

**Development of methods for the lead-oriented synthesis of
molecular scaffolds**

Steven Kane

Submitted in accordance with the requirements for the degree of

Doctor of Philosophy

The University of Leeds

School of Chemistry

November, 2015

Declaration

The candidate confirms that the work submitted is his/her own and that appropriate credit has been given where reference has been made to the work of others.

This copy has been supplied on the understanding that it is copyright material and that no quotation from the thesis may be published without proper acknowledgement.

© 2016 The University of Leeds and Steven Kane

Acknowledgements

I'd like to thank Adam and Steve for their support, guidance and mentoring throughout the past few years. Without that I would not be in the opportunity to write these acknowledgements. I'd like to thank Ian Churcher, my industrial supervisor, for the significant discussions about the LOS project. I am also thankful to the EPSRC and GSK for funding.

Team LOS!! Richard thanks for your continued ideas, singing and “alter ego”. Dan for always having a useful set of conditions to try and Phil reading parts of the thesis, continued suggestions and failing to teach me the rules of cricket.

GK my mann! What can I say? I don't think two Cypriot descendants would have had such difficulty communicating. Then again, I am only 54.6765% Cypriot so maybe it's not such a surprise. Kelly, it really wasn't your fault. Like ever. No way and maybe now it's in ink you can believe it? Thanks for the random half (/3 pints), the coffee (it's my turn), the walks, the rants and support. I'd like to thank Silvia for always being in that place during squash, for your stories, the pints and for always listening and giving your two cents worth.

I am grateful to the old man in G56 for reading the majority of this thesis, that stirrer bar and that cake #where_is_the_rest_of_the_cake? Howard for making Australian stereotypes true. Joan “as seen on TV” ML for the thrown back sass during the write up. Rong for the awesome cakes and the badminton lessons. The ghosts of G56 past; Charles-Hugues Claude Jean Lardeau for the continued talks about everything from breaking French news to the latest TV shows. Giorgia for the Italian lessons when playing squash and for all your stories about train trips. Francesco, Tom and Mark for help at the start of the PhD. Raj for naming the kid “Kane”. Martin for that laugh.

Alun, Murray and Dan. I would never have made it through if it wasn't for the coffee, trips to Reds, “chocolate” and banter. Thank you.

To the Wilson group throughout the ages (Ludwig, GP, Valeria, Dave, Hannah and GB). To Chris Hone for telling me he's a nice guy. Keeran for teaching me

squash can be a contact sport. Carlo for being the “Victor” to Chris’ “Jack”. Roberta for always “it’s a normal”. Phil W we still need to arrange that swim. I’d like to thank Charlotte for surviving having me and GK next to her for three years. Francis for the stories, the papers and the ideas of things to do in Leeds. The Lhasa squash club for some pretty good games.

For the people outside of Leeds that helped throughout the PhD; Matt, Ami, Adam, Ross and Tommy for the numerous trips around the UK. My family for their continual reassurance and being there for me to lean on (quite literally) when needed; mum, dad, Gary and Frankie. Lastly I’d like to thank Tanya for her work stories, cat videos, housing stories and listening to me rant about anything from obscure Scottish politics to a TV show when needed. I really can’t think how the last 8 months would have been without your encouragement, support and patience.

Abstract

There is an unmet and continuing need for diverse compounds with appropriate physicochemical properties for screening collections. This thesis focusses on the preparation of diverse scaffolds which may provide access to lead-like compounds after decoration. The approach was underpinned by robust connective reactions and cyclisations. Computational tools were used in the design and subsequent analysis of the compounds obtained.

Chapter 1 discusses the pharmaceutical sector and the challenges associated with creating and maintaining diverse screening collections. Molecular properties are key to the solving the problems with that industry. The concept of Lead-Oriented Synthesis (LOS) is introduced to help address these challenges.

Chapter 2 details the significant challenges which were encountered when attempting to use the Petasis reaction for LOS. Ultimately however, it was not possible to retool this reaction for the synthesis a library of diverse lead-like compounds.

Chapter 3 details the use of a computation protocol to direct the selection of a new connective reaction to support lead-oriented synthesis. The tools were used to compare five alternative connective reactions. On the basis of this analysis, the nitro-Mannich reaction was prioritised for experimental investigation.

Chapter 4 describes the preparation of small functionalised nitro adducts and the exploitation of a small toolkit of robust methodologies to access seven scaffolds. A virtual library of 2413 compounds was enumerated from the scaffold, of which 46% were found to be lead-like. It was concluded that the nitro-Mannich reaction can support lead-oriented synthesis.

Contents

Declaration	ii
Acknowledgements	iii
Abstract	v
1 Introduction	1
1.1 Introduction	1
1.2 Overview of the Drug Discovery Process	1
1.2.1 Characteristics of drug-like compounds.	2
1.2.2 Progression from leads to drug compounds: changing physicochemical properties.....	4
1.2.3 Characteristics of lead-like compounds	5
1.3 Availability of Lead Molecules.....	6
1.3.1 Natural Products.....	6
1.3.2 X generation: exploiting first in class	7
1.3.3 Fragment-based drug discovery.	7
1.4 Existing methodologies for generating diverse compound libraries.....	8
1.4.1 Diversity-oriented synthesis.....	10
1.4.1.1 Branching Pathways	11
1.4.1.2 Folding Pathways	13
1.4.1.3 Oligomer-based Approaches	14
1.4.2 Physicochemical properties of DOS libraries	16
1.4.3 Lead-oriented synthesis.....	17
1.4.3.1 Lead-oriented synthesis: Branching pathway.....	17
1.4.3.2 Lead-oriented synthesis: Folding pathway (1)	19
1.4.3.3 Lead-oriented synthesis: Folding pathway (2)	20
1.5 Project Outline	22
1.6 Summary	24
2 Investigation into suitability for the Petasis reaction to support lead- oriented synthesis	25
2.1 Petasis reaction: general characteristics	25
2.1.1 Physicochemical properties of compounds within libraries generated from the Petasis reaction.....	28
2.2 Reaction optimisation.....	29
2.3 Scope and limitations of the Petasis reaction.....	30

2.3.1	Synthesis of starting materials	30
2.3.2	Synthesis of cyclisation precursors	31
2.3.3	Factors influencing a diastereoselective Petasis reaction.....	33
2.3.3.1	Use of chiral amines	34
2.3.3.2	Use of chiral aldehyde	36
2.4	Design of cyclisation precursors from Petasis reaction	37
2.4.1	Synthesis of starting materials	38
2.4.2	Synthesis of cyclisation precursors	38
2.5	Utilising cyclisation precursors in subsequent cyclisation reactions	39
2.5.1	Iodine-mediated cyclisation	39
2.5.2	Ring closing metathesis	41
2.5.3	Carbodiimidazole coupling	41
2.6	Conclusions and summary	42
3	Development of methodology to determine a reactions suitability to support lead-oriented synthesis	43
3.1	Protocol to assess the lead-likeness of molecular scaffolds.....	43
3.1.1	Enumeration of virtual compound libraries.	43
3.1.2	Novelty assessment of molecular scaffolds.	44
3.1.3	Lead-likeness assessment of physical properties of final compounds.	45
3.2	Evaluation of Potential Reaction.....	47
3.2.1	Evaluation of β -Lactam Synthesis to support LOS.....	47
3.2.2	Evaluation of C-H Insertion to support LOS	48
3.2.3	Evaluation of SOMO-Activation to support LOS.....	49
3.2.4	Evaluation of nucleophilic opening of cyclic sulfamidates to support LOS	51
3.2.5	Evaluation of nitro-Mannich reaction to support LOS	52
3.2.6	Further interrogation of the virtual libraries generated	53
3.3	Reaction selection: nitro-Mannich reaction	54
4	Investigation into suitability for the nitro-Mannich reaction to support lead-oriented synthesis	55
4.1	nitro-Mannich reaction: general characteristics	55
4.2	Selection of a diastereoselective protocol for the nitro-Mannich reaction.....	57
4.2.1	Synthesis of starting materials	58

4.2.2	Synthesis of cyclisation precursors	59
4.3	Selection of a diastereoselective nitro-Mannich reaction protocol (2)	61
4.3.1	Catalyst screen	61
4.3.1.1	Synthesis of selected catalysts.....	61
4.3.2	Catalyst screen to identify suitable diastereoselective conditions	63
4.4	Design of Cyclisation precursors	66
4.4.1	Synthesis of starting materials	67
4.4.2	Synthesis of cyclisation precursors	67
4.4.2.1	Determining relative configuration of the nitro- Mannich reaction.....	69
4.5	Reduction of the nitro group	69
4.5.1	Determining the enantiomeric excess of the nitro-Mannich reaction.....	71
4.6	Utilising cyclisation precursors in subsequent cyclisation reactions	72
4.6.1	Cyclisation precursor 268	72
4.6.1.1	Cyclisation by Aminoarylation	72
4.6.1.2	Cyclisation by Cross-metathesis	73
4.6.2	Cyclisation precursor 237	73
4.6.2.1	Aminoarylation with 287.....	75
4.6.2.2	Cyclisation with Aminoarylation 289	76
4.6.2.3	Aminoarylation with 290.....	77
4.6.3	Cyclisation with substrate 289b	77
4.7	Review of molecular properties of compounds derived from prepared scaffolds	79
4.7.1	Assessment of Molecular weight and ALogP.....	79
4.7.1.1	Assessment of Fraction of sp ³ carbons.....	80
4.7.2	Assessment of Novelty.....	81
4.7.3	Principle moments of inertia study	82
4.7.4	Assessment of Synthetic economy.....	83
4.8	Conclusions	84
5	Experimental	85
5.1	Instrumentation and General Information.....	85

6	Appendices	145
6.1	Appendix 1: Cyclisation reactions	145
6.2	Appendix 2: Diversification reactions	146
6.3	Appendix 3: Novelty Assessment	150
6.4	Appendix 4: Individual cyclisation data	151
6.5	Appendix 5: Data for Molecular weight, F_{SP^3} plots	156
6.6	Appendix 6: Shape Analysis – Principal Moments of Inertia.....	158
6.7	Appendix 7: Crystallographic informations.....	161
6.8	Appendix 8: NOESY Spectra for 298.....	163
7	References	164

Abbreviations

Ac	acetyl
ACE	angiotensin converting enzyme
ADMET	adsorption, distribution, metabolism, excretion and toxicity
ap.	apparent
Ar	aromatic
b	broad
b.p.	boiling point
BAM	bis (amidine)
BINOL	1,1'-Bi-2-naphthol
BINAP	2,2'-bis(diphenylphosphino)-1,1'-binaphthyl
Bn	benzyl
Boc	<i>tert</i> -butyloxycarbonyl
Boc ₂ O	<i>tert</i> -butyldicarbonate
br	broad
BRSM	based on recovered starting material
bs	broad singlet
Bz	benzamide
CAN	cerium ammonium aitate
CAS	chemical abstracts service
Cbz	carboxybenzyl
CDI	carbodiimidazole
<i>cf.</i>	<i>confer</i> ; compare
CN	nitrile
CNS	central nervous system
COSY	correlation spectroscopy
CyJohnPhos	2-(dicyclohexylphosphino)biphenyl
d	doublet
d.r.	diastereomeric ratio
Da	dalton
dba	dibenzylideneacetone
DBU	1,8-diazabicyclo[5.4.0]undec-7-ene
DCE	dichloroethane
DCM	dichloromethane
dd	doublet of doublets
ddd	double double doublet
dddd	double double double doublet
ddt	double double triplet
DEPT	distortionless enhancement by polarization transfer

DIAD	diisopropyl azodicarboxylate
DIBAL	diisobutylaluminium hydride
DIPEA	diisopropyl amine
DMB	2,4-dimethoxybenzyl
DME	dimethoxyethane
DMF	dimethylformamide
DMP	dimethoxypropane
DMSO	dimethyl sulfoxide
DOS	diversity oriented synthesis
DPE-Phos	bis[(2-diphenylphosphino)phenyl] ether
DPPA	diphenyl phosphoryl azide
dq	double quartet
dt	double triplet
DTBP	2,6 di-tert-butyl pyridine
eq.	equivalent
ES	electrospray ionisation
Et	ethyl
ether	diethylether
EtOAc	ethyl acetate
EtOH	ethanol
FBDD	fragment-based drug discovery
FDA	food and drug administration
FGI	functional group interconversion
Fsp ³	fraction of sp ³ hybridised carbons
FT-IR	fourier transform infrared spectroscopy
HA	heavy atoms
HBA	hydrogen bond acceptor
HBD	hydrogen bond donor
HCTU	2-(6-Chloro-1H-benzotriazole-1-yl)-1,1,3,3-tetramethylaminium hexafluorophosphate
hept	heptet
HFIP	hexafluoroisopropanol
HG II	Hoyveda Grubbs 2 nd generation catalyst
HMBC	heteronuclear multiple-bond correlation spectroscopy
HMQC	heteronuclear multiple-quantum correlation spectroscopy
HPLC	high pressure liquid chromatography
HRMS	high resolution mass spectrometry
HTS	high throughput screen
IC ₅₀	half maximal inhibitory concentration
IR	infrared
<i>J</i>	spin-spin coupling constant

LC-MS	liquid chromatography mass spectrometry
LLAMA	lead likeness and molecular analysis
LogP	partition coefficient
LOS	lead-oriented synthesis
m	multiplet
m.p.	melting point
M.S.	molecular sieves
<i>m/z</i>	mass to charge ratio
<i>m</i> CPBA	<i>meta</i> -chloroperbenzoic acid
Me	methyl
MeCN	acetonitrile
MeOH	methanol
MIDA	<i>N</i> -methyliminodiacetic acid
MS	mass spectrometry
MW	molecular weight
NIS	<i>N</i> -iodosuccinimide
NMR	nuclear magnetic resonance
NOESY	nuclear overhauser effect spectroscopy
<i>o</i> -NsCl	2-nitrobenzenesulfonyl
petrol	petroleum spirit
PG	protecting group
Ph	phenyl
PhCF ₃	trifluoromethyltoluene
Phth	phthalimide
PMI	principal moment of inertia
PPB	plasma protein binding
ppm	parts per million
PSA	polar surface area
<i>p</i> TsOH	<i>para</i> -Toluenesulfonic acid
q	quartet
RCM	ring closing metathesis
R _f	retention factor
Rot	rotamer
rt	room temperature
RuPhos	2-dicyclohexylphosphino-2',6'-diisopropoxybiphenyl
s	singlet
SAR	structure activity relationship
<i>sat.</i>	saturated
<i>s</i> -DOSP	1-[[4-alkyl(C11-C13)phenyl]sulfonyl]-(2 <i>S</i>)-pyrrolidinecarboxylate
SMARTS	smiles arbitrary target specification
SnAP	Sn amine protocol
SOMO-Activation	singly occupied molecular orbital - activation

t	triplet
TBAF	tetra- <i>n</i> -butylammonium fluoride
TBDPS	<i>tert</i> -butyl diphenyl silyl
TBME	<i>tert</i> -butyl methyl ether
TBS	<i>tert</i> -butyl dimethyl silyl
<i>tert</i>	tertiary
TFA	trifluoroacetic Acid
THF	tetrahydrofuran
TLC	thin layer chromatography
TOCSY	total correlation spectroscopy
TOS	target oriented synthesis
Ts	4-toluenesulfonyl
tt	triple triplet
δ	chemical shift

1 Introduction

1.1 Introduction

The drug discovery process has undergone a rapid revolutionary change in recent years.¹ The growth of chemoselective transformations over the past decades has enabled the synthesis of previously challenging molecules. In addition, the advances made in understanding the cellular and molecular mechanisms behind diseases has allowed for the elucidation of additional drug targets.¹ As such it could have been expected that productivity of pharmaceutical industry would have increased. However up to 97% of all potential clinical candidates which enter phase 1 clinical trials fail to progress to market.²

1.2 Overview of the Drug Discovery Process

The main objective of drug discovery process is to identify new drugs which are effective, safe and meet an unmet clinical need.³ The different stages within drug discovery programmes are outlined in Figure 1. The first objective is to identify a target which is associated with the disease.⁴⁻⁶ This can be a protein active in the disease pathway (or present within the microorganism causing the disease), an enzyme, ion channel or nucleic acids.

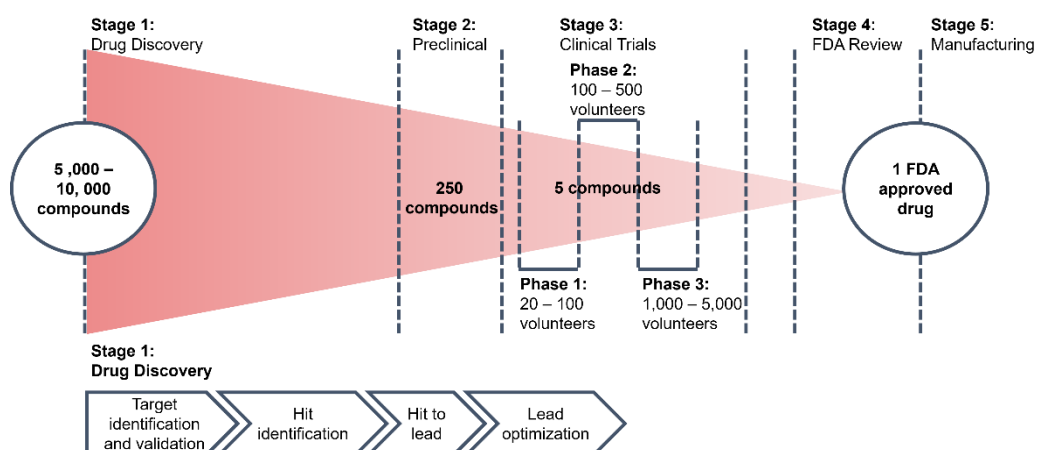


Figure 1: Stages of drug discovery process.

Once identified the target is then validated to ensure modulation provides relief from the disease state.³ A high throughput screen (HTS) can be implemented to

discover chemical compounds which interact with the target.^{5,6} As an alternative, computational docking may also be used to evaluate a library of compounds which are expected to interact with the target if its structure is known.^{4,5} A compound which binds and modulates the target is termed a “hit”.⁷ The best hits are then developed into leads and refined during lead optimisation to improve the potency, selectivity or safety of the compound.^{4,5,7} The final compound is designated the drug candidate; more extensive safety and metabolism studies are then performed.^{4,5,7} This whole process is costly, time-consuming and complex.⁷⁻⁹ Clinical development of a drug candidate is routinely prone to failure due to the uncertainties associated with predicting pharmacological and toxicological effects in humans.⁷⁻⁹

An analysis of the candidate’s pharmacokinetics properties can often prevent unsuitable molecules from advancing through the drug discovery process and thus help to decrease the number of failures.^{7,10,11} It has recently been recognised that the pharmacokinetic properties of the candidates are intrinsic properties of the molecules and it is therefore important for the medicinal chemist to optimise not only the drug-like properties but also the pharmacokinetic properties in lead molecules.¹²

1.2.1 Characteristics of drug-like compounds.

Drug-like properties refer to both the physical and adsorption, distribution, metabolism, excretion and toxicity (ADMET) properties of a molecule.^{4,13} For example, Lipinski’s “rule of 5” is a set of informal guidelines which take into account the molecular weight, hydrophobicity, hydrogen bond donor and acceptor capabilities of the molecule (summarised in Figure 2, Panel A entries 1-4).^{11,13,14} The guidelines are based on a statistical analysis of successfully marketed drugs and violation of more than one of these rules is unlikely to provide an orally viable drug.^{7,11} Shown in Figure 2 (Panel B) are the properties of the number one bestselling drug (as measured by sales from October-December 2013) Aripiprazole (**1**), an antipsychotic.¹⁵

Arguably the most important property of a drug is the LogP (a measure of lipophilicity).^{7,16-18} The higher this value the less likely the substance dissolves in aqueous environment which could lead to transport issues (rate of metabolism and

plasma protein binding are amongst other sources of transport issues).^{7,19–22} In addition, there is a correlation between greater lipophilicity and an increase in promiscuity; the toxicity of the compound could be amplified as binding interactions towards other targets could be significantly improved.^{7,19,20}

Entry	Physiochemical descriptors	Drug-like values	Physiochemical descriptors of Aripiprazole
1	Molecular Weight:	≤500	447.15
2	LogP :	≤5	4.90
3	Hydrogen bond donors:	≤5	1
4	Hydrogen bond acceptors:	≤10	5
5	Polar surface area:	≤70 Å ²	

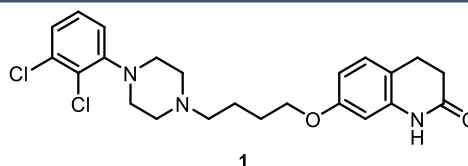


Figure 2: Summary of drug-like properties as defined by Lipinski and their idealised values (column 1).²³ The physiochemical properties of Aripiprazole (**1**), the bestselling drug in the final months of 2013 (column 2).¹⁵

Hydrogen bond donors and acceptors are atoms which either provide the hydrogen for a hydrogen bond or provide an electron rich atom to interact with the respective hydrogen.⁴ Too many of these interactions leads to poor membrane permeability, reducing the transport capability of the drug.⁴

The polar surface area is the sum of surface area of all the polar atoms and attached hydrogens.^{19,22,24} Although not part of Lipinski's original work, it is an additional parameter which has been shown to be a good indicator of how well a substance can be transported across cellular membranes.^{19,22,24}

Reactive functional groups are a further aspect to consider when evaluating the drug-like properties of a molecule. These groups are undesirable in a drug molecule as they could give a false hit (as it could react indiscriminately with the target) or increase the toxicity.^{7,25–29} In addition, some groups are undesirable as they are readily hydrolysed *in vivo* and as such are avoided as their hydrolysis could reveal a toxic function group or the molecule could lose some binding interactions. Common undesirable groups within drugs include (but are not limited to) electrophiles such as epoxides and Michael acceptors.^{25–28}

It should be noted however, that the above rules are only expected to serve as guidelines to the medicinal chemist and it is the balance of these properties which

determine the compounds suitability as a drug candidate.^{14,22} Indeed the rule of 5 is only applicable to orally bioavailable drugs and describes just adsorption issues, not the compounds bioavailability. If specific transport methods are employed, there is a more generous allowance for drug properties.^{14,30–32} There are also specific rules for drugs acting on the Central Nervous System.^{30,33–35}

1.2.2 Progression from leads to drug compounds: changing physiochemical properties

As previously discussed the lead compound is often altered within the drug discovery process to yield the drug candidate. This is done for a number of reasons including (but not limited to) improving ADMET properties and increasing binding to the target. Dichloroisoproterenol (**2**) was the first β -blocker to be developed (Figure 3 , Panel A).³⁶ However the low potency observed and the fact it is partial agonist/antagonist of the β_1 and β_2 -adrenergic receptors made it unsuitable as a drug.³⁶ Subtle structural modification resulted in the development of Propranolol (**3**), the first β -blocker to reach market which is a full antagonist of the β_1 and β_2 -adrenergic receptors.³⁷

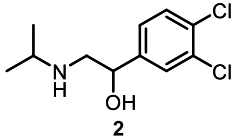
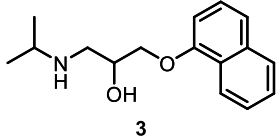
A: Physiochemical properties of Dichloroisoproterenol and Propranolol			
	Molecular Weight: 247.05 LogP: 2.88 HBD: 2 HBA: 2		Molecular Weight: 259.16 LogP: 2.58 HBD: 2 HBA: 3
Dichloroisoproterenol		Propranolol	
B: Changes in Physiochemical properties of dichloroisoproterenol and propranolol		C: Changes in Physiochemical properties of 67 lead drug pairs	
Δ Molecular Weight: +12.11	Δ LogP: -0.3	Δ Molecular Weight: +78.97	Δ LogP: +1.25
Δ HBD: 0	Δ HBA: +1	Δ HBD: -0.18	Δ HBA: +0.45

Figure 3: Panel A: Physiochemical properties of Dichlorisoproterenol (**2**) and propranolol (**3**). Panel B: Changes in physiochemical properties of selected lead-drug pair. Panel C: Property analysis of 67 lead and drug pairs. Values for the lead compounds were subtracted from matching properties of the drug molecules. Adapted from Teague *et al.*¹²

The molecular weight increased during the development of Propranolol from Dichlorisoproterenol (Figure 3 , Panel B). The number of hydrogen bond acceptors also increased with a slight decrease in LogP. Teague and co-workers analysed the difference between 67 lead compounds and the drug candidates derived from them.¹² By using such a large data set they were able to highlight some trends; chiefly

molecular weight, LogP and complexity are increased throughout the drug discovery process. It is therefore better to start from a smaller fragment so as to remain in drug-like chemical space on optimisation to the final lead compound.^{7,13,30}

1.2.3 Characteristics of lead-like compounds

If the information presented above is taken into account, a map of chemical space can be created such that the drug-like properties, as defined by Lipinski, represents the limits of chemical space. Since there is typically an increase in molecular weight and LogP throughout development¹² Churcher *et al.* have defined a region termed lead-like chemical space (Figure 4, Panel A). By their definition the limits of lead-like space is defined by the molecular properties outlined in Figure 4 (Panel B).⁷ By constraining the physiochemical properties of lead compounds, increases in molecular weight and LogP typically observed during development, the final compound should still remain within Lipinski's drug-like chemical space.

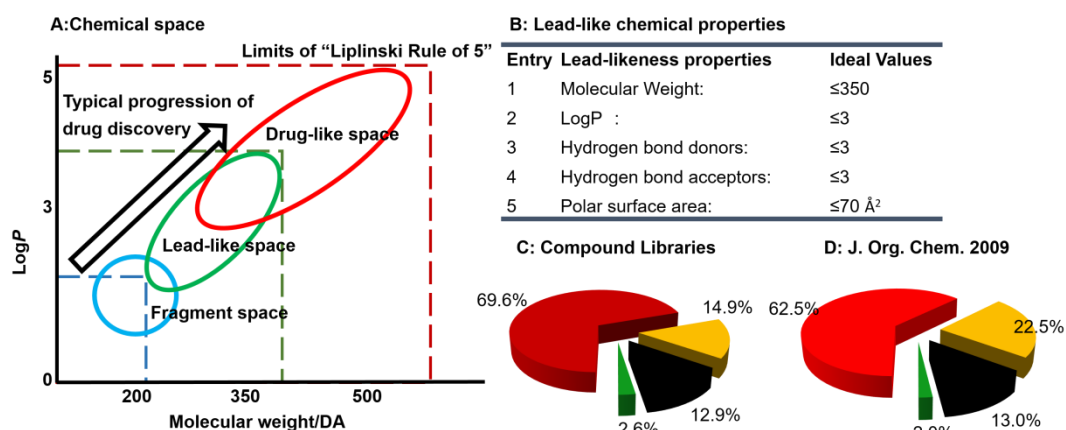


Figure 4: Panel A: Diagram of chemical space. Throughout lead optimisation, a compound tends to increase molecular weight and lipophilicity.¹² Panel B: Limits for the molecular properties of lead-like compounds as defined by Churcher *et al.*⁷ Panel C: Analysis of 4.9 million commercially available compounds for their lead-likeness.⁷ 2.6% of the compounds (green) survive successive filtering by molecular size ($14 \leq \text{number of heavy atoms} \leq 26$; failures shown in red), lipophilicity ($-1 \leq \text{LogP} \leq 3$; failures shown in orange) and presence of undesirable functional groups (failures shown in black). Panel D: Analysis of 13,194 compounds published in *J. Org. Chem.* 2009 for lead-likeness. Using the same criteria as before, on 2.0% of compounds pass all filters.⁷

Churcher *et al.* analysed the physiochemical properties of 4.9 million commercially available compounds from a variety of vendors.⁷ They found the vast majority of compounds (97.4%) fail at least one descriptor of lead-like properties. (Figure 4, Panel C).⁷ The same analysis was performed on synthetic methodology reported in the *Journal of Organic Chemistry* during 2009 showed that of the ca. 32,700 molecules synthesised only 690 (2.0%) of them would pass lead-like filters

(Figure 4, Panel D). As such there is an urgent need for the development of new methodology which is capable of reliably generating diverse compounds with properties within lead-like chemical space.⁷

1.3 Availability of Lead Molecules.

This section details traditional sources of lead compounds and their advantages and disadvantages before assessing the typical physiochemical properties associated with typical leads and assessing if they inhabit lead-like chemical space.⁴

1.3.1 Natural Products

Natural compounds have evolved to interact with specific biological targets to achieve a precise response; as such the use of natural products as sources for leads has been extensive.^{4,5} However, natural products are often complex and while they can have excellent potency, they provide little room for further chemical manipulation.⁴ As a result they are not generally lead-like as defined by Churcher.⁷ In addition, isolation of the active compound can prove difficult as it may be present in low concentration or unstable to purification techniques employed.³⁸ Taxol (**4**, Figure 5) is a key example, originally isolated from the Pacific Yew. It required 1,200 kg of bark to yield just 10 g of purified Taxol and it was not until 1993 (over 30 years since it was initially isolated) that a practical semi-synthetic synthesis was developed by Bristol–Myers–Squibb.³⁸

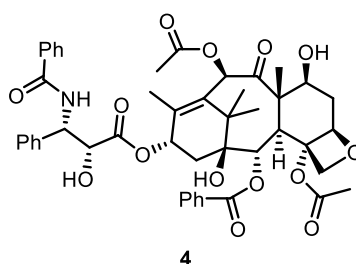


Figure 5: Taxol (**4**) is a complex anticancer agent, derived from natural sources.³⁸

1.3.2 X generation: exploiting first in class

As compounds with activity are identified, through academic research groups or within rival pharmaceutical companies, the reported structure can often be used as the lead compound.³⁸ The so called “best in class” approach has been used widely.^{38,39} The scaffold of the molecule is generally retained but the appendages are altered to maximise its effectiveness. Pro-drug strategies or different formulations can be used to circumvent patent protection.³⁸ Ranitidine (**5**, Figure 6), a histidine H₂ receptor agonist, was developed by the then Glaxo organisation in response to Cimetidine (**6**, Figure 6) developed by Smith, Kline and French.^{38,39}

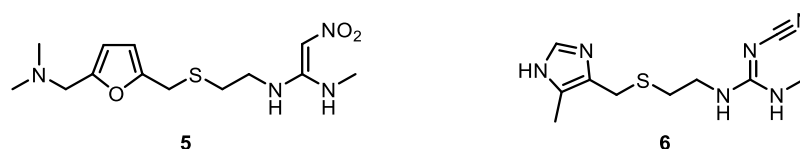


Figure 6: Cimetidine (**6**) was used as a lead compound for the development of Ranitidine (**5**) a histidine H₂ receptor agonists.^{38,39}

1.3.3 Fragment-based drug discovery.

Traditional HTS requires a large library of compounds to be prepared and screened in order to identify suitable hits. This increases both cost of development and time required to identify suitable compounds. Fragment-based drug discovery (FBDD) has grown as a complementary method for lead identification within drug discovery programs.^{38,40-42}

A major advantage of screening fragments is that a library of smaller fragments represents a much larger proportion of the available chemical space than a similarly sized library for higher molecular weight compounds.³⁹⁻⁴¹ In addition there are significantly more hits with a fragment-based screen compared to traditional HTS; the library screened therefore can be much smaller to obtain a comparable number of hits.^{39-41,43} This decreases both the time and cost associated with development of the screen.^{40,42}

A major disadvantage of this approach to lead identification is that the binding affinity of fragments is much lower than drug-like molecules. As a result, conventional HTS bio-assays for determining activity cannot readily be applied.^{38,40} Other techniques such as X-ray crystallography and NMR spectroscopy must be

used.^{38,40,42} The use of such techniques requires significantly more time for data collection and consequently they are not suitable to HTS. The compounds screened must also be very soluble since high concentrations are required to detect the weakly bound species which limits the availability of certain fragments.^{40,42}

Vemurafenib (or PLX4720) is a kinase inhibitor, and the first FDA approved drug discovered by FBDD.^{38,44,45} 7-Azaindole (**7**, Figure 7) was identified by Tsai and co-workers from an initial library of 20,000 fragments and was subsequently co-crystallised with Pim-1; however, as with most low-binding fragments multiple binding modes were identified.⁴⁵ Derivatisation of **7** quickly identified **8** which crystallised with Pim-1 in a single binding site. Derivatisation of **8** at the three and five positions as directed by the X-ray structure generated PLX4720 (**9**) which was found to be selective for B-Raf^{V600E} kinase (the most common oncogenic kinase) over wild type B-Raf (IC₅₀ of 13 and 160 nM respectively).^{44,45}

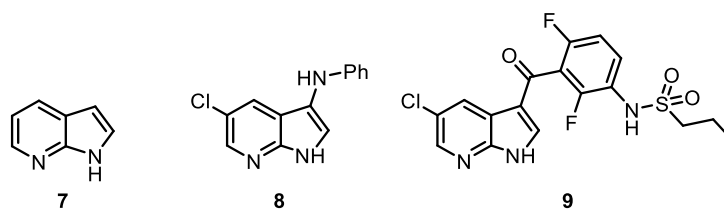


Figure 7: Azaindole (**7**) was the initial hit which was developed into a kinase inhibitor and the first FDA approved drug discovered from FBDD (**9**).^{44,45}

1.4 Existing methodologies for generating diverse compound libraries

Libraries of highly diverse small molecules are essential for enabling the efficient screening of chemical space. However diversity is a crude term often used to describe entirely different concepts. Lipkus *et al.* have used the concept of frameworks to quantitatively analyse the diversity of the CAS registry.⁴⁶ The concept of frameworks is demonstrated with Amikacin (**10**, Figure 8, Panel A).⁴⁶

By this method, it is only the constituent ring systems which are important, the side chain appendages are ignored for simplicity.⁴⁶ The simplest level, the graph level, is simply the ring systems with connecting chain atoms. At this stage, tetrahydrofuran and pyrroles would be classed as the same scaffold. The next level, the graph/node level, simply includes the heteroatoms present within the graph framework. At this level, piperidine could be differentiated from benzene but it would still have the same scaffold as pyridine. This is also called the

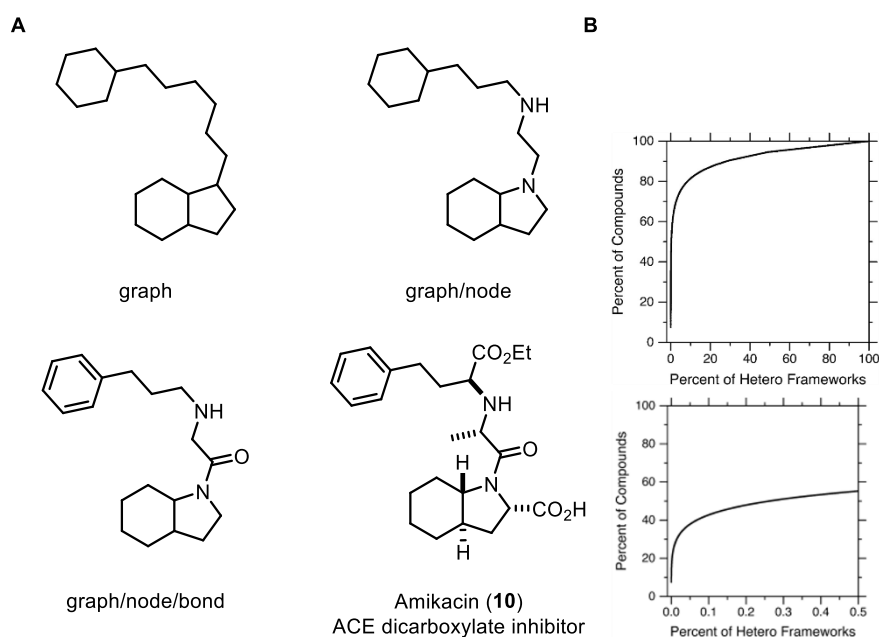


Figure 8: Panel A: Amikacin, a dicarboxylate ACE inhibitor, shown at graph, graph/node and graph/node/bond level of frameworks. Panel B: A plot of the percentage of frameworks vs the percentage of compounds which have that framework. An expanded view is shown below. Adapted from.⁴⁶

heteroframework. The final level, the graph/node/bond level, includes the oxidation states of the heteroframework. In this way pyridine rings can be differentiated from piperidine rings.

Lipkus *et al.* have used the concept of frameworks to analyse the diversity of the CAS registry.⁴⁶ From the analysis, they concluded that the 5% most common heteroframeworks represent ~75% of all compounds synthesised (Figure 8, Panel B and C).⁴⁶ Exploration of chemical space has therefore not been systematic, approximately half of all compounds synthesised are based on only 0.25% of known molecular scaffolds.⁴⁶⁻⁴⁹ The number of possible drug-like molecules is enormous and it is impossible to prepare all molecules to map the entire chemical space or indeed just biologically active space.^{46,50} As a consequence, skeletally-diverse structures must be synthesised to ensure maximal chemical space coverage.⁴⁹ With a more systematic approach to exploring new molecular scaffolds, novel leads may be discovered.⁵¹

1.4.1 Diversity-oriented synthesis

Diversity-oriented synthesis (DOS) is a technique aimed at the systematic exploration of chemical space. DOS aims to efficiently prepare libraries of compounds with diverse molecular structures.⁵¹⁻⁵³ There are three general descriptors of diversity:^{47,48,52-54}

1. Appendage diversity – in which the substituents on the scaffolds are varied.
2. Stereochemical diversity – in which the use of stereoselective reactions allows access to all possible stereoisomers.
3. Skeletal diversity – in which the scaffolds of small molecules are varied.

Target oriented synthesis (TOS) is used when there is a known compound of interest and the medicinal chemist will try many different types of chemistries to obtain the single scaffold (Figure 9, left). Combinatorial chemistry aims to explore the immediate vicinity of a particular target by variation of substituents, and is usually used in lead optimisation (Figure 9, centre). As a result, although many different compounds are synthesised they are often based on a conserved molecular scaffold. DOS differs considerably from combinatorial chemistry. Since it aims to explore broad areas of chemical space, few compounds with just the same molecular scaffold (Figure 9, right).⁴⁷

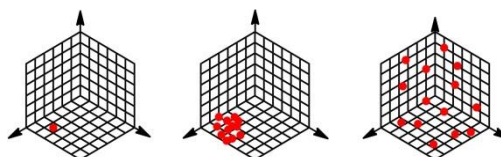


Figure 9: Schematic illustration of the major approaches to lead generation: target oriented synthesis (left), combinatorial chemistry (centre) and diversity oriented synthesis (right).⁴⁷

DOS employs a number of different strategies to obtain skeletal diversity (of which some can be used in combination to greatly increase complexity).⁵² Multi-component reactions are often extensively used.⁵⁵ Diversity can then be obtained by variation of each of the reactants. Three conceptually different approaches to exploration of chemical space using DOS are;

1. Branching pathways (Section 1.4.1.1)
2. Folding pathways (Section 1.4.1.2)
3. Oligomer-based approaches (Section 1.4.1.3)

Other approaches have been reviewed and are not discussed here.^{51,56,57}

1.4.1.1 Branching Pathways

Branching pathways (or ‘reagent based approaches’) are one of the more commonly employed strategies in DOS. Branching pathways involve the use of a substrate with many complementary functional groups (Figure 10) which are then exposed to a number of different reagents which couple the different functionalities in order to give distinct molecular scaffolds.^{47,49,52,54,58}

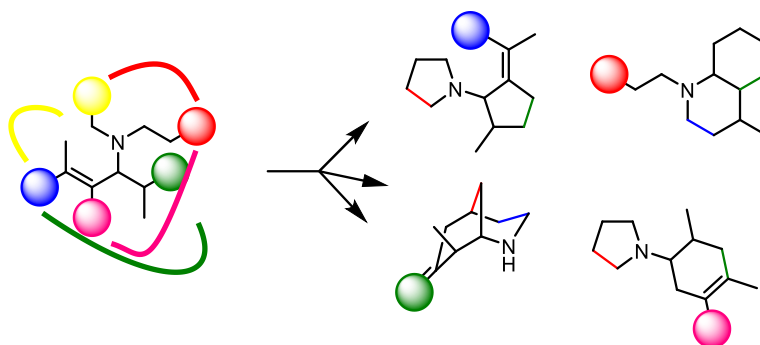
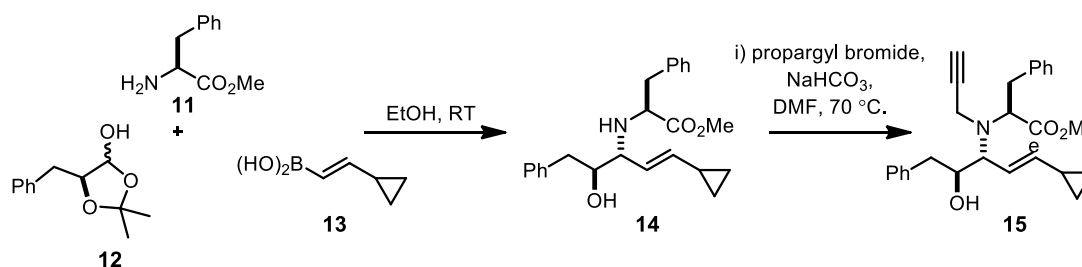


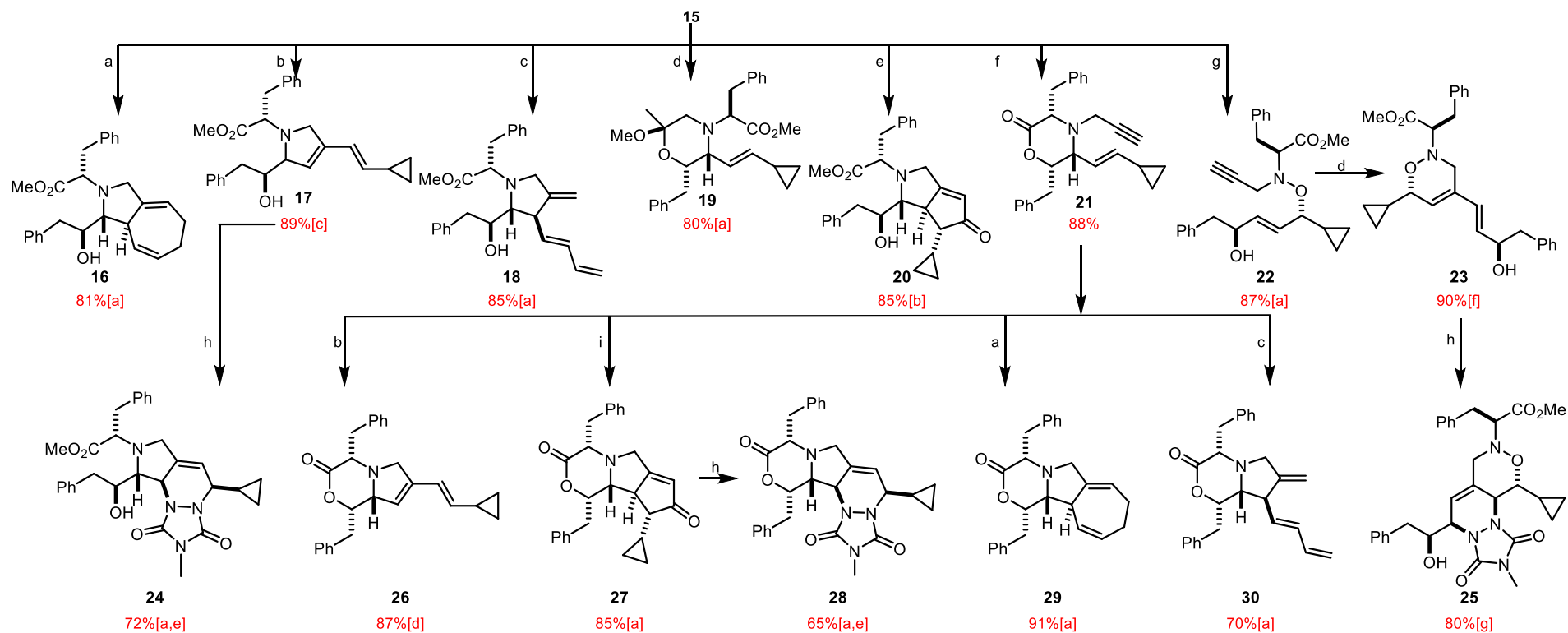
Figure 10: Schematic representation of a branching pathway route in Diversity-oriented synthesis.

This method becomes extremely efficient when the product of the reactions retains complementary functional groups which allow further diversification.^{52,58} Structural complexity is built up rapidly in four or five synthetic steps as shown in the work of Schreiber and co-workers.⁵⁸ Schreiber utilised the Petasis reaction to create the amino alcohol **14** (Scheme 1). Additional functionality was then incorporated with the selective *N*-alkylation with propargyl bromide to give **15**.⁵⁸



Scheme 1: Synthesis of amino alcohol **15** in two synthetic steps from available starting materials.⁵⁸

Alternative transition metal catalysis was employed to give products with distinct molecular scaffolds (Scheme 2): ruthenium-catalysed cycloheptadiene (\rightarrow **16**), ene-yne metathesis (\rightarrow **17**), palladium-catalysed cycloisomerisation (\rightarrow **18**), electrophilic activation of alkyne with gold (\rightarrow **19**), Pauson-Khand cyclisation



Scheme 2: The use of the Petasis reaction to create a polyfunctional starting material. Various transition metal catalysed reactions were then employed to couple the various functional groups and give access to distinct molecular scaffolds. Reaction conditions: a) $[\text{CpRu}(\text{CH}_3\text{CN})_3\text{PF}_6]$ (10 mol%), acetone, rt; b) Hoveyda-Grubbs second generation catalyst (10 mol%), DCM, reflux; c) $[\text{Pd}(\text{PPh}_3)_2(\text{OAc})_2]$ (10 mol%), benzene, 80 °C; d) NaAuCl_4 (10 mol%), MeOH, rt; e) $[\text{Co}_2(\text{CO})_8]$, trimethylamine *N*-oxide, NH_4Cl , benzene, rt; f) NaH, toluene, rt; g) *m*CPBA, THF, -78 – 0 °C; h) 4-methyl-1,2,4-triazoline-3,5-dione, DCM, rt; i) $[\text{Co}_2(\text{CO})_8]$, trimethylamine *N*-oxide, benzene, rt; [a] Single diastereoisomer; [b] > 10:1 d.r.; [c] *trans/cis* = 6.7:1; [e] from *trans* diene; [f] *trans/cis* = 3:1; [g] combined yield from the *trans* and *cis* dienes. *m*CPBA = *m*-chloroperbenzoic acid.

(→**20**), lactonisation (→**21**) and *N*-oxide mediated isomerisation (→**22**) which underwent the same gold mediated activation of alkyne previously (→**23**).

After the first generation of cyclised products, some were suitable substrates for further manipulation. Thus dienes **17** and **23** underwent a Diels Alder reaction to give tricycles **24** and **25**. The lactone **21** was subjected to some of the initial cyclisation used with **15** to give second-generation cyclisation products with increased complexity (**26-30**). In total, this strategy yielded over 15 distinct molecular scaffolds in two synthetic steps from a simple starting material (itself prepared in two steps from commercially available reagents).⁵⁸ Although not explored here, with variation of the starting reactants, additional scaffolds could be readily synthesised.

1.4.1.2 Folding Pathways

Folding Pathways (or ‘substrate-based control’) are the converse of branching pathways. Diversity is built into the route by varying the building blocks used and then under the same reaction conditions one can generate different molecular scaffolds (Figure 11).^{47,49,52,53} Diversity of the starting materials could be the use of acyclic and cyclic starting materials or varying the distance between reactive functional groups as well as appendage diversification.

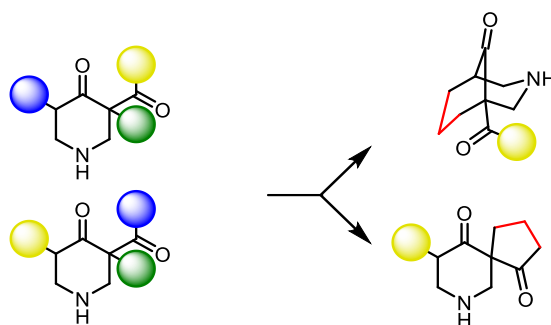
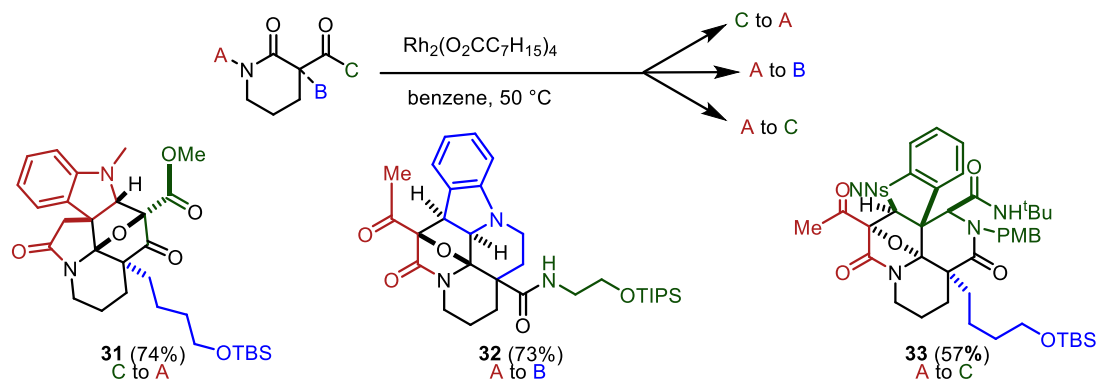


Figure 11: Schematic representation of a folding pathway.⁵⁴

Oguri and Schreiber reported the use of one such folding pathway to three distinct indole alkaloid architectures (**31-33**, Scheme 3).^{51,53,55} The rhodium catalysed cyclisation produced distinct structures based on the relative locations of the α -diazo carbonyl and the indole groups. As a result of the different ring closures, quite diverse products were obtained. Complex alkaloid-like products were obtained in just four reactions from commercially available starting materials.⁵³



Scheme 3: Three distinct alkaloid-like structures generated from folding pathway. The diverse structures were obtained by varying the distance between the reactive groups.⁵³

1.4.1.3 Oligomer-based Approaches

Oligomer-based approaches combine elements from both branching and folding pathways to provide a vastly powerful tool for generation of diverse molecular scaffolds. The starting material is often immobilised on a tag or a polymeric support (Figure 12) then various coupling strategies are employed to obtain a larger bound substrate.^{48,59} Then using suitable reactions, the product can be released from the bound support (Figure 12). This release step often “re-programmes” the substrate giving access to the diverse structures.^{48,51}

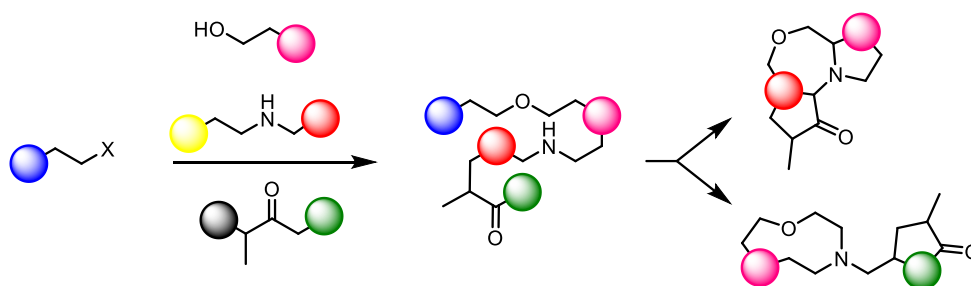


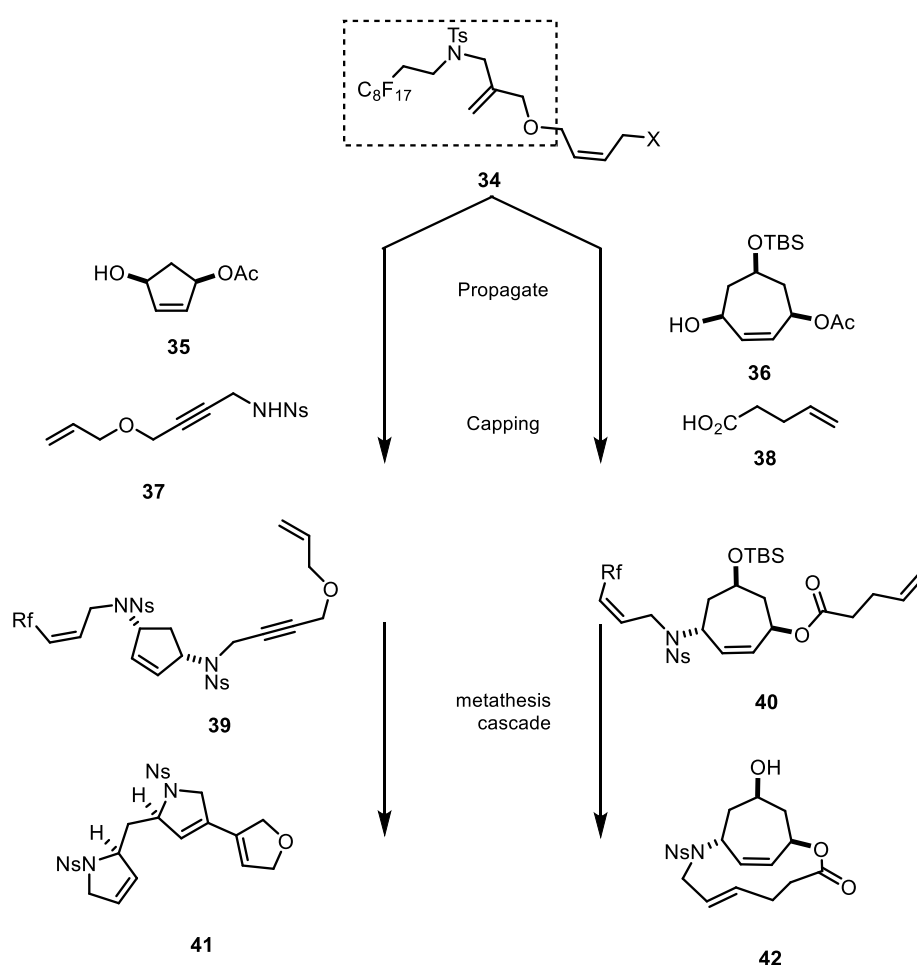
Figure 12: Schematic representation of a folding pathway

This strategy has been used within the Nelson group (Scheme 4).^{48,49} By using various a variable oligomer bound starting material (**34**) they were able, in a series of propagating and capping steps, add a variety of different building blocks (**35-38**) to synthesis a number of oligomer-bound structurally diverse intermediates. Then following alkene metathesis, the products were reprogrammed giving a large number of different scaffolds and removing the oligomer tag.

Exploiting variation of the position of the alkene bonds in the substrates, and subsequent competition between the formation of different ring sizes, 84 distinct

molecular scaffolds were obtained from only 92 products, of which 65% were novel.⁴⁸ A fact which demonstrates that the use of oligomer-based approaches can achieve the aims of DOS; the systematic exploration of chemical space.

An important advantage of this method was the use of the fluororous-tagged linker (R_F). This linker allowed rapid purification of all intermediates and final reagents with simple fluororous solid-phase extraction.⁴⁸ The broad scope of the metathesis reaction was another key feature which allowed the high diversity. It is only through using similarly tolerant reactions that diversity on this scale could be achieved, with the use of only six optimised reactions.⁴⁸



Scheme 4: Example of the oligomer-bound pathway used in DOS. The initial substrate is bound to a fluororous linker then rapidly extended before product release.⁴⁸ R_F = Fluorous tag.

One of the major challenges associated with DOS strategies is finding suitable reactions which tolerate a variety of functional groups.⁵¹ Since the aim of DOS is to achieve diversity in few steps, the use of protecting groups is avoided wherever possible.

1.4.2 Physiochemical properties of DOS libraries

The products obtained from the DOS approaches described in Section 1.4.1.1-1.4.1.3 were subjected to a computational analysis of their physiochemical properties. A plot of the molecular weight *vs* LogP was then created (Figure 13). From the data generated, only 10% of the scaffolds created have physiochemical properties suitable for the synthesis of a lead-like compounds (shown in green). Just 55% of the scaffolds have properties suitable for Lipinski's drug like space while the remaining 35% are outside lead-like chemical space. Since development of a drug candidate typically increases molecular weight and LogP, most of the products would be unsuitable for generation of a drug-like library. The products obtained are better described as drug-like or natural product-like due to the significant molecular weight which often lies well outside the lead-like chemical space as defined by Churcher (Section 1.2.2).^{7,51}

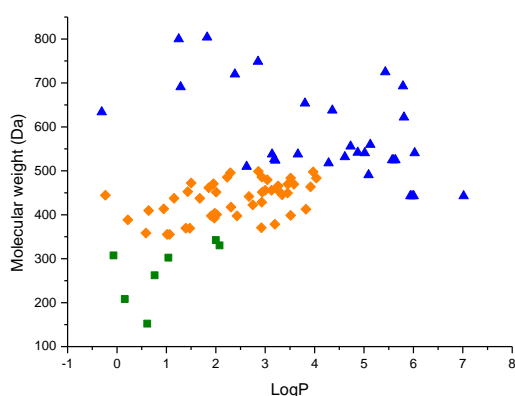


Figure 13: Analysis of the molecular weight and LogP of the products obtained from three DOS campaigns.^{48,52,53} Compounds which pass lead-like filters (green), Lipinski's rule of five (orange) and compounds beyond the Lipinski limit (blue).

1.4.3 Lead-oriented synthesis

In their review, Churcher *et al.* establish that traditional chemistries are inclined to producing molecules outwith “lead-like” space.^{7,13,26,50} Arrays are designed to give molecules with a broad range of properties and structural characteristics. Typically however, not all products are obtained from a planned array and as such the property profile of the entire array is often skewed.⁷ Generally the molecules which systematically fail are often the polar, more hydrophilic products (either through failure of the reaction under standard conditions or poor product recovery from standard work-up procedures).⁷

As such, the final array of compounds obtained often have a different physiochemical profile which a much higher mean LogP than planned (so called LogP drift).⁷ As a result, the authors call for new methodology to be developed to allow to more diverse and better quality lead compounds.⁷ Since the concept of Lead-Oriented Synthesis (LOS) was introduced a number of groups have attempted to address the need. Herein approaches which best attempt to address these challenges are discussed.

1.4.3.1 Lead-oriented synthesis: Branching pathway

Branching pathways (as seen in Section 1.4.1.1) can be used in the development of lead-like chemical libraries. “Rope-like molecules” as defined by Stockman *et al.* are linear compounds with complementary functional groups which allow the creation of fraction sp^3 (F_{sp^3}) carbon molecular structures.² These structures contain a variety of ring systems and the heteroatoms incorporated allow further diversification and subsequent SAR type analysis. The methodology is exquisitely demonstrated in Figure 14 (Panel A) where an example of a “rope like molecule” **43** gave rise to a small library of products with distinct molecular scaffolds; 6/5/5 fused tricycles (**44**, **45** and **46**); 6/6 fused cycles (**47**, **48** and **49**); 5/5 fused cycles (**50** and **51**); spirocycle (**52**) and single cycles tetrahydropyran (**53**) and cycloalkane (**54**).²

The products obtained from this small library were subjected to the same computational analysis of the physiochemical properties used in the DOS campaigns (Section 1.4.2). A plot of the molecular weight vs LogP was then created (Figure 14,

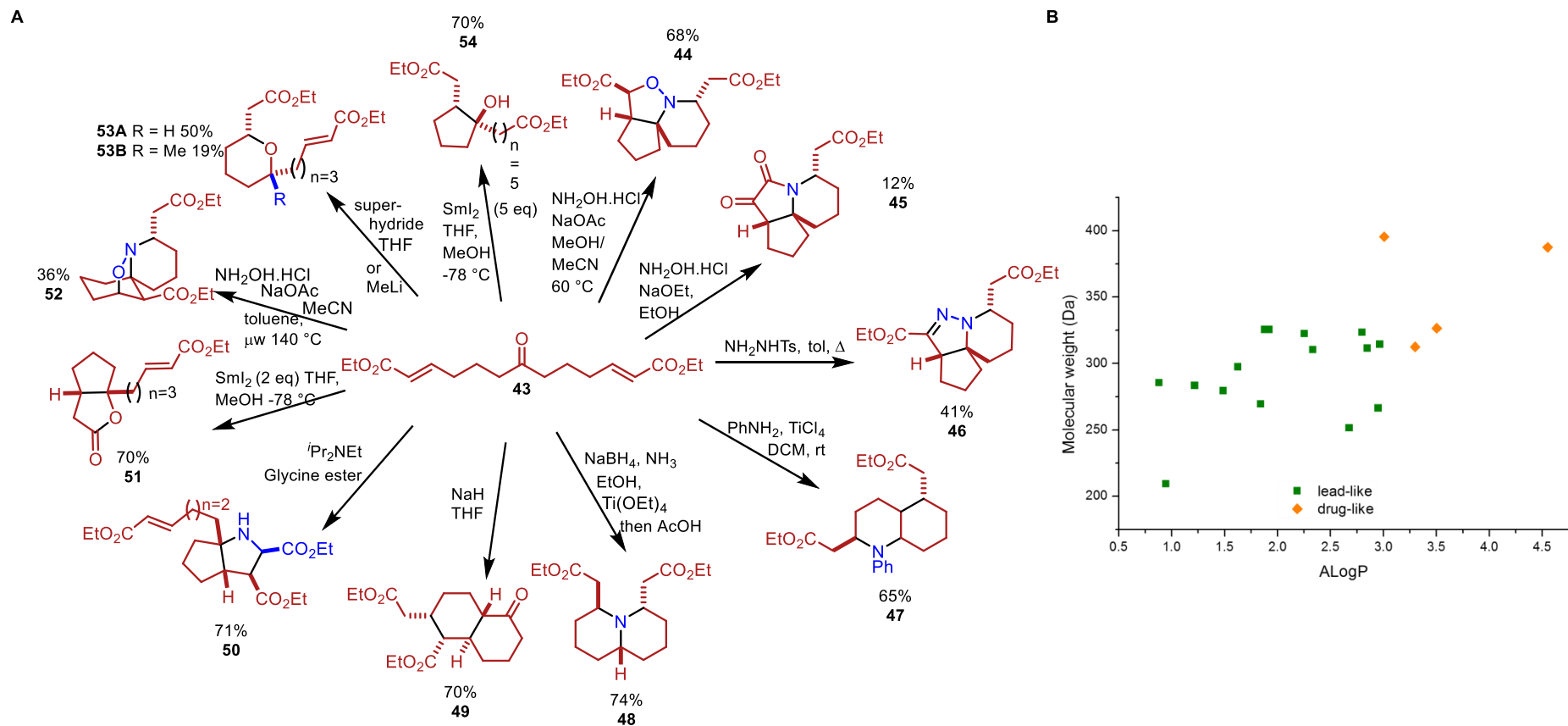


Figure 14: Panel A: An example of a “rope like molecule” **43** which undergoes a variety of cyclisation reactions to give scaffolds **44-57**. Panel B: Analysis of the physicochemical properties of these scaffolds generated reveal they occupy lead-like chemical space.

Panel B). As shown, seven out of the eleven scaffolds synthesised have molecular weight and LogP within lead-like chemical spaces as defined by Churcher *et al.*⁷ Further elaboration of scaffold **44** resulted in an additional library of compounds which was screened against three cancer cell lines and exhibited a range of biological activity. This demonstrates this is a practical methodology for rapid access scaffolds with high Fsp³ which can be further elaboration to give a library of molecules suitable for biological screening. The scaffolds were delivered in an average 1.25 steps from **43** per new scaffold.²

The only real disadvantage of this methodology is the limited number of sites remaining for diversification. Nine of the compounds only have the presence of one or two ester groups. Three of the scaffolds generated also have the presence of undesirable functional groups, namely N-O and N-N linkages.⁶⁰

1.4.3.2 Lead-oriented synthesis: Folding pathway (1)

Folding pathways (as seen in Section 1.4.1.2) can be used in the development of lead-like chemical libraries. The use of multicomponent reactions which allow variation of the components allows rapid access to diverse small molecules if systematic variation of each component is tolerated. SnAP (Sn Amine Protocol) as re-introduced by Bode *et al.* attempts to deliver highly functionalised Fsp³ rich heterocycles (Figure 15).⁶¹⁻⁶³ Treatment of an aldehyde with an amino tethered stannane in the presence of a copper catalyst led to the isolation of cyclic amines *via* radical addition to the imine (Figure 15, Panel A). A broad variety of (hetero) aryl and aliphatic aldehydes are tolerated with a variety of substitution patterns allowing the synthesis of six- to nine-membered heterocycles including diazapines and oxazepanes (**55-60**, Panel B).⁶¹⁻⁶³

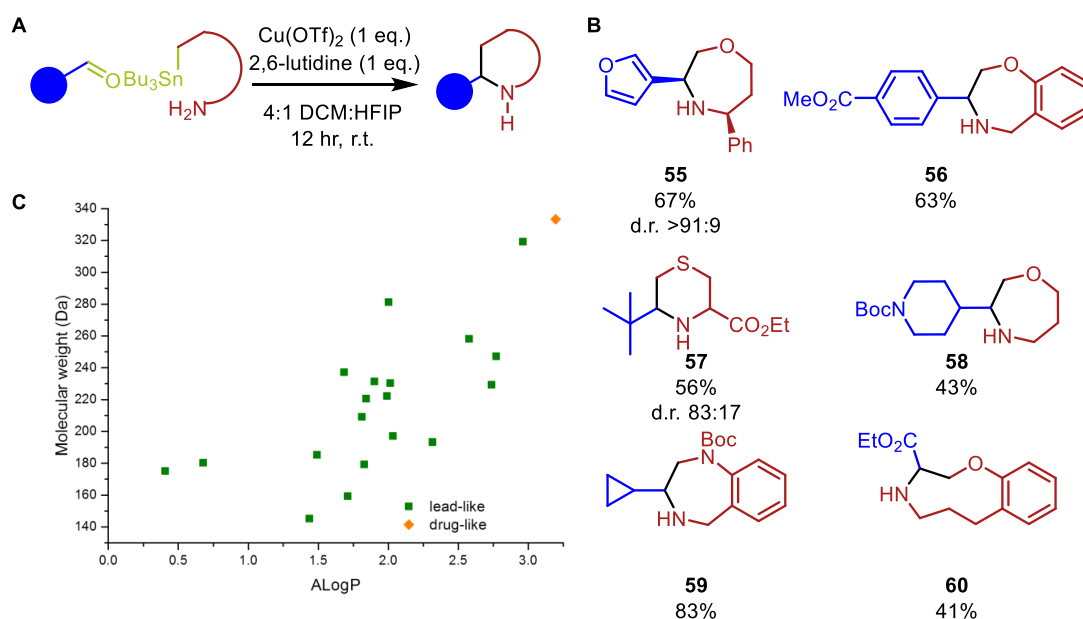


Figure 15: Panel A: Bode *et al.* utilisation of a novel copper mediated radical addition to various imines allows the synthesis of diverse range of heterocycles. Panel B: Selected examples of products obtained from this folding pathway.^{61–63} Panel C: Analysis of the physicochemical properties of these scaffolds generated *via* SnAP protocol reveal they are sufficiently small that may retain useful properties even after decoration.

When the molecular weight and LogP is calculated for the library members, as described previously (Section 1.4.2 and 1.4.3.1), data generated reveals that every compound except one falls within lead-like chemical space (Figure 15, Panel C). A key limitation of the SnAP protocol is that significant synthetic effort is required to make the tin reagents. The diversity of the subsequent library is also reduced since a common ring system would be present in a large percentage of the compounds generated. This could only be overcome by the synthesis of many different tin reagent.^{61–63}

1.4.3.3 Lead-oriented synthesis: Folding pathway (2)

Dixon *et al.* have recently disclosed a folding pathway towards highly functional, diverse pyrrolidinones employing a nitro-Mannich-lactamisation cascade (Figure 16, Panel A).⁶⁴ Treatment of the nitro ester with the imine (formed from the condensation of aldehyde and amine) led to the isolation of pyrrolidinones **61–66**. Systematic variation of different amines, aldehydes and nitro components allowed the synthesis of a library of highly substituted scaffolds with good diastereocontrol (Panel B).⁶⁴

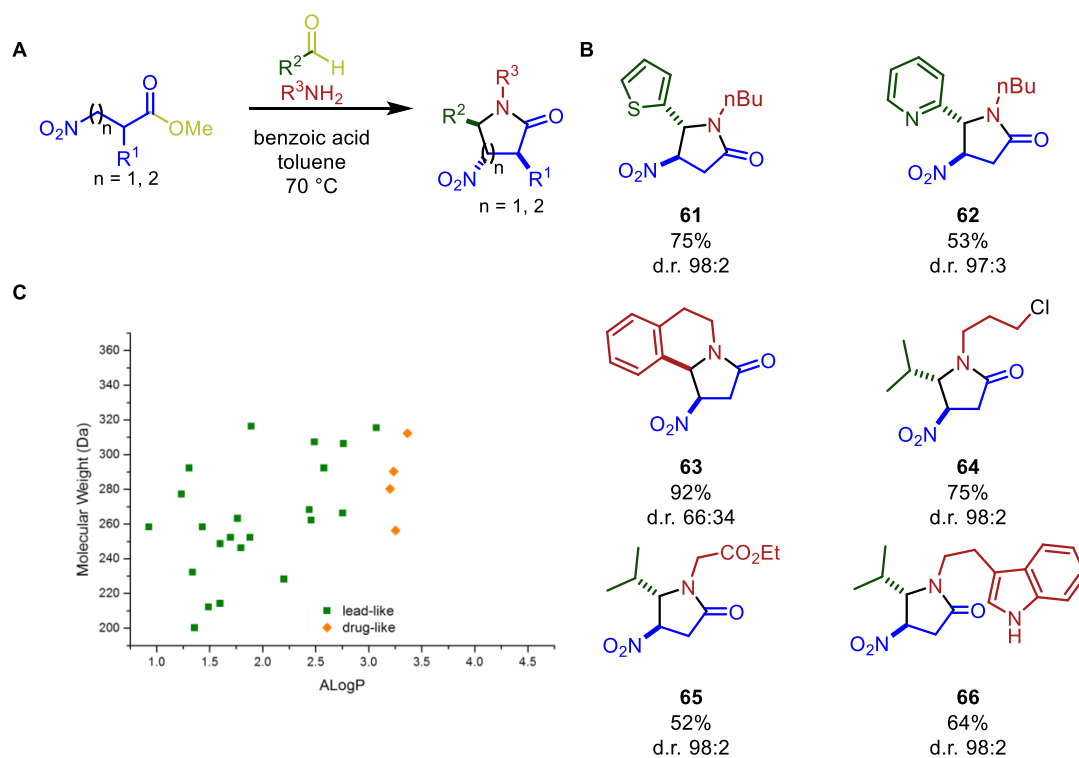


Figure 16: Panel A: Overview of the nitro-Mannich lactamisation developed by Dixon. Panel B: Selected examples of diverse pyrrolidones generated.⁶⁴ Panel C: Analysis of the physiochemical properties of these scaffolds reveal they occupy lead-like chemical space.

A plot of the physiochemical properties (Panel C) shows the majority of products obtained have physiochemical properties within lead-like chemical space. As seen with the work of Bode (Section 1.4.3.2) however, the only real limitation of this protocol is that the diversity of the subsequent library is reduced since a γ -lactam is found within the every compound in the library.

1.5 Project Outline

Traditionally within the Nelson group, DOS strategies implemented thus far have created libraries of compounds with unprecedented skeletal diversity (Section 1.4.1.3).^{48,49} However, the control of the physicochemical properties of the synthesised libraries has not been attempted, and as such they often display natural product-like or drug-like properties with high molecular weight and LogP (Section 1.4.2).

Recently, in collaboration with the Marsden group, efforts have been directed towards the synthesis of libraries possessing lead-like properties (Figure 17). The approach uses a connective reaction to give a highly functional cyclisation precursor. The cyclisation precursors generated are then subjected to a maximum of two cyclisation reactions to obtain scaffolds. This has been shown superbly with the iridium-catalysed allylic amination,⁶⁵ which has generated thirteen unique cyclisation precursors. (Figure 17, Panel A, selected example).

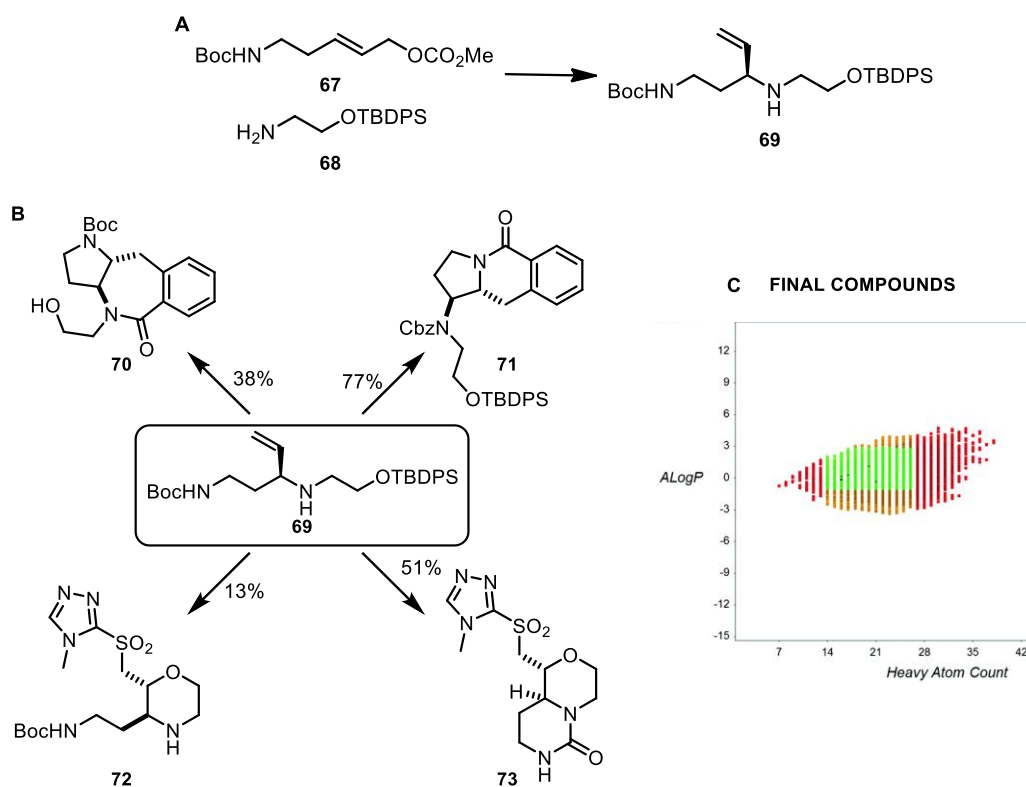


Figure 17: Panel A: An iridium-catalysed reaction between an amine and allylic carbonate. 13 cyclisation precursors synthesised.⁶⁵ Panel B: Selected lead-like scaffolds (**70-73**) prepared cyclisation precursor **69**.⁶⁵ Panel C: Distribution of the molecular properties of the virtual library. 59% of the compounds (green) survive successive filtering by molecular size ($14 \leq \text{number of heavy atoms} \leq 26$; failures shown in red) and lipophilicity ($-1 \leq \text{ALogPP} \leq 3$; failures shown in orange) and various structural filters; 0.27% of the compounds (shown in black) failed the structural filters.⁶⁵

Using a toolkit of just six cyclisation reactions a total of 52 diverse molecular scaffolds was synthesised from the thirteen precursors (Panel B, selected scaffolds). The compounds were then virtually decorated with a number of different medicinal chemistry capping groups and the molecular properties were analysed. By successive filtering, using the method described by Churcher (Section 1.2.3), and 59% of compounds were considered lead-like. (Panel C, Figure 17).

The aim of this project was to expand the number of connective reactions which could be used for the generation of lead-like chemical libraries (Figure 18). The connective reaction had to be tolerant of a variety of building blocks with diverse functional groups to permit different scaffold generating cyclisations. The scaffolds synthesised should also retain suitable functionality which would allow late stage decoration to give a library of compounds with suitable physiochemical properties to target broad regions of lead-like chemical space and thus demonstrate the potential of this strategy to underpin early-stage drug discovery. Once a potential connective reaction had been identified, a key outcome was generating a library of scaffolds.

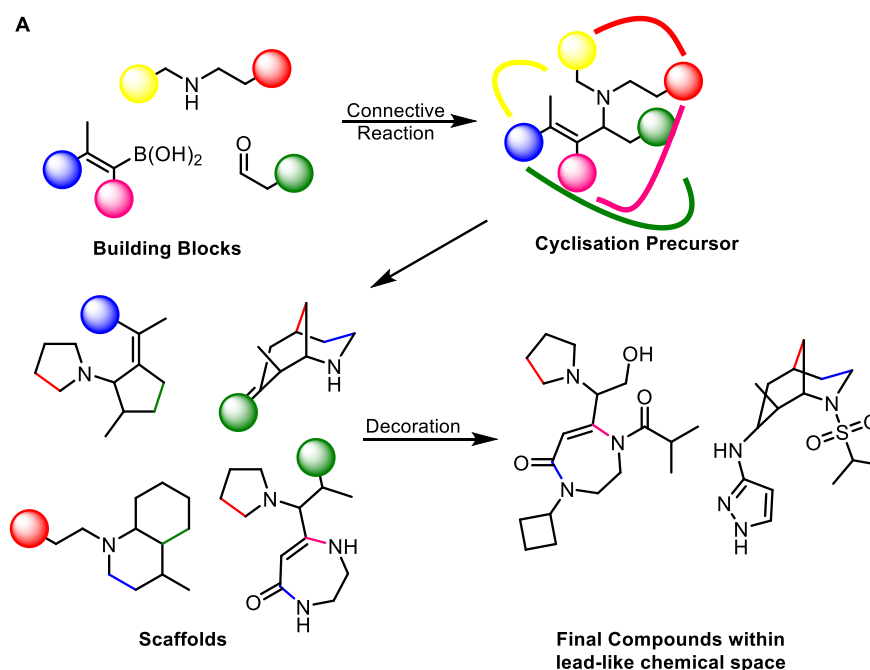


Figure 18: Common starting reagents with different functionalities are combined to give a cyclisation precursor; exposed to different reaction conditions yields diverse scaffolds which can then undergo decoration with traditional medicinal chemistry groups to give lead-like scaffolds. This approach is illustrated using the Petasis reaction.

1.6 Summary

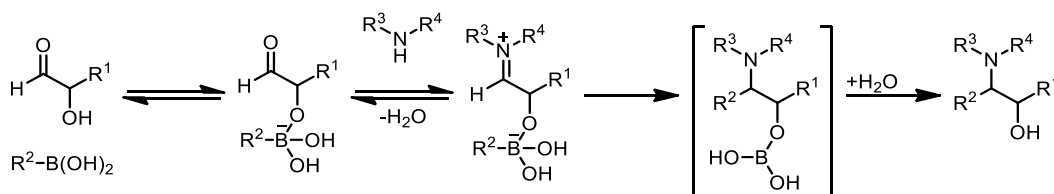
In order to improve productivity in the pharmaceutical sector, where traditionally up to 97% of lead compounds fail to make it to market, a new approach, lead-oriented synthesis was envisioned.⁷ A key challenge in lead-oriented synthesis is the identification of complementary and robust reactions with broad functional group compatibility that may be used to link building blocks. The project aimed to use a computational method to identify connective reactions which create scaffolds with the potential, after decoration, to yield lead-like small molecules. Once identified, a key challenge was optimise these reactions, and to exemplify them in the synthesis of lead-like scaffolds. If successful, it could greatly expand the relevant chemical space accessible to drug discovery programs targeting scaffolds which have traditionally been underrepresented in screening collections and could therefore significantly address the productivity within the pharmaceutical sector.

2 Investigation into suitability of the Petasis reaction for lead-oriented synthesis

This Chapter describes the potential of the Petasis borono-Mannich reaction (hereafter referred to as the Petasis reaction) as a connective reaction to support lead-oriented synthesis. A literature review is first given before a detailed description of the development of the Petasis reaction to support lead-oriented synthesis (LOS).

2.1 Petasis reaction: general characteristics

Multicomponent reactions are convergent reactions in which three or more starting materials react to form a product and are one of the best tools available to explore chemical space.⁶⁶⁻⁶⁸ With a large variety of commercially available materials and mild reaction conditions,⁶⁹⁻⁷³ the Petasis reaction (Scheme 5) could be suitable for synthesising a range of cyclisation precursors with the aim to explore lead-like chemical space.



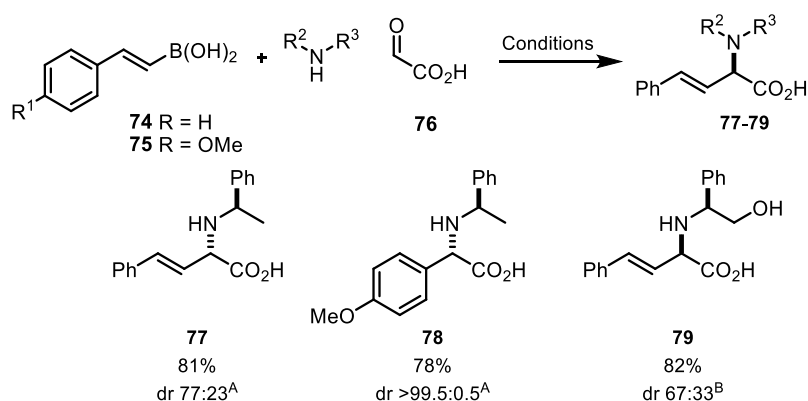
Scheme 5: Proposed mechanism for the Petasis reaction. The rate determining step is irreversible C-C bond formation when transferring R² moiety to imine.

The Petasis reaction exploits the combination of a α -hydroxyaldehyde, boron nucleophile and an amine to give a variety of differentially substituted amines (Scheme 5). While the mechanism is not fully understood, it has been proposed to involve the co-ordination of the boron nucleophile with the α -hydroxyl group of the aldehyde to give an electron rich boronate species.⁶⁷ Condensation with the amine gives an electrophilic iminium ion which facilitates the transfer of the R² component of the boronate. A final hydrolysis of boric acid provides substituted amine.

There are two major approaches to obtain enantio-enriched products from the Petasis reaction: the use of chiral substrates (e.g. chiral amines, boronic esters or

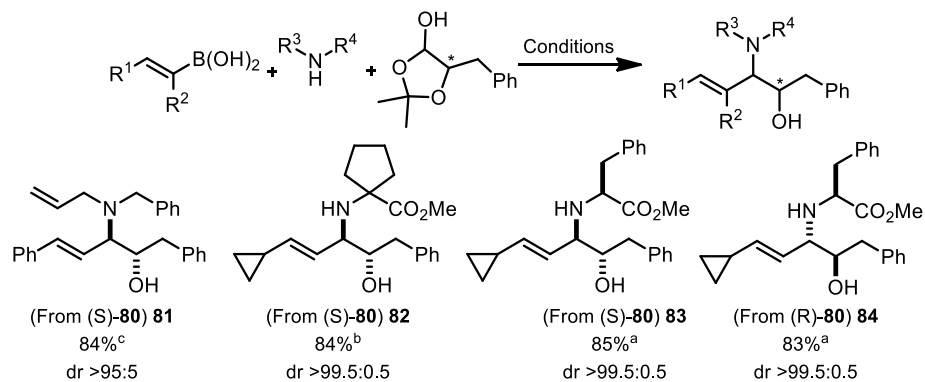
aldehydes) and organocatalysts.

The use of chiral amines has been accomplished successfully.^{70,74,75} Sterically unencumbered (*R*)-methylbenzylamine has been shown to yield amino acid **77** with modest diastereoselectivity (Scheme 6).⁷⁴ This methodology has been extended to electron rich aryl boron nucleophiles with slightly reduced selectivity (**78**).⁷⁶ With (*S*)-phenylglycinol, Petasis and co-workers reported improved diastereoselectivity to yield **79** with high diastereoselectivity (Scheme 6).⁷⁵



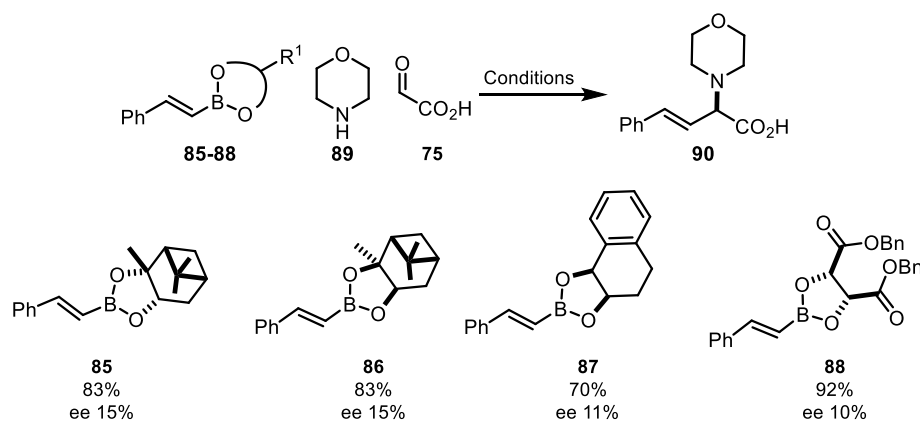
Scheme 6: Application of Petasis reaction for synthesis of enantio-enriched amino acids **77-79** via a chiral amine.⁷⁴⁻⁷⁶ Conditions: a) DCM, rt, 48 h; b) toluene, 25 °C, 30 h.

Schreiber and co-workers observed high diastereoselectivity in the Petasis reaction of a range of masked aldehydes (**81-84**, Scheme 7). This is shown with *N*-benzylallyl amine and 1,1-aminocyclopentane carboxylic acid giving anti amino alcohols **81** and **82** with high diastereocontrol.⁶⁹ The methodology has also been used with chiral amines; when using (*R*)-phenyl alanin emethyl ester, a different stereoisomer is obtained depending on the stereochemistry of the aldehyde (overriding the stereocontrol of amine) as shown with **83** and **84**.⁵⁸



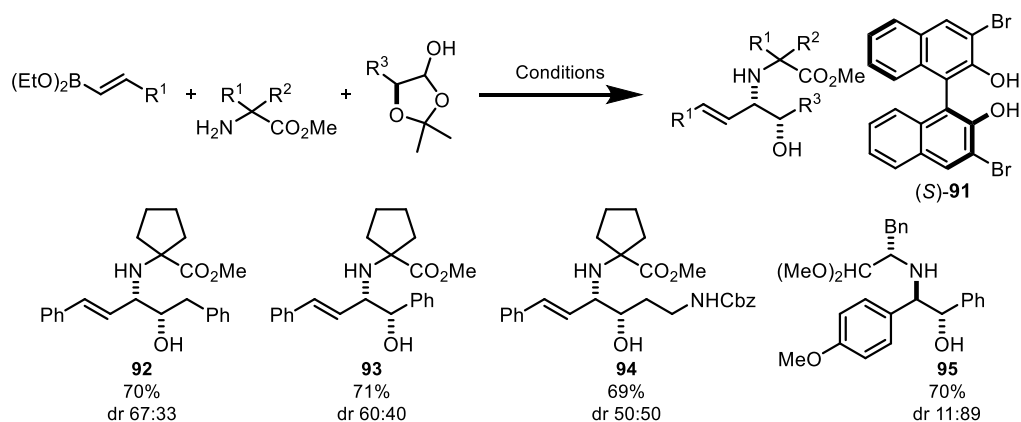
Scheme 7: Application of Petasis reaction for synthesis of diastereo-enriched amino acids **81-84** using a chiral aldehyde ((*S*)-**80** or (*R*)-**80**).^{58,69} *(*S*) or (*R*). Conditions: a) DCM-HFIP (90-10), rt; b) DCM-HFIP (75-25), rt; c) ethanol, rt.

The use of chiral boronic nucleophiles has received less attention, though Koolmeister and co-workers have successfully employed a range of chiral boronic esters **85-88** to give enantiomerically enriched amino acid **90** (Scheme 8).⁷⁷ The low levels of enantioselectivity excess observed could result from competing hydrolysis of the chiral moiety prior to the Petasis reaction.



Scheme 8: Application of Petasis reaction for synthesis of enantiomerically enriched amino acid **90** via chiral boronic esters.⁷⁷

Recently, organocatalysts has been successfully employed to yield the first Petasis reaction products with *syn* relative configuration. Schreiber and co-workers employed BINOL ligand (**91**) to overcome the inherent *anti*-diastereoselectivity of the Petasis reactants which increases the number of potential stereoisomers that can be produced. This is preliminary work but if successfully expanded, could overcome the major limitation of the Petasis reaction (**92-93**, Scheme 9) for library generation; namely that only one stereoisomer of product can be obtained. This is a complex reaction which is not fully selective as existing amine stereochemistry can override catalyst control giving *anti* isomer (e.g. with **95**).



Scheme 9: Application of Petasis reaction for synthesis of diastereo-enriched amino alcohols **92-95** via BINOL catalyst (*S*)-**91**.⁷⁸

2.1.1 Physiochemical properties of compounds within libraries generated from the Petasis reaction

The Petasis reaction has been shown, by the Neilsen and Schrieber groups, to be suitable for the synthesis of diverse heterocycles.^{71,78-82} However the properties of the compounds created, specifically the LogP and molecular weight, lie outside lead-like chemical space. Indeed when the properties of the Petasis products and the scaffolds generated within these libraries are calculated, over half the compounds (both cyclisation precursors and scaffolds) have physiochemical properties outside of lead-like chemical space (Figure 19).

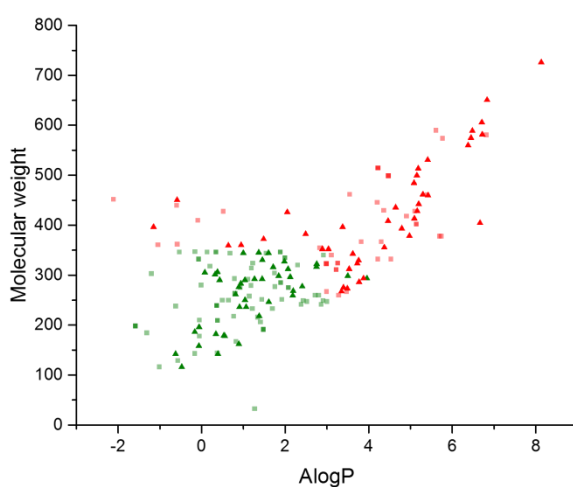


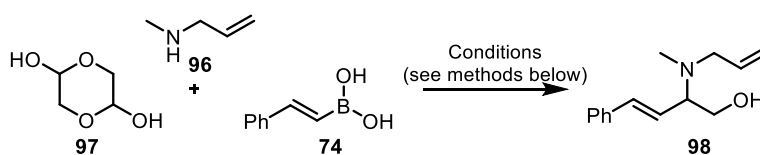
Figure 19: Analysis of the physiochemical properties of the products obtained from Petasis reaction campaigns.^{71,78-82} Note the high molecular weight which puts them beyond lead-like chemical space and indeed in some cases beyond drug like chemical space. Cyclisation precursors with physiochemical properties within lead-like chemical space (green triangles) and those outwith lead-like chemical space (red triangles). Scaffolds with physiochemical properties within lead-like chemical space (green squares) and those outwith lead-like chemical space (red squares).

In addition, many of cyclisation precursors and scaffolds have molecular weight and LogP approaching the limits of lead-like chemical space (275-350 Da and LogP of 2-3). If these were decorated to give screening compounds, their physiochemical properties are likely to be beyond the scope of LOS. It was envisioned that the Petasis reaction could be retooled to allow for the synthesis of cyclisation precursors (and in effect scaffolds) for the exploration of lead-like chemical space.

2.2 Reaction optimisation

Due to the conflicting reports in the literature, the first objective was to identify common reaction conditions before systematic investigation of different amines, boron nucleophiles and α -hydroxy aldehydes could be undertaken. Accordingly, *N*-methylallyl amine (**96**), *trans*-2-phenylvinylboronic acid (**74**) and glycolaldehyde (**97**) were used as model reactants for the Petasis reaction (Table 1).

Table 1: Initial exploration of the Petasis reaction.



Entry	Solvent	Temperature	Equivalent of 97	Yield (%)
1	Water	rt	1	64
2	Water	40 °C	1	Trace
3	Water	80 °C	1	-- [†]
4	Toluene	rt	1	64
5	THF	rt	1	65
6	DCE	rt	1	74
7	9:1 DCE-HFIP	rt	1	76 ^a
8	Water	rt	1	60 ^b
9	Water	rt	2	59 ^b
10	Water	rt	1.2	82 ^c
11*	DCE	rt	2	55 ^d
12	DCE	rt	1.2	84 ^c

Unless otherwise stated 1 eq. **96**, 0.5 eq. **97**, 1 eq. **74**, 48 h, rt ^a: 6 h; ^b: 1 eq. **96**; ^c: 0.6 eq. **96**; ^d: 1.2 eq. **96**; *4 Å MS; [†]No product observed by TLC or 500MHz ¹H NMR spectroscopy

It was found that even moderate heating led to significantly reduced isolated yields of the amino alcohol **98** (entries 1-3, Table 1). For the reaction at 40 °C, only a trace amount of product was observed in the crude reaction mixture by 500MHz ¹H NMR spectroscopy (entry 2). In addition no product was observed when the reaction was carried out at 80 °C (entry 3).

Next, a range of solvents was investigated: for example, polar and non-polar, protic and aprotic solvents (entries 1 and 4-6). Of these entries, most provided amino alcohol **98** in 60-65% yield. The maximum yield was obtained

in dichloroethane (74%, entry 6). It should be noted that the use of hexafluoroisopropanol (HFIP) as a co-solvent (entry 7) has been reported to significantly improve the yield of the Petasis reaction when using primary amines.^{67,69,83} Although having little effect on the yield when using amine **96** this solvent did significantly improve the rate of reaction, as a comparable yield was obtained in only six hours (entry 6).

Improved yields were obtained in when using **97** and **74** in slight excess (entries 10 and 12, greater than 80% yield). Having identified optimal reaction conditions, substrate scope was next explored.

2.3 Scope and limitations of the Petasis reaction.

2.3.1 Synthesis of starting materials

In order to investigate the functional group tolerance and scope of the Petasis reaction in the generation of cyclisation precursors a selection of amines, boronic nucleophiles and aldehydes was required (Figure 20). The boronic nucleophiles, glycolaldehyde (**97**) and all amines except for **105** and **107** were commercially available. The amine **107** was obtained from ethylene diamine (**111**) by treatment with di-*tert*-butyldicarbamate.⁸⁴ Reductive amination of **107** with benzaldehyde afforded the secondary amine **105** in modest yield (Figure 20).⁸⁵

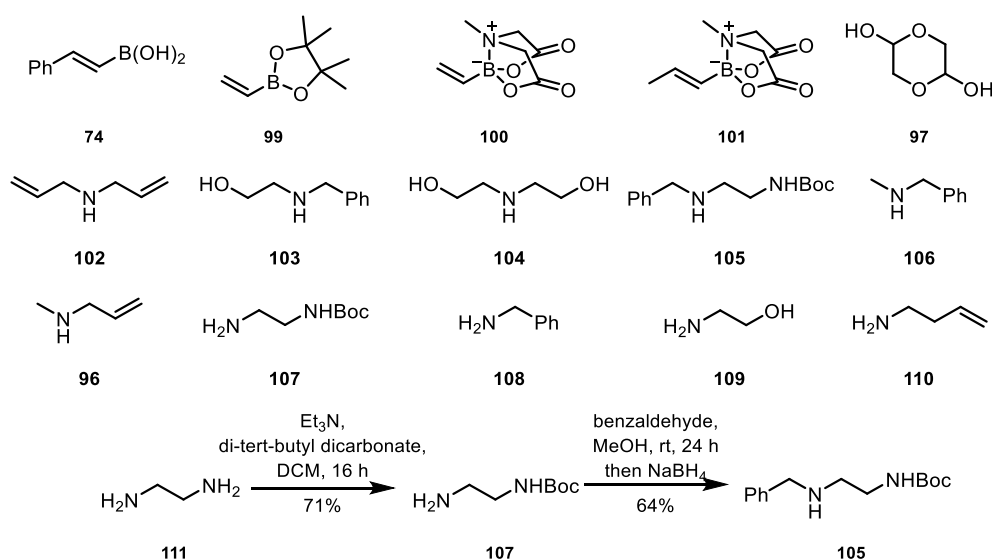
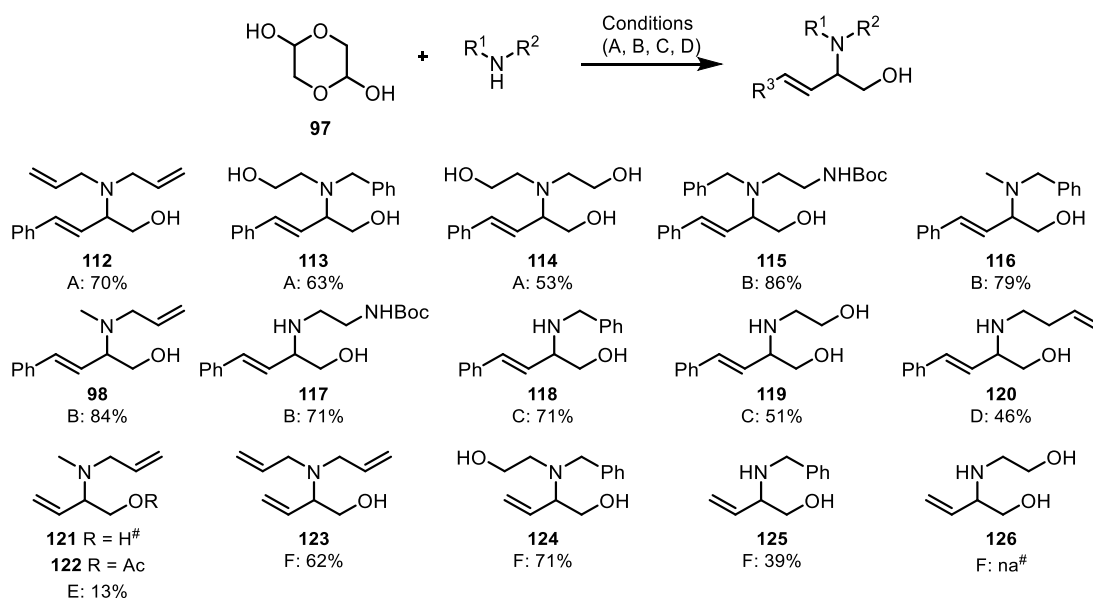


Figure 20: Boron nucleophiles, aldehydes and amines selected to investigate the functional group tolerance and reactivity in the Petasis reaction. Synthesis of amines **105** and **107**.

2.3.2 Synthesis of cyclisation precursors

With the relevant starting materials in hand, the next step was to synthesise the cyclisation precursors outlined in Table 2. In general, the reactions were successful; a broad range of amines and boron nucleophiles were successfully reacted with glycolaldehyde to give the corresponding amino alcohols (**112-126**). A series of secondary amines reacted efficiently under the reaction conditions providing amino alcohols **112-116** in yields ranging from 53-86%. Notably, with the exception of the diamine **111**, which required carbamate protection of the additional amine group, protecting groups were avoided.

Table 2: Scope of the Petasis reaction.



Unless otherwise stated: 1.2 eq. **97**, 1 eq. amine, A: 1.2 eq. **74**, H₂O, 48 h, rt; B: 1.2 eq. **74**, DCE, 48 h, rt; C: 1.2 eq. **74**, DCE:HFIP (90:10), 6 h, rt; D: 1.2 eq. **74**, KOH, H₂O, 48 h, rt; E: 1.2 eq. **99**, H₂O:THF (83:17), 48 h, rt then Ac₂O, Pyridine, 18 h, rt; F: 1.2 eq. **74**, H₂O:THF (83:17), 48 h, rt; #reaction did not proceed as judged by TLC and 500 MHz ¹H NMR Spectroscopy.

Yields with primary amines were significantly lower than those obtained with secondary amines with similar appendages (**117-120**). For example, *N*-methylallylamine provided the amino alcohol **98** in 84% yield, while butenylamine provided the amino alcohol **120** in 46% yield. Furthermore amino alcohol **114** was obtained in significantly greater yield than the amino alcohol obtained using *N*-ethanolamine (**119**, 53% versus 39%).

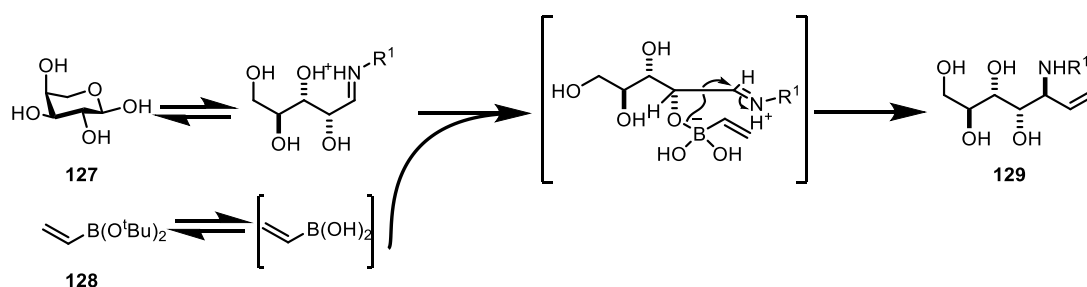
Polar functional groups were also found to give reduced yields, *N*-benzylethanolamine provided amino alcohol **113** in 63% yield, while bis(2-hydroxyethyl)amine (**104**) gave amino alcohol **114** in a 53% yield.

Vinyl boronic ester was unreactive under the conditions found to be effective for generation of the amino alcohol **121**. Additional boronate esters (**100-101**, Figure 20) were used but no conversion was observed with 500 MHz ¹H NMR spectroscopy or TLC. After extensive solvent screening, it was found that a THF-water solvent mixture was required to obtain sufficient reactivity (mass observed by LC-MS reaction monitoring and new alkene signals observed by 500 MHz ¹H NMR spectroscopy); however it was not possible to isolate **121**. Finally, after the Petasis reaction was complete, the reaction mixture was concentrated *in vacuo* then re-dissolved in pyridine, and acetic anhydride was added to the reaction mixture and stirred for 18 hours. This allowed, after purification, isolation of **122** in a 13% yield. Together, these results demonstrate the difficulties of using the vinylboronic ester and highlighted potential problems with isolation of these extremely polar amino alcohols.

The scope of additional amines was investigated (**123-126**) with the conditions developed for **100**. Secondary amines continued to provide greater yields of the corresponding amino alcohols compared with primary amines (**124** was obtained in a 71% yield while the amino alcohol **125** was obtained in a 39% yield). Amino alcohols which were more lipophilic were isolated in greater yields (**125** isolated in 39% yield but **126** was not isolated) as with *trans*-2-phenylvinylboronic acid products (**118** obtained in 71% while **119** was obtained in a 51% yield).

The yields obtained for the vinylboronic acid pinacol ester system continues to be lower than the corresponding *trans*-2-phenylvinylboronic acid system. This discrepancy in yields could be a result of reduced reactivity or poorer product isolation from the Petasis reaction as observed with reaction of *N*-methylallyl amine. This is particularly unsatisfactory since the products obtained from using the unsubstituted vinyl boron nucleophile are more attractive in library design; the phenyl group increases the LogP of the molecule by approximately two units⁸⁶ and many potential cyclisation reactions identified are unproven on 1,2-disubstituted alkenes.^{87,88}

A literature search revealed there is only one previous example of using an unsubstituted vinyl boronic acid ester in the Petasis reaction. Wong *et al.* used vinyl boronic acid dibutyl ester (**128**) as a reagent in a key step towards sialic acid derivatives (Scheme 10).⁸⁹ The ester was found to be unreactive in organic solvents but with a combination of ethanol and water, they obtained viable yields. They proposed that the ester is unreactive towards the Petasis reaction, but in the presence of water, the ester is hydrolysed to the more reactive vinyl boronic acid which then participates in the Petasis reaction to give **129**.



Scheme 10: Model proposed by Wong and co-workers to explain the reactivity of vinylboronic esters. The ester is first hydrolysed acid which is sufficiently reactive to participate in the Petasis reaction. Condition: EtOH-H₂O (80:20), 50 °C, 72 h, 55%. R = bis(4-methoxyphenyl)methyl

2.3.3 Factors influencing a diastereoselective Petasis reaction

With a working protocol for the Petasis reaction, priority was concentrated on controlling the stereochemical outcome of the reaction. As described in Section 2.1, the two approaches involve the use of a chiral reagent or organocatalysts. Given limited precedent in using organocatalysts, a selection of enantiomerically enriched amines and aldehydes were chosen (Figure 21).

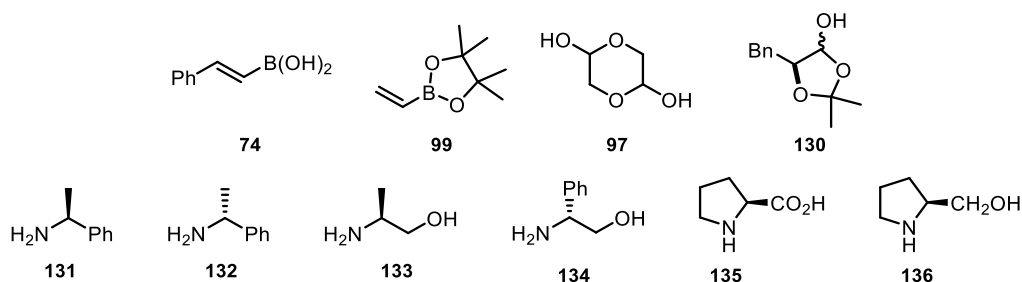
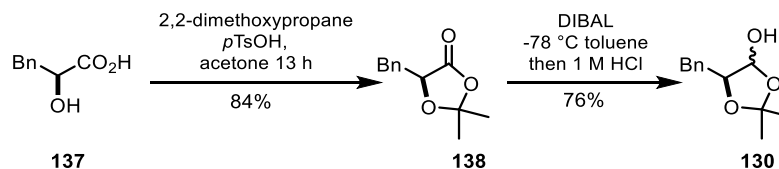


Figure 21: Boron nucleophiles, aldehydes and amines selected to investigate the requirements of a stereoselective Petasis reaction.

The boronic nucleophiles, glycolaldehyde (**97**) and all amines were commercially available. The masked α -hydroxyaldehyde **130** was obtained from acetonide formation of commercially available α -hydroxyacid **137**. Subsequent

reduction of the lactone (**138**) with diisobutyl aluminium hydride afforded lactol **130** (Scheme 11). With the relevant starting materials in hand, the diastereoselectivity of the Petasis reaction was explored.

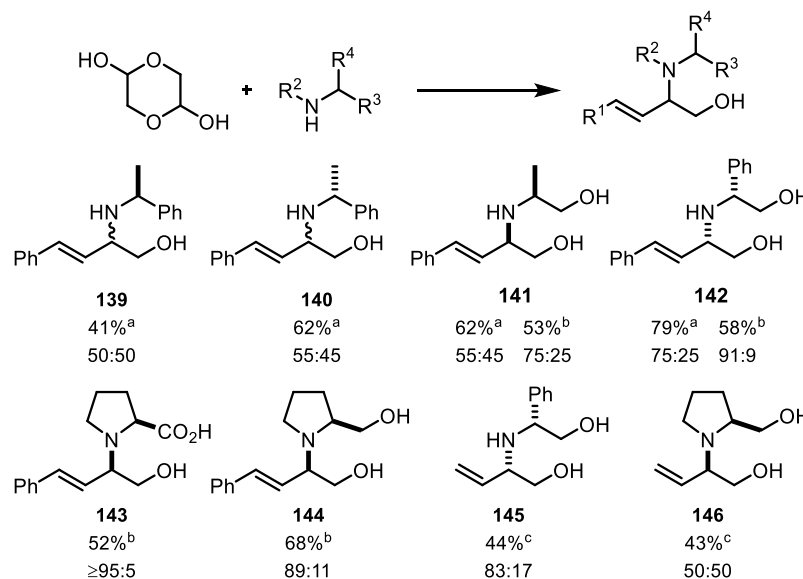


Scheme 11: Synthesis of lactol **130** from **137**.

2.3.3.1 Use of chiral amines

With the relevant starting materials in hand, the next step was to determine their selectivity in the synthesis of the cyclisation precursors summarised in Table 3. In general, amino alcohols afforded reasonable diastereoselectivity (greater than $\geq 75:25$) and the best selectivities were observed with phenyl vinyl boronic acid as the boron nucleophile.

Table 3: Investigation of factors required for the diastereoselective Petasis reaction.



Unless otherwise stated: 0.6 eq. **97**, 1 eq. amine, 48 h, rt; a) 1.2 eq. **74**, DCE; b) 1.2 eq. **74**, H₂O; c) 1.2 eq. **99**, DCE:HFIP (90:10); d) H₂O:THF (83:17);

Both (*R*)- and (*S*)-methylbenzylamine (**131** and **132**) failed to give any stereochemical control and a 50:50 diastereomeric ratio of products was obtained in each case (**139** and **140**). Both Petasis and Southwood have reported moderate levels of control (83:17 and 76:24 respectively) when (*S*)-Methylbenzylamine was used as

in auxiliary in the synthesis of amino acid **76**.^{75,74}

Choice of solvent was found to be crucially important in obtaining suitable selectivity. (2*S*)-2-Amino-1-propanol (**133**) was entirely unselective, giving a 55:45 mixture of diastereoisomers, when dichloroethane was the reaction solvent. However, switching the reaction solvent to water, a 75:25 ratio of diastereomeric products was obtained (as evidenced by 500 MHz ¹H NMR spectroscopy).

Given the proposed transition state, Figure 22, it is clear the steric clash between the methyl group and the styrenyl group of the boronic acid was insufficient to fully differentiate between the two possible diastereoisomers. The amino alcohol **145** (obtained from the Petasis reaction with (*R*)-2-amino-2-phenylethanol) resulted in an improved d.r. (75:25) with dichloroethane as the reaction solvent. As seen with (2*S*)-2-amino-1-propanol (**133**), greater selectivity was obtained (90:10) when water was used as the reaction solvent. The significant difference in selectivity is surprising, given that the stereocentre is remote from the stereogenic centre the expected transition state for the two amino alcohols was expected to be similar.

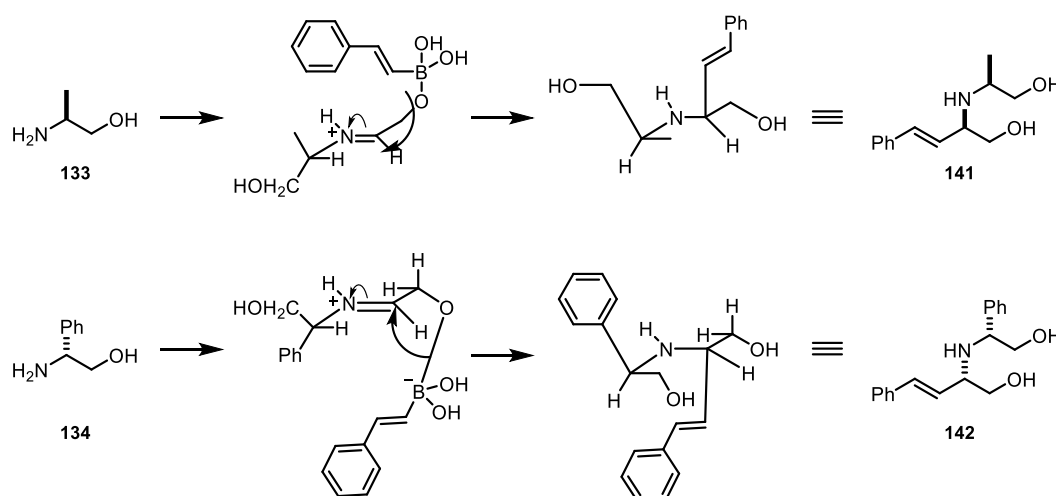


Figure 22: Proposed transition state for the synthesis of **141** and **142**.

Cyclic amines were found to be as efficient as acyclic secondary amines at controlling the stereochemistry of the reaction. The greatest diastereoselectivity was obtained with amino alcohols **143** and **144** obtained from L-proline and L-prolinol (d.r. $\geq 95:\leq 5$ and 90:10 respectively).

To investigate the differences in selectivity between the boronic nucleophiles, the two of the best performing amines, (2*R*)-2-amino-1-phenylethanol and L-prolinol were selected. In the case of (2*R*)-2-amino-1-phenylethanol, amino alcohol **144** was formed in reduced yield and selectivity (44% and d.r. 83:17). The selectivity with L-prolinol was completely lost, giving an equal mixture of diastereoisomers in a modest (43%) yield. The reduced diastereoselectivity observed *cf.* *trans*-2-phenylvinyl boronic acid is likely due to the decreased steric clash between the smaller vinyl group with the prolinol ring.

2.3.3.2 Use of chiral aldehyde

As mentioned previously (Section 2.1), chiral aldehydes have been used to good effect to control the outcome of the Petasis reaction. *N*-Methylallyl amine (**96**) and ethanol amine (**109**) were selected to investigate the stereocontrol exhibited by the protected aldehyde **130**.

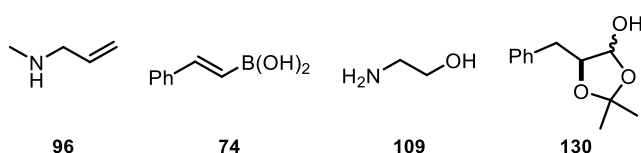


Figure 23: Secondary and primary amines **96** and **103** were chosen to investigate the stereochemical outcome of the Petasis reaction with aldehyde **130**.

With *N*-methylallyl amine, a single diastereoisomer was obtained, which is consistent with the reported literature (Figure 24).^{58,69} The selectivity observed is due to the aldehyde α -hydroxyl group being directly involved in the rate determining step. The proposed transition states for the two imines are shown in (Figure 24). The reduced 1,3-allylic strain in **TS2** ensures the anti diastereoisomer is the only product.

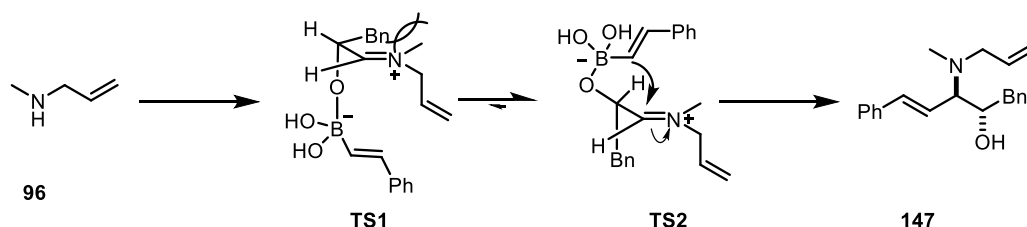


Figure 24: Diastereoselective transition state. The unfavourable 1,3-allylic strain is minimised in **B** yielding the anti diastereoisomer. Conditions: DCE-HFIP (90:10), rt, 30 h.

The reaction between that of **74**, ethanolamine (**109**) and **130** was unsuccessful. The amine (**109**) had previously given low yields when used with glycolaldehyde

and *trans*-phenylvinylboronic acid and had failed entirely when vinylboronic acid ester (**99**) was used. The reaction with ethanolamine, glyoxylic acid and *trans*-2-phenylvinylboronic acid (**74**) had also been previously attempted but as in this case, no reaction was observed when monitoring the reaction by TLC or LC-MS.

2.4 Design of cyclisation precursors from Petasis reaction

With a robust, stereoselective Petasis reaction protocol developed, the focus progressed to generating cyclisation precursors which would allow the synthesis of lead-like scaffolds. In total, six amines were chosen for the generation of cyclisation precursors (Figure 25).

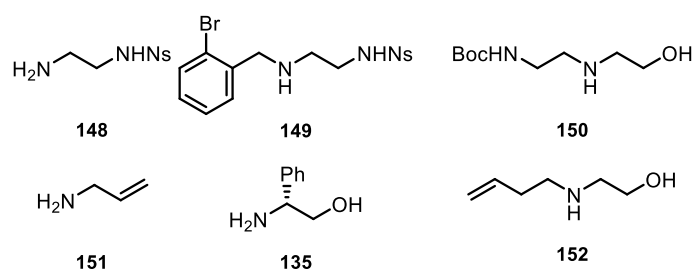
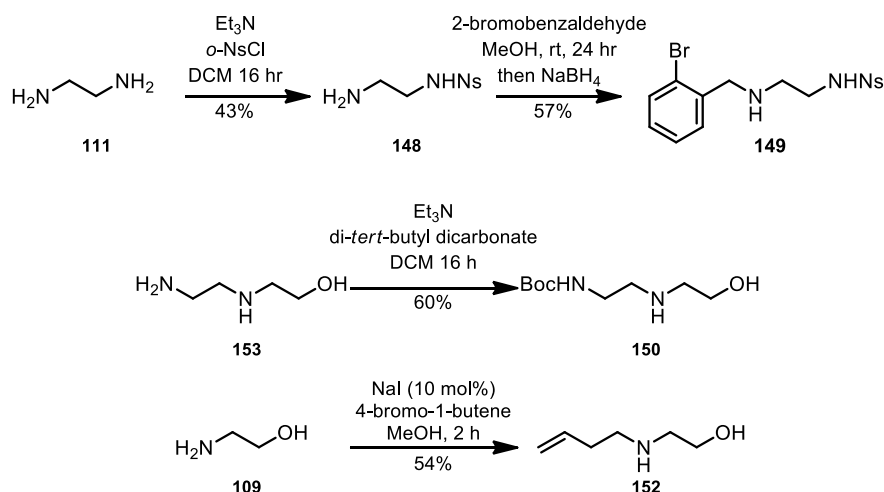


Figure 25: Amines selected to investigate the potential for the Petasis reaction to deliver scaffolds suitable for interrogating lead-like chemical space.

The amines were chosen based on a compromise between the observed reactivity in the scope and limitations of the Petasis reaction and a strong requirement to maintain the physiochemical properties. Thus primary amines **148**, **151** and **135** were chosen due to the success of related substrates and the potential to greatly increase the scaffold count by introducing a variety of different alkylating reagents. It had been found that secondary amines reacted more efficiently, thus **149**, **150** and **152** were chosen.

2.4.1 Synthesis of starting materials

Amine **149** was readily accessed via reductive amination of *ortho*-bromobenzaldehyde with *N*-nosyl-ethylenediamine (**148**) in modest yields (Scheme 12).⁹⁰ Diamine **153** was commercially available and protected as the carbamate **150** (Scheme 12). Finally ethanolamine (**109**) was coupled with 4-bromo-1-butene in the presence of sodium iodide to give amino alcohol **152**.⁹¹



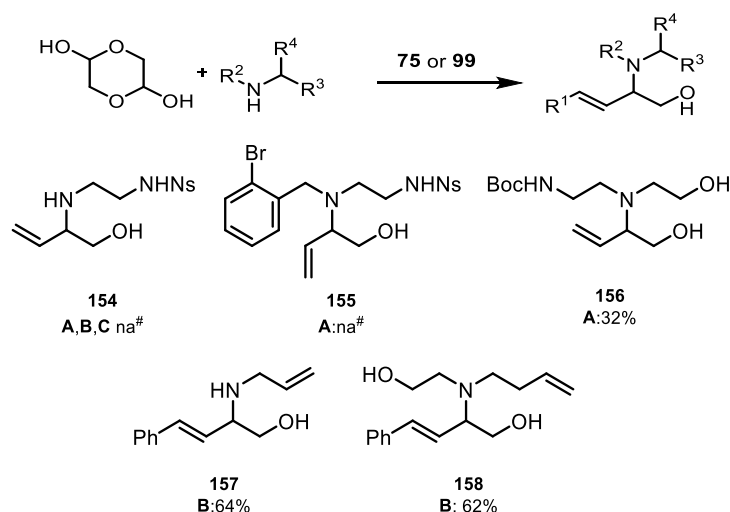
Scheme 12: Synthesis of amines **149**, **150** and **152**.

2.4.2 Synthesis of cyclisation precursors

With the relevant starting materials in hand, they were next reacted under conditions previously optimised (Section 2.2). Disappointingly amine (**148**) was unsuccessful in the optimised conditions. In each attempt, starting materials was recovered. Given the reduced reactivity for primary amines, coupled with the reduced reactivity of vinyl boronic ester (*cf.* *trans*-phenylvinylboronic acid), this substrate was expected to be difficult and subsequently deprioritised in favour of the remain amines.

Surprisingly amine **149** failed to give the tertiary amino alcohol **155**. This was particularly surprising given the success of the model system. The crude 500 MHz ¹H NMR spectrum did show diagnostic signals at 5.6 and 5.1ppm which correspond with equivalent signals observed with other cyclisation precursors; however the major component was unreacted amine and vinylboronic acid MIDA ester. Given the limited utility of the precursor, it was decided to prioritise another cyclisation precursor.

Table 4: Attempted synthesis of cyclisation precursors from Petasis reaction.



Unless otherwise stated: 0.6 eq. **97**, 1.2 eq. boron nucleophile, 1 eq. amine, 48 h, rt A: H₂O–THF (84:16), B: DCE:HFIP (90:10), 6 h, rt; C: H₂O–THF (83:17), 48 h, Et₃N (1.5 eq.) rt; #reaction did not proceed as judged by TLC or 500 MHz ¹H NMR spectroscopy. B: 40 °C

Amino alcohol (**150**) gave the expected cyclisation precursors (**156**) in a 32% yield. Allyl amine (**151**) and butenylethanamine (**152**) gave the corresponding amino alcohols (**157** and **158**) in yields exceeding 60%. The use of *trans*-phenylvinylboronic acid greatly increased the yield and viability of the reaction.

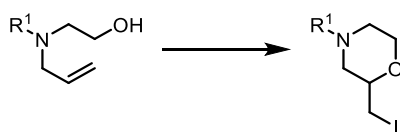
2.5 Utilising cyclisation precursors in subsequent cyclisation reactions

With the chosen cyclisation precursors in hand we next looked at cyclisation reactions. This Section outlines the attempts with three cyclisation reactions; iodine mediated etherification^{87,92}, carbodiimidazole coupling^{93–95} and ring closing metathesis.^{96–98}

2.5.1 Iodine-mediated cyclisation

Iodoetherification has been shown to be an efficient method for the synthesis of morpholine rings.^{87,92} Cyclisation precursors **113**, **124** and **146** were selected to determine if this was a suitable reaction. Accordingly molecular iodine was added to a solution of amino alcohol **113** and heated to 65 °C (Table 5, entry 1). However, only starting materials were observed. The solvent was changed and amino alcohol re-subjected to the reaction conditions however after 18 hours only starting material was observed by LC-MS and TLC (entry 2). Heating the reaction at reflux for an additional day still led to recovered starting material (entry 2).

Table 5: Studies towards iodine mediated cyclisation

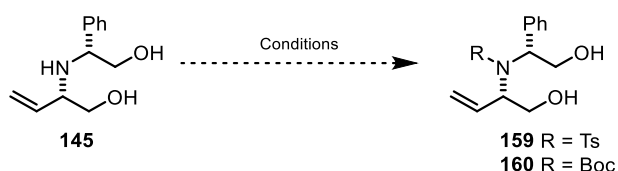


Entry	Substrate	Conditions	Outcome
1		I ₂ , 65 °C, MeCN	NR [#]
2	113	I ₂ , rt, THF, 18 hr then 65 °C, 18 hr	NR [#]
3		I ₂ , rt, THF then 65 °C, 18 hr	NR [#]
4		I ₂ , 65 °C, MeCN	NR [#]
5	146	NIS, Et ₃ N, MeCN, 65 °C, 18 hr.	NR [#]
6	146	NIS, TFA, MeCN, 65 °C, 18 hr.	NR [#]

[#]reaction did not proceed as judged by LC-MS (M+H for SM observed) or 500 MHz ¹H NMR spectroscopy (only evidence of starting material).

Given the precedent for the reaction used a monosubstituted alkene, amino alcohols **124** and **146** were selected (entries 3 and 4). However as with **113**, only starting material was observed. A different iodine source (entry 5) and reaction conditions were attempted, including stirring the amino alcohol **146** in TFA (an attempt to form the salt and quench the basic nitrogen), but suitable conditions were not obtained.

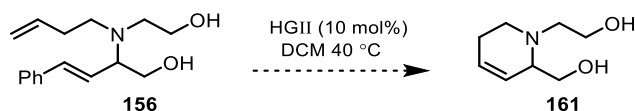
In addition to the precedent using only monosubstituted alkenes, basic amines were not used as substrates. Given the problems encountered with tertiary amine substrates, it was decided to use amino alcohol **145** and make the tosyl protected derivative (Scheme 13). However a complex mixture was obtained (as evidenced by TLC) and the expected mass was not observed by LC-MS. Given it was a significantly hindered secondary amine; it was possible either alcohols were tosylated and thus making them prone to elimination. Alternative protecting group such as *tert*-butyl carbamate returned unreacted starting materials, even after the addition of many equivalents, prolonged reaction times and heating.



Scheme 13: PG manipulation of cyclisation precursor **145**. Conditions: R = Ts; Et₃N, 4-TsCl, DCM, 16 h. PG = Boc; Et₃N, di-*tert*-butyl dicarbonate (1.5 eq. – 5 eq.), DCM, rt to 40 °C, 16-48 h.

2.5.2 Ring closing metathesis

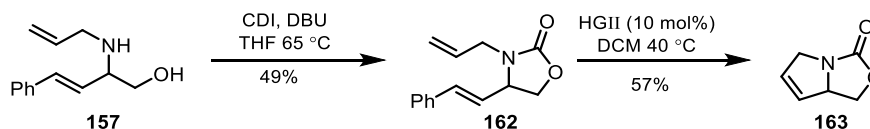
A ring closing metathesis (RCM), to give the tetrahydropyridine core, was attempted on amino alcohol **156** (Scheme 14). However only starting materials was recovered. Substrates containing a high density of heteroatoms have previously been shown to form chelates with the Ru catalyst with the Lewis-basic sites.⁹⁹ To circumvent this problem, the hydroxyl groups could have been protected however the steps required to attached, perform the RCM and subsequent removal would significantly reduce the synthetic utility of the process. This was especially true given that only a single scaffold could have been made.



Scheme 14: Attempted ring closing metathesis with amino alcohol **161**.

2.5.3 Carbodiimidazole coupling

Given the significant problems encountered with tertiary amine substrates for subsequent cyclisations, it was found that coupling of the secondary amine and primary alcohol group with carbodiimidazole furnished **162** in 49% yield (Scheme 15). This substrate was subjected to ring closing metathesis conditions attempted with **156** and gratifyingly fused bicyclic **163** was obtained (Scheme 15).



Scheme 15: Synthesis of bicyclic urea **163** from amino alcohol **157**.

Although the product only has one site for decoration, the success does suggest that the difficulties encountered with the use of the Petasis reaction was the presence of the basic nitrogen. Given the requirement of the amine for the Petasis reaction to proceed, and given the fact secondary amines reacted more efficiently, this is a limitation that was not possible to overcome.

2.6 Conclusions and summary

This chapter has detailed the significant challenges which were encountered when attempting to use the Petasis reaction for LOS. It was found that each building block required an optimised set of reaction conditions which meant it is less suitable for library design. The development of a diastereoselective protocol was detailed and it was found that the hydroxyl group of the amine and a large α -substituent was essential for good diastereo-stereocontrol. Ultimately however, the cyclisation precursors generated were unsuitable for further elaboration to give a diverse lead-like chemical library.

3 Development of methodology to determine the suitability of a reaction to support lead-oriented synthesis

This Chapter describes the use of a computation protocol to direct the selection of a new connective reaction to support lead-oriented synthesis. The computational approach was developed within the group by Dr Richard Doveston and has been used to direct the synthesis of over 50 lead-like molecular scaffolds.⁶⁵ An overview of the approach, including a description of the computational tool is given in Section 3.1. A detailed description of the process used to robustly compare different connective reactions is given in Section 3.2 and the process used to select a new connective reaction is described (Section 3.3).

3.1 Protocol to assess the lead-likeness of molecular scaffolds.

Previously within the group, Pipeline Pilot (Accelrys®) and Vortex (Dotmatics) software has been used to produce a robust tool for directing synthetic programmes towards the synthesis of novel lead-like scaffolds.⁶⁵ An overview of the functionality of the protocol is given in Figure 26. The protocols were designed to perform:

1. Enumeration of virtual compound libraries.
2. Novelty assessment of molecular scaffolds.
3. Lead-likeness assessment of physical properties of final compounds.

3.1.1 Enumeration of virtual compound libraries.

A virtual library of compounds was created by means of a three-step process. A connective reaction of interest, such as iridium-catalysed allylic amination^{100–106} was identified; the reactants specified and all possible product outcomes enumerated (step 1, Figure 26). The cyclisation precursors were then subjected up to two virtual cyclisation reactions (for a complete list of the cyclisation reactions used within the enumeration see Appendix 1 Figure 47) to generate a set of scaffolds (step 2, Figure 26). The number of scaffolds derived from a single cyclisation precursor was calculated and referred to as scaffold frequency.

These scaffolds were subsequently decorated virtually (at up to two sites) with a standard set of capping groups (for a complete list of capping groups see Appendix 2 Figure 50) to create the virtual library of final compounds (step 3, Figure 26).

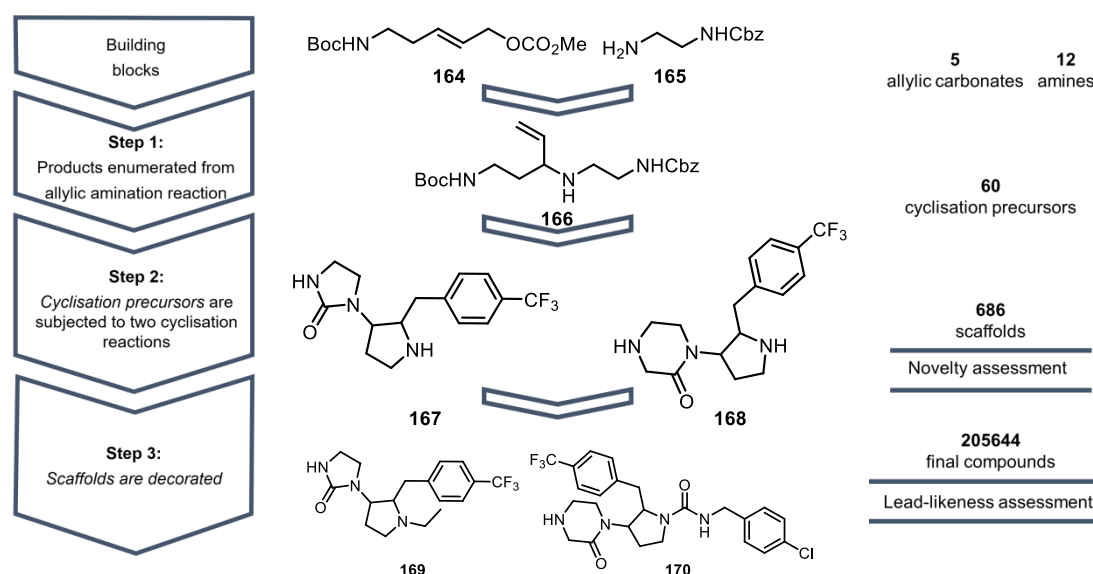


Figure 26: The computational protocol developed within the group. Step 1: Cyclisation precursors are generated from combinations of available building blocks. Step 2: Up to two cyclisation events generate a set of scaffolds which are then assessed for novelty. Step 3: Scaffolds were then decorated virtually using a standard set of capping groups to give final compounds which are assessed for lead-likeness.

3.1.2 Novelty assessment of molecular scaffolds.

Novelty was assessed at the scaffold level by way of a substructure count against a reference database (Figure 27). Murcko fragments¹⁰⁷ without α -attachments are generated for each scaffold and these are compared with Murcko fragments without α -attachments generated from a random 2% of compounds (~150,000 compounds) from the ZINC database of commercially available compounds.¹⁰⁸ A penalty is incurred for the scaffold each time a match within the ZINC database is found.

In addition, Murcko fragments with α -attachments are generated and these are also compared with the same randomly selected compounds from the ZINC database. With these two scores, it is possible to investigate both skeletal novelty (is the specific known without substituents) and appendage novelty (is the scaffold substitution pattern of the scaffold known).

Novelty assessment of scaffolds against ZINC database

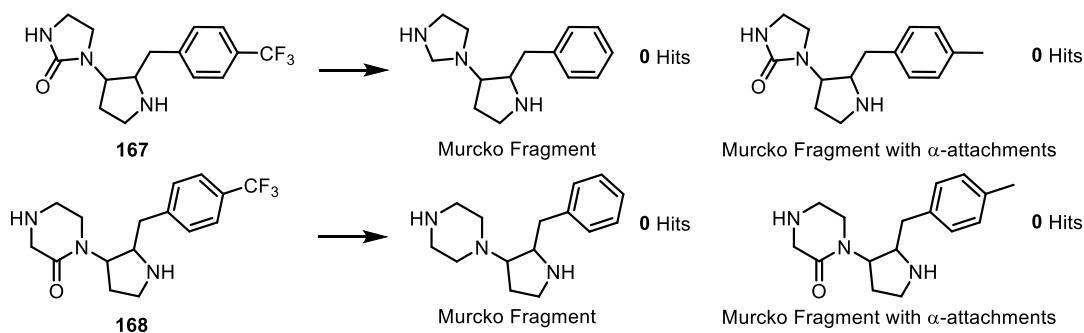


Figure 27: Novelty assessment. Two fragments are generated for each scaffold and compared with the ZINC database. The approach is illustrated for two exemplar scaffolds

3.1.3 Lead-likeness assessment of physical properties of final compounds.

Churcher *et al.* defined lead-like chemical space in their seminal paper.⁷ The properties (Section 1.2.3) include molecular size, lipophilicity, the potential for biological interaction and the presence of any un-desirable functional groups.⁷ A lead-likeness penalty scoring system has been devised; a penalty is incurred for each physical property which lies outwith lead-like chemical space (Figure 28). The further from those idealised values, the greater the penalty incurred.

The lead-likeness penalty was assessed for each final compound generated and these scores were combined to give a mean lead-likeness penalty score for each scaffold. As demonstrated in Figure 28 **169** has just one additional heavy atom compared with idealised values so incurs a small penalty for molecular weight but all remaining properties are within limits so it has an overall leadlikeness penalty of 1.

In contrast **170** has a higher molecular weight (32 heavy atoms) and a higher log P (3.8) so it incurs significant penalty in these areas and has a leadlikeness penalty score of 5. This would not be prioritised for synthesis. The scoring system implemented is outlined in Table 6, was based upon the optimal values previously defined and subsequent discussion with the authors.⁷

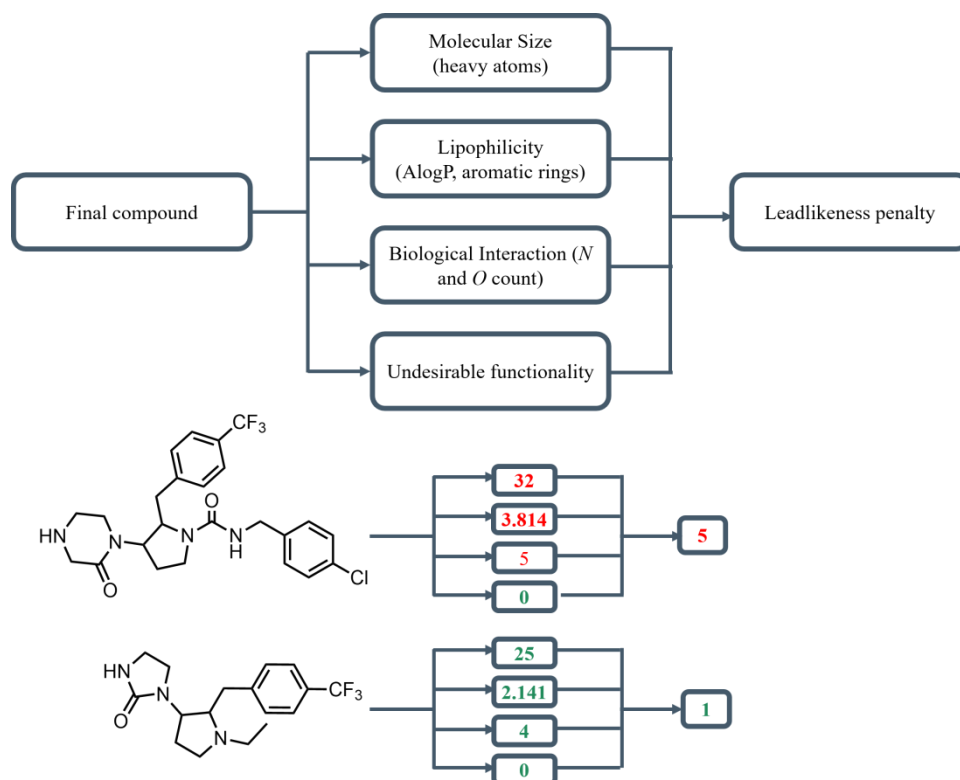


Figure 28: Lead-likeness assessment. The scoring system implemented is outlined in for the heavy atom count. For the full scoring penalty system see Appendix 1-4.

Property (measure)	Property Value	Property Score
Molecular size (heavy atoms)	17-24	0
	25, 16	1
	26, 15	2
	≥27-≤14	3
Lipophilicity (AlogP)	-1.0 - +3.0	0
	>3.0 and <-1.0	1
	>3.5 and <-1.5	2
	>4.0 and <-2.0	3
Number aromatic rings	1, 2	0
	0, 3	1
	4	2
	5	3
Biological Interaction (sum of N and O atoms)	<4	2
Undesirable Functionality (any substructure hit)*	n/a	5

*Functional groups penalised: Alkyl halide, Acyl halide, Aldehyde, Anhydride, Diazo, Dicarboxyl, Disulphide, Ester, Hydrazine, Isocyanate, Isothiocyanate, Michael acceptor, Peroxide, Quaternary ammonium

Table 6: The full scoring system used in generating a lead-likeness penalty

3.2 Evaluation of Potential Reaction

Before the Pipeline Pilot protocol could be utilised, the expected functional group tolerance, yields, diastereo- and enantioselectivity were thoroughly evaluated. With this information in hand, a selection of simple building blocks was then selected on the basis of the precedent for the potential connective reaction investigated and a virtual library was enumerated.

The lead-likeness penalty data was then examined for each reaction. For each scaffold, the number of compounds that can be derived and their average leadlikeness penalties are shown. In total, five potential reactions were evaluated for their applicability towards LOS

- 1) β -Lactam Synthesis (Section 3.2.1)
- 2) C-H Insertion (Section 3.2.2)
- 3) SOMO-Activation (Section 3.2.3)
- 4) Nucleophilic opening of cyclic sulfamidates (Section 0)
- 5) nitro-Mannich reaction (Section 3.2.5)

3.2.1 Evaluation of β -Lactam Synthesis to support LOS

A possible route towards cyclisation precursors considered was β -lactam synthesis (Kinugasa¹⁰⁹⁻¹¹¹ or Staudinger reaction¹¹²⁻¹¹⁵) followed by subsequent lactam opening with various reagents (Panel A, Figure 29). A virtual library was created using the protocol outlined above. For computational simplicity, 8 ketenes and 5 imines were used in the enumeration but these represent building blocks for both connective reactions (Panel B, Figure 29). In total 120 cyclisation precursors (lactam opening using 3 different reagents) and over 97,000 virtual final compounds were generated (Panel C, Figure 29).

Analysis of the enumerated library revealed that the majority of the scaffolds generated had a mean scaffold lead-likeness penalty greater than three (only 14% of final compounds generated had a lead-likeness penalty <3.2). Furthermore only 233 scaffolds were generated from the cyclisation precursors demonstrating poor synthetic economy.

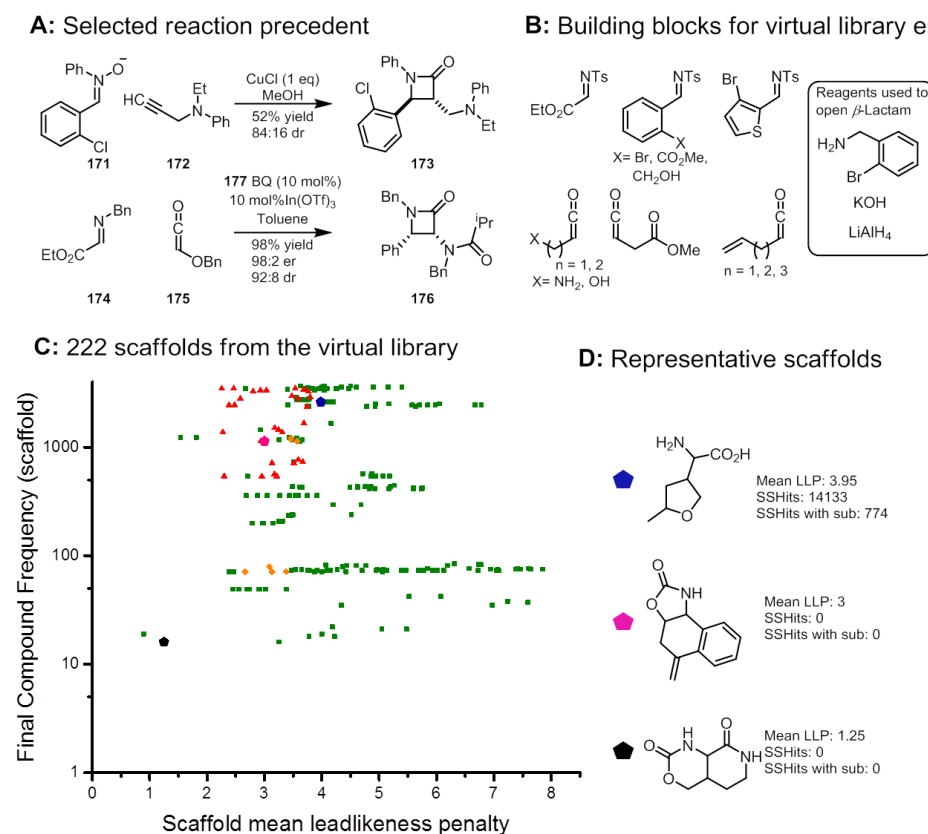


Figure 29: Panel A: Two representative examples of β -lactam synthesis. Panel B: The library of 5 imines, 8 ketenes and 3 ring opening reagents used in the virtual library enumeration. Panel C: Output for virtual library created, plot of scaffold frequency (total number of compounds generated from a single scaffold) vs the lead-likeness penalty. Highlighted area represents the most valuable area. Panel D: Representative scaffolds generated *via* library enumeration.

3.2.2 Evaluation of C-H Insertion to support LOS

Carbenoid insertion into C-H bonds α to heteroatoms has been studied extensively.^{116–124} As such they could provide cyclisation precursors with a desirable motif; namely four variable functional groups which could be reliably programmed (Panel A, Figure 30). A virtual library of 6 diazo compounds and 15 amine and alcohol coupling partners (Panel B, Figure 30) used to give 90 cyclisation precursors and over 472,000 virtual final compounds were generated (Panel C, Figure 30).

Subsequent analysis of the enumerated library revealed that the mean lead-likeness penalty was 3.66 (50% of all final compounds generated within the library had a lead-likeness penalty <3.2). Low novelty scores were obtained when scaffolds were compared with ZINC database (high degree of skeletal novelty) which established this as a promising connective reaction.

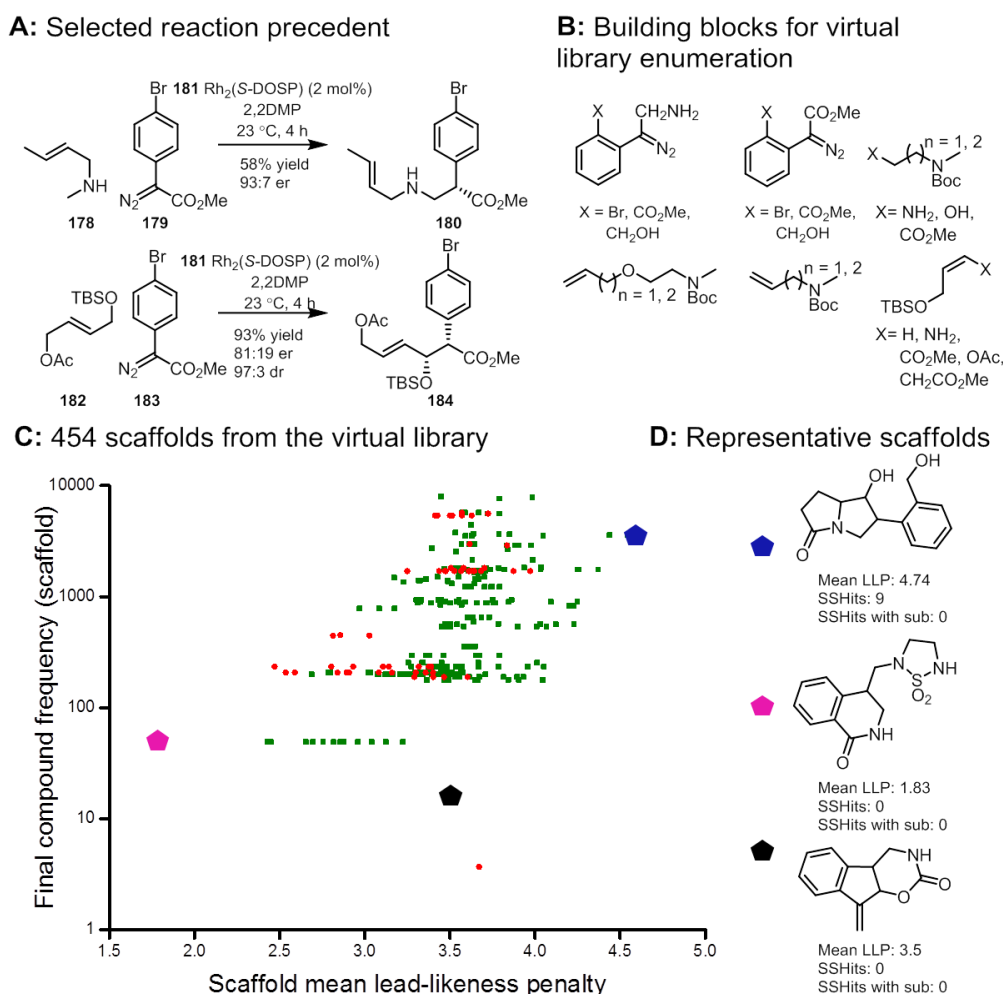


Figure 30: Panel A: Two representative of CH insertion into bonds α to heteroatoms. Panel B: The library of 6 diazo compounds and 15 amine and alcohol reagents used in the virtual library enumeration. Panel C: Output for virtual library created, plot of scaffold frequency (total number of compounds generated from a single scaffold) vs the lead-likeness penalty. Highlighted area represents the most valuable area. Panel D: Representative scaffolds generated *via* library enumeration.

3.2.3 Evaluation of SOMO-Activation to support LOS

SOMO-Activation, popularised by MacMillan^{125–129}, is a further potential connective reaction. High levels of enantioselectivity had been demonstrated and a high number of suitable starting materials could readily be obtained (Panel A, Figure 31).^{125–129} A virtual library of 6 SOMO donors and 11 SOMO acceptors (Panel B, Figure 31) was used to create 55 cyclisation precursors with over 748,000 virtual final compounds were generated (Panel C, Figure 31).

Following analysis of the enumerated library revealed a reasonable portion of scaffolds generated had a mean scaffold lead-likeness penalty less than three (50%

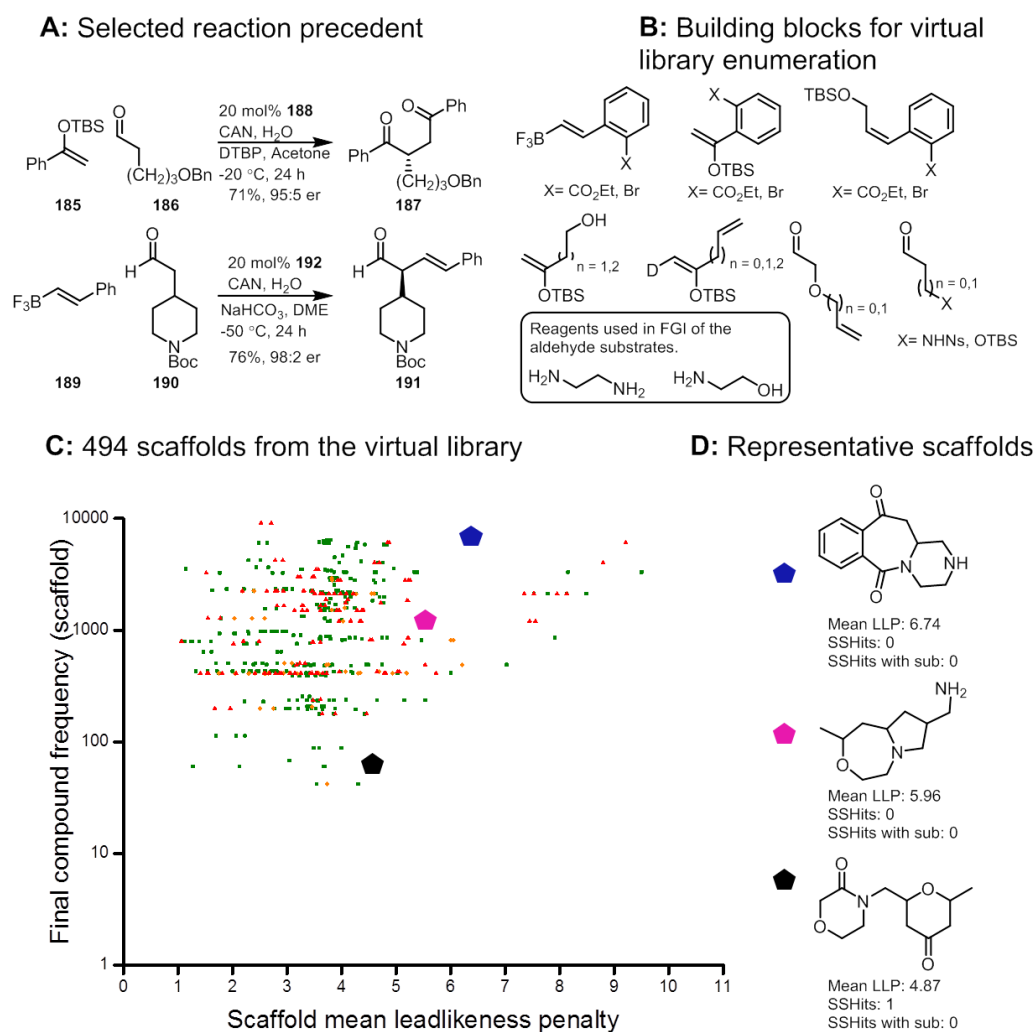


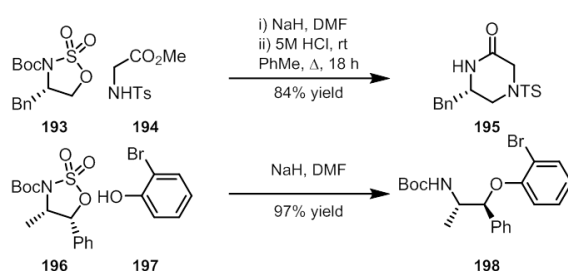
Figure 31: Panel A: Two representative examples of the SOMO activation. Panel B: The library of 11 SOMO acceptors and 6 SOMO donors used in the virtual library enumeration. Panel C: Output for virtual library created, plot of scaffold frequency (total number of compounds generated from a single scaffold) vs the lead-likeness penalty. Highlighted area represents the most valuable area. Panel D: Representative scaffolds generated *via* library enumeration.

of final compounds generated within the library had a lead-likeness penalty <3.2). However high novelty scores were observed across the majority of the library (Panel C, Figure 31) indicating low appendage novelty and skeletal novelty. In addition there were concerns over adequate diastereoselective control of the reaction.^{125–129}

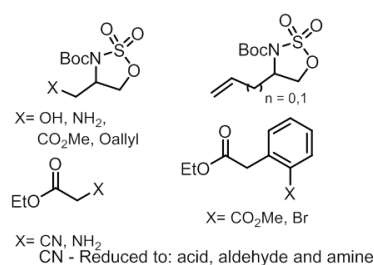
3.2.4 Evaluation of nucleophilic opening of cyclic sulfamidates to support LOS

Cyclic sulfamidates are versatile electrophilic reagents.^{130–136} They have been shown to undergo a facile, regiospecific nucleophilic substitution at the *O*-bearing centre (Panel A, Figure 32), yielding a valuable cyclisation precursor with the potential to vary each functional group.^{130–136} A virtual library of 6 cyclic sulfamidates and 4 nucleophiles (Panel B, Figure 32), gave 36 cyclisation precursors which resulted in over 459,000 virtual final were compounds (Panel C, Figure 32).

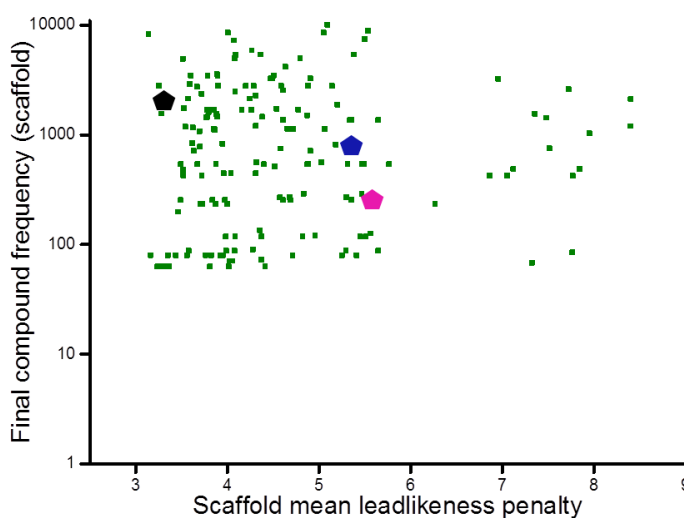
A: Selected reaction precedent



B: Building blocks for virtual library enumeration



C: 222 scaffolds from the virtual library



D: Representative scaffolds

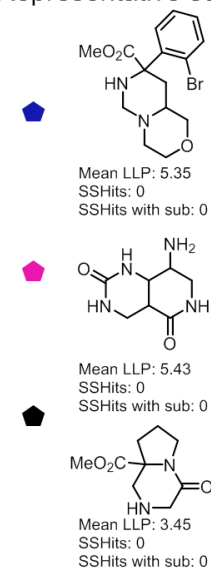


Figure 32: Panel A: Two representative examples of nucleophilic opening of cyclic sulfamidates. Panel B: The library of 6 cyclic sulfamidates and 4 nucleophile used in the virtual library enumeration. Panel C: Output for virtual library created, plot of scaffold frequency (total number of compounds generated from a single scaffold) vs the lead-likeness penalty. Highlighted area represents the most valuable area. Panel D: Representative scaffolds generated *via* library enumeration.

Resulting analysis of the virtual library contained very novel scaffolds as there are no substructure hits against the ZINC database. The scaffolds generated have a mean lead-likeness penalty >3, which may be attributed to the high number of

diversification sites (39% of all final compounds have a lead-likeness <3.2). However, there is poor stereocontrol when nucleophiles such as enolates are used (synthetically more attractive nucleophiles since a lactam would not be present in every compound), which make this connective reaction less suitable for LOS.

3.2.5 Evaluation of nitro-Mannich reaction to support LOS

The addition of a nitro reagent to imines is a reaction which gives access to 1,2-diamines upon reduction of the nitro functional group.¹³⁷ This powerful transformation has been studied extensively and with judicious choice of catalyst potentially all four stereoisomers of cyclisation precursors could be generated (Panel A, Figure 33).^{138–146} A virtual library, 10 imines and 7 nitro-components (Panel B, Figure 33) was used to give 70 cyclisation precursors with over 450,000 virtual final compounds generated (Panel C, Figure 33).

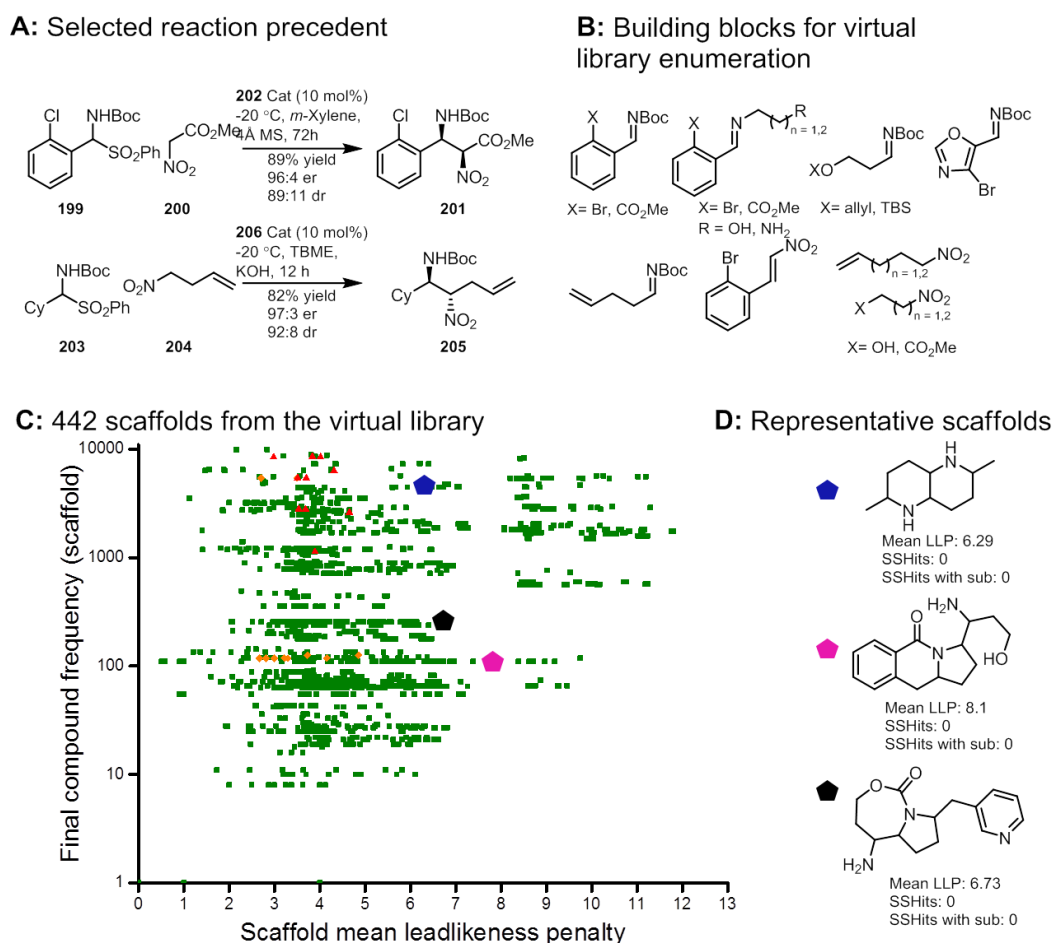


Figure 33: Panel A: Two representative examples of the nitro-Mannich reaction. Panel B: The library of 8 imines and 7 nitro components used in the virtual library enumeration. Panel C: Output for virtual library created, plot of scaffold frequency (total number of compounds generated from a single scaffold) vs the lead-likeness penalty. Highlighted area represents the most valuable area. Panel D: Representative scaffolds generated *via* the virtual library enumeration.

Ensuing analysis of the virtual library revealed a large number of scaffolds with a mean scaffold lead-likeness penalty less than three (49% of final compounds generated within the library had a lead-likeness penalty <3.2). In addition a substantial number of the scaffolds generated were extremely novel and a significant number of scaffolds could generate over 100 virtual final compounds which demonstrate the high diversity potential of the scaffolds.

3.2.6 Further interrogation of the virtual libraries generated

In addition to looking at the entire virtual library generated for each potential connective reaction, the libraries were further interrogated in order to identify the most promising cyclisation precursors. The data could be manipulated to give a plot of the final compound frequency vs. scaffold mean lead-likeness penalty for each individual cyclisation precursor. Representative cyclisation precursors generated from the nitro-Mannich reaction library are shown in Figure 34.

Each cyclisation precursor gives rise to over 20 highly novel scaffolds. In addition many scaffolds have suitable residual functional groups which could be exploited to create a plethora final compounds. However cyclisation precursors such as **206** are unsuitable for LOS as the majority of the scaffolds generated give a mean lead-likeness penalty >3, indicating poor physiochemical properties.

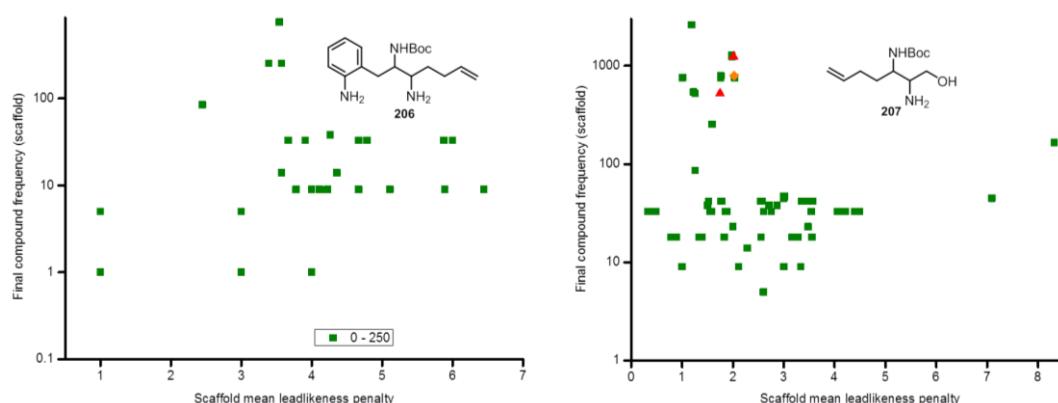


Figure 34: Output for two representative cyclisation precursors created from the nitro-Mannich reaction, plot of scaffold frequency (total number of compounds generated from a single scaffold) vs the lead-likeness penalty. Highlighted area represents the most valuable area.

In contrast, cyclisation precursor **207** would be prioritised since 32 scaffolds with over 30 virtual final compounds could potentially be synthesised. In addition

there are a further scaffolds with a favourable lead-likeness penalty but generate less than 30 virtual final compounds.

With the cyclisation precursors identified, a series of key reactions was then conceived to quickly determine the reactions suitability. If these preliminary reactions proved successful, the reaction could then be selected. For example, efficient access to required starting materials (if not commercially available) and suitable catalyst preparation had to be identified. Functional group interconversion conditions had to be identified and quickly realised (conversion of CN to amine, acid and aldehyde for cyclic sulfamidates or the reduction of the nitro functional group in nitro-Mannich library).

3.3 Reaction selection: nitro-Mannich reaction

The most valuable connective reactions can be identified by considering the novelty score, lead-likeness penalty, and synthetic economy involved (*i.e.* number of valuable scaffolds from a single cyclisation precursor) for a given reaction. Of the five reaction types, the nitro-Mannich reaction was selected due to the high number of potential cyclisation precursors generating scaffolds with favourable physicochemical properties (approximately one third of all scaffolds generated has a mean lead-likeness penalty <3.2). In addition, with the extensive use of various organocatalysts, potentially every stereoisomer of cyclisation precursors (and therefore scaffolds) could be synthesised.

The key reactions for demonstrating the potential of this reaction for LOS was the reduction of the nitro group. This was essential to realise the synthetic potential for the cyclisation precursors as well as removing an un-desirable functional group. In addition the reaction had to be diastereoselective therefore preparation of a suitable catalyst was required.

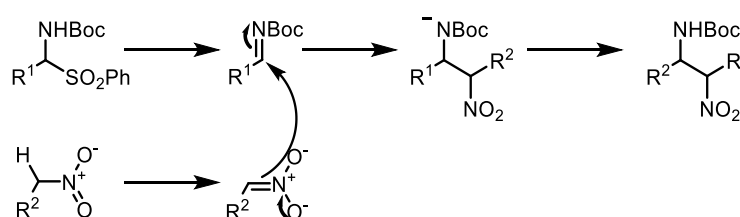
4 Investigation into suitability of the nitro-Mannich reaction to support lead-oriented synthesis

This Chapter describes the use of the nitro-Mannich reaction as a connective reaction to support lead-oriented synthesis. A literature review is first given before a detailed description of the development of the nitro-Mannich reaction towards the support of lead-oriented synthesis and the exemplification of this strategy.

4.1 nitro-Mannich reaction: general characteristics

The formation of C-C bonds is a fundamental process in organic chemistry.¹³⁷ The nitro-Mannich (or aza-Henry) reaction is an underutilised reaction which may have value in the synthesis of scaffolds due to the large variety of commercially available starting materials and mild reaction conditions.¹³⁷ Chapter 3 demonstrated that these scaffolds were lead-like (Section 3.2.5).

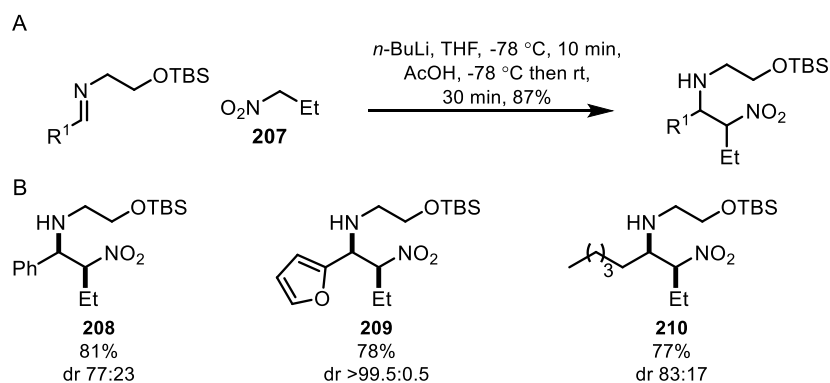
The mechanism of the nitro-Mannich reaction (Scheme 16)¹⁴⁷ is essentially the addition of a nitronate species to an imine electrophile creating the new C-C bond which upon protonation gives the product β -nitroamine (Scheme 16). The eponymous nitro group allows access to a wide range of synthetic targets through simple functional group interconversion to amine,¹⁴⁸ acid,¹⁴⁹ ketone,¹⁵⁰ and nitrile.¹⁵⁰



Scheme 16: Proposed mechanism for the nitro-Mannich reaction. The rate determining step is the irreversible C-C bond formation.

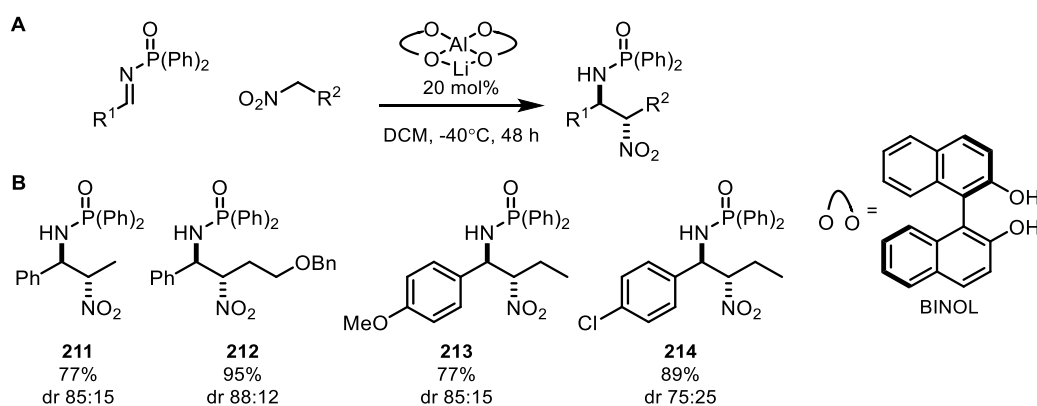
Early reports on the nitro-Mannich reaction were of limited synthetic use, being unselective¹³⁷ and often low yielding^{138,139}. The first stereoselective protocol with acyclic starting materials was reported in 1998¹⁴⁰. There now exist a large number of both enantio^{141,142}- and diastereoselective^{143,144} methods using a wide range of organometallic¹⁴⁵ and organo- catalysts¹⁴⁶.

Anderson described a diastereoselective method for the preparation of nitro amino alcohols (**208-210**, Scheme 17).¹⁵¹ The scope of the nitro component was not investigated and thus limited to nitropropane (**207**). More importantly however, electron rich imines could be used which is complementary to the electron deficient imines described below.



Scheme 17: Application of nitro-Mannich reaction for diastereoselective synthesis of nitroamines **208-210**. Panel A: An overview of the reaction described by Anderson.¹⁵¹ Panel B: Specific examples of diastereoselective products obtained using this method (**208-210**).

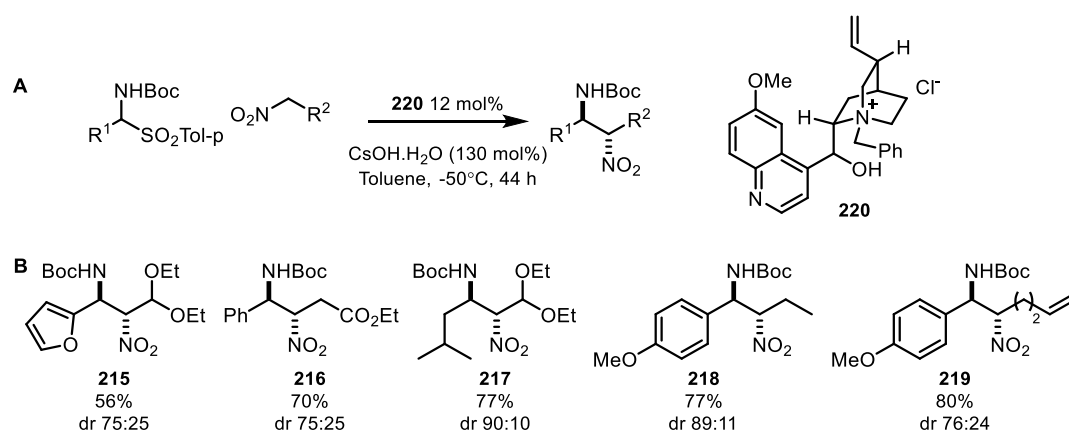
Shibasaki described a selective method using an organometallic catalyst (**211-214**, Scheme 18) which yielded products with good enantio- and diastereoselectivity.¹⁵² The catalyst exploits the dual activation of Brønsted basic and Lewis acidic sites, allowing excellent control in the synthesis of aryl substituted amines. The scope of the nitro component was limited to alkyl R^2 groups.



Scheme 18: Application of nitro-Mannich reaction for enantio-enriched synthesis of nitroamines **211-214** using an organometallic aluminium complex.¹⁵² Panel A: An overview of the reaction discovered by Shibasaki. Panel B: Specific examples of enantio- and diastereoselective products obtained using this method.

Palomo has released, independently from Herrera^{153,154}, an organocatalytic protocol using phase transfer catalysis (**215-219**, Scheme 19).¹⁵⁵⁻¹⁵⁷ Using a simple

commercially available cinchona-derived catalyst **220** good enantioselectivity was observed, with modest mixtures of diastereoisomers obtained in most cases. Significantly, in contrast to previously highlighted reports, a variety of functionalised nitro compounds were utilised giving nitro adducts with suitable functional groups and high cyclisation potential in practical diastereoselectivity (**215** to **219**).



Scheme 19: Application of nitro-Mannich reaction for enantio-enriched synthesis of nitroamines **215-219** using a cinchona-derived catalyst. Panel A: An overview of the reaction discovered by Palomo.¹⁵⁵⁻¹⁵⁷ Panel B: Specific examples of enantio- and diastereoselective products obtained using this method.¹⁵⁵⁻¹⁵⁷

4.2 Selection of a diastereoselective protocol for the nitro-Mannich reaction

Two cyclisation precursors were selected from the nitro-Mannich reaction library to investigate the diastereoselectivity of the reaction. A thorough investigation of the functional group tolerance of the reaction was not undertaken as the nitro-Mannich reaction is well-documented (Figure 35).¹³⁷ In addition to the cyclisation precursors, the cinchona-derived catalyst **222** was also chosen based on literature precedent (Figure 35).¹⁴³

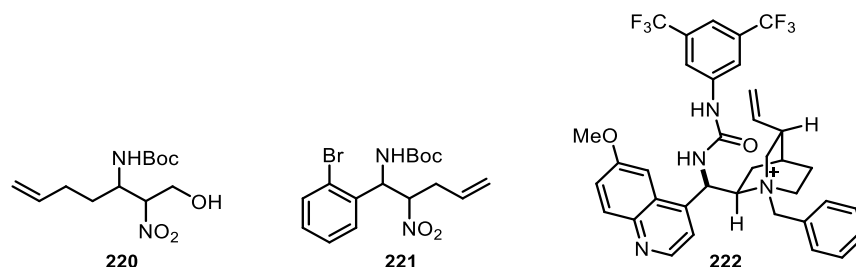
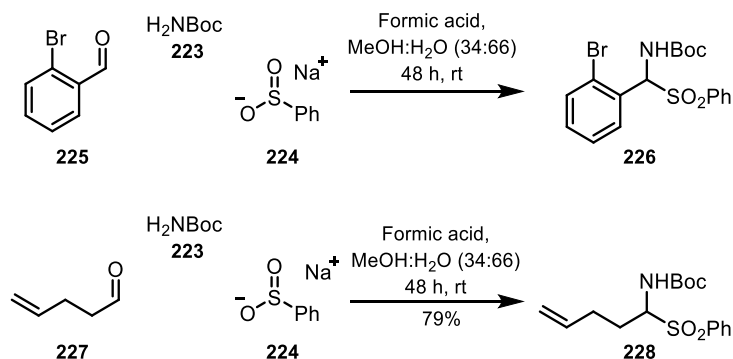


Figure 35: Two cyclisation precursors (**220**) and (**221**) identified from the computational protocol as having potential to explore lead-like chemical space. Cinchona-derived catalyst **222** was also selected as a catalyst system to identify suitable reaction conditions.

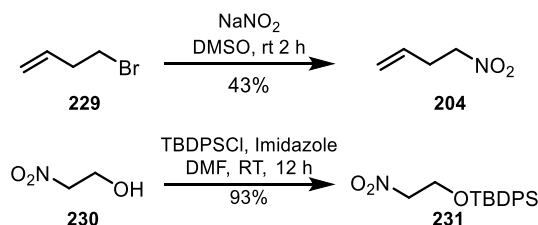
4.2.1 Synthesis of starting materials

The amidosulfone starting materials were readily obtained in a single step from commercially available materials. Accordingly *ortho*-bromobenzaldehyde (**225**) and pentenal (**227**) were condensed with *tert*-butyl carbamate (**223**) and benzenesulfonic acid (**224**) to give the corresponding amidosulfones **226** and **228** (Scheme 20)¹⁵⁸



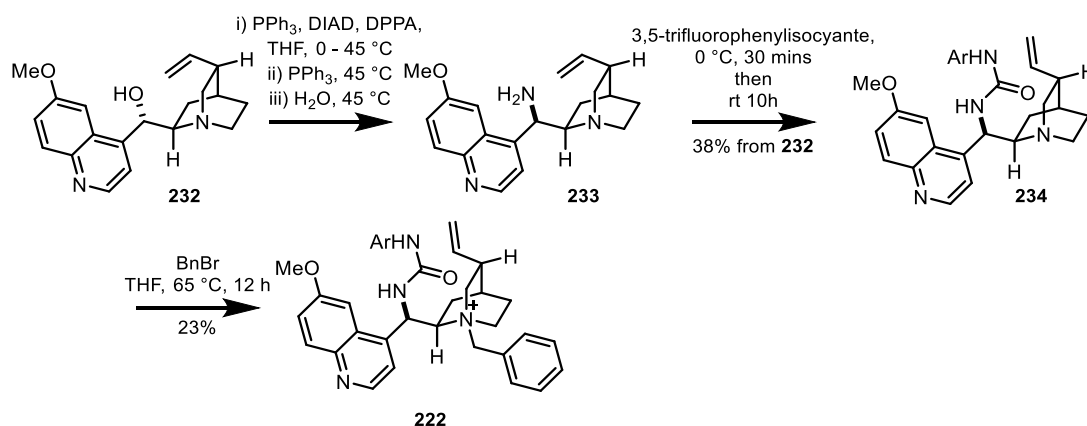
Scheme 20: Synthesis of amidosulfone **226** and **228**.

Nitrobutene (**204**) was readily prepared from 4-bromobutene (**229**) *via* displacement of the bromide group with sodium nitrite according to a modified literature procedure in modest yield (Scheme 21).¹⁵⁹ Nitroethanol (**231**) was protected by *tert*-butyldiphenylsilylation (**230**, Scheme 21).



Scheme 21: Synthesis of nitro compounds **204** and **231**.

The cinchona-derived catalyst (**222**) was selected as it was reported to give good enantio- and diastereo-control at mild reaction conditions.¹⁴³ Accordingly, a Mitsunobu reaction with DPPA and quinine (**233**) afforded primary amine **234** upon reduction of the azide with triphenylphosphine (Scheme 22).



Scheme 22: Synthesis of catalyst **222** from quinidine (**232**). Ar = 3,5-trifluoromethylphenyl

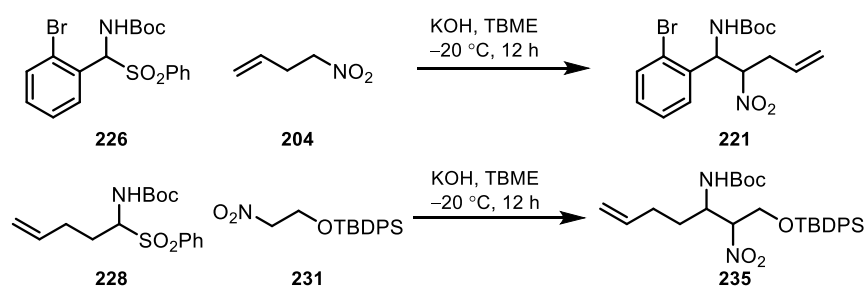
Subsequent urea formation with 3,5-trifluorophenylisocyanate gave the catalyst precursor **234**. A final alkylation with benzyl bromide gave the phase transfer catalyst **222** in modest yield (Scheme 22). Given the reaction route, and the modest yield of the alkylation step, the catalyst precursor **234** was also screened as a potential catalyst for the nitro-Mannich reaction.

4.2.2 Synthesis of cyclisation precursors

With the relevant catalysts and starting materials in hand, the nitro-Mannich reaction was then investigated. Initially the amidosulfone was added to a solution of the nitro component then the reaction mixture was cooled to -20 °C. The catalyst and potassium hydroxide was then added. The products (**221** and **235**) were obtained in good yields using the reaction conditions described without the addition of the organocatalysts (Table 7, entries 1 and 4).

Under the same reaction conditions, but with the addition of 5 mol% of catalyst **222**, the nitro adducts were again obtained in good yield (64-69%) and poor diastereocontrol (Table 7, entries 2 and 5). Although no *ortho*-substituted aryl components had been described¹⁴³ the result was surprising. In addition, the few examples of alkyl amidosulfones and alkyl nitro components reported, involve quite sterically large reagents which may have aided their control.

Table 7: nitro-Mannich reaction to give the cyclisation precursors **221** and **235**.



Entry	Product	Organocatalyst	d.r. <i>anti:syn</i> ^{A,B}	Yield
1		--	50:50	75%
2		222	55:45	64%
3		234	35:65	73%
4		--	50:50	64%
5		222	60:40	69%
6		234	35:65	61%

^ADetermined by 500 MHz ¹H NMR Spectroscopy of the crude reactions. ^B *anti:syn* w.r.t NHBoc and NO₂.

The most surprising result, the addition of 5 mol% of catalyst **234**, favoured the formation of the *syn* diastereoisomer albeit with modest control (entries 3 and 6). There are no reports of unalkylated cinchona-derived catalyst used in the nitro-Mannich reaction.

4.3 Selection of a diastereoselective nitro-Mannich reaction protocol (2)

4.3.1 Catalyst screen

Given the poor diastereocontrol observed using both cyclisation precursors, a more thorough investigation of a suitable catalytic system was then undertaken. As such, the bifunctional organocatalysts **220**, **236-240** (Figure 36) were selected based on the following criteria; coverage of a range of organocatalyst classes and ready availability.

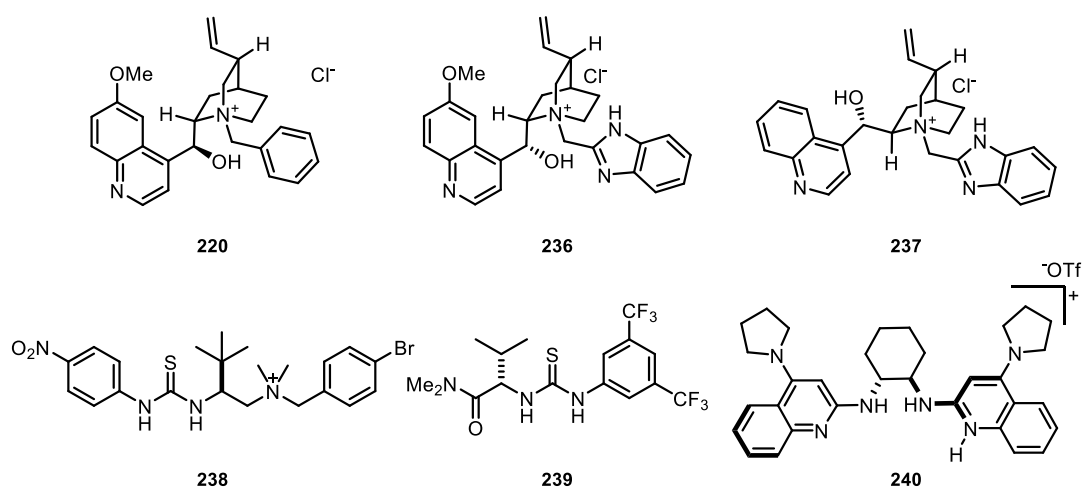
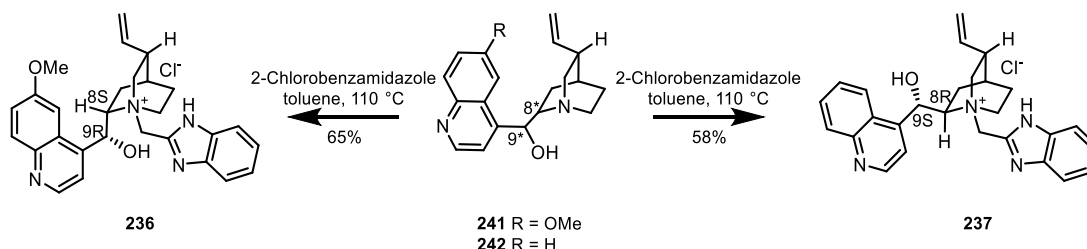


Figure 36: Chiral catalysts chosen for a screening of the nitro-Mannich reaction.

4.3.1.1 Synthesis of selected catalysts

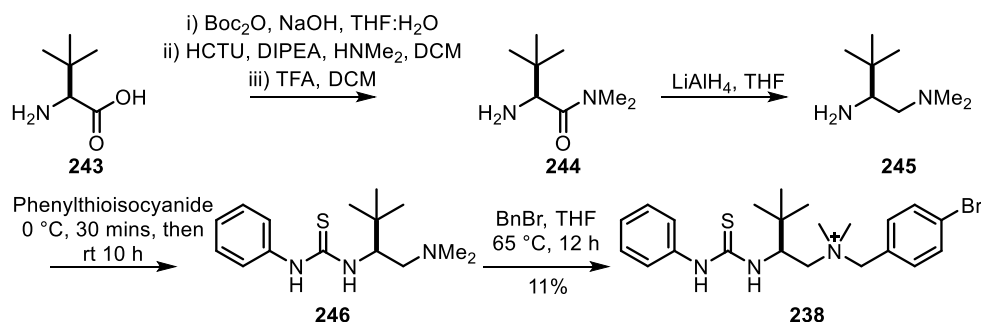
The cinchona-derived phase-transfer catalyst **220** was commercially available. Additional catalysts **236** and **237** were readily synthesised from alkylation of quinine (**241**) and cinchonine (**242**) with 2-chlorobenzimidazole in 65% and 58% yields respectively (Scheme 23).¹⁶⁰



Scheme 23: Synthesis of Zhang's cinchona alkaloid catalyst **236** and **237**.¹⁶⁰ *R or S

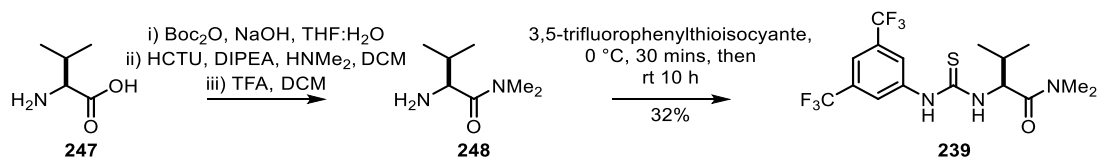
Zhao's catalyst **238** required the protection of *tert*-leucine **243** with *tert*-butyl carbamate, subsequent amide formation and deprotection gave the dimethyl amide derivative **244** (Scheme 24).¹⁶¹ This intermediate was then reduced to give diamine

245 with lithium aluminium hydride before thiourea formation with phenylthioisocyanate furnished **246**. Finally, alkylation with benzyl bromide gave phase transfer catalyst **238** in 11% yield from *tert*-leucine (**243**).¹⁶¹



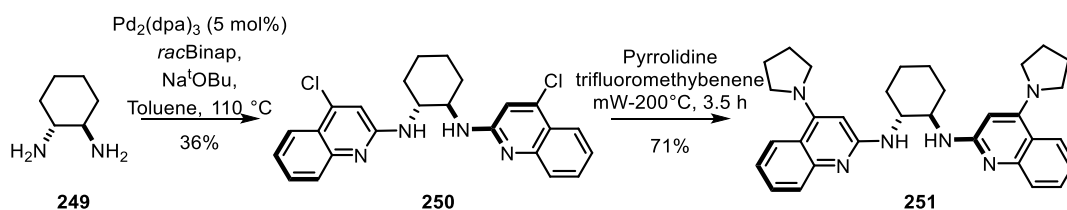
Scheme 24: Synthesis of Zhao's thiourea catalyst **238** from *tert*-Leucine **243**.¹⁶¹

Anderson's catalyst **239** was readily prepared in a similar route from valine (**247**).¹⁶² The amino acid was first protected as the carbamate derivative before amide formation with dimethylamine and deprotection gave the dimethyl amide derivative **248** (Scheme 25). Subsequent thiourea formation on the crude material afforded **239** in 32% yield from valine.¹⁶²



Scheme 25: Synthesis of Anderson's thiourea catalyst **239** from valine.

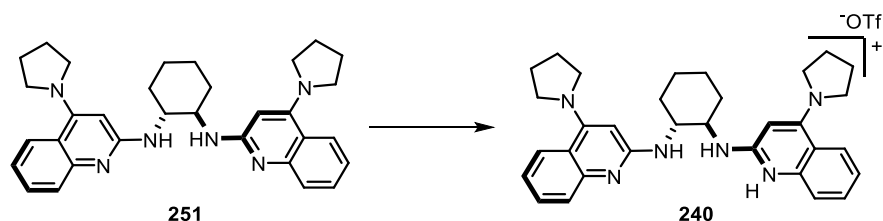
The final organocatalyst, Johnson's chiral bis (amidine) (BAM) Brønsted basic catalyst (**240**), was readily available in two steps.^{148,163} Regioselective Buchwald coupling of 2,4-dichloroquinoline with diaminocyclohexane **249** gave the amino chloro derivative **250** (Scheme 26). A final S_NAr reaction using pyrrolidine gave the catalyst precursor **251** (Scheme 26).^{148,163}



Scheme 26: Synthesis of precursor for Johnsons BAM Brønsted basic catalyst **251**.

The active catalyst (**240**) was formed immediately prior to its use by the addition of a sub stoichiometric amount of triflic acid to **251** (Scheme 27). Johnson

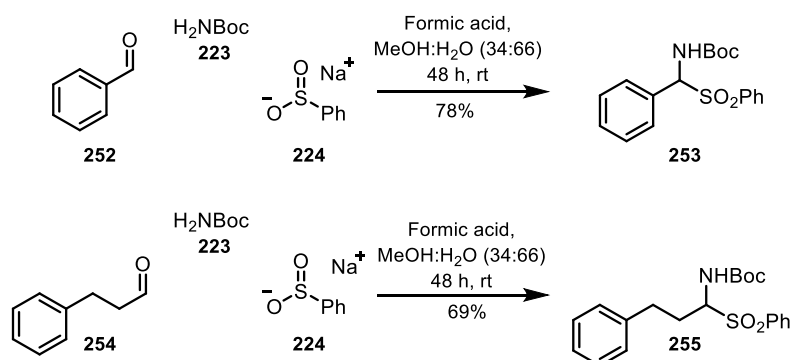
has shown that the amount of triflic acid added had a direct effect on the diastereoselectivity of the system.^{148,163}



Scheme 27: BAM Brønsted basic catalyst **240** was prepared by the addition of sub stoichiometric amount of triflic acid to (**251**) and used without further purification/analysis as described.

4.3.2 Catalyst screen to identify suitable diastereoselective conditions

With a number of different catalysts synthesised, a common set of reaction conditions were then established to compare the effectiveness of each catalyst. Amidosulfones **253** and **255**, readily prepared from the corresponding aldehydes (**252** and **254**, Scheme 28).



Scheme 28: Synthesis of amidosulfones **253** and **255**.

The amidosulfones were dissolved in toluene with nitroethane and 10 mol% of the catalyst then cooled to $-50\text{ }^{\circ}\text{C}$. At this point, caesium hydroxide was added and the reactions stirred for 48 h. The conditions chosen had previously been used by Palomo *et al.* with their work using catalyst **220** (see Section 4.1, Scheme 19). Summarised in Table 8 are the results from the catalyst screen with amino sulfone **255**.

The catalysts **220**, **236** and **237** performed best, with each giving $>60\%$ conversion and good diastereoselectivities (Table 8, entries 1-3). As the conditions employed had previously been optimised for cinchona catalyst **220** this was expected. Disappointingly, very little conversion was obtained with the use of catalyst **238** and when no organocatalyst was used (Table 8, entries 4 and 7).

Table 8: Screening of catalysts in the asymmetric nitro-Mannich reaction between phenyl amidosulfone (**253**) and nitro ethane.

Reaction scheme: **253** (phenyl amidosulfone) reacts with CsOH.H₂O (130 mol%), nitroethane (5 eq.) in toluene at -50°C for 44 h to yield **257** (nitro-Mannich adduct).

Entry	Organocatalyst	Conversion ^a	d.r. ^a
1	220 (10 mol%)	>90%	95:5
2	236 (10 mol%)	>60%	95:5
3	237 (10 mol%)	>90%	95:5
4	238 (10 mol%)	<5%	--
5	239 (10 mol%)	nd ^b	--
6	240 (10 mol%)	>50%	60:40
7	7 --	<5%	--

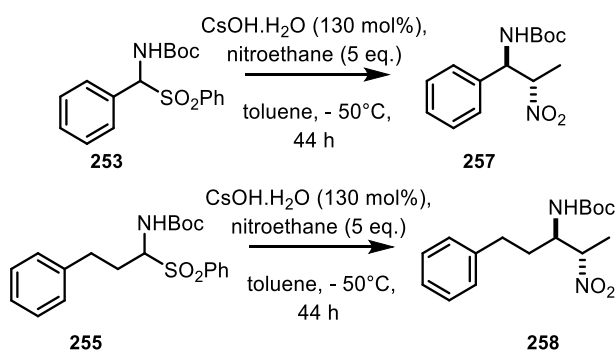
a) Determined by 500 MHz ¹H NMR spectroscopy of crude reaction mixture. b) 500 MHz ¹H NMR spectroscopy signals were extremely broad and therefore analysis was inconclusive.

Catalyst **239** provided reasonable conversion albeit with relatively poor diastereocontrol (60:40) which was significantly lower than that reported (entry 6).¹⁶³ This is likely due to the combination of two variables; under the literature procedure, there was no external base added to the reaction system, which may have limited the non-catalysed background reaction. In addition, the optimised conditions for Johnson's catalytic system were at higher temperatures (-20 °C).

Given these results, catalyst **220** and **237** were selected for further evaluation. The results are summarised in Table 9. Both catalysts were effective at promoting a diastereoselective nitro-Mannich reaction with amidosulfone **253**, in each case **257** was obtained with d.r. of 90:10 after purification (entries 1 and 3). The reaction was also scalable, allowing the synthesis of grams of **257** with catalyst **220** while maintaining high levels of diastereoselectivity (85:15, entry 2).

However, when **255** was used as the coupling partner, catalyst **220** was superior, with the nitro adduct **258** being isolated in a 60% yield with 93:7 d.r.

Table 9: Screening of catalysts (**220**) and (**237**) in the asymmetric nitro-Mannich reaction between model substrates on a preparative scale.



Entry	Substrate	Catalyst	Crude d.r. ^a	Yield	Purified d.r. ^a
1	255	220	82:18	83%	90:10
2	255	220	nd	43% ^b	85:15
3	255	239	75:25	76%	90:10
4	257	220	75:25	60% ^c	93:7
5	257	239	--	61%	60:40

^aDetermined by 500 MHz ¹H NMR spectroscopy. ^b50% conversion (85% BRSM). Reaction on 3.2 mmol scale. ^cMinor fraction isolated as 50:50 mixture of diastereoisomers in 19% yield.

4.4 Design of Cyclisation precursors

With a working diastereoselective protocol for the nitro-Mannich reaction, the pipeline pilot protocol was then used to identify the most useful cyclisation precursors. In total 18 imines and 11 nitro-components, were used to create a library with over two million virtual final compounds.

Because such a large amount of data was generated during the enumeration, the cyclisation precursors were first sorted according to the following criteria; cyclisation precursors ≤ 30 scaffolds with suitable physiochemical properties to interrogate lead-like chemical space was discarded. This left a focused library of 42 cyclisation precursors based on the combinations of aldimines with nitro components (Figure 37).

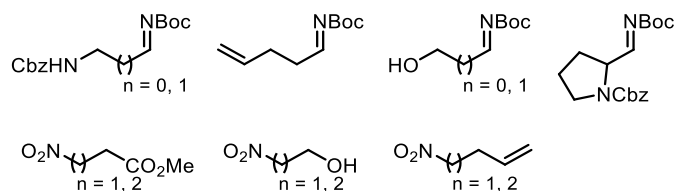


Figure 37: Amidosulfones and nitro compounds used to generate lead-like scaffolds.

From the list of 42 cyclisation precursors, **220** and **259** were chosen because they had over 30 potential scaffolds that could be accessed from each precursor (Figure 38). In addition, subtle variation of each reactant ($n = 0, 1$ or 2 respectively) the number of scaffolds obtained could be readily doubled or tripled from a common set of reaction conditions.

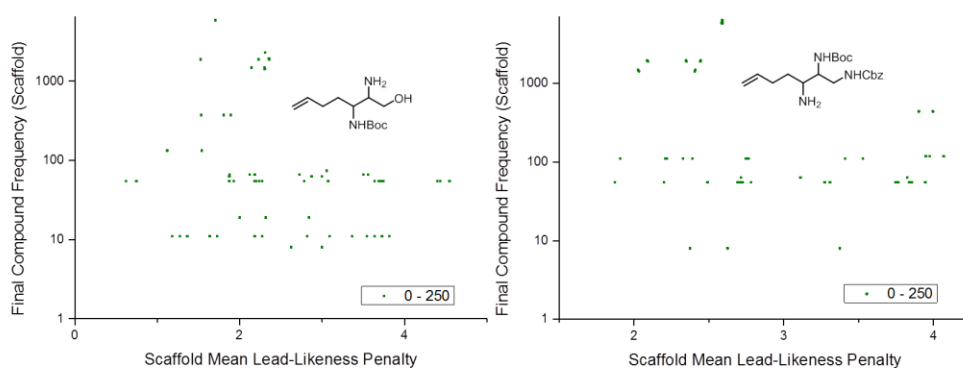
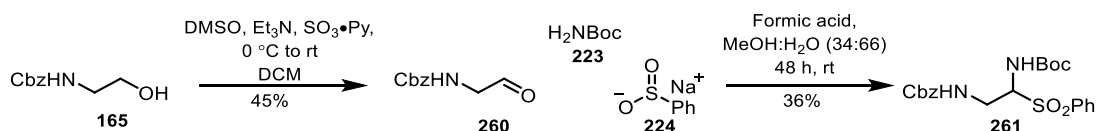


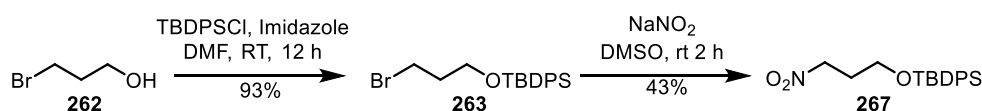
Figure 38: Output cyclisation precursors **220** (left) and **259** (right) selected for investigation. Plot of scaffold frequency (total number of compounds generated from a single scaffold) vs the lead-likeness penalty.

4.4.1 Synthesis of starting materials

With the selected cyclisation precursors, synthesis of the amidosulfones and nitro compounds was then undertaken. Amidosulfone **261** was prepared *via* Parikh-Doering oxidation of aminoethanol **165**. Subsequent amidosulfone formation with **223** and **224** provided **261** (Scheme 29).



3-Bromopropanol (**262**) was protected by *tert*-butyldiphenylsilylation (**263**, Scheme 30) then subsequent displacement of the bromide group with sodium nitrite gave the silyl protected nitropropanol **267**. (Scheme 30). Preparation of remaining starting materials has previously been described (Section 4.2.1).

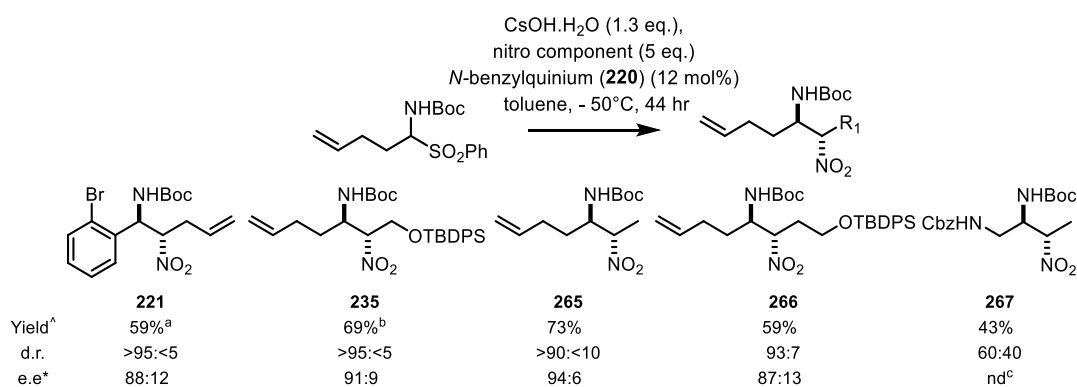


4.4.2 Synthesis of cyclisation precursors

With a significant number of starting materials prepared, the diastereoselectivity of the nitro-Mannich reaction was investigated. In general good levels of diastereocontrol was observed from a broad range of amidosulfones.

Cyclisation precursors **221** and **235** could now be synthesised in good yield and diastereocontrol (Table 10). After purification, both nitro amines could be obtained as almost a single diastereoisomer (d.r. 87:13 and 90:10 respectively).¹⁵⁵ Additional nitro compounds, **267** and nitroethane (**256**) were successfully reacted with aldimine **227** to give cyclisation precursors **265** and **266** respectively (Table 10).

Table 10: Scope of the nitro-Mannich reaction.



[^]Yield and diastereomeric mixture of purified product determined by 500MHz ¹H NMR spectroscopy. ^{*}Determined by reduction of the nitro group, formation of diastereomeric Mosher's amides. ^AMinor diastereoisomer isolated 13% (d.r. 60:41). ^BMinor diastereoisomer isolated 7% (d.r. 90:10) and a third fraction with a d.r. 60:40 (5% yield) was obtained. ^cee not determined due to the presence of significant amount of the other diastereoisomer.

Disappointingly however, amidosulfone **261** gave nitro adduct **267** in poor yield and diastereocontrol. In addition, a large amount of the enamine side product was observed which was difficult to remove. The poor diastereo control could be the result of coordination of NHCbz to the catalyst in place of the NHBoc. This alternative mode of coordination could give rise to another diastereoisomer.

4.4.2.1 Determining relative configuration of the nitro-Mannich reaction

The relative stereochemistry of the nitro-Mannich reaction had until now been assigned by analogy to the results of Palomo who had demonstrated that the *anti* diastereoisomer was obtained through suitable functional group manipulation.¹⁵⁵ In this study, the relative stereochemistry was independently confirmed when the minor diastereoisomer of nitro adduct **265**, *syn*-**265**, was crystallised from ethyl acetate and petrol (Figure 39) displaying *syn* relationship between nitro and NHBoc groups.

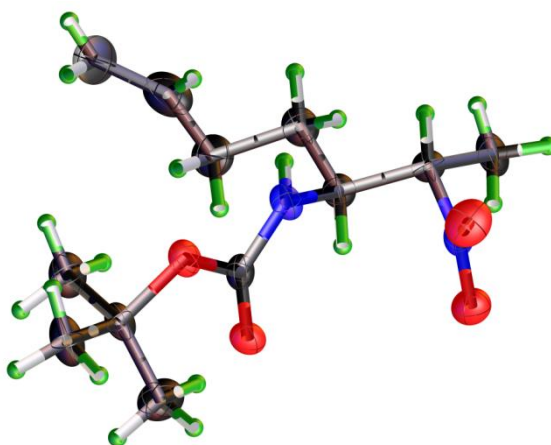


Figure 39: Confirmation of the relative configuration of a product of the nitro-Mannich reaction. The minor diastereoisomer of **265** was crystallised from EtOAc–petrol. Ellipsoids at 50% probability.

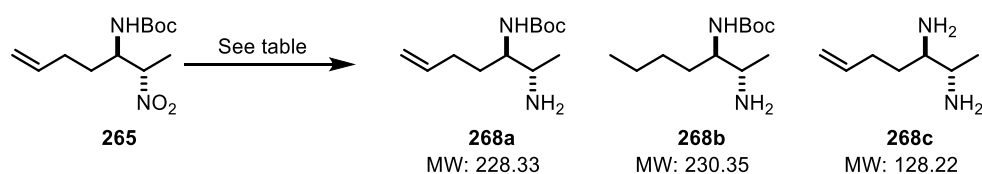
4.5 Reduction of the nitro group

With a suitable route for the synthesis of cyclisation precursors, the next aim was to reduce the nitro group to give access to 1,2-diamines. Using standard conditions¹⁴³, nickel chloride and sodium borohydride were added to a solution of **265**. After 60 minutes, TLC indicated the complete consumption of starting material however LC-MS analysis showed a mass of 231 (M+3) (Table 11 entry 1). After quenching and workup, 500 MHz ¹H NMR analysis of the crude reaction did not show any alkene signals, suggesting **268b** had been formed recovered **268a**.

Given the unexpected result, the reaction was repeated and at various time spots the reaction was quenched and analysed by LC-MS. At two minutes, 229 was observed by LC-MS corresponding to *MH*⁺ for amine **268a**. ¹H NMR analysis of the crude reaction showed a mixture of **265** and **268a** (based on the presence of two different terminal alkene signals in the 500 MHz ¹H spectrum obtained). However

by five minutes, only the fully reduced amine **268b** was observed by LC-MS and 500 MHz ^1H NMR. Although an unusual outcome, the reduction of alkenes with nickel and sodium borohydride is not unprecedented.¹⁶⁴

Table 11: Screening of conditions for the reduction of the nitro group in the presence of an alkene and carbamate group.

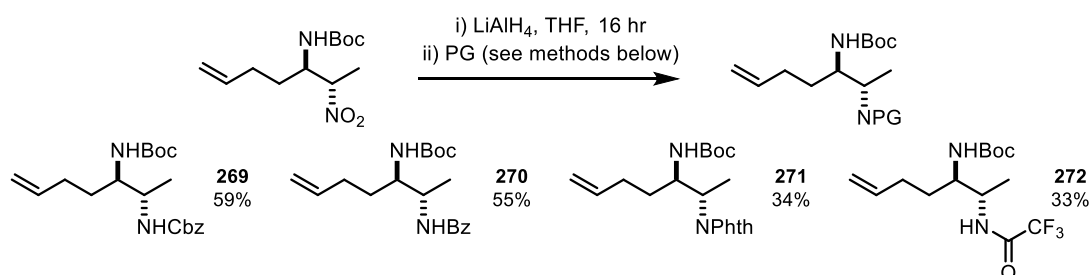


Entry	Conditions	Time	Outcome ^a
1	NiCl_2 , NaBH_4 20°C	2 minutes	Mixture of 265 and 268a
		5 minutes	268b
2	Zn , AcOH , 75°C	16 hr	Mixture of 268a and 268c
3	LiAlH_4	16 hr	268a present by LC-MS

^aDetermined by 500 ^1H NMR spectroscopy and LC-MS

Zinc has been extensively used with acid to reduce aryl nitro groups.¹⁶⁵ To this end, the nitro amine **265** was dissolved in acetic acid and heated to reflux for 16 hours. Pleasingly, these conditions did reduce the nitro group while leaving the alkene untouched however the carbamate protecting group was partially removed and a mixture of amine **268a** and diamine **268c** was obtained (entry 2). While the loss of the carbamate group was not unexpected, given the instability of *tert*-butyl carbamate groups to cleavage under acidic conditions,¹⁶⁶ the nitro-Mannich reaction is known with other protecting groups on the nitrogen (e.g. benzyl carbamate) which are stable to acid.

Fortunately, when a solution of cyclisation precursor **265** in THF was added to lithium aluminium hydride (1M in THF), amine **268a** in obtained. (entry 3). Amines such as **268a** are difficult to handle and analyse. Consequently, it was found to be more efficient to trap the amine with a protecting group complimentary to *tert*-butyl carbamate. Shown in Scheme 31 is the various differentially protected amines obtained from **265**.

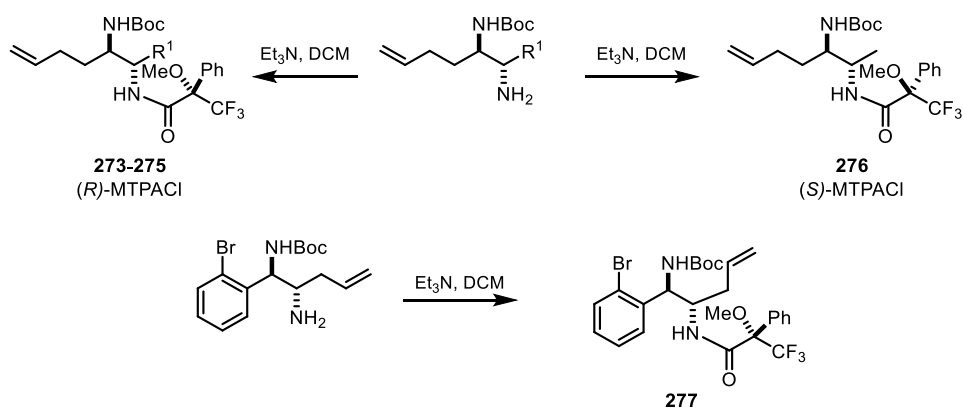


Scheme 31: Synthesis of differentially protected diamines **269-272**. Conditions; (i) **265** (1 eq.), THF, 1 M LiAlH₄ (2.1 eq.) then (ii) **269**: DCM, NaHCO₃, Cbz-Cl 18 h; **270**: DCM, benzyl anhydride, E₃N 18 h; **271**: Toluene, phthalic anhydride, E₃N, 110 °C, 48 h; **272**: TFA-Cl, E₃N, 18 h.

4.5.1 Determining the enantiomeric excess of the nitro-Mannich reaction

With a suitable route for the synthesis of cyclisation precursors and the reduction and more importantly a method for reducing the nitro group, the enantioselectivity of the diastereoselective adducts had to be determined. This was done *via* Mosher's amide analysis¹.

Accordingly, the nitro group of each cyclisation precursor was reduced with lithium aluminium hydride as described previously. To determine the enantiomeric excess, the amine was then reacted with (*R*) or (*S*) α -methoxy- α -trifluoromethylphenylacetyl chloride to give a pair of diastereoisomers (**273-277**, Scheme 32). The ee was determined *via* integration of the corresponding diastereoisomers within the crude 500 MHz ¹H NMR signals (e.e given in Table 10).



Scheme 32: Preparation of Mosher's amide derivatives. **273** R¹ = H (from **268**), **274** CH₂OTBDPS (from **237**), **275** CH₂CH₂OTBDPS (from **269**).

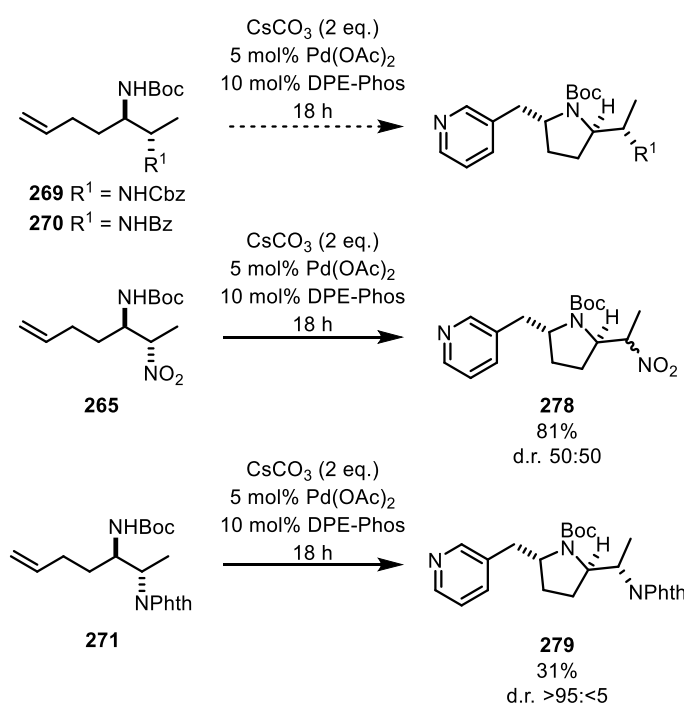
¹ The pseudo enantiomer of cat **220** was prepared and opposite configuration of nitro adducts was prepared. In addition, reduction of nitro group and preparation of benzamide derivatives was prepared. However a suitable method was not obtained.

4.6 Utilising cyclisation precursors in subsequent cyclisation reactions

4.6.1 Cyclisation precursor 265

4.6.1.1 Cyclisation by Aminoarylation

With the cyclisation precursors in hand, next the potential for making scaffolds was investigated. For this, the cyclisation precursors **235** and **265** were used. There had been success within the group using a palladium-catalysed aminoarylation reaction to give a range of pyrrolidine products.⁶⁵ Accordingly, **269** was treated with 5 mol% palladium acetate and 3-bromopyridine then heated to 110 °C. However the expected product was not observed (Scheme 33).



Scheme 33: [#]No mass observed by LC-MS analysis. 500 MHz ¹H NMR spectroscopy showed presence of starting material. 51% recovered starting material

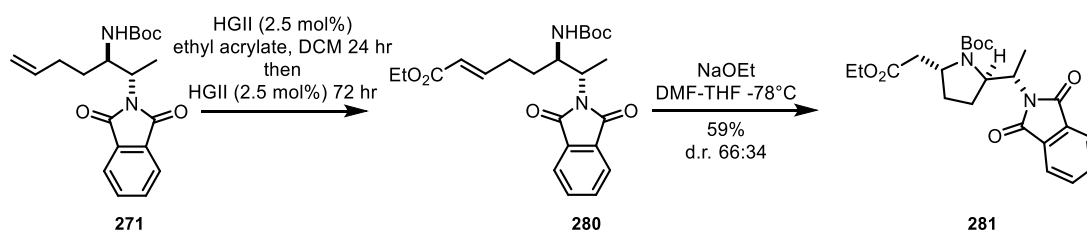
When heated for longer, 48 hr, still only **269** was observed. Attempted use of **270** also failed to give any of the desired product. Given the presence of the 1,2 nitrogen atoms, it was possible that co-ordination with the Pd between these atoms was preventing completion of the catalytic cycle. To test this, the nitro adduct **265** was subjected to aminoarylation conditions. Pleasingly, the pyrrolidine **278** was obtained in reasonable yield albeit with poor stereochemical control. This was perhaps unsurprising, given the possibility of epimerisation α to the nitro group but

it does demonstrate that with judicious choice of protecting group, aminoarylation was possible.

Pleasingly with the phthalimide protected amine (**271**), the pyrrolidine (**279**) was obtained with high diastereoselectivity in 31% yield. It should be noted that 51% of starting material was recovered indicating potential difficulty with these cyclisation reactions.

4.6.1.2 Cyclisation by Cross-metathesis

The cyclisation precursor **271** underwent efficient cross metathesis with ethyl acrylate to give $\alpha\beta$ unsaturated ester **280** (Scheme 34). The crude product was then reacted with sodium *tert*-butoxide without isolation to give pyrrolidine **281**. Unfortunately poor diastereocontrol was observed (d.r. 66:34, Scheme 34). Alternative bases were investigated but the diastereoselectivity could not be improved.

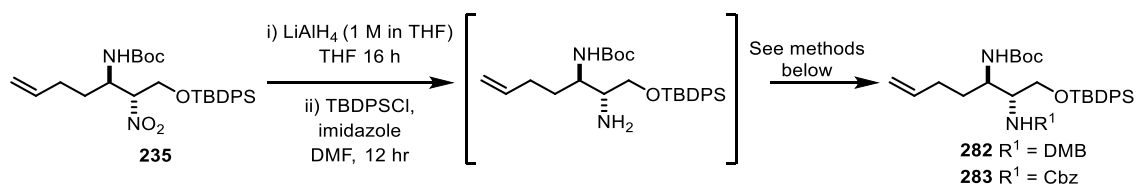


Scheme 34: Cross metathesis and aza-Michael reaction to give **281**. Alternative conditions were attempted (variation of base and solvent, see page 137 for full details) but the diastereoselectivity remained at 65:35.

4.6.2 Cyclisation precursor 235

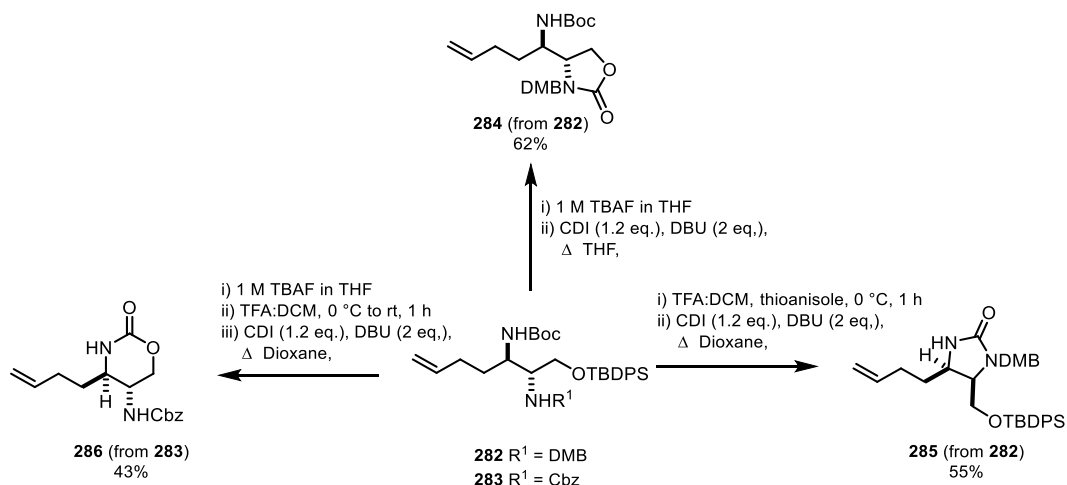
Cyclisation precursor **235**, with additional functionality could be used in two cyclisation reactions to give access to bicyclic scaffolds. To make use of the different functional groups, **235** was reduced with lithium aluminium hydride, and protected with dimethoxy benzaldehyde and benzyl chloroformate to give **282** and **283** respectively (Scheme 35).

The reduction of **235** was complicated due to the partial loss of the TBDPS group. While removal of a silyl group with lithium aluminium hydride is known¹⁶⁶ it was unexpected. However, the addition of an equivalent of TBDPS-Cl with imidazole prior to the amine protecting group was sufficient to solve this problem.



Scheme 35: Preparation of the differentially protected diamines **282** and **283**. (i) **235** (1 eq.), THF, 1 M LiAlH₄ (2.1 eq.) then (ii) **282**: MeOH, 2,4 dimethoxybenzaldehyde, MS, 65 °C 18 h then NaBH₄; 18 h, 43%; **283**: DCM, NaHCO₃, Cbz-Cl, 18 h, 48%.

With **282** the silyl protecting group was removed with TBAF to give the corresponding amino alcohol which was reacted directly with carbonyldiimidazole to give the oxazolodinone **284** (Scheme 36). In addition, the *tert* butyl carbamate group of amine **282** could be removed with TFA to give the corresponding diamine, which after the addition of carbodiimidazole gave the urea **285** (Scheme 36).



Scheme 36: Synthesis of first generation scaffolds. By judicious choice of protecting group manipulation, 3 scaffolds were obtained from the one reaction class (CDI coupling).

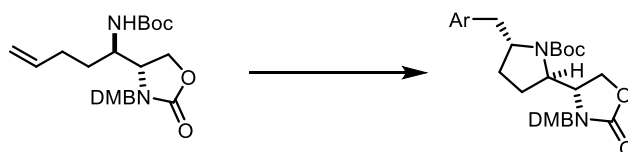
With amine **283**, the silyl protecting group was removed with TBAF and the *tert* butyl carbamate group was removed with TFA to give the corresponding amino alcohol, which after the addition of carbodiimidazole gave the six membered carbamate **286** (Scheme 36).

4.6.2.1 Aminoarylation with 284

It was envisaged that the aminoarylation chemistry and cross metathesis described with cyclisation precursor **265** could be used with the remaining functionality present in **284-286**. Taking the aminoarylation conditions developed within the group, **284** was added treated with 5 mol% of palladium acetate, 3-bromopyridine and heated to 110 °C (Table 12, entry 1). However the expected pyrrolidine was not obtained. Only starting material was observed by LC-MS and 500 MHz ¹H NMR spectroscopy. Heating for extended times, and addition of more palladium catalyst, the pyrrolidine was still not observed (Table 12, entries 2-3).

A series of different aryl bromides was then investigated to ensure that lack of activity observed was not the result of poor selection of coupling partner. In each case, however, only starting material was observed (Table 12, entries 4-5).

Table 12: Attempted aminoarylation with substrate **287**



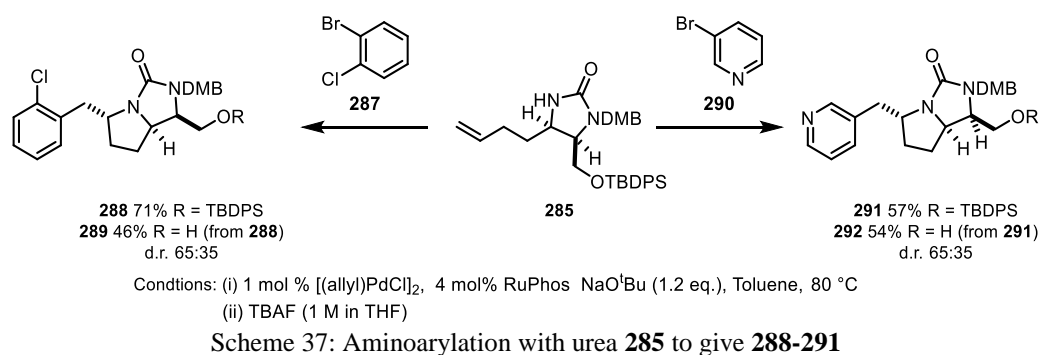
Entry	Catalyst	Time	Ar	Outcome
1	5 mol% Pd(OAc) ₂	18 h	3-bromopyridine	NR [#]
2	5 mol% Pd(OAc) ₂	36 h	3-bromopyridine	NR [#]
3	10 mol% Pd(OAc) ₂	48 h	3-bromopyridine	NR [#]
4	5 mol% Pd(OAc) ₂	18 h	5-bromopyrimidine	NR [#]
5	5 mol% Pd(OAc) ₂	18 h	1-chloro 2-bromobenzene	NR [#]
6	1 mol% Pd ₂ (allylCl) ₂	18 h	3-bromopyridine	NR [#]

Unless otherwise state, dioxane, CsCO₃ (2 eq.) and 10 mol% of ligand DPE-Phos used.[#]Mass for pyrrolidine was not observed by LC-MS. 500 MHz ¹H NMR showed starting material present after the specified time.

A different palladium source was also used; again only starting material was observed (entry 6). Given the comprehensive set of conditions attempted, it is clear that substrate **284** is not suitable for the aminoarylation reaction.

4.6.2.2 Cyclisation with Aminoarylation 285

Aminoarylation of cyclic carbonates had previously been described. In their system, the oxazolidinone was treated with 2 mol% of palladium allyl chloride, aryl bromide and heated to 80 °C. A range of different 5/5 fused systems was created with excellent stereocontrol. Accordingly, urea **285** was treated under the conditions with 1-bromo-2-chlorobenzene (**287**) and the imidazolone **288** was obtained (Scheme 37).

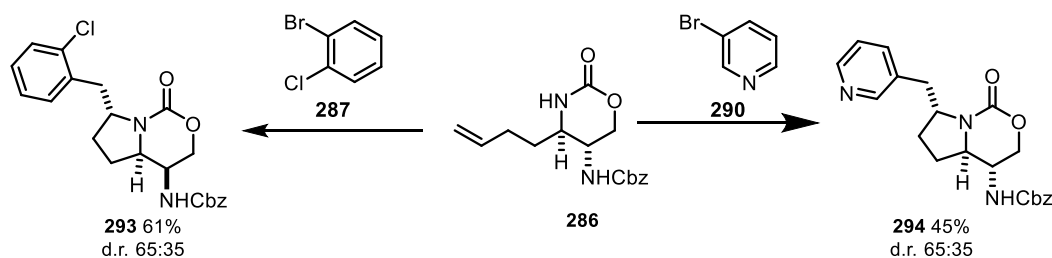


The presence of the silyl protecting group greatly complicated interpretation of the 500 MHz ¹H NMR spectra. It was therefore not trivial to determine the diastereoselectivity of the aminoarylation reaction. Consequently, the silyl protecting group was removed with TBAF to give imidazolone **289**. From this data, it was clear that the compounds was obtained in a 65:35 mixture of diastereoisomers (Scheme 37).

An additional scaffold was obtained when using 3-bromopyridine (**290**) as the coupling partner to give **291** in a modest yield and same diastereoselectivity (as observed in the preparation of **289**). The aminoarylation was attempted with 5-bromopyrimidine, however although the mass of the imidazolone was observed it was not possible to isolate cleanly and determine if the reaction had occurred. In each case, LC-MS analysis showed the [M-TBDPS], i.e. loss of the silyl protecting group however this was never isolated.

4.6.2.3 Aminoarylation with 286

Given the success of the amino arylation with **285**, **286** was treated with 2 mol% of palladium allyl chloride and 1-bromo-2-chlorobenzene (**287**) and heated to 80 °C and the pyrroloxazinone **293** was obtained (Scheme 38). As before, scaffold **293** was obtained in a 65:35 mixture of diastereoisomers. The methodology was exploited with 3-bromopyridine (**290**) as the coupling partner to give **294** in a modest yield and same diastereoselectivity.

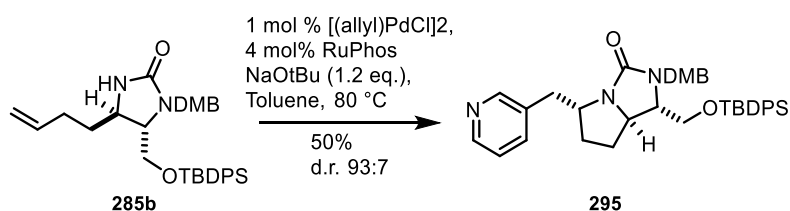


Conditions: 1 mol % [(allyl)PdCl]₂, 4 mol% RuPhos NaO^tBu (1.2 eq.), Toluene, 80 °C

Scheme 38: Aminoarylation with carbamate **286**.

4.6.3 Cyclisation with substrate 289

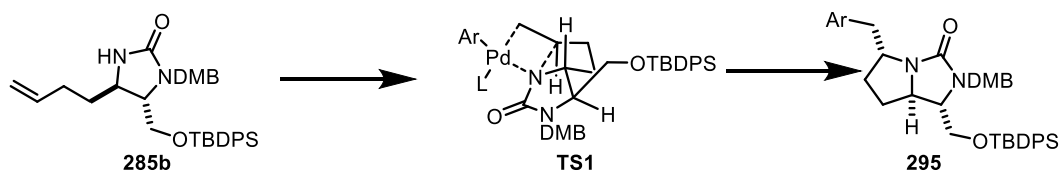
Given the poor diastereocontrol observed, something which was unexpected and at odds with the precedent, an alternative diastereoisomer of urea **285b** was prepared (Scheme 39) according the same reaction route; *syn* diastereoisomer from the nitro-Mannich reaction was reduced, protected with dimethoxybenzyl group and urea formed with CDI (as described for the *anti* diastereoisomer Scheme 36).



Scheme 39: Aminoarylation of substrate **285b**.

Using the same reaction conditions as for the *anti*, the aminoarylation reaction provided **295** as a single diastereoisomer. This result indicates that the poor diastereoselectivity observed with **285** was the result of the configuration set at the nitro-Mannich reaction and that there is a matched and mismatched effect with the relative configuration of the starting material and stereochemical outcome of the aminoarylation. As shown in Figure 40, conversions of **289b** and related substrates

is believed to occur through transition states such as **TS1** which minimises the ring strain.^{167,168} In the case of **285b** this is the lowest energy conformation which leads to the observed pyrroloimidazolone **295** in good diastereoselectivity.



Conditions: 1 mol % [(allyl)PdCl]₂, 4 mol% RuPhos, NaOtBu (1.2 eq.), Toluene, 80 °C

Figure 40: Transition state of **285b** towards pyrroloimidazolone **295**

The aminoarylation chemistry is well precedented to give the trans ring system with cyclic carbonates.^{167,168} Thus the stereochemical outcome of the aminoarylation was independently confirmed through a 500 MHz ¹H NMR 2D-NOESY experiment with **295** as depicted below. The stereochemistry of the remaining adducts was assigned by analogy.

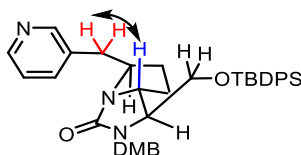
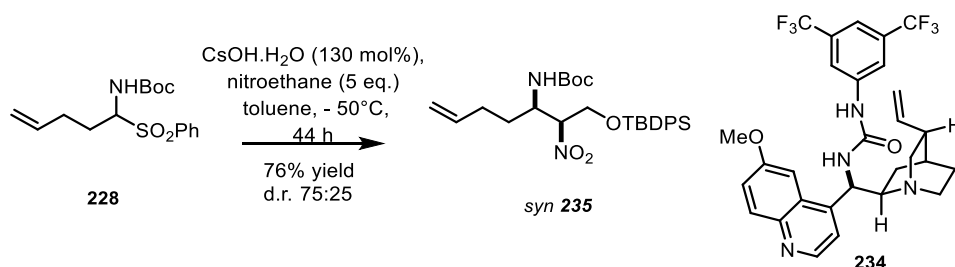


Figure 41: Structural confirmation about pyrroloimidazolone core came from the NOESY correlation between the 4-methyl protons (red), 7-H (blue) and 1-methyl protons (green) (see Section 6.8 for full details).

Given that failing, and the observation that an unalkylated cinchona urea catalyst **234** gave an enriched *syn* diastereoisomer, the nitro-Mannich reaction was attempted with this catalyst under the optimised reaction conditions.



Scheme 40: nitro-Mannich reaction with organocatalysts **234**.

Pleasingly, catalyst **234** provided *syn*-**235** as the major diastereoisomer in a 75:25 ratio (Scheme 40). On a preparative scale, the diastereoisomers could be separated to give an increased yield of the *syn* diastereoisomer.

4.7 Review of molecular properties of compounds derived from prepared scaffolds

To assess the value of the seven scaffolds prepared, a virtual library of functionalised compounds was enumerated using the protocol described previously. Except, the exemplar medicinal chemistry capping groups used in this enumeration was a carefully chosen sub section of the list used previously to more fully represent traditional capping groups used by medicinal chemists. In addition, the scaffolds prepared by aminoarylation reaction, only one capping group was exploited due to the variable nature of the reactant. The resulting virtual library comprised 2414 likely synthetically-accessible small molecules.

4.7.1 Assessment of Molecular weight and ALogP

First, the lead-likeness of the members of the virtual library was assessed (Figure 42). Compounds were successively filtered by molecular size ($14 \leq$ number of heavy atoms ≤ 26), lipophilicity ($-1 \leq$ ALogP ≤ 3) and undesirable structural features (Appendix 7: Table 15 for specific structural filters) using the same protocol as described. About 46% of the compounds in the virtual library had lead-like molecular properties, and the majority of the outlying compounds only narrowly failed the molecular property filters (heavy atoms: $\mu = 25.9$, $\sigma = 5.2$; ALogP: $\mu = 0.89$, $\sigma = 1.6$). By comparison, the ZINC database has just 23% of commercially available compounds which were lead-like.

Remarkably, it is also evident that, each one of the seven scaffolds allowed significant regions within lead-like chemical space to be targeted (For individual PMI scaffold graphs see Appendix 7: Figure 52). This unified synthetic approach thus specifically targeted lead-like chemical space.

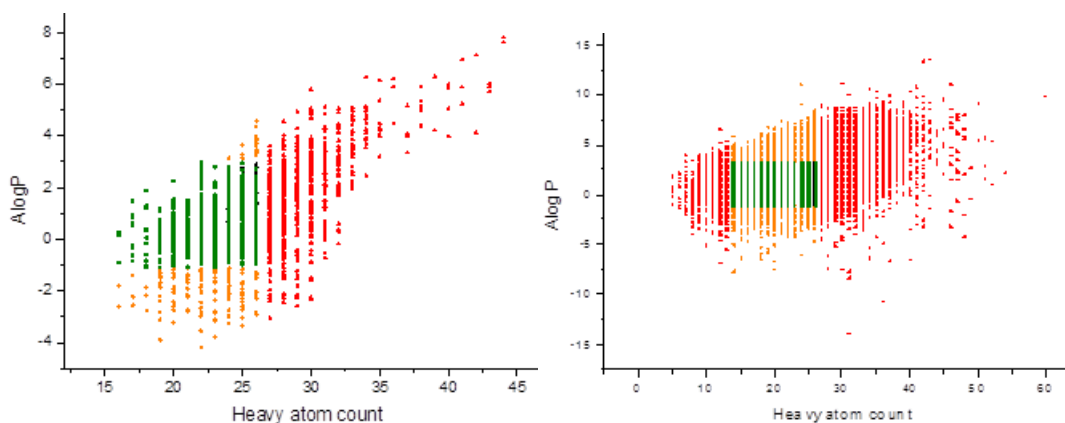


Figure 42: Analysis of the molecular properties of a virtual library of 2413 compounds derived from the seven molecular scaffolds and 2% of the ZINC database (90 911 randomly-selected compounds). Panel A: Distribution of the molecular properties of the virtual library. 46% of the compounds (green) survive successive filtering by molecular size ($14 \leq \text{number of heavy atoms} \leq 26$; failures shown in red) and lipophilicity ($-1 \leq \text{AlogP} \leq 3$; failures shown in orange) and various structural filters; 0.03% of the compounds (shown in black) failed the structural filters. Panel B: Distribution of the molecular properties of the compounds from the ZINC database. Using the same approach, 23% of the compounds survive the iterative filtering process, and 9% of the compounds fail a structural filter.

4.7.1.1 Assessment of Fraction of sp^3 carbons

Second, we determined the fraction of sp^3 hybridised carbon atoms (Fsp^3) in the virtual compounds (Figure 43). It has previously been shown that Fsp^3 correlates strongly with success because compounds in the discovery phase have lower Fsp^3 than marketed drugs.¹⁶⁹ It has thus been stated that accessing more three-dimensional lead compounds is a desirable goal.¹⁶⁹

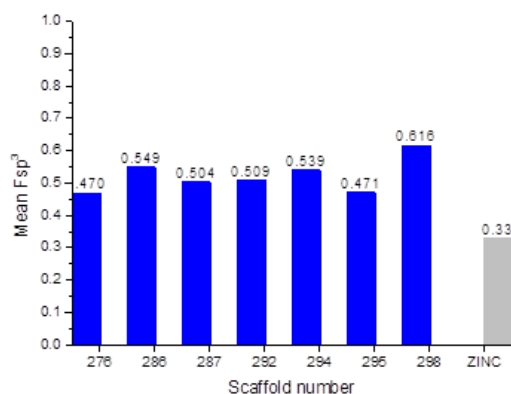


Figure 43: Mean Fsp^3 of the compounds from the ZINC database (red) and our virtual library (mean for the compounds based on each of the seven scaffolds, green).

The mean Fsp^3 of the virtual compounds (0.52) compared very favourably with that of the random sample of compounds from the ZINC database (0.33). Thus, our synthetic approach can yield compounds with significantly greater sp^3 character than most commercially-available compounds, thereby expanding the range of molecular

architectures available within lead-like chemical space and offering more flexibility in lead optimisation.

4.7.2 Assessment of Novelty

Third, the novelty and diversity of the seven scaffolds was assessed. A substructure search was performed in which the ZINC database was interrogated with each of the deprotected scaffolds. In general the bicyclic scaffolds were extremely novel with no substructures found within the ZINC database or CAS registry.

The diversity of, and relationship between, the scaffolds was assessed using a hierarchical analysis. The hierarchical framework analysis applied the ‘scaffold tree’ approach described by Schuffenhauer and co-workers. The results are summarized in Figure 44.

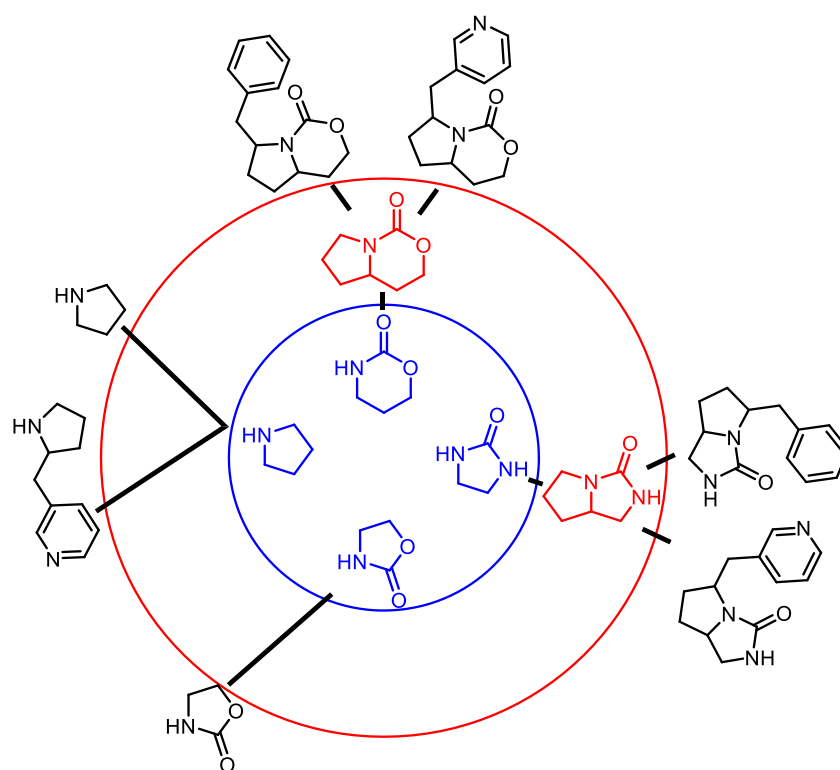


Figure 44: The hierarchal relationship between the 7 distinct molecular frameworks at the graph/node/bond level (black) and 5 parental frameworks (blue). Daughter frameworks are shown in red. The scaffolds that represent each framework are indicated.

It was found that seven frameworks were represented at the graph-node-bond level, which were related hierarchically to 4 “parent” frameworks. There is

significant scaffold diversity at each level of hierarchy, meaning that the scaffolds are not simply closely related derivatives.

4.7.3 Principle moments of inertia study

An alternative metric to access the three dimensionality of the compound was to conduct a Principal moments of inertia (PMI) study. The same 90,911 randomly selected compounds from the ZINC database used in Figure 45 was used to compare the shape diversity of the virtual library created from the scaffolds. For each compound, the two normalised PMI values were determined for a low energy conformation (For individual PMI plots of each scaffold, see Appendix 7: Figure 52).

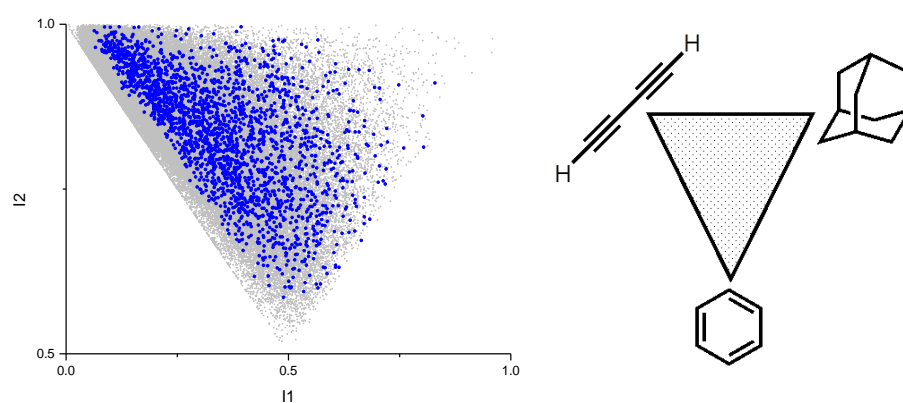


Figure 45: A normalised principal moment of inertia plot to show the shapes of the 2413 virtual compounds in relation to three idealised shapes; a rod, disk and sphere. A systematic shift away from the flat-linear edge of the graph can be observed for the virtual compounds derived from seven scaffolds (blue) when compared to 90 911 randomly selected compounds from ZINC database (grey).

By dividing the PMI plot into 20 bins (Figure 46), the three dimensionality of the library can be assessed by comparison to the same fraction of the ZINC database used in Figure 42. Notably, while 44% of the compounds in ZINC database fall within the first bin (i.e. lie along the flat-linear edge of the PMI plot in Figure 45), only 1.3% of the 2413 virtual library compounds fall within this bin. In addition, more than >80% of the virtual compound library falls in bins ≥ 4 (*cf.* <10% of the ZINC library of compounds). This is an additional indication that the methodology developed will target Fsp^3 rich compounds which may serve as better leads for drug discovery.

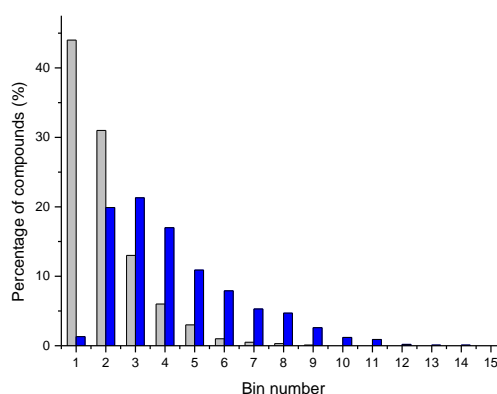


Figure 46: The relative proportions of the compounds found when the PMI was divided into twenty bins for 2% of the ZINC database (grey) versus the virtual library of compounds (blue). As a greater percentage of the virtual compound library occupies bins >3 a systematic shift away from the flat-linear edge of chemical space is observed. 15 of 20 bins shown.

4.7.4 Assessment of Synthetic economy

In total, seven diverse molecular scaffolds were prepared from just two different cyclisation precursors. Initially, pairs of building blocks were combined using a single connective reaction, the nitro-Mannich reaction, before a divergent synthetic approach was used to convert these cyclisation precursors into seven molecular scaffolds. This approach exploited a toolkit of just four cyclisation reactions, and required on average just 1.57 operations per scaffold from the key connective reaction (nitro-Mannich reaction). Furthermore, the unified and modular nature of the strategy means that it has the potential to deliver many additional scaffolds through expansion of the range of building blocks used (e.g. by use of homologated, and stereo- or region isomerically substituted variants).

4.8 Conclusions

This thesis has detailed the significant problems associated with the drug discovery. It described a new approach, termed lead-oriented synthesis, and highlighted the problems and potential advantages associated with this methodology (Chapter 1).

In Chapter 2, the problems encountered when attempting to re-tool the Petasis reaction for LOS was described in detail. While the reaction had been shown repeatedly^{71,78-82} it was suitable for the generation of chemical libraries, the properties of these compounds were outwith lead-like chemical space and it proved difficult to adapt the reaction.

Chapter 3 described the use of a computation protocol to direct the selection of a new connective reaction to support lead-oriented synthesis. The computational approach was developed within the group previously.⁶⁵ It then described the process used to robustly compare different connective reactions is given to select a new connective reaction.

This chapter has described the use of the nitro-Mannich reaction in support of lead-oriented synthesis. In combination of with the computation protocol, a diastereoselective protocol was identified. The unified synthetic approach yielded molecular scaffolds that were novel, diverse and lead-like. It was shown that functionalization of the scaffolds would allow significant lead-like chemical space to be targeted that complements that occupied by commercially-available molecules.

A key challenge in lead-oriented synthesis is still the identification of complementary and robust reactions with broad functional group compatibility, particularly convergent reactions that may be used to link building blocks. As such an increased armoury of such robust convergent reactions would crucially expand the relevant chemical space accessible to drug discovery programmes, and may help to address the grand challenge of increasing productivity in the pharmaceutical sector.

5 Experimental

5.1 Instrumentation and General Information

All non-aqueous reactions were performed under an atmosphere of nitrogen unless otherwise stated. Water-sensitive reactions were performed in oven-dried glassware, cooled under nitrogen before use. Solvents were removed *in vacuo* using a Büchi rotary evaporator and a Vacuubrand PC2001

Tetrahydrofuran (THF), DCM, toluene and CH₃CN were dried and purified by means of a Pure Solv MD solvent purification system (Innovative Technology Inc.). Anhydrous *N,N*-dimethylformamide (DMF) and 1,4-dioxane was obtained in SureSeal bottles from Sigma-Aldrich. All other solvents used were of chromatography or analytical grade. Petrol refers to petroleum spirit (b.p. 40-60 °C). Ether refers to diethyl ether. Commercially available starting materials were obtained from Sigma-Aldrich, Fluka, Acros or Alfa-Aesar and were used without purification unless stated.

Thin layer chromatography (TLC) was carried out on aluminium backed silica (Merck silica gel 60 F₂₅₄) plates supplied by Merck. Visualisation of the plates was achieved using an ultraviolet lamp ($\lambda_{\text{max}} = 254 \text{ nm}$), KMnO₄, anisaldehyde or ninhydrin. LC-MS was performed using an Agilent 1200 series LC system comprising of a Bruker HCT Ultra ion trap mass spec, a high vacuum degasser, a binary pump, a high performance autosampler and micro well plate autosampler, an autosampler thermostat, a thermostat column compartment and diode array detector. The system used Phenomenex Luna C18 50 x 2mm 5 micron column and two solvent systems: MeCN/H₂O + 0.1% Formic acid or MeCN/H₂O.

Flash chromatography was carried out using silica gel 60 (60-63 μm particles) supplied by Merck or using Biotage silica. Strong cation exchange solid phase extraction (SCX-SPE) was carried out using pre-packed Discovery DSC-SCX cartridges supplied by Supleco. Mass-directed HPLC purification was carried out using an Agilent 1260 Infinity HPLC system comprising an Agilent 6120 Quadrupole LC/MS and Agilent G1968D active splitter.

Optical rotation measurements were carried out at the sodium D-line (589 nm) on a Schmidt and Haensch H532 or an Optical Activity AA-1000 polarimeter instrument; concentrations are g/100 mL, temperatures given in °C, optical rotations are given in $10^{-1}\text{degcm}^2\text{g}^{-1}$ (units are omitted). Infrared spectra were recorded on a Perkin-Elmer One FT-IR spectrometer with absorption reported in wavenumbers (cm^{-1}).

High resolution mass spectra (HRMS) were recorded on a Bruker Daltonics micrOTOF or Bruker MaXis Impact spectrometer with electrospray ionisation (ESI) source. Where EI ionisation was required, a Waters/Micromass GCT Premier spectrometer was used.

Proton (^1H) and carbon (^{13}C) NMR spectral data were collected on a Bruker Advance 400, 500 or 600, Bruker DPX500 or DPX300 spectrometers. Chemical shifts (δ) are quoted in parts per million (ppm) and referenced to the residual solvent peak or downfield of tetramethylsilane. Coupling constants (J) are quoted in Hertz (Hz) and splitting patterns reported in an abbreviated manner: app. (apparent), s (singlet), d (doublet), t (triplet), q (quartet), m (multiplet). Assignments were made with the aid of COSY, DEPT-135, HMQC, HMBC, TOCSY and NOESY experiments.

A Julabo FT902 Immersion Cooler was used to cool the reaction mixture to $-50\text{ }^\circ\text{C}$ where required.

General Method A1

Glycolaldehyde dimer (**97**) (0.6 eq.) was added to a stirred solution of *trans*-2-phenylvinylboronic acid (**74**) (1.2 eq.) in water (10 mL/mmol substrate). The reaction mixture was stirred at rt for 10 mins. The amine (1 eq.) added, stirred for 48 hr and 5M HCl_(aq) was added until the pH of the reaction mixture was 1. The aqueous layer was washed with DCM (3 × 30 mL/mmol substrate), K₂CO₃ was added until the pH of the reaction mixture was 10 and the aqueous layer was extracted with DCM (3 × 30 mL/mmol substrate), dried (MgSO₄), filtered and concentrated *in vacuo* to give a crude product.

General Method A2

This procedure is identical to procedure A1 except DCM (10 mL/mmol substrate) was used as a solvent.

General Method A3

This procedure is identical to procedure A1 except DCE–HFIP (9:1 v/v, 10 mL/mmol substrate) was used as a solvent.

General Method A4

Glycolaldehyde dimer (**97**) (0.6 eq.) was added to a stirred solution of vinylboronic acid pinacol ester (**100**) (1.2 eq.) in water–THF (83:17 v/v, 10 mL/mmol substrate, 10 mL/mmol substrate). The reaction mixture was stirred at rt for 10 mins. The amine (1 eq.) added, stirred for 48 hr and 5M HCl_(aq) was added until the pH of the reaction mixture was 1. The aqueous layer was washed with DCM (3 × 30 mL/mmol substrate), K₂CO₃ was added until the pH of the reaction mixture was 10 and the aqueous layer was extracted with DCM (3 × 30 mL/mmol substrate), dried (MgSO₄), filtered and concentrated *in vacuo* to give a crude product.

General Method B

Aldehyde (1.5 eq.), *tert*-butyl carbamate (1 eq.) and sodium benzenesulfinate (1.5 eq.) were suspended in H₂O–MeOH (66:34) and formic acid was added (0.32 mL/mmol substrate) and the reaction mixture was stirred in a sealed flask at rt for 2 days. The reaction mixture was filtered, yielding a white precipitate which was

washed with ether (20 mL/mmol substrate) and water (20 mL/mmol substrate) and concentrated *in vacuo* to give the title compound.

General Method C

To a stirred solution of sodium nitrite (1.05 eq.) in DMSO (0.3 M) was added 5-bromobut-1-ene (1 eq.), and the reaction mixture was stirred at rt for 2 hr. The pale yellow solution was then partitioned between water (50 mL/mmol substrate) and ether (50 mL/mmol substrate), and the organic phase was separated. The aqueous layer was extracted with ether (5 × 30 mL/mmol substrate), and the combined organic extracts were washed with brine (3 × 30 mL/mmol substrate) then dried (MgSO₄), filtered and concentrated *in vacuo* to give a crude mixture.

General Method D

According to the procedure⁸⁴ *tert*-butyl-diphenylsilyl chloride (1.1 eq.) added dropwise to the stirred solution of alcohol (1 eq.) and imidazole (3 eq.) in DMF (0.4 M) over 1 hr. The reaction mixture was left to stir for a further 12 hr then water and DCM was added. The phases were separated and the aqueous phase was extracted with DCM (3 × 10 mL/mmol substrate). The combined organic phase was washed with *sat.* NaHCO_{3(aq)}, water, and brine, then dried (MgSO₄), filtered and concentrated *in vacuo* to give a crude mixture.

General Method E

Amidosulfone (1 eq.) was suspended in toluene (0.2 M) and the nitro compound (5 eq.) was added and the resulting mixture was cooled to -50 °C. Freshly acquired CsOH.H₂O (5 eq.) was added and the resulting suspension was stirred vigorously for 48 h. 1 M HCl (until pH 3) was added and the solution was allowed to warm to ambient temperature. The aqueous layer was extracted with DCM (3 × 30 mL/mmol substrate), then the combined organic extracts were dried (Na₂SO₄), filtered and concentrated *in vacuo* to give a crude product.

General Method F

Substrate (1 eq.) was dissolved in THF (0.4 M) and added drop wise to stirred 1 M solution of LiAlH₄ (2.1 mL/mmol substrate). The mixture was stirred for 18 h then H₂O (1 mL per 1 g of LiAlH₄), 2 M NaOH (2 mL per 1 g of LiAlH₄) and H₂O (3 mL per 1 g of LiAlH₄) was added in that order and left to stir for 30 mins. The reaction mixture was then concentrated *in vacuo*, dissolved in EtOAc (50 mL/ mmol substrate) washed successively with water (3 × 30 mL/mmol substrate) and brine (3 × 30 mL/mmol substrate), and then dried (MgSO₄), filtered and concentrated *in vacuo* to give a crude product.

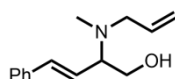
General Method G

By **General Method F**, then crude amine was dissolved in DCM (0.2 M) then Et₃N (3 eq.) and (*R*)-MPTA-Cl (1.2 eq.) or (*S*)-MPTA-Cl (1.2 eq) was added and the reaction stirred for 19 h. The reaction mixture was diluted with ether (3 ml) and water (1 ml) and the layers separated. The aqueous layer was extracted with ether (3 × 3 mL), the organic layers dried (Na₂SO₄), filtered and concentrated *in vacuo*. The crude material was then analysed by 500 MHz ¹H NMR spectroscopy to determine the diastereomeric ratio.

General Method H

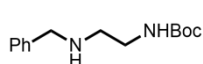
[(allyl)Pd(Cl)]₂ (1 mol%), CyJohnPhos (4 mol%), and NaO^tBu (1.2 eq.) then a solution of the substrate (1 eq.) and the aryl halide (1.2 eq.) in toluene (4 mL/mmol substrate) was added and heated to 80 °C for 18 h. The reaction mixture was cooled to rt and *sat.* NH₄Cl_(aq) (2 mL/mmol substrate) and EtOAc (5 mL/mmol substrate) were added. The aqueous layer was extracted with ethyl acetate (4 x 5 mL/mmol substrate). The combined organic layers were dried (Na₂SO₄), filtered, and concentrated *in vacuo*.

(3E)-2-[Methyl(allyl)amino]-4-phenylbut-3-en-1-ol (98)



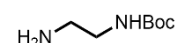
By **General Method A1**, using *N*-allylmethylamine (0.16 mL, 1.67 mmol), filtered through a silica plug, eluting with DCM–MeOH (90:10) gave the *amino alcohol* **98** (0.241 g, 84%) as a yellow liquid; R_f 0.20 (90:10 DCM–MeOH); δ_H (500 MHz, $CDCl_3$); 7.41 (2H, d, J 7.5, Ar), 7.36 (2H, t, J 7.5, Ar), 7.29 (1H, t, J 7.5, Ar), 6.56 (1H, d, J 16.0, 4-H), 6.17 (1H, dd, J 16.0 and 9.0, 3-H), 5.87 (1H, ddd, J 17.2, 13.7 and 10.2, allyl 2-H), 5.23 (1H, d, J 17.2, allyl 3- H_A), 5.19 (1H, d, J 10.2, allyl 3- H_A), 3.66 (1H, app t, J 10.4, 1- H_A), 3.60 (1H, dd, J 10.4 and 5.4, 1- H_B), 3.44 (1H, td, J 9.0 and 5.4, 2-H), 3.27 (1H, dd, J 13.7 and 6.5, allyl 1- H_A), 3.08 (1H, dd, J 13.7 and 6.5, allyl 1- H_B) 2.31 (3H, s, NMe); δ_C (75 MHz, $CDCl_3$); 136.5 (Ar), 136.0 (4-C), 134.9 (allyl 2-C), 128.6 (Ar), 127.8 (Ar), 126.4 (Ar), 123.7 (allyl 1-C), 117.5 (3-C), 65.8 (2-C), 61.1 (1-C), 56.9 (allyl 3-C), 36.5 (NMe), OH not observed; ν_{max}/cm^{-1} (neat); 3401, 2977, 1449 and 1045; m/z (ES) 218.2; HRMS Found: 218.1537, ($C_{14}H_{19}NO$ MH^+ requires 218.1539). This compound has previously been prepared but characterisation data has not been reported.

***tert*-Butyl-*N*-[2-(benzylamino)ethyl]carbamate (**105**)⁸⁵**



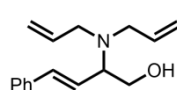
tert-Butyl-*N*-(2-ethylamino)carbamate (**107**) (0.31 g, 1.9 mmol), in MeOH (1 mL, 2 M) was added to benzaldehyde (1.2 eq.), 4 Å MS in MeOH (20 mL, 0.1 M) and stirred for 16 hr. Sodium borohydride (5 eq.) was added in small portions over 60 mins and reaction mixture stirred for 4 hr. The reaction mixture was concentrated *in vacuo*, partitioned between EtOAc (80 mL) and water (80 mL), the organic layer was extracted with 0.5 M HCl_(aq) (5 × 30 mL) and the combined aqueous layers were neutralised by the addition of 2 M NH₄OH (pH 10). The aqueous layer was then extracted with chloroform (5 × 20 mL), combined, dried (MgSO₄), filtered and concentrated *in vacuo* then purified by column chromatography eluting with DCM–EtOH–NH₄OH (84:14:2)⁸⁵, to give the amino carbamate⁸⁵ **105** (0.27 g, 64%) as a colourless oil; R_f 0.35 (90:10 DCM–MeOH); δ_H (500 MHz, CDCl₃); 7.35–7.30 (4H, m, Ar), 7.26–7.21 (1H, m, Ar), 4.92 (1H, bs, NH), 3.79 (2H, s, benzyl 1-H₂), 3.24 (2H, t, *J* 5.5, ethyl 2-H₂), 2.75 (2H, t, *J* 5.5, ethyl 1-H₂), 1.49 (1H, bs, NH), 1.44 (9H, s, Boc); δ_C (125 MHz, CDCl₃); 156.1 (C=O), 139.0 (Ar 1-C), 129.0 (Ar), 128.7 (Ar), 127.3 (Ar), 92.0 (Boc 2-C), 53.5 (benzyl C-1), 47.5 (ethyl C-2), 40.6 (ethyl C-1), 28.5 (Boc 3-C); *m/z* (ES) 251.2; HRMS Found: 251.1752, (C₁₄H₂₂N₂O₂ MH⁺ requires 251.1754).

***tert*-Butyl-*N*-(2-ethylamino)carbamate (**107**)⁸⁴**



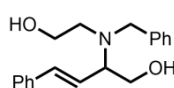
According to the procedure⁸⁴ di-*tert*-butyl dicarbonate (2.3 g, 10.6 mmol) was dissolved in DCM (200 mL) and added dropwise to the stirred solution of ethylene diamine (3.7 mL, 54.6 mmol) in DCM (200 mL) over 8 hr. The reaction mixture was left to stir for a further 12 hr and then concentrated *in vacuo*. The crude mixture was purified by flash chromatography, eluting with DCM–MeOH (90:10), to give the aminocarbonate⁸⁴ **107** (1.20 g, 71%) as a viscous yellow oil; R_f 0.10 (90:10 DCM–MeOH); δ_H (500 MHz, CDCl₃); 4.96 (1H, bs, NH), 3.17 (2H, d, *J* 5.4, 2-H₂), 2.81 (2H, t, *J* 5.4, 1-H₂), 1.54 (2H, bs, NH₂), 1.45 (9H, s, Boc); δ_C (125 MHz, CDCl₃); 156.2 (C=O), 79.2 (Boc 2-C), 43.3 (2-C), 41.9 (1-C), 28.4 (Boc 3-C); ν_{max}/cm⁻¹ (film); 3358, 2977, 1698, 1526, 1256; *m/z* (ES) 161.1; HRMS Found: 161.1293, (C₇H₁₆N₂O₂ MH⁺ requires 161.1290).

(3E)-2-(Diallylamino)-4-phenylbut-3-en-1-ol (112)¹⁷⁰



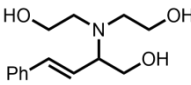
By **General Method A1**¹⁷⁰, using diallylamine (0.32 mL, 2.6 mmol), filtered through a silica plug, eluting with DCM–MeOH (90:10) gave the amino alcohol¹⁷⁰ **112** (0.44 g, 70%). R_f 0.25 (90:10 DCM–MeOH); δ_H (500 MHz, $CDCl_3$); 7.38–7.35 (5H, m, Ar), 6.52 (1H, d, J 16.0, 4-H), 6.11 (1H, dd, J 16.0 and 7.6, 3-H), 5.85 (2H, ddd, J 18.2, 10.0, 5.5, allyl 2- H_2), 5.17–5.27 (4H, m, allyl 3-H), 3.55–3.67 (3H, m, 1-H and 2-H), 3.42–3.39 (2H, m, allyl 1- H_B), 3.25 (1H, bs, OH), 2.99 (2H, dd, J 8.1, allyl 3- H_A); δ_C (75 MHz, $CDCl_3$); 136.5 (Ar), 136.2 (4-C), 135.0 (allyl 2-C), 128.7 (Ar), 127.9 (Ar), 126.4 (Ar), 123.8 (3-C), 117.7 (allyl 1-C), 62.3 (2-C), 61.0 (1-C), 52.4 (allyl 3-C); ν_{max}/cm^{-1} (neat) 3401, 2159, 1449 and 1032; m/z (ES) 244.2; HRMS Found: 244.1704, ($C_{16}H_{21}NO$ MH^+ requires 244.1696).

(3E)-2-[(2-Hydroxyethyl)benzylamino]-4-phenylbut-3-en-1-ol (113)



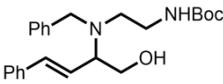
By **General Method A1**, using *N*-benzylaminoethanol (0.240 mL, 1.69 mmol), filtered by through a silica plug, eluting with DCM–MeOH (90:10) gave the *amino alcohol* **113** (0.30 g, 63%) as a brown oil; R_f 0.30 (90:10 DCM–MeOH); δ_H (500 MHz, $CDCl_3$); 7.36–7.22 (10H, m, Ar), 6.44 (1H, d, J 16.0, 4-H), 6.06 (1H, dd, J 16.0 and 9.0, 3-H), 3.80 (1H, d, J 6.0, benzyl H_A), 3.74 (1H, d, J 6.0, benzyl H_B), 3.67–3.54 (2H, m, hydroxyethyl 2-H), 3.52–3.38 (2H, m, hydroxyethyl 1-H), 2.91 (1H, ddd, J 14.0, 9.0 and 4.8, 2-H), 2.77–2.71 (1H, m, 1- H_A), 2.56 (1H, dt, J 14.0 and 3.4, 1- H_B), 2.34–2.15 (2H, bs, OH); δ_C (75 MHz, $CDCl_3$); 136.5 (Ar), 134.7 (4-C), 128.7 (Ar), 128.4 (Ar), 128.1 (Ar), 127.9 (Ar), 127.6 (Ar), 126.9 (Ar), 126.4 (Ar), 123.4 (3-C), 69.7 (benzyl 1-C) 63.9 (2-C), 61.8 (1-C), 59.6 (hydroxyethyl 1-C), 51.9 (hydroxyethyl 2-C); ν_{max}/cm^{-1} (neat); 3368, 2159, 1452; m/z (ES) 298.2; HRMS Found: 298.1803, ($C_{19}H_{23}NO_2$ MH^+ requires 298.1802).

(3E)-2-[Bis(2-hydroxyethyl)amino]-4-phenylbut-3-en-1-ol (114)

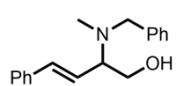
 By **General Method A1**, using bis(hydroxyethyl)amine (0.17 mL, 1.42 mmol), filtered by through a silica plug, eluting with DCM–MeOH (90:10) gave the *amino alcohol* **114** (0.24 g, 53%) as a pale yellow oil; R_f 0.15 (90:10 DCM–MeOH); δ_H (500 MHz, $CDCl_3$); 7.25–7.35 (5H, m, Ar), 6.51 (1H, d, J 16.0, 4-H), 6.05 (1H, dd, J 16.0 and 8.4, 3-H), 4.05 (3H, bs, OH), 3.76 (2H, dd, J 10.8 and 2.8, 1-H₂), 3.62 (4H, dd, J 11.5 and 4.6, hydroxyethyl 1-H), 3.56–7.52 (1H, m, 2-H), 2.88 (2H, J 13.8, 10.3 and 3.3, hydroxyethyl 2-H_A), 2.60 (2H, dt, J 3.3, hydroxyethyl 2-H_B); δ_C (75 MHz, $CDCl_3$); 136.5 (Ar), 134.7 (4-C), 128.7 (Ar), 127.9 (Ar), 126.4 (Ar), 123.4 (3-C), 63.9 (2-C), 61.8 (1-C), 59.6 (hydroxyethyl 1-C), 51.9 (hydroxyethyl 2-C); ν_{max}/cm^{-1} (neat); 3368, 2159, 2030, 1976, 1072, 1033; m/z (ES) 252.2; HRMS Found: 252.1595, ($C_{14}H_{21}NO_3$ MH^+ requires 252.1594).

(3E)-2-[(*tert*-Butylethylcarbamate)benzylamino]-4-phenylbut-3-en-1-ol

(115)

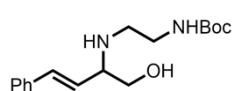
 By **General Method A2**, using *tert*-butyl-*N*-(2-{benzylamino}ethyl) carbamate (0.2 g, 0.8 mmol) in DCE (1 mL), filtered by through a silica plug, eluting with DCM–MeOH (90:10) gave the *amino alcohol* **115** (0.26 g, 86%) as a yellow oil. R_f 0.15 (90:10 DCM–MeOH); δ_H (500 MHz, $CDCl_3$); 7.43–7.19 (10H, m, Ar), 6.58 (1H, d, J 16.0, 4-H), 6.01 (1H, dd, J 16.0, 7.6, 3-H), 3.68 (1H, dd, J 10.6, benzyl 1-H_A), 3.47 (1H, d, J 10.6, benzyl 1-H_B), 3.36 (1H, td, J 7.6 and 4.0, 2-H), 3.24–3.18 (1H, bs, OH or NH), 2.95–2.87 (4H, m, ethyl 1-H₂ and 2-H₂), 2.85 (1H, dd, J 12.3 and 4.0, 1-H_B), 2.71 (1H, dd, J 12.3 and 4.0, 1-H_A), 1.26 (9H, s, Boc), NH or OH not observed; δ_C (125 MHz, $CDCl_3$); 158.7 (C=O), 136.4 (Ar), 135.7 (Ar) 132.4 (4-C), 128.6 (Ar), 128.5 (Ar), 127.9 (Ar), 127.7 (Ar), 127.2 (Ar), 126.5 (Ar), 117.3 (3-C), 74.9 (Boc 2-C), 66.4 (1-C), 64.5 (2-C), 61.3 (ethyl 2-C), 59.4 (ethyl 1-C), 40.8 (benzyl), 28.4 (Boc 3-C); ν_{max}/cm^{-1} (neat); 3353 2976 1693 1518 1392 1252 1170; m/z (ES) 396.24.

(3E)-2-(Benzyl(methyl)amino)-4-phenylbut-3-en-1-ol (116)¹⁷⁰



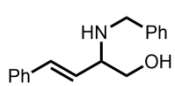
By **General Method A2**¹⁷⁰, using *N*-methylbenzylamine (0.18 mL, 1.4 mmol), filtered by through a silica plug, eluting with DCM–MeOH (90:10) gave the amino alcohol¹⁷⁰ **116** (0.30 g, 79%) as a brown oil; R_f 0.15 (90:10 DCM–MeOH); δ_H (500 MHz, $CDCl_3$); 7.41 (2H, d, J 7.4, Ar), 7.35–7.31 (6H, m, Ar), 7.28 (2H, d, J 7.4, Ar), 6.57 (1H, d, J 16.0, 4-H), 6.20 (1H, dd, J 16.0 and 9.2, 3-H), 3.77 (1H, d, J 13.0, benzyl 1- H_B), 3.69 (1H, app t, J 10.4, 1- H_A), 3.58 (1H, dd, J 10.4 and 5.4, 1- H_B), 3.54 (1H, d, J 13.0, benzyl 1- H_A), 3.46 (1H, dd, J 9.2 and 5.4, 2-H), 2.48 (1H, bs, OH), 2.27 (3H, s, methyl); δ_C (125 MHz, $CDCl_3$); 141.5 (Ar), 130.9 (4-C), 130.2 (Ar), 129.6 (Ar), 129.5 (Ar), 129.6 (Ar) 129.0 (Ar), 128.7 (Ar), 127.1 (Ar), 115.1 (3-C), 67.5 (benzyl 1-C), 60.9 (2-C), 59.5 (1-C), 36.2 (NMe); ν_{max}/cm^{-1} (neat); 3306, 2959, 1650, 1458; m/z (ES) 268.2; HRMS Found: 268.1700, ($C_{18}H_{21}NO$ MH^+ requires 268.1696).

(3E)-2-[(*tert*-Butylethylcarbamate)amino]-4-phenylbut-3-en-1-ol (117)



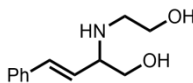
By **General Method A2**, using butyl-*N*-(2-ethylamino)carbamate (0.27g, 1.7 mmol, in 1 mL of DCE), filtered by flash chromatography, eluting with DCM–MeOH (90:10) gave the *amino alcohol* **117** (0.37 g, 71%) as yellow oil; R_f 0.22 (90:10 DCM–MeOH); δ_H (500 MHz, $CDCl_3$); 7.32 (2H, d, J 7.5, Ar), 7.25 (2H, t, J 7.5, Ar), 7.18 (1H, t, J 7.5, Ar), 6.48 (1H, d, J 16.0, 4-H), 5.95 (1H, dd, J 16.0 and 7.9, 3-H), 5.42 (1H, bs, NH), 3.69–3.64 (2H, m, OH and 2-H), 3.48–3.46 (1H, m, ethyl 1-H), 3.33 (1H, d, J 5.0, 1-H), 3.19–3.17 (2H, m, ethyl 2- H_2), 2.76 (1H, dd, J 11.7 and 5.5, 1- H_B), 2.61 (1H, dd, J 11.7 and 5.5, 1- H_A), 1.42 (1H, bs, NH), 1.39 (9H, s, Boc); m/z (ES) 307.3.

(3E)-2-(Benzylamino)-4-phenylbut-3-en-1-ol (118)¹⁷¹



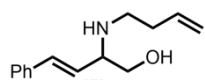
By **General Method A3**¹⁷¹, using *N*-benzylamine (0.15 mL, 1.4 mmol), DCE–HFIP (14 mL), filtered by through a silica plug, eluting with DCM–MeOH (90:10) gave the amino alcohol¹⁷¹ **118** (0.25 g, 70%) yellow oil; R_f 0.18 (90:10 DCM–MeOH); δ_H (500 MHz, $CDCl_3$); 7.39 (2H, d, J 7.4, Ar), 7.37–7.26 (8H, m, Ar), 6.58 (1H, d, J 15.9, 4-H), 6.06 (1H, dd, J 15.9 and 8.0, 3-H), 4.16 (1H, bs, NH), 3.93 (1H, d, J 13.2, benzyl 1- H_B), 3.74 (1H, d, J 13.2, benzyl 1- H_A), 3.70 (1H, dd, J 10.1 and 4.5, 1- H_A), 3.51 (1H, app t, J 10.1, 1- H_B), 3.41 (1H, td, J 8.0 and 4.5, 2-H), 2.48 (1H, bs, OH); δ_C (125 MHz, $CDCl_3$); 136.5 (Ar), 133.0 (4-C), 128.6 (Ar), 128.5 (Ar), 128.2 (Ar), 127.8 (Ar), 127.6 (Ar), 127.4 (Ar), 127.1 (Ar), 126.4 (3-C), 64.9 (benzyl 1-C), 61.6 (2-C), 51.0 (1-C); ν_{max}/cm^{-1} (film); 3335, 2970, 2873, 1594, 1371, 1264; m/z (ES) 208.1; HRMS Found: 208.1335, ($C_{17}H_{19}NO$ MH^+ requires 208.1332).

(3E)-2-[(2-Hydroxyethyl)amino]-4-phenylbut-3-en-1-ol (119)



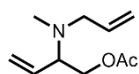
By **General Method A3**, using *N*-ethanolamine (0.12 mL, 2 mmol), DCE–HFIP (14 mL), followed by flash chromatography, eluting with DCM–MeOH (90:10) gave the *amino alcohol* **119** (0.16 g, 39%) as yellow oil; R_f 0.15 (90:10 DCM–MeOH); δ_H (500 MHz, $CDCl_3$); 7.28–7.25 (5H, m, Ar), 6.46 (1H, d, J 15.8, 4-H), 5.96 (1H, dd, J 15.8 and 8.1, 3-H), 3.65 (3H, app bs, hydroxyethyl 2-H, 1- H_A), 3.50 (1H, d, J 13.5, 1- H_B), 3.33 (1H, app bs, 2-H), 2.84 (1H, d, J 4.3, hydroxyethyl 1- H_A), 2.68 (1H, app bs, hydroxyethyl 2- H_B), 2.40 (3H, bs, NH, OH and OH); δ_C (75 MHz, $CDCl_3$); 136.5 (Ar), 133.3 (4-C), 128.7 (Ar), 128.6 (Ar), 128.2 (Ar), 126.4 (3-C), 65.0 (1-C), 62.6 (2-C), 61.1 (hydroxyethyl 2-C), 48.7 (hydroxyethyl 1-C); ν_{max}/cm^{-1} (neat); 3368, 2159, 2030, 1976, 1072, 1033; m/z (ES) 208.1; HRMS Found: 208.1335, ($C_{12}H_{17}NO_2$ MH^+ requires 208.1332).

(3E)-2-(But-3-enylamino)-4-phenylbut-3-en-1-ol (120)



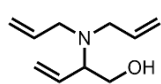
By **General Method A1**, using *N*-butenylamine hydrochloride (0.25 g, 2.3 mmol) and Et₃N (1 eq.) followed by SCX column, eluting with *sat.* NH₃ in MeOH, gave the *amino alcohol* **120** (0.23 g, 46%) as a dark yellow oil. R_f 0.21 (90:10 DCM–MeOH); δ_H (500 MHz, CDCl₃); 7.38 (2H, d, *J* 7.4, Ar), 7.32 (2H, t, *J* 7.4, Ar), 7.23 (1H, d, *J* 7.4, Ar), 6.55 (1H, d, *J* 15.9, 4-H), 6.03 (1H, dd, *J* 15.9 and 7.9, 3-H), 5.79 (1H, ddt, *J* 17.2, 10.2 and 6.8, 3'-H), 5.10 (1H, dd, *J* 10.2 and 1.6, butenyl 4-H_A), 5.06-5.04 (1H, m, butenyl 4-H_B), 3.68 (1H, dd, *J* 10.5 and 4.6, butenyl 2-H_A), 3.46 (1H, dd, *J* 10.5 and 7.9, butenyl 2-H_B), 3.35 (1H, dt, *J* 7.9 and 6.0, 2-H), 2.82 (1H, dt, *J* 11.5 and 6.0, 1-H_A), 2.63 (1H, dt, *J* 11.5 and 6.0, 1-H_B), 2.29-2.26 (3H, m, 1'-H and NH or OH), 2.02 (1H, bs, NH or OH); δ_C (75 MHz, CDCl₃); 141.4 (Ar), 136.3 (4-C), 132.6 (butenyl 3-C), 129.0 (Ar), 128.6 (Ar), 127.7 (Ar), 126.4 (3-C), 116.6 (butenyl 4-C), 64.8 (1-C), 62.3 (butenyl 2-C), 46.1 (2-C), 34.5 (butenyl 1-C); ν_{max}/cm⁻¹ (neat); 3436, 1976, 1416; *m/z* (ES) 218.2; HRMS Found: 218.1537, (C₁₄H₁₉NO *MH*⁺ requires 218.1539).

2-[(Allyl)methylamino]-but-3-enyl acetate (122)



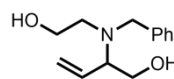
By **General Method A4**, using *N*-allylmethylamine (0.14 mL, 1.5 mmol) the solvent was removed *in vacuo* after 48 hr. The crude material was dissolved in pyridine (1.5 mL), acetic anhydride (0.14 mL, 1.45 mmol) was added and the reaction mixture stirred at rt for 18 hr. The solvent was removed *in vacuo* followed by flash chromatography, eluting with DCM–MeOH (90:10) gave the *amino acetate* **122** (36 mg, 13%) as a dark brown oil; R_f 0.30 (90:10 DCM–MeOH); δ_H (500 MHz, CDCl₃); 5.98 (1H, dddd, *J* 17.1, 10.2, 7.7 and 6.1, allyl 2-H), 5.81 (1H, ddd, *J* 17.4, 10.4 and 9.1, 3-H), 5.51 (1H, dd, *J* 10.2 and 1.1, allyl 3-H_A), 5.43-5.40 (2H, m, 4-H₂), 5.38 (1H, dd, *J* 17.1 and 1.2, allyl 3-H_B), 3.80 (1H, dd, *J* 12.3 and 4.8, 1-H_A), 3.77 (1H, dd, *J* 12.3 and 4.8, 1-H_B), 3.65 (1H, td, *J* 8.5 and 4.8, 2-H), 3.55 (1H, dd, *J* 13.3 and 6.1, allyl 1-H_B), 3.35 (1H, dd, *J* 13.3 and 7.7, allyl 1-H_A), 2.59 (3H, s, NMe), 2.02 (3H, s, acetate methyl); δ_C (75 MHz, CDCl₃); 177.0 (C=O), 129.9 (allyl 2-C), 128.5 (3-C), 124.2 (allyl 3-C), 122.8 (3-C), 67.4 (2-C), 60.8 (1-C), 56.9 (allyl 1-C), 36.5 (NMe), 22.2 (acetate methyl); ν_{max}/cm⁻¹ (neat); 3326, 2928, 1714, 1580, 1413; *m/z* (ES) 183.4; Unable to observe *MH*⁺ in mass spectrometer.

2-[Bis(allyl)amino]but-3-en-1-ol (**123**)



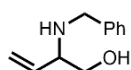
By **General Method A4**, using diallylamine (0.19 mL, 2.5 mmol), filtered through a silica plug, eluting with Petrol–EtOAc (50:50) gave the *amino alcohol* **123** (0.25 g, 62%) as an orange oil; R_f 0.20 (90:10 DCM–MeOH); δ_H (500 MHz, $CDCl_3$); 5.78 (2H, ddd, J 17.3, 10.2 and 8.1, allyl 2- H_2), 5.70 (1H, ddd, J 17.3, 10.5, 8.1 3-H), 5.29 (1H, dd, J 10.5, 4-H), 5.17-5.12 (5H, m, allyl 3-H, 4- H_B), 3.55-3.53 (2H, m, allyl 1- H_A), 3.48-3.45 (2H, m, allyl 1- H_B), 3.43 (1H, bs, OH), 3.33 (2H, app d, J 14.2, 1- H_2), 2.90 (1H, dd, J 14.2 and 8.1, 2-H). δ_C (75 MHz, $CDCl_3$); 136.2 (4-C), 135.0 (allyl 2-C), 123.8 (3-C), 117.7 (allyl 1-C), 62.3 (2-C), 61.0 (1-C), 52.4 (allyl 3-C); ν_{max}/cm^{-1} (film); 2978, 2930, 1473, 1452, 1145 ; m/z (ES) 168.2; HRMS Found: 168.1382, ($C_{10}H_{17}NO$ MH^+ requires 168.1383).

2-[Benzyl(2-hydroxyethyl)amino]but-3-en-1-ol (**124**)



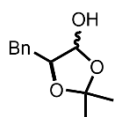
By **General Method A4**, using *N*-benzylaminoethanol (0.21 mL, 1.5 mmol) followed by flash chromatography, eluting with DCM–MeOH (90:10) gave the *amino alcohol* **124** (0.26 g, 71%) yellow oil; R_f 0.25 (90:10 DCM–MeOH); δ_H (500 MHz, $CDCl_3$); 7.42-7.10 (5H, m, Ar) 5.74 (1H, ddd, J 17.3, 10.5 and 8.3, 3-H), 5.33 (1H, dd, J 10.5 and 1.3, 4- H_B), 5.18 (1H, dd, J 17.3 and 1.3, 4- H_B), 3.85 (1H, d, J 13.7, 1- H_A), 3.62 (2H, app t, J 10.7, benzyl 1- H_2), 3.50 (1H, dd, J 13.7 and 5.4, 1- H_B), 3.34-3.32 (1H, m, 2-H), 2.90 (2H, dd, J 14.0, 4.0, hydroxyethyl 1- H_2), 2.56 (2H, dt, J 14.0 and 4.0, hydroxyethyl 2- H_2); δ_C (125 MHz, $CDCl_3$); 139.3 (Ar), 130.5 (3-C), 130.0 (Ar), 129.8 (Ar), 129.3 (Ar), 124.7 (4-C), 64.7 (benzyl 1-C), 60.4 (1-C), 57.5 (hydroxyethyl 2-C), 53.8 (2-C), 50.1 (hydroxyethyl 1-C). ν_{max}/cm^{-1} (film); 3321, 2932, 2879, 1472, 1371, 1265, 1025; m/z (ES) 222.2; HRMS Found: 222.1493, ($C_{13}H_{19}NO_2$ MH^+ requires 222.1489).

2-(Benzylamino)but-3-en-1-ol (**125**)¹⁷²



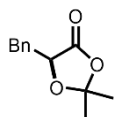
By **General Method A4**, using *N*-benzylamine (0.16 mL, 1.5 mmol) followed by flash chromatography, eluting with DCM–MeOH (90:10) gave the amino alcohol¹⁷² **125** as a yellow oil (68 mg, 39%); R_f 0.15 (90:10 DCM–MeOH); δ_H (500 MHz, CDCl₃); 7.51-7.23 (5H, m, Ar) 5.72 (1H, ddd, J 17.2, 10.1 and 8.1, 3-H), 5.26-5.20 (2H, m, 4-H₂), 3.92 (1H, d, J 13.1, benzyl H_A), 3.69 (1H, d, J 13.1, benzyl H_B), 3.62 (1H, dd, J 10.6 and 4.4, 1-H_A), 3.44 (1H, dd, J 10.6 and 8.1, 2-H), 3.26 (1H, dd, J 10.6 and 4.4, 1-H_B), 3.18 (2H, bs, NH, OH); δ_C (125 MHz, CDCl₃); 138.9 (Ar), 136.4 (4-C), 128.6 (Ar), 128.5 (Ar), 127.4 (Ar), 118.6 (3-C), 64.3 (1'-C), 62.2 (2-C), 50.7 (1-C); ν_{max}/cm^{-1} (film); 3292, 2930, 2875, 1602, 1453, 1371, 1009; m/z (ES) 178.2; HRMS Found: 178.1223, (C₁₁H₁₅NO MH^+ requires 178.1226).

(5*S*)-5-Benzyl-2,2-dimethyl-1,3-dioxolan-4-ol (**130**)¹⁷³



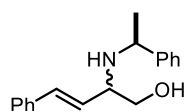
According to the procedure¹⁷³ **138** was dissolved in dry toluene (20 mL) under an inert atmosphere (N₂) and stirred at -78 °C. DIBAL (1M, 3.9 mL, toluene) was added over 10 minutes and the reaction left to stir for 30 minutes. 1 M HCl_(aq) (4 mL) was added over 15 mins and the reaction allowed to warm to rt. Dilution with water (100 mL) and extraction with EtOAc (150 mL), dried (MgSO₄), and filtered then concentrated *in vacuo* gave the protected aldehyde¹⁷³ (**130**) (0.38 g, 76%) as a yellow oil; R_f 0.20 (90:10 DCM–MeOH); δ_H (300 MHz, CDCl₃); 7.34-7.19 (10H, m, Ar), 5.26 (1H, dt, J 6.9 and 2.5, 4-H^{Maj}), 5.22 (1H, dt, J 7.0 and 3.4, 4-H^{Min}), 4.28 (1H, td, J 6.9 and 2.5, 5-H^{Maj}), 4.21 (1H, td, J 7.0 and 3.4, 5-H^{Min}), 3.04 (2H, bs, OH), 2.96 (2H, dd, J 14.0 and 7.0, benzyl H₂^{Maj}), 2.89 (2H, dd, J 14.0 and 6.5, benzyl H₂^{Min}), 1.57 (3H, s, Me^{Min}), 1.51 (3H, Me^{Maj}), 1.46 (3H, s, Me^{Min}), 1.34 (3H, s, Me^{Maj}).

(5S)-5-Benzyl-2,2-dimethyl-1,3-dioxolan-4-one (138)¹⁷³



According to literature procedure¹⁷³ L-3-phenyllactic acid (0.54g, 3 mmol) was added to a solution of *p*-toluenesulfonic acid (30 mg), 2,2-dimethoxypropane (3 mL) in acetone (20 mL) and stirred at rt for 17 hr. The reaction mixture was concentrated *in vacuo* then dissolved in EtOAc (30 mL). This was washed with NaHCO₃ (3 × 10 mL), brine (3 × 10mL), dried (MgSO₄), and filtered through a plug of silica eluting with DCM–MeOH (90:10) to give the protected acid¹⁷³ **138** (0.54 g, 84%) as an amorphous solid; R_f 0.25 (90:10 DCM–MeOH); δ_H (300 MHz, CDCl₃); 7.33-7.08 (5H, m, Ar), 4.58 (1H, dd, *J* 6.3 and 4.2, 5-H), 3.11 (1H, dd, *J* 14.5 and 4.2, benzyl 1-H_A), 2.97 (1H, dd, *J* 14.5 and 6.3, benzyl 1-H_B), 1.41 (3H, s, Me), 1.27 (3H, s, Me); δ_C (75 MHz, CDCl₃); 151.5 (C=O), 135.8 (Ar), 129.8 (Ar), 128.4 (Ar), 127.1 (Ar), 75.0 (benzyl 1-C), 37.7 (2C), 26.9 (Me), 26.2 (Me); *m/z* (ES) 229.1; HRMS Found: 229.0825, (C₁₂H₁₄O₃ MH⁺ requires 229.0835).

(3E)-2-[(1-Phenylethyl)amino]-4-phenyl-but-3-en-1-ol (139)

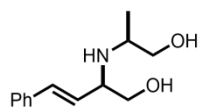


By **General Method A2**, using (*R*)-*N*-methylbenzylamine (0.18 mL, 1.4 mmol), filtered through a silica plug, eluting with DCM–MeOH (90:10) and SCX column, eluting with *sat.* NH₃ in MeOH gave the *amino alcohol* **139** (0.15 g, d.r. 50:50, 41%) as a dark brown amorphous solid; *R_f* 0.10 (90:10 DCM–MeOH); δ_{H} (500 MHz, CDCl₃); 7.32–7.17 (20H, m, Ar), 6.39 (1H, d, *J* 15.8, 4-H^{Dias A}), 6.29 (1H, d, *J* 16.0, 4-H^{Dias B}), 5.90 (2H, ddd, *J* 16.4, 9.1 and 7.8, 3-H^{Dias A and B}), 3.93 (2H, q, *J* 10.9 and 6.8, ethyl 1-H^{Dias A and Dias B}), 3.65–3.57 (1H, m, 1-H_A^{Dias B}), 3.57–3.44 (1H, m, 1-H_A^{Dias A}), 3.38–3.31 (3H, m, 1-H_B^{Dias B}, 2-H^{Dias A} and 1-H_B^{Dias A}), 3.04 (1H, dq, *J* 8.5 and 4.6, 2-H^{Dias A}), 2.08 (4H, bs, NH and OH^{Dias A and B}), 1.30 (3H, d, *J* 5.0, ethyl 2-H₃^{Dias A}), 1.29 (3H, d, *J* 5.1, ethyl 2-H₃^{Dias B}); δ_{C} (75 MHz, CDCl₃); 138.6 (4-C^{Dias B}), 137.2 (4-C^{Dias A}), 129.7 (Ar^{Dias A}), 129.5 (Ar^{Dias B}), 129.2 (Ar^{Dias A}), 129.1 (Ar^{Dias A}), 129.0 (Ar^{Dias B}), 128.8 (Ar^{Dias B}), 128.7 (Ar^{Dias A}), 128.6 (Ar^{Dias B}), 128.5 (Ar^{Dias A}), 127.5 (Ar^{Dias B}), 127.1 (Ar^{Dias B}), 128.4 (Ar^{Dias A}), 127.9 (Ar^{Dias A}), 127.6 (Ar^{Dias B}), 127.1 (Ar^{Dias B}), 127.0 (Ar^{Dias A}), 120.2 (3-C^{Dias A}), 119.3 (3-C^{Dias B}), 64.1 (ethyl 2-C^{Dias B}), 63.5 (ethyl 2-C^{Dias A}), 58.5 (1-C^{Dias A}), 57.1 (1-C^{Dias B}), 43.5 (2-C^{Dias A} + 2-C^{Dias B}), 21.4 (ethyl 2-C^{Dias A}), 19.1 (ethyl 2-C^{Dias B}); ν_{max} /cm⁻¹ (neat); 3340, 3053, 2983, 1265, 736; *m/z* (ES) 168.2; HRMS Found: 268.1697, (C₁₈H₂₁NO *MH*⁺ requires 268.1696).

Reaction was performed with (*S*)-*N*-methylbenzylamine (0.18 mL, 1.4 mmol), filtered through a silica plug, eluting with DCM–MeOH (90:10) and SCX column, eluting with *sat.* NH₃ in MeOH gave the *amino alcohol* **140** (0.15 g, 35%) as a dark brown amorphous solid. Data collected was identical to that obtained above.

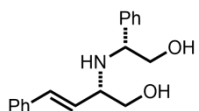
(3E)-2(R)-{[(2S)-2-Hydroxy-1-methylethyl]amino}-4-phenylbut-3-en-1-ol

(141)



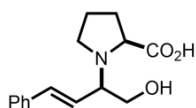
By **General Method A1**, using (*S*)-2-amino-1-propanol (0.14 mL, 1.5 mmol) followed by flash chromatography, eluting with DCM–MeOH (90:10) gave the *amino alcohol* **141** (0.209 g, d.r. 75:25, 53%) (brown oil); R_f 0.15 (90:10 DCM–MeOH); δ_H (500 MHz, $CDCl_3$); 7.38 (1H, d, J 7.5, Ar), 7.32–7.30 (2H, m, Ar), 7.26 (2H, m, Ar), 6.56 (1H, d, J 15.9, 4-H), 6.07 (1H, dd, J 15.9 and 7.8, 3-H), 3.68 (1H, dd, J 10.8 and 4.5, 1- H_A), 3.62 (1H, dd, J 10.8 and 4.5, 1- H_B), 3.52 (1H, dd, J 10.6 and 7.2, propanyl 1- H_B), 3.47 (1H, dd, J 7.8 and 4.5, 2-H), 3.36 (1H, dd, J 10.6 and 5.6, propanyl 1- H_A), 2.95–2.91 (1H, m, propanyl H^{Min}), 1.88 (3H, bs, NH, OH and OH), 1.12 (3H, d, J 6.6, propanyl 3-H); ν_{max}/cm^{-1} (film); 3380, 2987, 1607; m/z (ES) 222.2; HRMS Found: 222.1484, ($C_{13}H_{19}NO_2$ MH^+ requires 222.1489).

(3E)-2(S)-{[(2R)-2-Hydroxy-1-phenylethyl]amino}-4-phenylbut-3-en-1-ol (142)



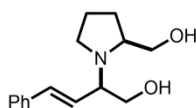
By **General Method A1**, using *N*-phenylglycinol (0.20 g, 1.5 mmol) followed by flash chromatography, eluting with DCM–MeOH (90:10) gave the *amino alcohol* **142** (0.24 g, d.r. ≥ 95 : ≤ 5 , 58%) as brown amorphous solid; R_f 0.25 (90:10 DCM–MeOH); δ_H (500 MHz, $CDCl_3$); 7.38 (2H, d, J 7.5, Ar), 7.32 (3H, m, Ar), 7.26 (5H, m, Ar), 6.56 (1H, d, J 16.0, 4-H), 6.07 (1H, dd, J 16.0 and 7.6, 3-H), 3.68 (1H, dd, J 10.6 and 4.5, 1- H_A), 3.62 (1H, dd, J 10.6 and 4.5, 1- H_B), 3.52 (1H, dd, J 10.8 and 7.2, hydroxyphenylethyl 1-H), 3.47 (1H, dd, J 7.6 and 4.4, 2-H), 3.36 (1H, dd, J 10.8 and 5.6, hydroxyphenylethyl 2- H_B), 2.97–2.92 (1H, m, hydroxyphenylethyl 2- H_A), 1.88 (1H, s, NH), 1.12 (2H, bs, OH). δ_C (75 MHz, $CDCl_3$); 139.9 (Ar 1-C), 136.4 (Ar), 133.6 (4-C), 129.7 (Ar), 128.8 (Ar), 128.5 (Ar), 128.0 (Ar), 127.8 (Ar), 127.7 (Ar), 126.4 (3-C), 126.3 (3-C), 69.4 (hydroxyphenylethyl 1-C), 67.3 (hydroxyphenylethyl 1-C), 66.5 (2-C), 61.7 (1-C), 61.1 (1-C), 60.2 (hydroxyphenylethyl 2-C); ν_{max}/cm^{-1} (neat); 3060, 2975, 2925, 1531, 1265, 1025; m/z (ES) 284.2.

(3E)-(2R)-[(2S)-2-(Carboxylic acid)pyrrolidine]-4-phenylbut-3-en-1-ol (143)



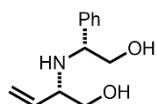
By **General Method A2**, using L-proline (0.16 g, 1.4 mmol) followed by flash chromatography, eluting with H₂O-ⁱPr-EtOH (45:33:22) gave the *amino acid* **143** (0.19 g, d.r. ≥95:≤5, 52%) as a clear oil; R_f 0.15 (90:10 DCM-MeOH); δ_H (500 MHz, CDCl₃); 7.46 (2H, d, *J* 7.5, Ar), 7.42 (2H, d, *J* 7.5, Ar), 7.31 (1H, t, *J* 7.5, Ar), 6.78 (1H, d, *J* 15.9, 4-H), 6.06 (1H, dd, *J* 15.9 and 7.6, 3-H), 4.20 (1H, d, *J* 10.4, pyrrolidine 2-H), 4.17 (1H, dd, *J* 8.4 and 3.4, 1-H_A), 3.86-3.79 (2H, m, 2-H and 1-H_B), 3.59 (1H, dd, *J* 10.4 and 6.6, pyrrolidine 3-H_A), 2.99 (1H, ddd, *J* 12.9, 10.4 and 6.6, pyrrolidine 3-H_B), 2.44 (1H, dd, *J* 12.9 and 6.4, pyrrolidine 5-H_B), 1.98-1.92 (1H, m, pyrrolidine 5-H_A), 1.85 (1H, dd, *J* 12.9 and 6.4, pyrrolidine 4-H_B), 1.71 (1H, dd, *J* 12.9 and 6.4, pyrrolidine 4-H_A), 1.25 (2H, bs, OH); δ_C (125 MHz, CDCl₃); 173.8 (C=O), 141.4 (Ar), 134.8 (4-C), 127.7 (Ar-C), 127.0 (Ar-C), 126.7 (Ar-C), 115.9 (3-C), 70.8 (2-C), 66.0 (1-C), 61.7 (pyrrolidine 2-C), 56.7 (pyrrolidine 3-C), 30.1 (pyrrolidine 5-C), 23.6 (pyrrolidine 4-C); ν_{max}/cm⁻¹ (neat); 3055, 1739, 1265; *m/z* (ES) 262.2; HRMS Found: 262.1435, (C₁₅H₁₉NO₃ *MH*⁺ requires 262.1438).

(3E)-(2R)-[(2S)-2-(Hydroxymethyl) pyrrolidine]-4-phenylbut-3-en-1-ol 144



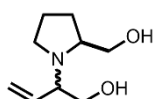
By **General Method A3**, using L-prolinol (0.16 g, 1.4 mmol), DCE-HFIP (14 mL), filtered through a silica plug, eluting with EtOAc gave the *amino alcohol* **144** (0.19 g, d.r. 89:11, 68%) as a brown oil; R_f 0.20 (90:10 DCM-MeOH) δ_H (500 MHz, CDCl₃); 7.40 (2H, d, *J* 7.5, Ar), 7.42 (2H, d, *J* 7.5, Ar), 7.31 (1H, t, *J* 7.5, Ar), 6.78 (1H, d, *J* 16.0, 4-H), 6.06 (1H, dd, *J* 16.0 and 7.6, 3-H), 4.05-3.98 (3H, m, 1-H_A, and hydroxymethyl H₂), 3.86-3.76 (2H, m, 2-H and 1-H_B), 2.99 (1H, ddd, *J* 12.4, 10.9 and 6.4, pyrrolidine 3-H_B), 2.84-2.79 (1H, m, pyrrolidine 2-H) 2.38 (1H, dd, *J* 11.6 and 6.9, pyrrolidine 5-H_B), 1.98-1.92 (1H, m, pyrrolidine 5-H_A), 1.89-1.81 (1H, m, pyrrolidine 3-H_A), 1.78 (1H, dt, *J* 12.4 and 6.5, pyrrolidine 4-H_B), 1.73 (1H, dt, *J* 12.4 and 6.5, pyrrolidine 4-H_A), 1.35 (2H, bs, OH); δ_C (125 MHz, CDCl₃); 136.5 (Ar), 135.2 (4-C), 128.7 (Ar-C), 127.9 (Ar-C), 126.4 (Ar-C), 123.7 (3-C), 63.4 (2-C), 63.7 (hydroxymethyl 1-C) 61.7 (1-C), 61.4 (pyrrolidine 2-C), 46.5 (pyrrolidine 5-C), 27.7 (pyrrolidine 3-C), 24.6 (pyrrolidine 4-C); ν_{max}/cm⁻¹ (neat); 3053, 2970, 1612, 1454; *m/z* (ES) 248.2; HRMS Found: 248.1643, (C₁₅H₂₁NO₂ *MH*⁺ requires 248.1645).

(2S)-{[(1R)-2-Hydroxy-1-phenylethyl]amino}-but-3-en-1-ol (145)



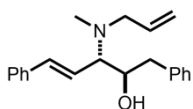
By **General Method A4**, using *N*-phenylglycinol (0.20 g, 1.5 mmol) followed by flash chromatography, eluting with DCM–MeOH (90:10) then DCM–EtOH–NH₄OH (85:15:1) gave the *amino alcohol* **145** (0.24 g, d.r. 83:17, 44%) as brown amorphous solid; R_f 0.10 (90:10 DCM–MeOH); δ_H (500 MHz, CDCl₃); 7.37-7.33 (6H, m, Ar^{Maj, Min}), 7.29 (4H, m, J 7.5, Ar^{Maj, Min}), 5.69 (1H, ddd, J 17.3, 10.4, 6.6, 3-H^{Min}), 5.60 (1H, ddd, J 17.1, 10.4, 8.4, 3-H^{Maj}), 5.25 (1H, d, J 17.1, 4-H^{A Maj}), 5.23 (1H, d, J 17.3, 4-H^{A Min}), 5.16 (1H, d, J 10.4, 4-H^{B Min}), 5.13 (1H, d, J 10.3, 4-H^{B Maj}), 3.93 (1H, dd, J 8.9 and 4.5, hydroxyphenylethyl 1-H^{Maj}), 3.89 (1H, dd, J 6.8 and 4.9, hydroxyphenylethyl 1-H^{Min}), 3.76 (1H, dd, J 10.9 and 4.9, hydroxyphenylethyl 2-H^{A Min}), 3.66-3.63 (2H, m, 1H^{B Maj} and hydroxyphenylethyl 2-H^{B Min}), 3.59 (1H, dd, J 10.6 and 4.5, 1H^{A Maj}), 3.55 (1H, dd, J 10.6 and 4.5, hydroxyphenylethyl 2-H^{B Maj}), 3.47-3.43 (2H, m, 1-H^{2 Min}), 3.41 (1H, dd, J 10.6 and 8.9, hydroxyphenylethyl 2-H^{A Maj}), 3.29 (1H, dd, J 12.0 and 6.6, 2-H^{Min}), 3.09 (1H, app dd, J 8.4 and 4.5, 2-H^{Maj}), 2.12 (3H, bs, 3 \times NH or OH), 3 \times NH or OH not observed; δ_C (125 MHz, CDCl₃) 140.0 (Ar 1-C^{Maj}), 141.1 (Ar 1-C^{Min}), 137.7 (3-C^{Min}), 136.7 (3-C^{Maj}), 128.7 (Ar^{Maj}), 128.6 (Ar^{Min}), 127.7 (Ar^{Min}), 127.6 (Ar^{Maj}), 127.5 (Ar^{Maj}), 127.2 (Ar^{Min}), 118.5 (4-C^{Maj}), 117.0 (4-C), 67.1 (hydroxyphenylethyl 1-C^{Maj}), 66.4 (hydroxyphenylethyl 1-C^{Min}), 65.3 (2-C^{Maj}), 64.0 (2-C^{Min}), 61.7 (1-C^{Min}), 61.0 (1-C^{Maj}), 60.4 (hydroxyphenylethyl 1-C^{Min}), 59.6 (hydroxyphenylethyl 1-C^{Maj}); ν_{max}/cm^{-1} (neat); 3082, 2980, 1602, 1454, 1264; m/z (ES) 208.2; HRMS Found: 208.1329, (C₁₂H₁₇NO₂ MH^+ requires 208.1332).

2-[(2*S*)-2-(Hydroxymethyl)pyrrolidin-1-yl]-but-3-en-1-ol (146)



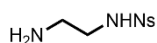
By **General Method A4**, using (*S*)-(+)-2-Pyrrolidinemethanol (0.13 mL, 2 mmol), filtered through a silica plug, eluting with DCM–MeOH (90:10) gave the *amino alcohol* **146** (0.15 g, d.r. 50:50, 43%); R_f 0.05 (90:10 DCM–MeOH); δ_H (500 MHz, $CDCl_3$); 5.80 (2H, m, 3- $H^{Dais\ 1}$ and $Dias\ 2$), 5.50 (1H, d, J 15.9 4- $H_A^{Dias\ 1}$), 5.43 (1H, d, J 15.7 4- $H_A^{Dias\ 2}$), 5.35 (2H, m, 4 H_B $H^{Dais\ 1}$ and $Dias\ 2$), 4.17 (2H, dd, J 8.4 and 3.4, 1- H_A), 3.86 (5H, m, 2- $H^{Dais\ 1}$ and $Dias\ 2$ and 1- $H_B^{Dais\ 1}$ and $Dias\ 2$), 3.59 (1H, dd, J 10.4 and 6.6, pyrrolidine 3- $H_A^{Dias\ 1}$), 3.59 (1H, dd, J 9.5 and 6.8, pyrrolidine 3- $H_A^{Dias\ 2}$), 3.20 (4H, m, pyrrolidine 2- $H^{Dais\ 1}$ and $Dias\ 2$), 2.99 (2H, m, pyrrolidine 3- $H_B^{Dais\ 1}$ and $Dias\ 2$), 2.44 (1H, dd, J 12.9 and 6.4, pyrrolidine 5- $H_B^{Dias\ 2}$), 2.45 (2H, dd, J 12.9 and 7.1, pyrrolidine 5- $H_B^{Dias\ 1}$), 1.98-1.92 (2H, m, pyrrolidine 5- H_A), 1.87-1.86 (2H, m, pyrrolidine 4- $H_B^{Dais\ 1}$ and $Dias\ 2$), 1.74-1.71 (2H, m, pyrrolidine 4- $H_A^{Dias\ 1}$ and $Dias\ 2$), 1.25 (4H, bs, OH); δ_C (125 MHz, $CDCl_3$); 134.5 (3- $C^{Dais\ 1}$), 134.8 (3- $C^{Dias\ 2}$), 118.9 (4- $C^{Dais\ 1}$), 117.7 (4- $C^{Dias\ 2}$), 68.8 (2- $C^{Dais\ 1}$), 70.8 (2- $C^{Dias\ 2}$), 66.2 (1- $C^{Dais\ 1}$), 64.9 (1- $C^{Dias\ 2}$), 62.4 (hydroxymethyl 1- $C^{Dais\ 1}$), 61.4 (hydroxymethyl 1- $C^{Dias\ 2}$), 56.7 (pyrrolidine 3- $C^{Dais\ 1}$), 55.7 (pyrrolidine 3- $C^{Dias\ 2}$), 48.9 (pyrrolidine 2- $C^{Dais\ 1}$), 50.4 (pyrrolidine 2- $C^{Dias\ 2}$), 30.6 (pyrrolidine 5- $C^{Dais\ 1}$), 30.5 (pyrrolidine 5- $C^{Dias\ 2}$), 23.6 (pyrrolidine 4- $C^{Dias\ 1}$ and $Dias\ 2$); ν_{max}/cm^{-1} (neat); 3054, 2982, 1421, 1264; m/z (ES) 172.1; HRMS Found: 172.1332, ($C_9H_{17}NO_2$ MH^+ requires 172.1332).

(4E)-3-[(Allyl)methylamino]-1,5-diphenylpent-4-en-2-ol (147)



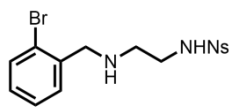
By **General Method A3**, using (5S)-5-benzyl-2,2-dimethyl-1,3-dioxolan-4-ol (0.19 g, 0.9 mmol), *N*-methylallylamine (1 mmol), DCE–HFIP (14 mL), filtered through a silica plug, eluting with hexane then DCM–MeOH (90:10) gave the *amino alcohol* (**147**) (0.20 g, d.r. $\geq 95:\leq 5$, 72%) as a brown oil; R_f 0.35 (90:10 DCM–MeOH); δ_H (500 MHz, $CDCl_3$); 7.43 (2H, d, J 7.5, Ar), 7.35 (3H, t, J 7.5, Ar), 7.32–7.22 (5H, m, Ar), 6.50 (1H, d, J 16.0, 5-H), 6.31 (1H, dd, J 16.0 and 10.0, 4-H), 5.83 (1H, ddt, J 16.6, 10.2 and 6.5, allyl 2-H), 5.19–5.12 (2H, m, allyl 3-H₂), 4.19 (1H, dd, J 14.0 and 5.5, 1-H_A), 3.24 (1H, dd, J 14.0 and 5.5, 1-H_B), 3.11 (1H, dd, J 10.0 and 5.5, 2-H), 2.94 (1H, dd, J 9.1 and 5.0, 3-H), 2.77 (2H, d, J 6.5, allyl 1-H₂), 2.31 (3H, s, Me), 1.66 (1H, bs, OH); δ_C (125 MHz, $CDCl_3$); 138.5 (5-C), 136.3 (allyl 3-C), 134.3 (Ar), 133.8 (Ar), 129.3 (Ar), 128.7 (Ar), 128.4 (Ar), 128.1 (Ar), 126.6 (Ar), 126.3 (Ar) 117.4 (4-C), 115.3 (allyl 3-C), 71.1 (1-C), 70.5 (2-C), 57.8 (3-C), 40.4 (allyl 1-C), 39.0 (NMe); ν_{max}/cm^{-1} (neat); 3055, 2932, 1722, 1493, 1057; m/z (ES) 308.4; HRMS Found: 308.2024, ($C_{21}H_{25}NO$ MH^+ requires 308.2009).

***N*-(2-Aminoethyl)-2-nitrobenzene-1-sulfonamide (148)⁹⁰**



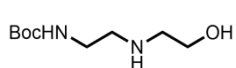
According to the procedure⁹⁰ Et₃N (1.5 mL, 15 mmol) was added to a suspension of ethylene diamine (0.5 mL, 7.5 mmol) in DCM (20 mL). The suspension was stirred for 10 min until it became a clear solution, after which 2-nitrophenylsulphonylchloride (1.7 g, 7.7 mmol) was added. The reaction mixture was stirred at rt for 16 hr and then diluted with DCM (100 mL) and water (100 mL). The phases were separated and the aqueous phase was extracted with DCM (3 × 100 mL). The combined organic phase was washed with *sat.* NaHCO_{3(aq)} (15 mL), water (15 mL) and brine (15 mL), dried (MgSO₄), filtered and concentrated *in vacuo* to give the amine¹⁷⁴ **148** (0.78 g, 43%) as an yellow oil; R_f 0.05 (90:10 DCM–MeOH); δ_H (500 MHz, MeOD); 8.03–8.00 (1H, m, Ar), 7.80–7.78 (1H, m, Ar), 7.76–7.73 (2H, m, Ar), 3.21 (2H, t, J 6.0, 2-H₂), 3.01 (2H, t, J 6.0, 1-H₂); δ_C (75 MHz, MeOD) 149.5 (Ar C-2), 135.5 (Ar C-1), 133.7 (Ar), 133.6 (Ar), 131.7, (Ar) 126.2 (Ar), 41.4 (C-2), 40.6 (C-1); ν_{max}/cm^{-1} (neat); 3736, 3650, 2918, 1541, 1275; m/z (ES) 268.1; HRMS Found: 268.0359, ($C_8H_{11}N_3O_4S$ MH^+ requires 268.0362).

***N*-(2-[(2-Bromophenyl)methyl]amino)ethyl)-2-nitrobenzene-1-sulfonamide
(149)**



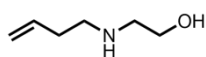
N-(2-aminoethyl)-2-nitrobenzene-1-sulfonamide (**148**) (0.43 g, 1.72 mmol) was added to 2-bromobenzaldehyde (0.6 ml, 5.5 mmol) in ethanol (15 mL) and stirred at 79 °C for 4 hr. Sodium borohydride (5 eq.) was added in small portions over 60 mins and reaction mixture stirred for 4 hr. The reaction mixture was concentrated *in vacuo*, partitioned between EtOAc (40 mL) and water (40 mL). The organic layer was then extracted with 0.5 M HCl_(aq) (5 × 30 mL) and the combined aqueous layers were neutralised by the addition of 2 M NH₄OH. The aqueous layer was then extracted with DCM (5 × 20 mL), combined, dried (MgSO₄), filtered and concentrated *in vacuo* and purified by column chromatography eluting with DCM–EtOH–NH₄OH (84:14:2) to give the amino alcohol¹⁷⁵ **149** (0.41 g, 57%); *R_f* 0.10 (90:10 DCM–MeOH); δ_{H} (500 MHz, CDCl₃); δ_{C} (125 MHz, MeOH); 8.30 (2H, d, *J* 8.7, Ns), 8.05 (2H, d, *J* 8.7, Ns), 7.55 (1H, d, *J* 7.5, Ar), 7.37 (1H, d, *J* 7.5, Ar), 7.29 (1H, t, *J* 7.5, Ar), 7.13 (1H, d, *J* 7.5, Ar), 3.89 (2H, s, benzyl H₂), 3.67 (2H, dd, *J* 5.5 and 4.9, 1-H₂), 2.79 (2H, dd, *J* 5.5 and 4.9, 2-H₂), 2.35; δ_{C} (75 MHz, MeOH); 149.2 (Ns), 136.49 (Ns), 132.8 (Ns), 132.7 (Ns), 128.84 (Ns), 138.8 (Ar C-2), 132.9 (Ar C-1), 130.4 (Ar), 128.8 (Ar), 126.2 (Ns), 124.1 (Ar), 111.6 (Ar), 60.7 (benzyl 1-C), 53.2 (C-1), 50.3 (C-2); ν_{max} /cm⁻¹ (neat); 3392, 2938, 1439, 1275; *m/z* (ES) 416.02 and 418.02.

***tert*-Butyl *N*-{2-[(2-hydroxyethyl)amino]ethyl}carbamate (**150**)¹⁷⁶**



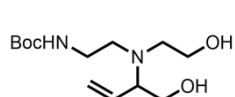
Et₃N (0.48 mL, 3.47 mmol) was added to a suspension of *N*-(2-hydroxyethyl)ethylene diamine (0.28 mL, 2.60 mmol) in DCM (10 mL). The suspension was stirred for 10 min, after which di-*tert*-butyl dicarbonate (0.38 g, 1.73 mmol) was added. The reaction mixture was stirred at rt for 16 hr and then diluted with DCM (10 mL) and water (10 mL). The phases were separated and the aqueous phase was extracted with DCM (3 × 10 mL). The combined organic phase was washed with *sat.* NaHCO_{3(aq)} (15 mL) and brine (15 mL), dried (MgSO₄) and concentrated *in vacuo* and purified by column chromatography eluting with DCM–EtOH–NH₄OH (84:14:2) to give the amine alcohol¹⁷⁶ **150** (0.21 g, 60%) as an amorphous colourless solid; *R_f* 0.10 (90:10 DCM–MeOH); δ_H (500 MHz, CDCl₃); 4.97 (1H, bs, NH or OH), 3.66 (2H, m, hydroxyethyl 2-H₂), 3.23 (2H, dd, *J* 11.2 and 5.6, 2-H₂), 2.78 (4H, m, 1-H₂, hydroxyethyl 1-H₂), 2.07 (2H, bs, NH or OH) 1.47 (9H, s, Boc); δ_C (75 MHz, CDCl₃); 156.2 (C=O), 80.6 (Boc 2-C), 61.0 (2-C), 50.7 (hydroxyethyl 2-C), 48.9 (hydroxyethyl 1-C), 40.4 (1-C), 28.4 (Boc 3-C); ν_{max}/cm⁻¹ (neat); 3329, 2976, 2932, 1692, 1529, 1366, 1279, 1172; *m/z* (ES) 205.2; HRMS Found: 205.1555, (C₉H₂₀N₂O₃ *MH*⁺ requires 205.1567).

2-[(But-3-en-1-yl)amino]hydroxyethyl-1-ol (152**)⁹¹**



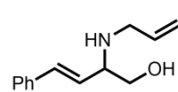
According to the procedure⁹¹ sodium iodide (55 mg, 0.37 mmol) was added to a solution of 4-bromo-1-butene (0.50 g, 3.7 mmol) and 2-aminoethanol (0.89 mL, 18.53 mmol) in MeOH (8 mL). The reaction mixture was heated under reflux for 2 hr, then cooled to rt and evaporated *in vacuo*. The residue was partitioned between *sat.* NH₄Cl_(aq) (20 mL) and EtOAc (20 mL). The aqueous layer was made basic with 40% sodium hydroxide and extracted with EtOAc (3 × 15 mL). The combined organic layers were dried (MgSO₄) and concentrated *in vacuo* to afford the amino alcohol⁹¹ **152** (0.20 g, 54%) as a colourless oil; *R_f* 0.10 (90:10 DCM–MeOH); δ_H (500 MHz, CDCl₃); 5.79 (1H, ddt, *J* 17.2, 10.1 and 6.7, butenyl 3-H), 5.10 (1H, d, *J* 17.2, butenyl 4-H_A), 5.05 (1H, d, *J* 10.1, butenyl 4-H_B), 3.64 (2H, dd, *J* 5.5 and 4.9, hydroxyethyl 2-H₂), 2.78 (2H, dd, *J* 5.5 and 4.9, hydroxyethyl 1-H₂), 2.70 (2H, app t, *J* 6.7, butenyl 2-H₂), 2.26 (2H, dd, *J* 13.6 and 6.7, butenyl 1-H₂), 1.82 (2H, bs, NH, OH); *m/z* (ES) 116.2.

2-[(*tert*-Butylethylcarbamate)2-hydroxyethylamino]but-3-en-1-ol (**156**)



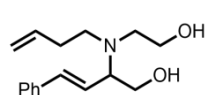
By **General Method A4**, using amine **150** (70 mg, 0.3 mmol) followed by SCX column and flash chromatography, eluting with DCM–EtOH–NH₄OH (84:14:2), gave the *amino alcohol* **156** (30 mg, 30%) as a brown oil; R_f 0.20 (90:10 DCM–MeOH); δ_H (500 MHz, MeOD); 5.64 (1H, ddd, J 17.5, 10.6 and 8.1, 3-H), 5.16 (1H, d, J 10.6, 4-H_A), 5.10 (1H, d, J 17.5, 4-H_B), 3.50–3.45 (2H, m, hydroxyethyl 2-H), 3.42–3.39 (2H, m, 1-H₂), 3.38 (1H, dd, J 8.1 and 5.4, 2-H), 3.20–3.17 (2H, m, ethylcarbamate 2-H₂), 3.02–2.97 (2H, m, hydroxyethyl 1-H₂), 2.72–2.65 (2H, m, ethylcarbamate 1-H₂), 2.62 (1H, bs, NH), 2.46 (2H, bs, OH), 1.32 (9H, s, Boc); δ_C (75 MHz, MeOD); 158.7 (C=O), 134.9 (hydroxybutene 3-C), 119.5 (hydroxybutene 4-C), 80.9 (Boc 2-C), 67.0 (ethylcarbamate 2-C), 63.2 (ethylcarbamate 1-C), 61.4 (hydroxybutene 2-C), 54.1 (hydroxyethyl 2-C), 52.4 (hydroxybutene 1-C), 49.6 (hydroxyethyl 1-C), 28.9 (Boc 3-C); $\nu_{\max}/\text{cm}^{-1}$ (neat); 3335, 3053, 2873, 1454, 1264; m/z (ES) 276.2.

(*3E*)-2-(Allylamino)-4-phenylbut-3-en-1-ol (**157**)



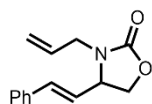
By **General Method A3**, using allylamine (0.15 mL, 1.69 mmol) filtered through a silica plug, eluting with DCM–MeOH (90:10) gave the *amino alcohol* **157** (0.34 g, 64%) as a yellow oil; R_f 0.10 (90:10 DCM–MeOH); δ_H (500 MHz, CDCl₃); 7.30 (2H, d, J 7.5, Ar), 7.23 (2H, t, J 7.5, Ar), 7.16 (1H, t, J 7.5, Ar), 6.49 (1H, d, J 16.0, 4-H), 5.94 (1H, dd, J 16.0 and 8.8, 3-H), 5.83 (1H, dddd, J 17.0, 10.3, 6.3 and 4.7, allyl 2-H), 5.12 (1H, dd, J 17.0 and 1.3, allyl 3-H_A), 5.0 (1H, dd, J 10.3 and 1.3, allyl 3-H_B), 3.64 (1H, dd, J 10.6 and 4.4, 1-H_A), 3.43 (1H, dd, J 10.6 and 8.0, 1-H_B), 3.31–3.25 (2H, m, 2-H and allyl 1-H_A), 3.12 (1H, d, J 6.3, allyl 1-H_B), 2.37 (2H, bs, NH and OH); δ_C (75 MHz, CDCl₃); 149.5 (Ar), 136.6 (4-C), 132.9 (allyl 2-C), 128.6 (Ar), 128.6 (Ar), 128.6 (Ar), 127.8 (3-C), 116.17 (allyl 3-C), 64.9 (1-C), 61.7 (2-C), 49.6 (allyl 1-C); $\nu_{\max}/\text{cm}^{-1}$ (neat); 3436, 2927, 1642, 1416; m/z (ES) 204.2; HRMS Found: 204.1387, (C₁₃H₁₇NO MH^+ requires 204.1383).

(3E)-2-[(But-3-en-1-yl)-2-hydroxyethylamino]-4-phenylbut-3-en-1-ol (158)



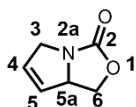
By **General Method A3**, using amine **152** (0.20 g, 1 mmol), followed by flash chromatography, eluting with DCM–MeOH (90:10) gave the *amino alcohol* **158** (0.21 g, 62%) as a yellow oil; R_f 0.25 (90:10 DCM–MeOH); δ_H (500 MHz, $CDCl_3$); 7.36 (2H, d, J 7.5, Ar), 7.31 (2H, t, J 7.5, Ar), 7.25 (1H, d, J 7.5, Ar), 6.52 (1H, d, J 16.0, 4-H), 6.10 (1H, dd, J 16.0 and 8.4, 3-H), 5.81 (1H, ddt, J 17.2, 10.2 and 6.6, butenyl 3-H), 5.11 (1H, d, J 17.2, butenyl 4- H_A), 5.07 (1H, d, J 10.2, butenyl 4- H_B), 3.69-3.55 (4H, m, 1-H, hydroxyethyl 2-H), 3.52-3.45 (1H, m, 2-H), 2.86 (1H, dt, J 13.6 and 9.2, hydroxyethyl 1- H_A), 2.70 (1H, dt, J 13.6 and 7.8, hydroxyethyl 1- H_B), 2.65 (1H, dd, J 13.2 and 6.6, butenyl 2- H_A), 2.59 (1H, dt, J 13.2 and 6.6, butenyl 2- H_B), 2.45 (2H, bs, OH), 2.26 (2H, d, J 13.1 butenyl 1- H_2). δ_C (75 MHz, $CDCl_3$); 136.7 (Ar-C1), 136.5 (C-4), 134.5 (butenyl C-4), 128.6 (Ar), 127.8 (Ar), 126.4 (Ar), 124.1 (C-3), 116.6 (butenyl C-3), 64.1 (2-C), 61.7 (1-C), 60.0 (hydroxyethyl 2-C), 51.6 (butenyl 2-C), 50.1 (hydroxyethyl 1-C), 33.1 (butenyl 1-C); ν_{max}/cm^{-1} (neat); 3412, 2928, 1612, 1443; m/z (ES) 262.2. $C_{16}H_{23}NO_2$

4-[(1E)-2-Phenylethenyl]-3-(allyl)-1,3-oxazolidin-2-one (**162**)¹⁷⁷



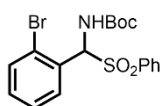
CDI (0.18 g, 1.1 mmol) and DBU (0.32 mL, 2.2 mmol) were added to a solution of **157** (0.20 g, 0.98 mmol) in THF (10 mL) and the resulting mixture was stirred at rt for 16 hr under N₂. After this time the reaction mixture was concentrated *in vacuo*, re-dissolved in EtOAc (6 mL) and washed with brine (3 mL). The organic phase was then dried over MgSO₄, filtered then concentrated *in vacuo* and the resulting yellow oil purified by flash chromatography eluting with EtOAc–MeOH (100:0 to 95:5) to give the title compound¹⁷⁷ **162** (0.11 g, 49%) as a yellow oil; R_f 0.25 (90:10 DCM–MeOH); δ_H (500 MHz, CDCl₃); 7.39 (2H, d, *J* 7.5, Ar), 7.37–7.33 (2H, m, Ar), 7.32–7.28 (1H, m, Ar), 6.60 (1H, d, *J* 15.7, phenylethenyl 2-H), 5.99 (1H, dd, *J* 15.7 and 8.9, phenylethenyl 1-H), 5.82–5.70 (1H, m, allyl 2-H), 5.23 (1H, d, *J* 10.2, allyl-3-H_A), 5.19 (1H, d, *J* 17.1, allyl 3-H_B), 4.48 (1H, app t, *J* 8.5, 4-H), 4.40 (1H, dd, *J* 15.8 and 8.1, allyl 1-H_A), 4.11 (1H, dd, *J* 15.8 and 4.7, allyl 1-H_B), 4.04 (1H, dd, *J* 8.5 and 7.5, 5-H_A), 3.57 (1H, dd, *J* 15.6 and 7.5, 5-H_B); δ_C (75 MHz, CDCl₃); 157.8 (C=O), 136.0 (Ar), 135.3 (phenylethenyl 2-C), 131.9 (allyl 2-C), 128.8 (Ar), 128.7 (Ar), 126.7 (Ar), 125.2 (phenylethenyl 2-C), 118.7 (allyl 3-C), 67.3 (5-C), 58.3 (4-C), 44.6 (allyl 1-C); ν_{max}/cm⁻¹ (neat); 3390, 3252, 2933, 2515, 2029, 1976, 1748; *m/z* (ES) 230.1.

4,5-Dihydropyrrolo[2,5-a]oxazol-2-one (**163**)¹⁷⁷



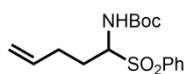
Grubbs' catalyst 2nd gen. (30 mg, 0.034 mmol) was added at rt to a solution of **162** (80 mg, 0.34 mmol) in DCM (20 mL). The resulting mixture was heated at 55 °C and stirred for 48 hr. After this time the reaction mixture was concentrated *in vacuo* and the resulting oil purified by flash chromatography eluting with EtOAc–Petrol (50:50) to give the title compound¹⁷⁷ **163** (24 mg, 57 %) as a brown oil; R_f 0.75 (90:10 DCM–MeOH); δ_H (300 MHz, CDCl₃); 6.06 (1H, app dt, *J* 6.0 and 3.3, 4-H), 5.92 (1H, dd, *J* 6.0 and 3.0, 5-H), 4.79–4.69 (1H, m, 5a-H), 4.62 (1H, app t, *J* 8.5, 6-H_A), 4.41 (1H, dd, *J* 3.3 and 2.0, 3-H_A), 4.25 (1H, dd, *J* 8.5 and 5.1, 6-H_B), 3.83 (1H, dd, *J* 3.3 and 2.0, 3-H_B); δ_C (75 MHz, CDCl₃); 163.3 (C=O), 131.0 (C-4), 128.9 (C-5), 68.7 (C-6), 64.6 (C-5a), 54.8 (C-3); ν_{max}/cm⁻¹ (neat); 3353, 3005, 2981, 1690, 1275; *m/z* (ES) 126.05; HRMS Found: 126.0545, (C₆H₇NO *MH*⁺ requires 126.0550).

***tert*-Butyl-*N*-([2-bromophenyl]{phenylsulfonyl)methyl)carbamate (**226**)**



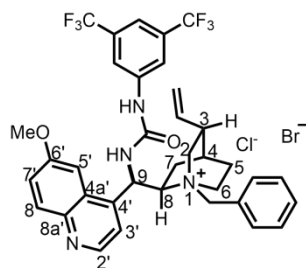
By **General Method B**, using *tert*-butyl carbamate (0.50 g, 4.2 mmol), benzene sulfinic sodium salt (0.84 g, 6.3 mmol) and *o*-bromobenzaldehyde (1.16 g, 6.3 mmol), followed by filtration, washing with water (100 mL) and hexane (100 mL) gave the title compound (**226**) (1.57 g, 88%); R_f : 0.60 (10:90, EtOAc–hexane); δ_H (500 MHz, $CDCl_3$); 8.04–7.84 (2H, m, Ar), 7.67–7.51 (2H, m, Ar), 7.48–7.33 (5H, m, Ar), 6.60 (1H, bs, NH), 5.80 (1H, bs, CH), 1.28 (9H, s, Boc); δ_C (75 MHz, $CDCl_3$); 153.3 (C=O), 135.3 (Ar), 133.9 (Ar), 133.2 (Ar), 130.7 (Ar), 129.8 (Ar), 129.2 (Ar), 128.8 (Ar), 127.9 (Ar), 126.7 (Ar), 126.4 (Ar), 79.9 (Boc 2-C), 72.3 (1-C), 28.01 (Boc 3-C); ν_{max}/cm^{-1} (neat); 3055, 2978, 2306, 1726, 1422, 1264; HRMS Found: 227.9652 and 229.9632, ($C_8H_7BrNO_2$ MH^+ requires 227.9654 and 229.9654 MH^+ minus $^tBu-SO_2Ph$). This compound has previously been prepared but characterisation data has not been reported.

***tert*-Butyl-*N*-(1-[phenylsulfonyl]pent-4-en-1-yl)carbamate (**228**)¹⁵⁸**



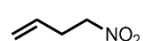
By **General Method B**, using *tert*-butyl carbamate (3.74 g, 31 mmol), benzene sulfinic sodium salt (8.6 g, 46 mmol) and pentenal (5 mL, 35 mmol). After 4 days, followed by filtration, washing with water (5 × 100 mL) and hexane (5 × 100 mL), and drying to give the title compound¹⁵⁸ (**228**) (8.06 g, 80%) as an amorphous white solid; R_f : 0.70 (10:90, EtOAc–hexane); δ_H (500 MHz, $CDCl_3$); 7.94–7.90 (2H, m, Ar), 7.69–7.51 (3H, m, Ar), 5.77 (1H, m, 4-H), 5.06 (2H, m, 5-H₂), 4.93 (1H, d, NH), 4.87 (1H, d, 1-H), 2.44–2.28 (2H, m, 3-H), 2.24–2.13 (1H, m, 2-H_A), 1.91–1.86 (1H, m, 2-H_B), 1.21 (9H, s, Boc); δ_C (75 MHz, $CDCl_3$); 153.5 (C=O), 136.8 (Ar), 135.8 (4-C), 133.8 (Ar), 129.2 (Ar), 129.0 (Ar), 116.7 (5-C), 80.7 (Boc 2-C), 70.0 (1-C), 29.3 (3-C), 27.9 (Boc 3-C), 25.6 (2-C); ν_{max}/cm^{-1} (neat); 3339, 2978, 1720, 1518, 1309, 1143; HRMS Found: 184.1332 ($C_{10}H_{18}NO_2$ requires MH^+ 184.1332 minus $^tBu-SO_2Ph$). This reaction was completed on 4.2 mmol scale with benzene sulfinic sodium salt (6.3 mmol) and pentenal (6.3 mmol) using **General Method C** and the yield was 76%.

1-[(8*S*, 9*S*)-1-Benzyl-6'-methoxycinchonan-1-ium-9-yl]-3-[3,5-bis(trifluoromethyl)phenyl]urea bromide (222)¹⁴³

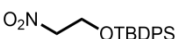


To a stirred solution (toluene 0.1 M) of **234** (0.20 g, 0.35 mmol) was added benzylbromide (1.0 eq.) and the solution was heated to 65 °C. After 12 hr, the mixture was allowed to cool to ambient temperature and concentrated *in vacuo* and purified by column chromatography eluting with ether-MeOH (100:0 to 85:15) the columned eluting with DCM-MeOH (100:0 to 90:10) to give the title compound (0.053 mg, 23%) as a yellow solid; R_f : 0.30 (90:10, DCM-MeOH); δ_H (500 MHz, $CDCl_3$); 8.69 (1H, d, J 4.7, 2'-H), 7.97 (1H, d, J 9.3, 8'-H), 7.69 (1H, bs, 5'-H), 7.61 (1H, d, J 4.7, 3'-H), 7.45 (1H, dd, J 9.3 and 2.6, 7'-H), 5.74 (1H, ddd, J 17.5, 10.3 and 7.5 vinyl 1-H), 4.95-5.10 (2H, m, vinyl 2-H₂), 4.72 (1H, d, J 10.7, 9-H), 4.00 (3H, s, OCH_3), 3.32 (1H, ddd, J 15.6, 10.5 and 2.3, 6-H_A), 3.28 (1H, dd, J 13.6 and 9.9, 2-H_A), 3.16 (1H, app q, J 10.7, 8-H), 2.79 (1H, ddd, J 15.6, 13.8 and 4.9, 6-H_B), 2.56 (1H, ddd, J 13.6, 4.7 and 2.3, 2-H_B), 1.60-1.57 (3H, m, 7-H_A and 5-H_A), 1.56-1.54 (1H, br m, 4-H), 1.53-1.50 (2H, m, 7-H_B and 5-H_B), 1.47-1.40 (1H, br m, 3-H), 2 \times NH not observed; m/z (ES) 669.3.

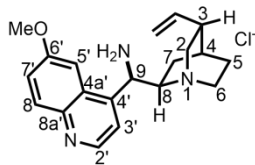
Nitrobut-3-ene (204)¹⁵⁹

 According to **General Method C**, using 4-bromobutene (0.75 mL, 7.4 mmol), sodium nitrite (0.60 g, 8.4 mmol) followed by flash chromatography, eluting with ether-Hexane (5:95) gave the title compound¹⁵⁹ (0.32 g, 43%) as a yellow oil; R_f : 0.20 (5:95, ether-hexane); δ_H (500 MHz, $CDCl_3$); 5.78 (1H, ddd, J 17.0, 11.2 and 8.5, 3-H), 5.10 (1H, d, J 11.2, 4-H_A), 5.06 (1H, d, J 17.0, 4-H_B), 4.46-4.35 (2H, m, 1-H₂), 2.87-2.85 (2H, m, 2-H₂); δ_C (75 MHz, $CDCl_3$); 131.8 (3-C), 118.8 (4-C), 74.7 (1-C), 31.3 (2-C); Unable to observe MH^+ in mass spectrometer.

***tert*-Butyl(2-nitroethoxy)diphenylsilane (231)**¹⁷⁸

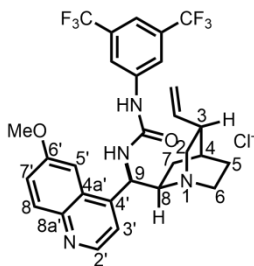
 **General Procedure D**, using nitroethanol (1.2 mL, 16.8 mmol), TBDPS-Cl (3.3 mL, 17.7 mmol), imidazole (2.28 g, 33.6 mmol), followed by flash chromatography, eluting with EtOAc–Hexane (10:90) gave the title compound¹⁷⁸ (5.2 g, 93%); *R*_f: 0.70 (10:90, EtOAc–hexane); δ_H (500 MHz, CDCl₃); 7.35-7.28 (4H, d, *J* 7.4, Ar), 7.25-7.10 (6H, m, Ar), 4.78 (2H, t, *J* 8.7 1-H₂), 4.23 (2H, t, *J* 8.7, 2-H₂), 1.29 (9H, s, ^tBu). *m/z* (ES) 330.2.

9-Amino-(9-deoxy)-*epi*-quinine (233)¹⁷⁹



Quinidine (6.13 mmol) and triphenylphosphine (2.11 g, 7.35 mmol) were dissolved in THF (30 mL) and the solution was cooled to 0 °C. DIAD (1.52 mL, 7.35 mmol) was added in one portion. A solution of diphenyl phosphoryl azide (1.63 mL, 7.35 mmol) in THF (13 mL) was then added dropwise at 0 °C. The mixture was allowed to warm to rt and stirred for 12 hr. The solution was then heated at 50 °C for 2 hr. Triphenylphosphine (2.29 g, 7.97 mmol) was then added and heating was maintained until the gas evolution had ceased (3 hr). The solution was cooled to rt, water (0.7 mL) was added, and the solution was stirred for 12 hr. The reaction mixture was concentrated *in vacuo* and the residue was dissolved in DCM (30 mL), then HCl_(aq) (10 %, 30 mL) was added. The phases were separated then the aqueous phase was washed with DCM (3 × 30 mL), then *sat.* NH₄OH was added (pH 12) and the aqueous layer was extracted with DCM (330 mL), dried (Na₂SO₄) and concentrated *in vacuo*. The crude material was purified by flash chromatography, eluting with EtOAc-MeOH then DCM-*sat.* methanolic ammonia-NH₄OH (85:15.5:0.5) the title compound¹⁷⁹ as yellowish viscous oil (0.84g, 40%). Note, some polar impurities were still present but it is easier to purify after the next step; R_f: 0.05 (90:10, DCM-MeOH); δ_H (500 MHz, CDCl₃); 8.69 (1H, d, *J* 4.7, 2'-H), 7.97 (1H, d, *J* 9.3, 8'-H), 7.69 (1H, bs, 5'-H), 7.61 (1H, d, *J* 4.7, 3'-H), 7.45 (1H, dd, *J* 9.3 and 2.6, 7'-H), 5.74 (1H, ddd, *J* 17.5, 10.3 and 7.5 vinyl 1-H), 4.95-5.10 (2H, m, vinyl 2-H₂), 4.72 (1H, d, *J* 10.7, 9-H), 4.00 (s, 3H, OCH₃), 3.32 (1H, ddd, *J* 15.6, 10.5 and 2.3, 6-H_A), 3.28 (1H, dd, *J* 13.6 and 9.9, 2-H_A), 3.16 (1H, app q, *J* 10.7, 8-H), 2.79 (1H, ddd, *J* 15.6, 13.8 and 4.9, 6-H_B), 2.56 (1H, ddd, *J* 13.6, 4.7 and 2.3, 2-H_B), 1.60-1.57 (3H, m, 7-H_A and 5-H_A), 1.56-1.53 (1H, br m, 4-H), 1.52-1.48 (2H, m, 7-H_B and 5-H_B), 1.47-1.45 (1H, br m, 3-H), 2 × NH not observed; *m/z* (ES) 325.2.

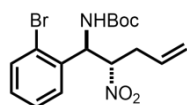
1-[(8*S*, 9*S*)-6'-Methoxycinchonan-1-ium-9-yl]-3-[3,5-bis(trifluoromethyl)phenyl]urea (234)¹⁸⁰



A solution of a **233** (0.9 mmol, 0.26 g) in anhydrous THF (1.1 mL) was added slowly to a solution of 3,5-bis(trifluoromethyl)phenyl isocyanate (1.0 mmol, 0.26 g, 0.5) in anhydrous THF (3 mL) at 0 °C. The reaction mixture was allowed to warm to rt and stirred overnight. The resulting mixture was concentrated in vacuo. The residue was purified followed by flash chromatography, eluting with DCM–MeOH (90:10) then DCM–EtOH–NH₄OH (85:15:1) affording the title compound¹⁸⁰ as a pale yellow amorphous solid (0.345 g, 70%): *R_f*: 0.15 (90:10, DCM–MeOH); *R_f*: 0.25 (90:10 DCM–MeOH); δ_{H} (300 MHz, MeOH); 8.66 (1H, d, *J* 4.6, 2'-H), 7.96–7.89 (3H, m, 8'-H, 5'-H, Ar) 7.79 (1H, d, *J* 2.8, Ar), 7.55 (1H, d, *J* 4.7, 3'-H), 7.43 (1H, s, Ar), 7.39 (1H, dd, *J* 9.2 and 2.6, 7'-H), 5.90 (1H, ddd, *J* 17.0, 10.5 and 6.1 vinyl 1-H), 5.65 (1H, dd, *J* 10.2 and 6.4), 5.16 (1H, d, *J* 17.4, vinyl 2-H_A), 5.09 (1H, d, *J* 10.5, vinyl 2-H_B), 4.75 (1H, d, *J* 10.5, 9-H), 4.01 (3H, s, OCH₃), 3.21 (3H, dt, *J* 14.3, 8.1, 6-H_A and 2-H_A) 2.98 (3H, dd, *J* 14.4, 9.6, 8-H, 6-H_B and 2-H_B), 2.71 (1H, m, 4-H), 2.27 (2H, q, *J* 12.7, 9.2, 7-H_A and 5-H_A), 1.19 (2H, m, 7-H_B and 5-H_B), 2 × NH not observed; *m/z* (ES) 579.2; HRMS Found: 579.2204 (C₂₉H₂₈F₆N₄O₂ MH⁺ requires 579.2189)

***tert*-Butyl-*N*-[(1*R*, 2*S*)-1-(2-bromophenyl)-2-nitropent-4-en-1-yl] carbamate**

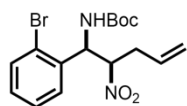
(221)



By **General Method E**, using amino sulfone (**226**) (0.213 g, 0.5 mmol), nitrobutene (0.26 g, 2.5 mmol) and *N*-benzylquinium chloride (12 mol%), followed by flash chromatography, eluting with EtOAc–Hexane (90:10) gave the *title compound* (0.11 g, d.r. >95:<5, 59%); $[\alpha]_D^{22}$ -17.3 (c. 0.5, CHCl₃); R_f : 0.40 (10:90, EtOAc–hexane); δ_H (500 MHz, CDCl₃); 7.62 (1H, d, *J* 8.0, Ar), 7.34 (1H, t, *J* 7.3, Ar), 7.31 (1H, d, *J* 7.3, Ar), 7.23 (1H, d, *J* 8.0, Ar), 5.75 (1H, ddd, *J* 16.9, 9.4, 7.3, 4-H), 5.63 (1H, dd, *J* 9.4, 1.1, 5-H_B), 5.43 (1H, d, *J* 16.9, 1.1, 5-H_A), 5.21 (1H, d, *J* 10.1, 1-H), 5.18-5.09 (1H, m, 2-H), 2.81 (1H, ddd, *J* 13.0, 10.5, 7.3, 3-H_A), 2.69 (1H, dd, *J* 10.5, 7.3, 3-H_B), 1.47 (9H, s, Boc), NH not observed; δ_C (75 MHz, CDCl₃); 154.8 (C=O), 133.9 (Ar), 133.4 (2-C), 131.1 (Ar), 130.3 (Ar), 130.2 (Ar), 129.9 (Ar), 128.1 (Ar), 122.6 (1-C), 89.4 (4-C), 80.6 (Boc 2-C), 54.8 (5-C), 35.4 (3-C), 28.2 (Boc 3-C); ν_{max}/cm^{-1} (neat); 3362, 2854, 1690, 1518; *m/z* (ES) 407.1 and 409.2; HRMS Found: 407.0580, 409.0560 (C₁₆H₂₁BrN₂O₄ *MH*⁺ requires 407.0574, 409.5752).

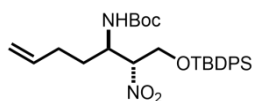
There was an additional fraction with *syn* isomer as the major component (d.r. 60:40) 13% yield.

***tert*-Butyl-*N*-[(1*R*, 2*R*)-1-(2-bromophenyl)-2-nitropent-4-en-1-yl] carbamate**



R_f : 0.40 (10:90, EtOAc–hexane); δ_H (500 MHz, CDCl₃); 7.61 (1H, d, *J* 8.0), 7.34 (1H, t, *J* 7.5, Ar), 7.22 (2H, t, *J* 7.6, Ar), 6.08 (1H, d, *J* 8.6, NH), 5.80 (1H, ddd, *J* 16.6, 9.6, 7.2, 2-H), 5.57 (1H, dd, *J* 9.6, 1.5, 1-H_A), 5.25 (1H, dd, *J* 16.6, 1.5, 1-H_B), 5.10 (2H, m, 5-H, 4-H), 2.95-2.86 (1H, m, 3-H_A), 2.75-2.66 (1H, m, 3-H_B), 1.47 (9H, s, Boc); δ_C (75 MHz, CDCl₃); 154.8 (C=O), 133.9 (Ar), 133.4 (2-C), 131.1 (Ar), 129.9 (Ar), 128.1 (Ar), 128.0 (Ar), 127.6 (Ar), 120.5 (1-C), 88.8 (4-C), 80.5 (Boc 2-C), 54.6 (3-C), 35.5 (3-C), 28.4 (Boc 3-C); ν_{max}/cm^{-1} (neat); 3362, 2854, 1690, 1518; *m/z* (ES) *m/z* (ES) 407.1 and 409.2; HRMS Found: 407.0580, 409.0560 (C₁₆H₂₁BrN₂O₄ *MH*⁺ requires 407.0574, 409.5752).

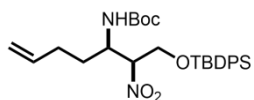
***tert*-Butyl-*N*-[(2*R*, 3*R*)-1-{(*tert*-butyldiphenylsilyl)oxy}-2-nitrohept-6-en-3-yl]carbamate (235)**



By **General Method E**, using amino sulfone (**228**) (0.65 g, 2 mmol), nitro-compound (**231**) (3.3 g, 10 mmol) and *N*-benzylquinium chloride (12 mol%), followed by two concurrent flash chromatography columns; eluting with DCM–Hexane (50:50) gave the *title compound* (0.85 g, d.r. 80:20, 83%) then second column eluting with TBME–Hexane (8:92) to give the *title compound*: (0.68 g, d.r. $\geq 95:\leq 5$, 69%); $[\alpha]_{\text{D}}^{22}$ 7.6 (c. 0.9, CHCl₃); R_f : 0.30 (8:92, TBME–hexane); δ_{H} (500 MHz, CDCl₃); 7.71–7.64 (4H, m, Ar), 7.45–7.30 (6H, m, Ar), 5.80–5.67 (1H, ddd, J 16.3, 8.5 and 7.0, 6-H), 5.00 (1H, d J 8.5, 7-H_B), 4.98 (1H, d J 16.3, 7-H_A), 4.68 (1H, app bs, 2-H), 4.62 (1H, d, J 9.4, NH), 4.03–3.97 (1H, m, 3-H), 3.93 (1H, d, J 12.0, 1-H_B), 3.72 (1H, d, J 7.5, 1-H_A), 2.11 (1H, dt, J 16.9 and 7.0, 5-H_B), 1.99 (1H, dt, J 14.5 and 7.0, 5-H_A), 1.47–1.45 (2H, m, 4-H₂), 1.44 (9H, s, Boc), 1.02 (9H, s, ^tBu); δ_{C} (125 MHz, CDCl₃); 155.0 (C=O), 136.5 (7-C), 135.6 (Ar), 135.5 (Ar), 135.5 (Ar), 132.3 (Ar), 130.1 (Ar), 126.0 (Ar), 125.8 (Ar), 124.5 (Ar), 115.3 (7-C), 91.6 (3-C), 80.1 (Boc), 62.4 (1-C), 50.0 (3-C), 31.4 (5-C), 29.8 (4-C), 28.2 (Boc), 27.3 (SiC(CH₃)₃), 26.6 (^tBu); $\nu_{\text{max}}/\text{cm}^{-1}$ (neat); 3310, 2980, 1710, 1485; m/z (ES) 513.3; HRMS Found: 513.2782, (C₂₈H₄₀N₂O₅Si MH^+ requires 513.2779).

The minor diastereoisomer was isolated in 7% yield with $>90:<10$ d.r.

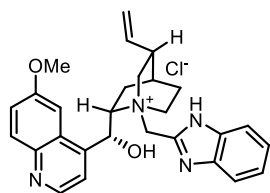
***tert*-Butyl-*N*-[(2*S*, 3*R*)-1-{(*tert*-butyldiphenylsilyl)oxy}-2-nitrohept-6-en-3-yl) carbamate (235)**



(0.07 g, d.r. 90:10, 7%); R_f : 0.32 (8:92, TBDMS–hexane); δ_H (500 MHz, $CDCl_3$); 7.62 (2H, d, J 7.0, Ar) 7.60–7.56 (2H, m, Ar), 7.45–7.30 (2H, m, Ar), 7.39 (4H, d, J 7.0, Ar), 5.72 (1H, ddd, J 16.0, 13.0 and 6.3, 6-H), 5.01 (1H, d J 13.0, 7- H_B), 4.98 (1H, d J 16.0, 7- H_A), 4.85 (1H, d, J 10.2, NH), 4.77 (1H, dd, J 9.2 and 4.0, 2-H), 4.22–4.14 (1H, m, 3-H), 3.93 (2H, app dd, J 11.3 and 4.0, 1- H_2), 2.09 (2H, dd, J 14.0 and 6.3, 5- H_2), 1.35 (2H, m, 4- H_2), 1.44 (9H, s, Boc), 1.02 (9H, s, t Bu); δ_C (125 MHz, $CDCl_3$); 155.2 (C=O), 136.6 (6-C), 135.4 (Ar), 134.8 (Ar), 132.5 (Ar), 130.2 (Ar), 129.6 (Ar), 127.9 (Ar), 127.7 (Ar), 127.5 (Ar), 116.1 (7-C), 91.8 (3-C), 80.0 (Boc), 63.1 (1-C), 49.0 (3-C), 30.0 (5-C), 29.7 (4-C), 28.2 (Boc), 27.8 (SiC(CH₃)₃), 26.6 (Boc); ν_{max}/cm^{-1} (neat); 3310, 2980, 1710, 1485; m/z (ES) 513.3; HRMS Found: 513.2782, (C₂₈H₄₀N₂O₅Si MH^+ requires 513.2779).

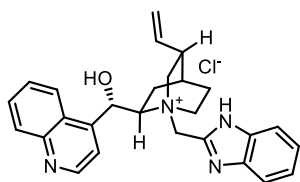
In addition a mixture of both diastereoisomers was obtained with d.r. of 50:50 (5% yield).

***N*-[1*H*-1,3-Benzodiazol-2-ylmethyl]quininium chloride (236)¹⁶⁰**



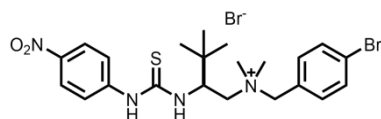
To a suspension of quinine (0.32 g, 1 mmol) in toluene (4 mL) was added 2-chloromethylbenzimidazole (0.18 g, 1.1 mmol), and the mixture was stirred at reflux for 3 h then cooled to rt and filtered. The crude material was purified by flash chromatography, eluting with DCM–MeOH (90:10) gave the title compound¹⁶⁰ (0.32 g, 65%) as a pink solid; R_f : 0.32 (80:20, DCM–MeOH); δ_H (500 MHz, $CDCl_3$); 8.78 (1H, d, J 4.6, 2'-H), 8.03 (1H, d, J 9.4, 8'-H), 7.92 (1H, d, J 4.8, 5'-H), 7.74-7.13 (5H, m, Ar), 6.76 (1H, d, J 1.7, Ar), 6.12-6.03 (1H, m, vinyl 1-H), 5.35-5.27-5.18 (2H, m, vinyl 2-H₂), 4.76 (1H, t, J 9.5, 9-H), 4.15 (1H, t, J 9.5, 8-H), 3.97 (3H, s, OMe), 3.90-3.82 (2H, m, benzyl H₂), 3.42 (1H, m, 6-H_A), 2.79 (1H, m, 6-H_B), 2.41 (2H, m, 2-H_A and 3-H), 2.31 (1H, s, 2-H_B), 1.89-1.98 (4H, m, 5-H₂ and 7-H₂), 1.03 (1H, m, 4-H), NH and OH not observed; m/z (ES) 455.2.

***N*-[1*H*-1,3-Benzodiazol-2-ylmethyl]cinchoninium chloride (237)¹⁶⁰**



To a suspension of cinchonine (0.29 g, 1 mmol) in toluene (4 mL) was added 2-chloromethylbenzimidazole (0.18 g, 1.1 mmol), and the mixture was stirred at reflux for 3 h then cooled to rt and filtered. The crude material was purified by flash chromatography, eluting with DCM–MeOH (90:10) gave the title compound¹⁶⁰ (0.27 g, 58%) as a red solid; R_f : 0.15 (80:20, DCM–MeOH); δ_H (500 MHz, $CDCl_3$); 8.87 (1H, d, J 4.6, 2'-H), 7.83-7.80 (2H, m, 8'-H and 5-H), 7.51-7.45 (3H, m, Ar), 7.27-7.16 (3H, m, Ar), 6.70-6.67 (1H, m, Ar), 6.60 (1H, bs, OH), 5.93 (1H, m, vinyl 1-H), 5.30-5.23 (2H, m, vinyl 2-H₂), 4.85 (1H, m, 9-H), 4.71 (1H, t, J 5.2, 9-H), 4.07 (1H, t, J 11.2, 8-H), 3.97 (2H, m, benzyl H₂), 2.62-2.55 (2H, m, 6-H₂), 2.35-1.78 (4H, m, 5-H₂ and 7-H₂), 0.87-0.82 (1H, m, 4-H), NH and OH not observed; m/z (ES) 425.

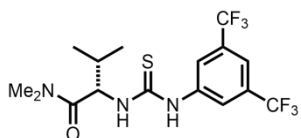
***N*-{(4-Bromobenzyl)-*N,N*-dimethyl-2-[(4-nitrophenyl)thioureido]}-*tert*-butyl]ethanaminium bromide (238)¹⁶²**



According to modified¹⁶⁶ procedure, di-*tert*-butyl dicarbonate (1.40 g, 6.4 mmol) was added to a solution of valine (0.50 g, 4.3 mmol), NaOH (2 eq.) in THF–H₂O (50:50, 20 mL) and stirred overnight. The reaction mixture was diluted with DCM (100 mL) and 1 M HCl_(aq) (pH 2). The organic layer was washed with 1 M HCl_(aq) (3 × 15 mL), brine (2 × 10 mL), dried (Na₂SO₄) and concentrated *in vacuo*. The crude residue was dissolved in DCM (20 mL, 0.3 M) and HCTU (6.4 mmol), DIPEA (8.6 mmol) was added at 0 °C. Dimethylamine (4 mL, 1 M in EtOH) was then added dropwise and the reaction mixture was vigorously stirred at rt. After 4 hr, the resulting solution was diluted with H₂O (100 mL) and DCM (100 mL), the organic layer was separated, washed with 1 M HCl_(aq) (3 × 15 mL), brine (2 × 10 mL), dried (Na₂SO₄) and concentrated *in vacuo*. The crude product was dissolved TFA–DCM (2:8 mL), stirred at rt overnight. The resulting solution was diluted with H₂O (100 mL) organic layer was extracted with H₂O (3 × 50 mL) then the combined aqueous layer was basified with *sat.* NaHCO_{3(aq)} (pH 10) and extracted with DCM (3 × 30 mL). The combined organic phases were dried (Na₂SO₄), concentrated *in vacuo*. Crude residue was filtered through a silica plug, eluting with DCM–MeOH (90:10) then dissolved in THF (10 mL) and added dropwise to LiAlH₄ (2mL in 1 M THF) at 0 °C. The reaction mixture was then heated at 75 °C for 24 h. The reaction mixture was cooled to 0 °C and H₂O (0.08 mL), NaOH (0.16 mL) then H₂O (0.24 mL) was added and stirred for 3 hr then filtered through celite and the filtrate concentrated *in vacuo*. The crude residue was then dissolved into DCM (4 mL), and the isothiocyanate (5 mmol) was added and stirred overnight. The reaction mixture was concentrated *in vacuo* then dissolved in a solution of MeCN (5.0 mL). Benzyl bromide (2 eq.), was added dropwise and the resulting mixture was stirred at rt overnight. The reaction mixture was concentrated *in vacuo* residue was purified by flash chromatography eluting with DCM–MeOH (100:0 to 90:10) to afford the title compound¹⁶² (0.27 g, 11%); R_f: 0.40 (90:10, DCM–MeOH); δ_H (500 MHz, CDCl₃); 10.54 (1H, s, NH), 9.42 (1H, d, *J* 12.0, NH), 8.12 (2H, d, *J* 8.1, Ar), 8.03 (2H, d, *J* 8.1, Ar), 7.62 (2H, d, *J* 7.3, Ar), 7.41 (2H, d, *J* 7.3, Ar), 4.97–4.93 (1H, d, *J* 12.0, benzyl H_A), 4.65–4.62 (1H, d, *J*

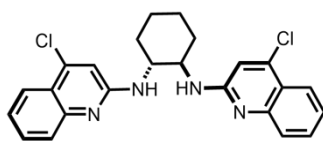
12.0, benzyl H_B), 4.41-4.35 (1H, m, 2-H), 3.61-3.58 (2H, d, *J* 12.0, 1-H₂), 3.25 (3H, s, Me), 3.18 (3H s, Me), 1.13 (9H, s, ^tBu); δ_C (75 MHz, CDCl₃); 181.2 (C=S), 145.6 (Ar), 134.5 (Ar), 132.7 (Ar), 131.7 (Ar), 130.5 (Ar), 126.1 (Ar), 125.5 (Ar), 124.2 (Ar), 67.8 (benzyl CH₂), 67.5 (1-C), 56.3 (2-C), 50.6 (Me), 49.8 (Me), 37.1 (^tBu 2-C), 26.4 (^tBu 3-C); ν_{max}/cm⁻¹ (neat); 2963, 1575, 1508, 1330, 1257, 1109, 851, 727; *m/z* (ES) 493.1; HRMS Found: 493.1269, (C₂₂H₃₀Br₂N₄O₂S *MH*⁺ requires 493.1273).

(2S)-3-(3,5-bis(trifluoromethyl)phenyl)thioureido-(isopropyl)-N,N-dimethylacetamide (**239**)¹⁶¹



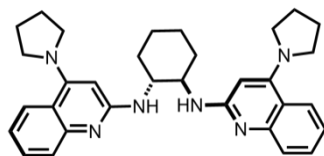
According to modified procedure¹⁶⁶, di-*tert*-butyl dicarbonate (1.4 g, 6.4 mmol) was added to a solution of valine (0.5 g, 4.3 mmol), NaOH (2 eq.) in THF–H₂O (50:50, 20 mL) and stirred overnight. The reaction mixture was diluted with DCM (100 mL) and 1 M HCl_(aq) added until pH 2. The organic layer was washed with 1 M HCl_(aq), brine, dried (Na₂SO₄) and concentrated *in vacuo*. The crude residue was dissolved in DCM (20 mL) and HCTU (6.4 mmol), DIPEA (8.6 mmol) was added at 0 °C. Dimethylamine (2 mL, 1 M in EtOH) was then added dropwise and the reaction mixture was vigorously stirred at rt. After 4 h, the resulting solution was diluted with H₂O (100 mL) and DCM (100 mL), the organic layer was separated, washed with 1 M HCl_(aq) (3 × 30 mL), brine (2 × 15 mL), dried (Na₂SO₄) and concentrated *in vacuo*. The crude residue was dissolved TFA–DCM (2:4 mL), stirred at rt overnight. The reaction solution was diluted with H₂O (100 mL) and organic layer was extracted with H₂O (3 × 30 mL) then the combined aqueous layer was basified with *sat.* NaHCO_{3(aq)} (pH 10) and extracted with DCM (5 × 30 mL). The combined organic phases were dried (Na₂SO₄), concentrated *in vacuo*. The crude residue was filtered through a silica plug, eluting with DCM–MeOH (90:10) gave a crude material which was added a solution of isothiocyanate 11 (1.4 g, 5.18 mmol) in DCM (20 mL) at rt the crude material was added and the reaction was stirred at rt overnight, then concentrated *in vacuo* then purified by flash chromatography eluting with DCM–MeOH (100:0 to 90:10) to give the acetamide (**239**)¹⁶¹ (0.58 g, 32%); R_f: 0.15 (90:10, DCM–MeOH) δ_H (500 MHz, CDCl₃); 9.35 (1H, s, NH), 8.40 (1H, d, *J* 7.7, NH), 8.03 (2H, s, Ar), 7.47 (1H, s, Ar) 5.25 (1H, app t, *J* 8.1, 1'-H), 3.38 (3H, s, Me), 3.05 (3H, s, Me), 2.08 (1H, tt, *J* 14.2 and 8.1, 1-H), 1.12 (3H, d, *J* 6.8, Me), 1.07 (3H, d, *J* 6.8, Me); *m/z* (ES) 416.2; C₁₆H₁₉F₆N₃O₅

(1*R*,2*R*)-*N,N*-Bis(4-chloroquinolin-2-yl)cyclohexane-1,2-diamine (250)¹⁶³



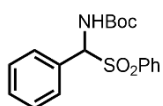
A flame-dried flask was charged with Pd(dba)₂ (0.057 g, 0.063 mmol), *rac*-BINAP (0.039 g, 0.063 mmol), sodium *tert*-butoxide (0.363 g, 3.78 mmol), (*R,R*)-diaminocyclohexane (0.143 g, 1.26 mmol), and 2,4-dichloroquinoline (0.5 g, 2.25 mmol), and the reaction vessel was placed under an argon atmosphere. Toluene (13 mL) was added, and the resulting red-brown solution was heated at 85 °C, after 3 hr, the reaction was cooled to 25 °C and diluted with EtOAc. The reaction mixture was washed with *sat.* NH₄Cl_(aq) (3 × 30 mL), dried (Na₂SO₄) and concentrated *in vacuo*. Flash chromatography, eluting with EtOAc–Hexane (10:90) gave the title compound¹⁶³ **250** (0.20 g, 36%) as an amorphous yellow powder; *R_f*: 0.20 (10:90, EtOAc–Hexane); δ_H (500 MHz, CDCl₃); 7.91 (2H, d, *J* 8.2), 7.69 (2H, d, *J* 8.2), 7.56 (2H, dd, *J* 8.2 and 7.3), 7.24 (2H, dd, *J* 8.2 and 7.3), 6.42 (2H, s), 5.75 (2H, bs), 4.09 (2H, m), 2.35 (2H, d, *J* 12.0), 1.83 (2H, m), 1.50-1.34 (4H, m); δ_C (75 MHz, CDCl₃); 156.8, 148.9, 142.6, 130.9, 126.5, 124.4, 122.9, 121.9, 112.6, 56.5, 33.1, 25.2; ν_{max}/cm⁻¹ (neat); 3220, 2930, 1601; *m/z* (ES) 437.2; HRMS Found: 437.1295, (C₂₄H₂₂Cl₂N₄ *MH*⁺ requires 437.1300).

(1*R*,2*R*)-*N,N*-Bis(4-(pyrrolidin-1-yl)quinolin-2-yl)cyclohexane-1,2-diamine (251)¹⁶³



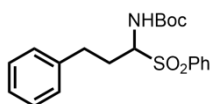
A microwave vial (10 mL) was charged with **250** (0.1 g, 0.23 mmol), pyrrolidine (0.6 mL, 4.6 mmol), and trifluoromethylbenzene (3 mL, 0.15 M). This suspension was heated at 200 °C and stirred in the microwave for 3.5 h. The reaction was then concentrated and purified by flash chromatography eluting with DCM–MeOH (95:5, to 80:20) to provide a light brown solid. This material was dissolved in dichloromethane and then washed with 3 M NaOH (4 × 10 mL), dried (Na₂SO₄) and concentrated *in vacuo*. The material was then triturated with hexanes to afford the diamine (**251**)¹⁶³ as a light brown powder (73 mg, 71%); *R*_f: 0.15 (95:5, DCM–MeOH) δ_H (500 MHz, CDCl₃); 7.73 (2H, d, *J* 7.8), 7.40 (2H, d, *J* 7.5), 7.40 (2H, dd, *J* 8.0 and 7.5), 7.00 (2H, dd, *J* 8.0 and 7.5), 5.82 (2H, bs), 5.27 (2H, s), 4.10 (2H, bs), 3.26 (4H, bs), 3.10 (4H, bs), 2.32 (2H, s), 1.90-1.70 (10H, m), 1.55-1.35 (4H, m); δ_C (75 MHz, CDCl₃); 153.2, 152.0, 125.0, 122.4, 119.9, 115.6, 88.6, 56.6, 53.4, 52.2, 31.8, 25.4, 24.3, 23.3; ν_{max}/cm⁻¹ (neat); 3259, 3056, 2927, 2855, 2935, 1591, 1529; *m/z* (ES) 507.4; HRMS Found: 507.3239, (C₃₈H₃₈N₆ MH⁺ requires 507.3236).

***tert*-Butyl *N*-[1-(benzenesulfonyl)-(phenyl)methyl]carbamate (253)**¹⁸¹



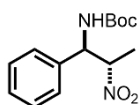
By **General Method B**, using *tert*-butyl carbamate (0.50 g, 4.2 mmol), benzene sulfinic sodium salt (1.03 g, 6.3 mmol) and benzaldehyde (0.64 g, 6.3 mmol), followed by filtration, washing with water (100 mL) and hexane (100 mL) gave the amidosulfone¹⁸¹ **253** (1.14 g, 78%) an amorphous white solid; *R*_f: 0.45 (10:90, EtOAc–hexane); δ_H (500 MHz, CDCl₃); 7.91-7.90 (2H, d, *J* 7.2, Ar), 7.65-7.63 (1H, m, Ar), 7.55-7.52 (2H, d, *J* 7.3, Ar), 7.42-7.39 (5H, m, Ar), 5.93 (1H, d, *J* 10, NH), 5.74-7.72 (1H, d, *J* 10, CH), 1.26 (9H, bs, Boc); δ_C (75 MHz, CDCl₃); 153.5 (C=O), 136.8 (Ar), 133.9 (Ar), 129.8 (Ar), 129.8 (Ar), 129.4 (Ar), 129.0 (Ar), 128.9 (Ar), 128.7 (Ar), 81.2 (Boc 2-C), 73.9 (1-C), 28.0 (Boc 3-C); ν_{max}/cm⁻¹ (neat); 3355, 2982, 1698, 1509, 1309, 1144; Due to instability, unable to get an accurate high mass for title compound. C₁₈H₂₁NO₄S

***tert*-Butyl *N*-[1-(benzenesulfonyl)-3-phenylpropyl]carbamate (**255**)¹⁸²**



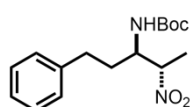
By **General Method B**, using *tert*-butyl carbamate (0.50 g, 4.2 mmol), benzene sulfinic sodium salt (1.03 g, 6.3 mmol) and hydrocinnamaldehyde (0.84 g, 6.3 mmol), followed by filtration, washing with water (100 mL) and hexane (100 mL) gave the amidosulfone¹⁸² **255** (1.09 g, 69%) an amorphous white solid; R_f : 0.40 (10:90, EtOAc–hexane); δ_H (500 MHz, $CDCl_3$); 7.90-7.87 (4H, d, J 7.4, Ar), 7.58-7.50 (6H, m, Ar), 7.32-7.16 (10H, m, Ar), 5.18 (1H, d, J , $NH^{Rot A}$), 5.02 (1H, d, J , $NH^{Rot B}$), 4.86 (1H, d, J , 1- $H^{Rot B}$), 4.59 (1H, d, J , 1- $H^{Rot A}$), 2.57-2.97 (6H, m, 3- $H^{Rot B}$, 3- $H^{Rot A}$, 2- $H_A^{Rot B}$, 2- $H_A^{Rot A}$), 2.57-2.97 (2H, m, 2- $H_B^{Rot B}$, 2- $H_B^{Rot A}$) 1.22 (9H, s, Boc^{Rot B}), 1.05 (9H, s, Boc^{Rot A}); δ_C (75 MHz, $CDCl_3$); 153.5 (C=O), 136.8 (Ar), 133.9 (Ar), 129.8 (Ar), 129.8 (Ar), 129.4 (Ar), 129.0 (Ar), 128.9 (Ar), 128.7 (Ar), 81.2 (1-C), 73.9 (Boc 2-C), 34.8 (3-C), 31.2 (2-C), 28.0 (Boc 3-C); ν_{max}/cm^{-1} (neat); 3355, 2982, 1698, 1509, 1309, 1144; Due to instability, unable to get an accurate high mass for title compound. $C_{18}H_{21}NO_4S$

***tert*-Butyl-*N*-(2-nitro-3-phenylpropyl)carbamate (**257**)¹⁵⁷**



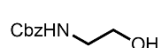
By **General Method E**, using amino sulfone (**253**) (0.173 g, 0.5 mmol), nitroethane (0.17 mL, 2.5 mmol) and *N*-benzylquinium chloride (10 mol%), filtered through a silica plug, eluting with EtOAc–Hexane (90:10) gave the nitro amine¹⁵⁷ **257** (0.11 g, d.r. 93:7. 82%) an amorphous white solid; R_f : 0.30 (10:90, EtOAc–hexane); δ_H (500 MHz, $CDCl_3$); 7.39-7.29 (6H, m, Ar^{Maj and Min}), 7.27-7.21 (4H, m, Ar^{Maj and Min}), 5.57 (1H, app bs, NH^{Min}), 5.32 (1H, d, J 8.7, NH^{Maj}), 5.19 (1H, dd, J 8.9 and 6.4, 2- H^{Maj}), 5.10 (1H, app bs, 2- H^{Min}), 4.92 (2H, app bs, 3- $H^{Maj and Min}$), 1.53 (6H, d, J 6.4, 1- $H_3^{Maj and Min}$), 1.44 (18H, s, Boc^{Maj and Min}); δ_C (75 MHz, $CDCl_3$); 155.4 (C=O^{Maj and Min}), 140.6 (Ar^{Maj and Min}), 129.1 (Ar^{Min}), 129.0 (Ar^{Maj}), 128.6 (Ar^{Maj}), 128.4 (Ar^{Min}), 126.8 (Ar^{Maj}), 126.4 (Ar^{Min}), 86.7 (2- C^{Min}), 85.7 (2- C^{Maj}), 77.2 (Boc 2- $C^{Maj and Min}$), 57.4 (3- $C^{Maj and Min}$), 28.2 (Boc 3- $C^{Maj and Min}$), 17.0 (1- $C^{Maj and Min}$); ν_{max}/cm^{-1} (neat); 3345, 1711, 1602, 1508; m/z (ES) 280.3.

tert-butyl N-(2-nitro-4-phenylpentan-3-yl)carbamate (258)¹⁵⁷



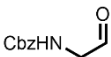
By **General Method E**, using amino sulfone (**255**) (0.18 g, 0.5 mmol), nitroethane (0.17 g, 2.5 mmol) and *N*-benzylquinium chloride (12 mol%), followed by flash chromatography, eluting with EtOAc–Hexane (90:10) gave the nitro amine¹⁵⁷ **258** (0.12 g, d.r. 90:10, 63%) an amorphous white solid; R_f : 0.40 (10:90, EtOAc–hexane); δ_H (500 MHz, C_6D_6); 7.16-7.08 (4H, m, Ar), 7.06-7.01 (2H, m, Ar), 6.99 (2H, d, J 7.3, Ar), 6.91 (2H, d, J 7.3, Ar), 4.62 (1H, d, J 9.9, NH^{Maj}), 4.26 (1H, d, J 9.0, NH^{Min}), 4.23-4.19 (1H, m, 2- H^{Min}), 3.98 (1H, dq, J 6.8 and 4.6, 2- H^{Maj}), 3.86 (1H, m, 3- H^{Maj}), 3.75-3.67 (1H, m, 3- H^{Min}), 2.39 (2H, dd, J 14.0 and 7.7, 4- H_2^{Maj}), 2.28-2.20 (2H, m, 4- H_2^{Min}), 1.41 (9H, s, Boc^{Min}), 1.37 (9H, s, Boc^{Maj}), 1.30-1.13 (4H, m, 4- H_2^{Maj} and Min) 1.00 (3H, d, J 6.8, 1- H_3^{Maj}), 0.84 (3H, d, J 6.8, 1- H_3^{Maj}); δ_C (75 MHz, C_6D_6); 155.6 ($C=O^{Maj}$), 155.2 ($C=O^{Min}$), 141.0 (Ar Maj), 140.8 (Ar Min), 128.6 (Ar Maj), 128.5 (Ar Min), 128.4 (Ar Maj), 128.2 (Ar Min), 127.8 (Ar Min), 126.3 (Ar Maj), 85.7 (2- C^{Maj}), 85.4 (2- C^{Min}), 79.4 (Boc 2- C^{Min}), 79.3 (Boc 2- C^{Maj}), 53.0 (3- C^{Min}), 52.2 (3- C^{Maj}), 33.9 (5- C^{Maj} and Min), 32.2 (4- C^{Maj}), 31.2 (4- C^{Min}), 28.2 (Boc 3- C^{Maj} and Min), 15.9 (1- C^{Maj}), 14.6 (1- C^{Min}); ν_{max}/cm^{-1} (neat); 3315, 2985, 1687, 1520; m/z (ES) 381.2; HRMS Found: 381.1784, ($C_{16}H_{24}N_2O_4$ *MNa* requires 381.1784).

Benzyl (2-hydroxyethyl)carbamate (165)¹⁸³



According to the procedure⁸⁴ a solution of benzyl chloroformate (4.7 mL, 3.3 mmol) added dropwise to the stirred solution of ethanolamine (1.81 mL, 30 mmol), $NaHCO_3$ (3 eq.) in DCM (0.2 M) over 1 hr. The reaction mixture was left to stir for a further 12 hr and then concentrated *in vacuo* to give a crude mixture which was purified by flash chromatography, eluting with EtOAc–Hexane (10:90) gave the title compound¹⁸³ (5.3 g, 91%) as a white amorphous solid; R_f : 0.25 (10:90, EtOAc–hexane); δ_H (500 MHz, $CDCl_3$); 7.48-7.27 (5H, m, Ar), 5.11 (2H, s, benzyl H_2), 3.73 (2H, d, J 4.8, 1- H_2), 3.37 (2H, d, J 4.8, 2- H_2), 2.04 (1H, bs, OH or NH), NH or OH not observed; m/z (ES) 196.2;

Benzyl (2-oxoethyl)carbamate (260)^{184,185}

 To a stirred solution of DMSO (6.4 mL) in DCM (0.3 M) was added sulphur trioxide pyridine complex (7.20 g) at 0 °C. The resultant mixture was stirred for 15 mins and a solution of benzyl (2-hydroxyethyl)carbamate (2.0 g, 10 mmol), (1 eq.) in DCM (0.2 M) was added dropwise. After stirring for 1 hr at 0 °C, Et₃N (3 eq.) was added, and the resulting mixture was allowed to warm into rt. After 30 mins, the reaction mixture was quenched with 10% HCl_(aq) (60 mL) and the resulting mixture extracted with ethyl acetate (3 × 200 mL). The combined organic layers were washed with *sat.* NaHCO_{3(aq)}, brine then dried (MgSO₄) and concentrated *in vacuo* to give a crude mixture which was flash chromatography, eluting with EtOAc–Hexane (10:90) gave the title compound^{184,185} (0.874 g, 45%); R_f: 0.10 (10:90, EtOAc–hexane) δ_H (300 MHz, CDCl₃); 9.66 (1H, d, *J* 5.0, 1-H), 7.44-7.28 (5H, m, Ar), 5.40 (1H, bs, NH), 5.14 (2H, s, benzyl CH₂), 4.16 (2H, d, *J* 5.0, 2-H₂); δ_C (125 MHz, CDCl₃); 196.2 (1-C), 136.1 (Ar), 128.5 (Ar), 128.3 (Ar), 128.1 (Ar), 67.2 (2-C), 51.7 (benzyl CH₂), C=O not observed; *m/z* (ES) 194.1.

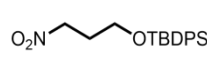
***tert*-Butyl-*N*-[1-(benzenesulfonyl)-1-methyl-*N*-benzyloxycarbonylamino] carbamate (261)**

By **General Method B**, using *tert*-butyl carbamate (0.45 g, 3.8 mmol), benzene sulfinic sodium salt (0.64 g, 3.8 mmol) and aldehyde **260** (0.54 g, 0.37 mmol), followed by filtration, washing with water (100 mL) and hexane (100 mL) then purified by flash chromatography eluting with Petrol–EtOAc (70:30) give the *title compound* (**261**) (0.43 g, 36%) an amorphous white solid; R_f : 0.15 (10:90, EtOAc–hexane); δ_H (300 MHz, $CDCl_3$); 7.90 (4H, d, J 7.5, Ar^{RotA and RotB}), 7.61 (12H, t, J 7.5, Ar^{RotA and RotB}), 7.50 (4H, t, J 7.5, Ar^{RotA and RotB}), 5.91 (2H, d, J 10.3, NH^{RotA and RotB}), 5.72 (1H, t, J 8.7, NH^{RotB}), 5.10–4.96 (6H, m, benzyl^{RotA and RotB} and 1-H^{RotA and RotB}), 4.01–3.83 (1H, m, 2-H_A^{RotA}), 3.82–3.75 (1H, m, 2-H_A^{RotB}), 3.50–3.40 (1H, m, 2-H_B^{RotA}), 3.37–3.30 (1H, m, 2-H_B^{RotB}), 1.43 (9H, s, Boc^{RotA}), 1.20 (9H, s, Boc^{RotB}), NH^{RotA} not observed; δ_C (75 MHz, $CDCl_3$); 156.8 (C=O^{RotA and RotB}), 153.9 (C=O^{RotA and RotB}), 136.6 (Ar^{RotA and RotB}), 136.1 (Ar^{RotA and RotB}), 134.1 (Ar^{RotA and RotB}), 129.3 (Ar^{RotA and RotB}), 129.1 (Ar^{RotA and RotB}), 128.5 (Ar^{RotA and RotB}), 128.1 (Ar^{RotA and RotB}), 128.0 (Ar^{RotA and RotB}), 80.8 (Boc 2-C^{RotA and RotB}), 71.0 (1-C^{RotB}), 69.9 (1-C^{RotA}), 67.1 (benzyl CH₂^{RotA}), 66.8 (benzyl CH₂^{RotB}), 38.7 (2-C^{RotA and RotB}), 28.3 (Boc 3-C^{RotB}), 27.9 (Boc 3-C^{RotA}); ν_{max}/cm^{-1} (neat); 3100, 3090, 1742, 1730, 1450; Unable to observe MH^+ in mass spectrometer.

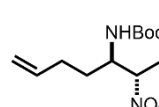
***tert*-Butyl(3-bromopropoxy)diphenylsilane (263)**¹⁸⁶

General Procedure D, using 3-bromopropanol (6.5 mL, 10 mmol), TBDPS-Cl (3.12 mL, 12 mmol) and imidazole (2.04 g, 30 mmol), filtered through a silica plug eluting with EtOAc–Hexane (10:90) gave the *title compound*¹⁸⁶ (3.20 g, 85%) as a yellow oil; R_f : 0.60 (10:90, EtOAc–hexane); δ_H (500 MHz, $CDCl_3$); 7.48–7.33 (4H, m, Ar), 7.25–7.10 (6H, m, Ar), 3.79 (2H, t, J 8.7, 3-H₂), 3.57 (2H, m, 1-H₂), 1.90 (2H, m, 2-H₂), 1.32 (9H, s, Boc). Unable to observe MH^+ in mass spectrometer.

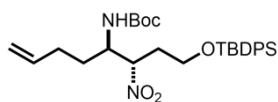
***tert*-Butyl(3-nitropropoxy)diphenylsilane (264)**¹⁷⁸

 According to **General Method C**, using *tert*-butyl(3-bromopropoxy) diphenylsilane (**263**) (2.199 g, 5.8 mmol), sodium nitrite (0.80 g, 11.6 mmol), followed by flash chromatography, eluting with EtOAc–Petrol (20:80) gave the title compound¹⁷⁸ (0.86 g, 43%) as slight yellow solid; *R*_f: 0.50 (10:90, EtOAc–hexane); δ_H (500 MHz, CDCl₃); 7.48–7.33 (4H, m, Ar), 7.25–7.10 (6H, m, Ar), 4.68 (2H, m, 1-H₂), 3.79 (2H, t, *J* 8.7, 3-H₂), 1.90 (2H, m, 2-H₂), 1.32 (9H, s, ^tBu);¹⁷⁸

***tert*-Butyl-*N*-(2-nitro)hept-6-en-3-yl) carbamate (265)**

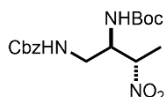
 By **General Method E**, using amino sulfone (**228**) (1.63 g, 5 mmol), nitroethane (1.7 mL, 25 mmol) and *N*-benzylquinium chloride (12 mol%), followed by flash chromatography, eluting with EtOAc–Hexane (90:10) gave the *title compound* (0.94 g, d.r. 90:10, 73%) as an amorphous solid; *R*_f: 0.4 (10:90, EtOAc–hexane); [α]_D¹⁹ +18.1 (*c.* 1.59, CHCl₃); δ_H (500 MHz, CDCl₃); 5.77 (2H, ddt, *J* 17.0, 10.2 and 6.7 6-H^{Maj and Min}), 5.03 (4H, app t, *J* 14.3, 7-H^{Maj and Min}), 4.88 (2H, d, *J* 9.1, NH^{Maj and Min}), 4.69 (1H, dd, *J* 12.1 and 6.4, 2-H^{Maj}), 4.51 (1H, m, 2-H^{Min}), 3.98 (2H, app t, *J* 10.0, 3-H^{Maj and Min}), 2.28–2.15 (2H, m, 5-H^{A Maj and Min}), 2.15–2.05 (2H, m, 5-H^{B Maj and Min}), 1.70–1.59 (2H, m, 4-H^{A Maj and Min}), 1.53 (6H, d, *J* 6.4, 1-H^{3 Maj and Min}), 1.45 (9H, s, Boc^{Min}), 1.45 (9H, s, Boc^{Maj}), 1.39–1.35 (2H, m, 4-H^{B Maj and Min}); δ_C (125 MHz, CDCl₃); 155.6 (C=O^{Min}), 155.3 (C=O^{Maj}), 136.80 (6-C^{Min}), 136.7 (6-C^{Maj}), 116.1 (7-C^{Min}), 115.9 (7-C^{Maj}), 85.64 (2-C^{Maj and Min}), 79.96 (Boc 2-C^{Min}), 79.83 (Boc 2-C^{Maj}), 53.9 (3-C^{Min}), 53.0 (3-C^{Maj}), 30.0 (5-C^{Maj}), 29.8 (5-C^{Min}), 28.9 (4-C^{Maj and Min}), 28.25 (Boc 3-C^{Maj}), 28.0 (Boc 3-C^{Min}), 16.3 (1-C^{Maj and Min}); ν_{max}/cm⁻¹ (neat); 3327, 2992, 1712, 1530. The minor diastereoisomer of this compound was subsequently crystallised from EtOAc:Hexanes. The crystal structure showed the *syn* relationship (see Section 0: Figure 39 and Section 6.8: Appendix 8: Table 16).

***tert*-Butyl (1-((*tert*-butyldiphenylsilyloxy)-2-nitro oct-7-en-4-yl)carbamate
(266)**



By **General Method E**, using amino sulfone (**228**) (0.256 g, 0.5 mmol), nitro-compound (**264**) (0.86 g, 2.5 mmol) and *N*-benzylquinium chloride (10 mol%), followed by two concurrent flash chromatography columns; eluting with DCM–Hexane (25:75) then second column eluting with TBME–Hexane (4:96) to give the *title compound* as an amorphous solid (0.19 g, d.r. \geq 90:10, 63%); R_f : 0.20 (4:96, TBME–Hexane); δ_H (500 MHz, $CDCl_3$); 6.49 (2H, d, J 7.2, NH), 5.72 (1H, ddd, J 16.9, 12.9 and 6.5, 6-H), 5.04–4.98 (2H, m, 7-H₂), 4.51 (1H, app dt, J 15.1 and 7.2, 2-H), 4.27 (1H, app ddd, J 11.3, 8.5 and 3.7, 5-H), 2.10–2.02 (2H, m, 4-H₂), 2.00–1.92 (1H, m, 5-H_A), 1.75–1.66 (1H, m, 5-H_A), 1.55 (9H, s, Boc), 1.21 (3H, d, J 7.2, 1-H₃); δ_C (125 MHz, $CDCl_3$); 161.2 (q J 39.1, C=O), 150.9 (C=O), 136.3 (6-C), 116.4 (7-C), 87.1 (Boc 2-C), 61.1 (2-C), 48.7 (3-C), 30.0 (4-C), 27.4 (Boc 3-C), 27.2, (5-C), 17.3 (1-C) ν_{max}/cm^{-1} (neat); 3100, 3090, 1742, 1730, 1450.

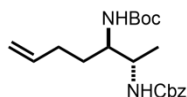
***tert*-Butyl-*N*-(2-nitro-3-methyl-[*N*-benzyloxycarbonylamino])carbamate
(267)**



By **General Method E**, using amino sulfone (**213**) (0.22 g, 0.5 mmol), nitroethane (0.17 g, 2.5 mmol) and *N*-benzylquinium chloride (12 mol%), followed by flash chromatography, eluting with EtOAc–Hexane (30:70) gave *title compound* (79 mg, d.r. 60:40, 43%) as an amorphous solid; R_f : 0.15 (30:70, EtOAc–hexane); δ_H (500 MHz, $CDCl_3$); 7.33 (10H, m, Ar), 5.54 (1H, bs, NH), 5.30 (1H, d, J 10.6 NH), 5.20 (2H, s, benzyloxycarbonyl^{Maj}), 5.09 (2H, s, benzyloxycarbonyl^{Min}), 4.84-4.77 (1H, app bs, 2-H^{Min}), 4.76-4.67 (1H, m, 3-H^{Maj}), 4.18 (1H, d, J 10.6, 2-H^{Maj}), 4.13 (1H, m, 3-H^{Min}), 3.92-3.84 (1H, m, 1-H_A^{Maj}), 3.79 (1H, dd, J 14.4 and 7.5, 1-H_B^{Maj}), 3.43 (1H, dd, J 13.6 and 7.5, 1-H_A^{Min}), 3.32 (1H, m, 1-H_A^{Min}), 2.19-2.12 (3H, m, 3-H₃^{Maj}), 1.90 (1H, d, J 6.5, 3-H₃^{Min}), 1.59 (9H, s, Boc^{Maj}), 1.42 (9H, s, Boc^{Min}), 2 \times NH not observed; δ_C (75 MHz, $CDCl_3$); 159.7 (C=O^{Maj} and ^{Min}), 158.3 (C=O^{Maj} and ^{Min}), 129.3 (Ar^{Maj} and ^{Min}), 128.5 (Ar^{Maj} and ^{Min}), 128.2 (Ar^{Min} and ^{Min}), 128.1 (Ar^{Min} and ^{Min}), 81.1 (2-C^{Maj}), 81.0 (2-C^{Min}), 78.1 (Boc 2-C^{Maj}), 78.0 (Boc 2-C^{Min}), 69.7 (2-C^{Maj} and ^{Min}), 67.2 (3-C^{Min}), 67.0 (3-C^{Maj}), 53.3 (4-

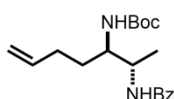
C^{Maj}), 52.2 (4-C^{Min}), 28.2 (Boc 3-C^{Maj}), 27.9 (Boc 3-C^{Maj}), 16.4 (1-C^{Maj} and Min); $\nu_{\max}/\text{cm}^{-1}$ (neat); 3389, 2997, 1732, 1717, 1640, 1580; m/z (ES) 367.17.

Benzyl *tert*-butyl hept-6-ene-2,3-diyl dicarbamate (269)



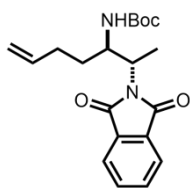
By **General Method F**, using nitro adduct (**265**) (2.6 g, 10 mmol) in THF (25 mL), LiAlH₄ (21 mL of 1 M solution), H₂O (0.8 mL), NaOH (1.6 mL), H₂O (2.4 mL). The crude material was then dissolved in THF (0.1 M) and benzyl chloroformate (14 mL, 10 mmol), E₃N (3 eq.) was added and the reaction stirred for 18 h. give a crude material which was purified by flash chromatography, eluting with DCM–MeOH (100:0 to 95:5) gave the *title compound* (2.14 g, 59%); R_f : 0.35 (10:90, EtOAc–hexane); δ_{H} (500 MHz, MeOH); 7.58 (2H, d, J 8.3, Ar), 7.11–7.01 (3H, m, Ar), 5.50 (1H, ddt, J 17.1, 10.4 and 6.6, 6-H), 4.73 (1H, dd, J 17.1 and 1.4, 7-H_A), 4.66 (1H, dd, J 10.4 and 1.4, 7-H_B), 4.10 (2H, s, benzyl H₂), 3.89–3.81 (1H, m, 2-H), 3.48 (1H, m, 3-H), 1.87 (1H, dt, J 14.0 and 6.6, 5-H_A), 1.77 (1H, dt, J 14.0, 6.6, 5-H_B), 1.31 (1H, dddd, J 14.0, 9.0, 7.0, 4.1, 4-H_A), 1.20–1.05 (10H, m, 4-H_B and Boc), 0.9 (3H, d, J 6.7, 1-H₃), 2 \times NH not observed; δ_{C} (125 MHz, MeOH); 169.1 (C=O), 154.2 (C=O), 138.8 (6-C), 136.0 (Ar), 132.2 (Ar), 129.3 (Ar), 128.7 (Ar), 115.4 (7-C), 75.7 (Boc 2-C), 63.4 (benzyl), 62.3 (3-C), 55.4 (2-C), 32.2 (4-C), 31.3 (5-C), 28.8 (Boc 3-C), 15.6 (1-C); $\nu_{\max}/\text{cm}^{-1}$ (neat); 3308, 2987, 1750, 1712, 1528; m/z (ES) 363.4.

***tert*-Butyl ((2*S*,3*R*)-2-benzamidohept-6-en-3-yl)carbamate (270)**



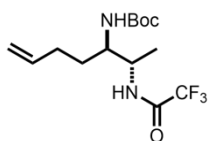
By **General Method F**, using nitro adduct (**265**) (2.6 g, 10 mmol) in THF (25 mL), LiAlH₄ (21 mL of 1 M solution), H₂O (0.8 mL), NaOH (1.6 mL), H₂O (2.4 mL). The crude amine was dissolved in DCM (0.1 M) and benzyl anhydride (2.22 g, 10 mmol) and E₃N (3 eq.) was added and the was stirred for 18 hr. The reaction mixture was then concentrated *in vacuo* and purified by flash chromatography, eluting with EtOAc–Hexane (90:10) gave the *title compound* (1.83 g, 55%); R_f: 0.40 (20:80, EtOAc–Hexane); δ_H (500 MHz, MeOH); 7.85 (2H, d, *J* 7.5, Ar), 7.57 (1H, *J* 7.5, Ar), 7.49-7.46 (2H, m, Ar) 5.89 (1H, ddt, *J* 17.1, 10.2 and 6.6, 6-H), 5.08 (1H, dd, *J* 17.1 and 1.4, 7-H_A), 5.05 (1H, dd, *J* 10.2 and 1.4, 7-H_B), 4.22-4.20 (1H, m, 3-H), 3.63–3.60 (1H, m, 2-H), 1.87 (1H, dt, *J* 14.0 and 6.6, 5-H_A), 1.77 (1H, dt, *J* 14.0 and 6.6, 5-H_B), 1.41 (9H, s, Boc), 1.37 (1H, m, 4-H_B), 1.31 (1H, dddd, *J* 14.0, 9.0, 7.0, 4.1, 4-H_A), 1.26 (3H, d, *J* 6.7, 1-H₃), 2 × NH not observed; δ_C (125 MHz, MeOH); 158.2 (C=O), 158.3 (C=O), 148.1 (6-C), 138.0 (Ar), 128.6 (Ar), 128.4 (Ar), 128.1 (Ar), 115.2 (7-C), 75.7 (Boc 2-C), 62.3 (3-C), 55.4 (2-C), 32.2 (4-C), 31.3 (5-C), 28.8 (Boc 3-C), 15.6 (1-C); ν_{max}/cm⁻¹ (neat); 3340, 2968, 1703, 1618; *m/z* (ES) 333.22; HRMS Found: 333.2174, (C₁₉H₂₈N₂O₃ *MH*⁺ requires 333.2172).

***tert*-Butyl (2-(1,3-dioxoisindolin-2-yl)hept-6-en-3-yl)carbamate (271)**



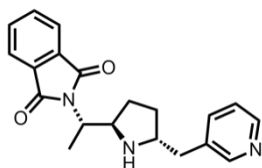
By **General Method F**, using nitro adduct (**265**) (2.6 g, 10 mmol) in THF (25 mL), LiAlH₄ (21 mL of 1 M solution), H₂O (0.8 mL), NaOH (1.6 mL), H₂O (2.4 mL). The crude amine was dissolved in toluene (0.1 M) and phthalic anhydride (2.22 g, 10 mmol) and E₃N (3 eq.) was added and the reaction mixture was heated to reflux for 48 hrs. The reaction mixture was then concentrated *in vacuo* and purified by flash chromatography, eluting with EtOAc–Hexane (50:50) gave the *title compound* **271** (1.22 g, 34%) as an amorphous white solid; R_f: 0.40 (20:80, EtOAc–Hexane); δ_H (500 MHz, CDCl₃); 8.06–8.03 (2H, m, Phth^{Min}), 7.96–7.93 (2H, m, Phth^{Min}), 7.87–7.79 (2H, m, Phth^{Maj}), 7.75–7.70 (2H, m, Phth^{Maj}), 5.86–5.69 (2H, m, 6-H^{Maj and Min}), 5.05–4.99 (4H, m, 7-H₂^{Maj and Min}), 4.44 (2H, d, *J* 9.8, NH^{Maj}), 4.34 (1H, app q, *J* 7.1, 2-H^{Min}), 4.18 (1H, app q, *J* 7.1, 2-H^{Maj}), 4.22–4.14 (1H, m, 3-H^{Maj}), 4.12–4.04 (1H, m, 3-H^{Min}), 2.20–2.02 (4H, m, 4-H₂^{Maj and Min}), 1.54 (6H, dd, *J* 7.7, 1-H₃^{Maj and Min}), 1.50–1.42 (4H, m, 5-H₂^{Maj and Min}), 1.41 (18H, s, Boc^{Maj and Min}); δ_C (125 MHz, CDCl₃); 168.9 (C=O^{Min}), 168.3 (C=O^{Maj}), 155.8 (C=O^{Min}) 155.6 (C=O^{Maj}), 137.6 (6-C^{Maj}), 137.0 (6-C^{Min}), 136.0 (Ar^{Min}), 133.84 (Ar^{Maj}), 131.87 (Ar^{Maj}), 131.80 (Ar^{Min}), 123.24 (Ar^{Min}), 123.13 (Ar^{Maj}), (7-C^{Min}), 115.2 (7-C^{Maj}), 79.1 (Boc 2-C^{Maj}), 78.8 (Boc 2-C^{Min}), 52.6 (2-C^{Maj}), 52.5 (2-C^{Min}), 50.7(3-C^{Maj}), 50. (3-C^{Min}), 31.1 (4-C^{Maj}), 30.5 (4-C^{Min}), 30.1 (5-C^{Maj}), 29.2 (5-C^{Min}), 28.2 (Boc 3-C^{Maj}), 28.1 (Boc 3-C^{Min}), 15.6 (1-C^{Min}), 14.0 (1-C^{Maj}); ν_{max}/cm⁻¹ (neat); 3301, 2980, 1730, 1715, 1496; *m/z* (ES) 359.2; HRMS Found: 359.1971, (C₂₀H₂₆N₂O₄ MH⁺ requires 359.1965).

***tert*-Butyl (2-(2,2,2-trifluoroacetamido)hept-6-en-3-yl)carbamate (272)**



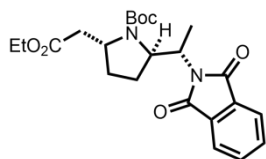
By **General Method F**, using nitro adduct (**265**) (0.26 g, 1 mmol) in THF (25 mL), LiAlH₄ (2.1 mL of 1 M solution), H₂O (0.08 mL), NaOH (0.16 mL), H₂O (0.24 mL), then trifluoroacetyl chloride (1.2 eq.), followed by flash chromatography, eluting with EtOAc–Hexane (90:10) gave the *title compound* (0.11 g, 33%); R_f: 0.30 (20:80, EtOAc–Hexane); δ_H (500 MHz, CDCl₃); 6.49 (2H, d, *J* 7.2, NH), 5.72 (1H, ddd, *J* 16.9, 12.9 and 6.5, 6-H), 5.04–4.98 (2H, m, 7-H₂), 4.51 (1H, app dt, *J* 15.1 and 7.2, 2-H), 4.27 (1H, app ddd, *J* 11.3, 8.5 and 3.7, 5-H), 2.10–2.02 (2H, m, 4-H₂), 2.00–1.92 (1H, m, 5-H_A), 1.75–1.66 (1H, m, 5-H_B), 1.55 (9H, s, Boc), 1.21 (3H, d, *J* 7.2, 1-H₃); δ_C (125 MHz, CDCl₃); 161.2 (q *J* 39.1, C=O), 150.9 (C=O), 136.3 (6-C), 116.1 (q, *J* 288.1, CF₃^{Maj}), 116.4 (7-C), 87.1 (Boc 2-C), 61.1 (2-C), 48.7 (3-C), 30.0 (4-C), 27.4 (Boc 3-C), 27.2, (5-C), 17.3 (1-C); ν_{max}/cm⁻¹ (neat); 3290, 2993, 1723, 1610, 1485; *m/z* (ES) 325.2.

***tert*-Butyl 2-(1-(1,3-dioxoisindolin-2-yl)ethyl)-5-(pyridin-3-ylmethyl)pyrrolidine-1-carboxylate (279)**



By **General Method H**, using **271** (43 mg, 0.12 mmol), 3-bromopyridine (0.14 mmol), followed by flash chromatography, eluting with DCM–EtOH–NH₄OH (97:2:1 to 84:14:2) gave the *title compound* (16 mg, d.r. >95:<5, 31%); R_f: 0.1 (97:2:1 DCM–EtOH–NH₄OH); δ_H (500 MHz, CDCl₃); 8.09 (2H, d, *J* 8.1, pyridinyl 2-H and 4-H), 7.59–7.49 (4H, m, Ar), 7.42 (1H, m, pyridinyl 6-H), 7.11 (1H, app s, pyridinyl 5-H), 4.29 (2H, m, 5-H and ethyl 1-C), 3.75 (1H, ddd, *J* 11.7, 8.0 and 3.5, 2-H), 2.89 (1H, d, *J* 13.6, 5-methyl H_B) 2.52 (1H, *J* 13.6, 5-methyl H_A), 1.57 (2H, dd, *J* 8.2, 5.4, 4-H₂), 1.50–1.37 (2H, m, 3-H₂), 1.25 (9H, s, Boc), 1.11 (3H, d, *J* 8.0, ethyl 2-H₃); δ_C (125 MHz, CDCl₃); 175.57 (Phth), 173.41 (Phth), 162.0 (C=O) 147.8(pyridinyl 2-C), 139.2 (pyridinyl 4-C), 135.3 (Phth), 124.9 (Phth), 136.8 (pyridinyl 2-C), 135.3 (pyridinyl 6-C), 125.7 (pyridinyl 5-C), 77.4 (Boc 2-C), 61.7 (2-C), 49.3 (ethyl 1-C), 40.8 (benzyl 5-C), 33.5 (3-C), 32.2 (5-C), 28.5 (Boc 3-C), 28.4 (4-C), 15.7 (ethyl 2-C); ν_{max}/cm⁻¹ (neat); 3330, 2980, 1722, 1716, 1601; *m/z* (ES) 435.3; HRMS Found: , (C₂₅H₂₉N₃O₄ MH⁺ requires). Note: 51% of starting material was also recovered.

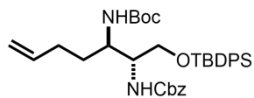
(2*R*,5*R*)-tert-Butyl 2-((*S*)-1-(1,3-dioxoisindolin-2-yl)ethyl)-5-(2-ethoxy-2-oxoethyl)pyrrolidine-1-carboxylate (281**)**



To a solution of **271** (0.16 g, 0.4 mmol) in DCM (7 mL), was added ethyl acrylate (2.4 mmol), followed by Hoveyda-Grubbs 2nd generation catalyst (2.5 mol%) as a solid. The solution was stirred for 24 h, at which time another portion of catalyst (2.5 mol%) was added. The solution stirred for a further 72 h, concentrated *in vacuo*. The crude material was dissolved in DMF–THF, cooled to -78 °C and NaOEt (1.5 eq.) was added. After 40 min, *sat.* NH₄Cl_(aq) was added. The aqueous phase was extracted with EtOAc (3 × 30 mL) The combined organic layers were washed with water (2 × 10 mL), brine (1 × 10 mL), dried with MgSO₄, filtered and concentrated *in vacuo* followed by flash chromatography, eluting with EtOAc–Hexane (90:10) gave the *title compound* (**281**) (0.11 g, d.r. 65:35, 59%); *R_f*: 0.35 (20:80, EtOAc–Hexane); δ_H (500 MHz, CDCl₃); 7.85–7.78 (8H, m, Ar), 4.49 (1H, ddd, *J* 15.5, 9.6 and 1.5, 5-H^{Maj}), 4.41 (1H, dd, *J* 15.5, 9.6 and 3.5, 5-H^{Min}), 4.35 (2H, m, 2-H^{Maj} and ^{Min}), 4.29 (2H, dt, *J* 7.3 and 3.1, ethyl 1-H^{Maj} and ^{Min}), 4.18 (1H, q, *J* 7.2, ethyl 2-H^{Maj}), 4.17 (1H, q, *J* 7.2, ethyl 2-H^{Min}), 2.83 (1H, dd, *J* 15.5 and 3.5, 5'-H_A^{Maj}), 2.87 (1H, dd, *J* 15.5 and 3.5, 5'-H_A^{Min}), 2.78 (1H, dd, *J* 15.5 and 3.5, 5'-H_B^{Min}), 2.74 (1H, dd, *J* 15.5 and 3.5, 5'-H_B^{Maj}), 2.21 (6H, d, *J* 6.2, ethyl 2-H₂), 2.10–1.97 (2H, m, 4-H_A^{Maj} and ^{Min}), 1.93 (2H, m, 3-H_A^{Maj} and ^{Min}), 1.82–1.71 (4H, m, 3-H_B^{Maj} and ^{Min} and 4-H_B^{Maj} and ^{Min}), 1.52 (9H, s, Boc^{Min}), 1.43 (9H, s, Boc^{Maj}), 1.26 (3H, d, *J* 7.1 OCH₂CH₃^{Min}), 1.25 (3H, t, *J* 7.1 OCH₂CH₃^{Maj}); δ_C (125 MHz, CDCl₃); 175.6 (C=O^{Maj}), 175.4 (C=O^{Min}), 173.4 (Phth C=O^{Maj} and ^{Min}) 158.3 (C=O^{Min}), 157.9 (C=O^{Maj}) 137.9 (Phth^{Maj} and ^{Min}), 136.8 (Phth^{Maj} and ^{Min}), 126.6 (Phth^{Maj} and ^{Min}), 79.2 (Boc^{Maj}), 79.0 (Boc^{Min}), 64.6 (5-C^{Maj} and ^{Min}), 64.5 (ethyl 2-C^{Maj} and ^{Min}), 59.0 (OCH₂CH₃^{Maj} and ^{Min}), 54.3 (2-C^{Min}), 53.9 (2-C^{Maj}), 37.3 (5'-ethyl-C^{Min}), 36.5 (5'-ethyl-C^{Maj}), 27.3 (3-C^{Maj} and ^{Min}), 27.5 (4-C^{Maj} and ^{Min}), 26.1 (Boc^{Min}), 26.0 (Boc^{Maj}), 24.5 (2' ethyl CH₃^{Maj} and ^{Min}), 17.0 (OCH₂CH₃^{Maj} and ^{Min}); ν_{max}/cm⁻¹ (neat); 3289, 1714,1705; *m/z* (ES) 431.2; HRMS Found: 431.1738, (C₂₃H₂₇N₂O₄ MH⁺ requires 431.1732).

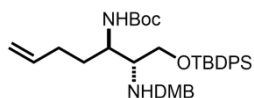
Note: the following conditions were also attempted but the diastereoselectivity obtained was the same as above (65:35). (i) NaOMe (1.5 eq.) in DMF–THF -78 °C; (ii) K^tBu (1.5 eq.) in DMF–THF -78 °C; (iii) K^tBu (1.5 eq.) in DMF -78 °C.

Benzyl tert-butyl (1-((tert-butyldiphenylsilyl)oxy)hept-6-ene-2,3-diyl) dicarbamate (283)



By **General Method F**, using nitro adduct (**235**) (1.06 g, 2 mmol), in THF (5 mL), LiAlH₄ (5 mL of 1 M solution), H₂O (0.16 mL), NaOH (0.32 mL), H₂O (0.48 mL). Note LiAlH₄ partially removed TBDPS group therefore the crude residue is dissolved in DMF (0.3 M), TBDPS-Cl (0.52 mL, 2 mmol), imidazole (3 eq.) were added and stirred for 18 h then water (100 mL) and DCM (20 mL) was added. The phases were separated and the aqueous phase was extracted with DCM (3 × 20 mL). The combined organic phase was washed with *sat.* NaHCO_{3(aq)} (3 × 20 mL), water (2 × 20 mL), and brine (1 × 20 mL), then dried (MgSO₄) and concentrated *in vacuo* to give a crude amine which was dissolved in DCM (0.1 M). NaHCO_{3(aq)} (3 eq.) and benzyl chloroformate (0.28 mL, 2 mmol) were added and the reaction stirred for 18 h. to give a crude material which was purified by flash chromatography, eluting with EtOAc–Hexane (90:10) gave the *title compound* **283** (0.59 g, 48%); R_f: 0.30 (20:80, EtOAc–Hexane); δ_H (500 MHz, CDCl₃); 7.63 (4H, dd, *J* 7.5 and 1.5, Ar), 7.45–7.30 (11H, m, Ar), 5.86–5.72 (1H, m, 6-H), 5.38 (1H, t, *J* 7.8, 2-H), 5.12–4.91 (3H, m, 3-H and 7-H₂), 3.86 (1H, d, *J* 9.3, benzyl H_A), 3.80 (2H, m, 1-H₂), 3.75 (1H, d, *J* 9.3, benzyl H_B), 2.17–2.02 (2H, m, 5-H₂), 1.57 (2H, dd, *J* 12.3, 5.4, 4-H₂), 1.43 (9H, s, Boc), 1.08 (9H, s, ^tBu), 2 × NH not observed; δ_C (125 MHz, CDCl₃); 156.3 (C=O), 156.0 (C=O), 137.7 (6-C), 135.7 (Ar), 132.6 (Ar), 130.4 (Ar), 135.5 (Ar), 134.9 (Ar) 130.3 (Ar), 130.1 (Ar), 129.8 (Ar), 128.6 (Ar), 128.4 (Ar), 128.2 (Ar), 128.1 (Ar), 115.3 (7-C), 79.2 (Boc 2-C), 66.9 (benzyl CH₂), 63.7 (1-C), 53.5 (2-C), 52.8 (3-C), 32.5 (4-C), 30.3 (5-C), 30.0 (SiC(CH₃)₃), 28.4 (Boc 3-C), 26.9 (SiC(CH₃)₃); ν_{max}/cm⁻¹ (neat); 3297, 2993, 1720, 1601; *m/z* (ES) 617.2; HRMS Found: 617.3419, (C₃₆H₄₈N₂O₅Si *MH*⁺ requires 617.3405).

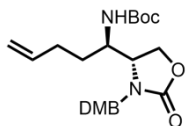
***tert*-Butyl ((2R)-1-((*tert*-butyldiphenylsilyl)oxy)-2-((2,4-dimethoxybenzyl)amino)hept-6-en-3-yl)carbamate (282)**



By **General Method F**, using nitro adduct (**235**) (3.08 g, 6 mmol), in THF (15 mL), LiAlH₄ (13 mL of 1 M solution), H₂O (0.54 mL), NaOH (0.96 mL), H₂O (1.44 mL). Note LiAlH₄ partially removed TBDPS group therefore the crude residue is dissolved in DMF (0.3 M), TBDPS-Cl (1.56 mL, 6 mmol), imidazole (3 eq.) were added and stirred for 18 h then water (100 mL) and DCM (40 mL) was added. The phases were separated and the aqueous phase was extracted with DCM (3 × 40 mL). The combined organic phase was washed with *sat.* NaHCO_{3(aq)} (3 × 40 mL), water (2 × 40 mL), and brine (1 × 40 mL), then dried (MgSO₄) and concentrated *in vacuo* to give a crude amine which was dissolved in MeOH (0.2 M) and 2,4-dimethoxybenzaldehyde (0.33 g) was added then the reaction heated to reflux for 12 hr. After the reaction had cooled to rt, NaBH₄ (5eq.) was added and left to stir for 3 hours. The reaction mixture was concentrated *in vacuo*, partitioned between EtOAc (40 mL) and water (40 mL), the organic layer was extracted with 0.5 M HCl_(aq) (5 × 30 mL) and the combined aqueous layers were neutralised by the addition of 2 M NH₄OH_(aq) (pH 10). The aqueous layer was then extracted with chloroform (5 × 30 mL), combined, dried (MgSO₄), filtered and concentrated *in vacuo* followed by flash chromatography, eluting with EtOAc–DCM (90:10) gave the *title compound* (1.63 g, 43%); R_f: 0.10 (20:80, EtOAc–Hexane); δ_H (500 MHz, CDCl₃); 7.66–7.60 (4H, m, Ar), 7.45–7.33 (6H, m, Ar), 7.10 (1H, d, *J* 8.1, DMB 6-H), 6.42 (1H, d, *J* 2.4, DMB 3-H), 6.40 (1H, dd, *J* 8.1 and 2.4, DMB 5-H), 5.79 (1H, ddt, *J* 17.0, 9.9 and 6.6, 6-H), 5.41 (1H, bs, NH), 4.97 (1, d, *J* 17.0, 7-H_A), 4.92 (1H, d, *J* 9.9, 7-H_B), 3.81–3.78 (4H, m, 3-H, OMe), 3.75 (3H, s, OMe), 3.78–3.74 (3H, m, 2-H, 1-H₂), 3.68 (2H, s, benzyl), 2.07 (2H, dd, *J* 13.7 and 6.8 5-H_A), 2.01 (1H, dd, *J* 14.9 and 6.8, 5-H_A), 1.53–1.46 (2H, m, 4-H₂), 1.43 (9H, s, Boc), 1.08 (9H, s, ^tBu), NH not observed; δ_C (125 MHz, CDCl₃); 163.7 (C=O), 159.1 (DMB 4-C), 155.9 (DMB 2-C), 137.7 (6-C), 134.9 (Ar), 133.9 (Ar), 132.3 (Ar), 129.2 (DMB 6-C), 128.9 (Ar), 126.9 (Ar), 126.9 (Ar), 127.9 (Ar), 127.8 (Ar), 127.8 (Ar), 120.5 (DMB 1-C), 113.7 (7-C), 102.9 (DMB 6-C), 97.7 (DMB 3-C), 76.4 (Boc), 63.0 (1-C), 55.3 (2-C), 55.2 (3-C), 30.7 (5-C), 29.7

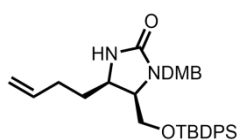
(4-C), 27.6 (Boc 3-C), 26.8 (^tBu), 25.7 (^tBu); $\nu_{\max}/\text{cm}^{-1}$ (neat); 3310, 2983, 1716, 1620; m/z (ES) 632.9; C₃₇H₅₂N₂O₅Si.

***tert*-Butyl ((*R*)-1-((*R*)-3-(2,4-dimethoxybenzyl)-2-oxooxazolidin-4-yl)pent-4-en-1-yl)carbamate (**284**)**



TBAF (2.5 mL, 1 M in THF) was added to **282** (1.21 g, 2 mmol) in THF (0.5 M) and stirred for 2 h. H₂O (5 ml) was added and the aqueous layer was extracted with DCM (3 × 15 mL), dried (MgSO₄), concentrated *in vacuo* then filtered through a plug of silica eluting with DCM-EtOAc (75:25) to give the crude *amino alcohol*. The amino alcohol was dissolved in DMF (0.13 M) and CDI (4.5 eq.) was added then mixture was heated at 110 °C for 18 h until consumption. The reaction mixture was then concentrated *in vacuo* and purified by SCX solid phase extraction eluting with *sat* NH₃ in MeOH then flash column chromatography eluting with EtOAc–Hexane (50:50) gave **284** (0.52 g, 62%); δ_{H} (500 MHz, MeOH) 7.24 (1H, d, *J* 8.2, DMB 6-H), 6.59 (1H, d, *J* 2.4, DMB 3-H), 6.53 (1H, dd, *J* 8.2, 2.4, DMB 5-H), 5.84 (1H, ddt, *J* 17.0, 10.1, 6.0, pentenyl 4-H), 5.18–4.92 (2H, m, pentenyl 5-H₂), 4.58 (1H, d, *J* 14.8, 3-benzyl H_A), 4.42 (1H, d, *J* 14.8, 3-benzyl H_B), 4.24 (1H, dd, *J* 9.2, 5.7, 1-H_A), 4.16–4.07 (2H, m, 1-H_B, pentenyl 1-H), 3.86 (3H, s, OMe), 3.82 (3H, s, OMe), 3.60 (1H, ddd, *J* 9.2, 5.1 and 1.9, 2-H), 2.18 (1H, dt, *J* 14.2 and 6.0, pentenyl 3-H_B), 2.10 (1H, dt, *J* 14.2 and 6.0, pentenyl 3-H_B), 1.49 (9H, s, Boc), 1.42–1.30 (2H, m, pentenyl 2-H₂). δ_{C} (75 MHz, MeOD) 162.7 (C=O), 160.7 (DMB 4-C), 160.4 (DMB 2-C), 158.4 (Boc), 138.6 (pentenyl 4-C), 132.5 (DMB 1-C), 117.4 (DMB 6-C), 116.1 (pentenyl 5-C), 105.8 (DMB 5-C), 99.4 (DMB 3-C), 72.8 (Boc 3-C), 64.3 (1-C), 59.1 (2-C), 56.0 (OMe), 55.9 (OMe), 49.8 (3-C), 40.8 (benzyl 1-C), 31.4 (4-C), 30.7 (5-C), 28.8 (Boc 3-C); m/z (ES) 421.7% C₂₂H₃₂N₂O₆

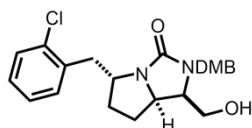
(4R,5R)-4-(But-3-en-1-yl)-5-(((*tert*-butyldiphenylsilyl)oxy)methyl)-1-(2,4-dimethoxybenzyl)imidazolidin-2-one (285)



A solution of **282** in DCM (125 mL) at 0 °C was treated with thioanisole (2.00 mL, 19.0 mmol) and trifluoroacetic acid (30.6 mL, 0.456 mol). The mixture was stirred at rt for 40 min. The reaction mixture was quenched with saturated NaHCO₃ (60 mL) at 0 °C and extracted with DCM (3 × 50 mL). The organic layers were combined, dried (MgSO₄), then concentrated *in vacuo* to give the crude *amino alcohol*. The amino alcohol was dissolved in DMF (0.13 M) and CDI (1.3 eq.) was added then mixture was heated at 110 °C for 18 h until consumption of the starting material. The reaction mixture was then concentrated *in vacuo* and purified by SCX solid phase extraction eluting with *sat* NH₃ in MeOH then flash column chromatography eluting with EtOAc–Hexane (50:50) gave **285** (0.52 g, 62%); 7.52 (2H, dd, *J* 8.1, 1.6 Ar^{Rot A and Rot B}), 7.49–7.46 (6H, m, Ar^{Rot A and Rot B}), 7.33–7.22 (12H, m, Ar^{Rot A and Rot B}), 6.90 (1H, d, *J* 8.1, DMB 6-H^{Rot A}), 6.86 (1H, d, *J* 8.1, DMB 6-H^{Rot B}), 6.35 (1H, d, *J* 2.4, DMB 3-H^{Rot A}), 6.33 (1H, d, *J* 2.4, DMB 3-H^{Rot B}), 6.31 (1H, d, *J* 8.4, DMB 5-H^{Rot A}), 6.30 (1H, d, *J* 8.2, DMB 5-H^{Rot B}), 5.73–5.60 (2H, m, 3-H^{Rot A and Rot B}), 4.90 (1H, d, *J* 17.1, 4-H_A^{Rot B}), 4.90 (1H, d, *J* 17.2, 4-H_A^{Rot A}), 4.82–4.79 (2H, m, 4-H_B^{Rot A and Rot B}), 4.22 (1H, t, *J* 15.1, 2-methyl H_A^{Rot A}), 3.93 (1H, d, *J* 15.1, 2-methyl H_A^{Rot B}), 3.89 (2H, d, *J* 15.5, 2-methyl H_A^{Rot B}), 3.79 (2H, bs, NH^{Rot A and Rot B}), 3.65 (3H, s, OMe^{Rot A}), 3.65 (6H, s, OMe^{Rot A and Rot B}), 3.62 (1H, d, *J* 5.2, 5-H^{Rot B}), 3.61 (1H, d, *J* 5.2, 5-H^{Rot A}), 3.59 (1H, d, *J* 5.7, 4-H^{Rot A}), 3.56 (1H, d, *J* 5.7, 4-H^{Rot B}), 3.50 (3H, s, OMe^{Rot B}), 2.75 (1H, d, *J* 8.5, 1-methylH_B^{Rot A}), 2.66–2.49 (1H, m, 1-methylH_A^{Rot A}), 2.36 (1H, t, *J* 8.5, 1-methylH_B^{Rot B}), 2.29 (1H, t, *J* 7.9, 1-methylH_A^{Rot B}), 1.95–1.84 (2H, m, butenyl 3-H_A^{Rot A and Rot B}), 1.77–1.66 (2H, m, butenyl 3-H_B^{Rot A and Rot B}), 1.62 (2H, m, butenyl 2-H_B^{Rot A and Rot B}), 1.37 (2H, m, butenyl 2-H_A^{Rot A and Rot B}), 1.10 (9H, s, ^tBu^{Rot A}), 0.97 (9H, s, ^tBu^{Rot B}); δ_C (125 MHz, CDCl₃); 163.7 (C=O^{Rot A and B}), 159.1 (DMB 4-C^{Rot A and B}), 157.7 (DMB 2-C^{Rot B}), 157.6 (DMB 2-C^{Rot A}), 136.9 (Ar^{Rot A}), 136.6 (Ar^{Rot B}), 134.9 (Ar^{Rot B}), 134.8 (Ar^{Rot A}), 134.7 (Ar^{Rot A}), 134.3 (Ar^{Rot B}), 133.9 (Ar^{Rot B}), 132.27 (Ar^{Rot A}), 132.1 (DMB 1-C^{Rot A and B}), 129.3 (Ar^{Rot A}), 128.9 (Ar^{Rot A}), 128.8 (Ar^{Rot B}), 128.5 (Ar^{Rot B}), 126.9 (Ar^{Rot B}), 126.8 (Ar^{Rot A}), 126.5 (Ar^{Rot B}), 126.1 (Ar^{Rot A}), 120.5 (DMB 3-C^{Rot A and B}), 113.7 (7-

$C^{\text{Rot A and B}}$, 102.9 (DMB 5- $C^{\text{Rot A and B}}$), 97.7 (DMB 6- $C^{\text{Rot A}}$), 96.9 (DMB 6- $C^{\text{Rot B}}$), 63.0 (4- $C^{\text{Rot B}}$), 62.8 (4- $C^{\text{Rot A}}$), 59.8 (5- $C^{\text{Rot A and B}}$), 55.5 (OMe $^{\text{Rot A}}$), 55.4 (OMe $^{\text{Rot B}}$), 54.5 (5-methyl C), 54.3 (5-methyl $C^{\text{Rot B}}$), 54.0 (OMe $^{\text{Rot A and B}}$), 38.7 (2-methyl $C^{\text{Rot A and B}}$), 30.7 (butenyl 2- $C^{\text{Rot A}}$), 29.7 (butenyl 2- $C^{\text{Rot B}}$), 27.6 (butenyl 1- $C^{\text{Rot A and B}}$) 26.0 ($\text{Si}(\text{CH}_3)_3^{\text{Rot A}}$), 25.9 ($\text{Si}(\text{CH}_3)_3^{\text{Rot B}}$), 21.80 ($^t\text{Bu}^{\text{Rot A and B}}$); $\nu_{\text{max}}/\text{cm}^{-1}$ (neat) ; m/z (ES) 559.7.

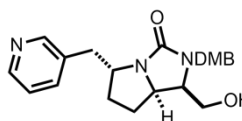
(1*R*,5*R*,7*aR*)-5-[(2-Chlorophenyl)methyl]-2-(2,4-dimethoxybenzyl)-1-(hydroxymethyl)tetrahydro-1*H*-pyrrolo[1,2-*c*]imidazolidin-3-one (289)



By **General Method H**, using **285** (0.20 g, 0.45 mmol), 1-bromo-2-chlorobenzene (0.54 mmol), followed by flash chromatography, eluting with EtOAc–Hexane (90:10) gave **288** (0.21 g, 71%) however analysis of 500 MHz ¹H NMR spectrum was non trivial; 1 M TBAF (0.12 mL) was added to **288** in THF (0.5M) and stirred for 2 h. H₂O (5 ml) was added and the aqueous layer was extracted with DCM (3 × 5 mL), dried (MgSO₄) and passed through a plug of silica eluting with DCM–EtOH–Et₃N (90:9:1) to give the *title compound* (65 mg, d.r. 65:35, 46%); After purification, the sample became contaminated with grease from the highvac. R_f: 0.15 (97:2:1 DCM–EtOH–NH₄OH); δ_H (500 MHz, CDCl₃); 7.40 (1H, dd, *J* 8.0 and 1.8, chlorobenzyl 3-H^{Maj}), 7.38 (1H, dd, *J* 8.0 and 1.8, chlorobenzyl 3-H^{Min}), 7.33 (2H, dt, *J* 8.0 and 1.8, chlorobenzyl 5-H^{Maj and Min}), 7.19 (2H, m, Ar^{Maj and Min}), 7.14 (2H, m, Ar^{Maj and Min}), 7.13 (2H, t, *J* 8.0, DMB 6-H^{Maj and Min}), 6.47 (1H, d, *J* 2.4, DMB 5-H^{Min}), 6.46 (1H, d, *J* 2.4, DMB 5-H^{Maj}), 6.43 (2H, dd, *J* 8. and 2.4, DMB 3-H^{Maj and Min}), 4.58 (1H, d, *J* 14.9, 2-benzyl H_B^{Maj}), 4.51 (1H, d, *J* 15.0, 2-benzyl H_B^{Min}), 4.28 (1H, d, *J* 14.9, 2-benzyl H_A^{Maj}), 4.23 (2H, ddd, *J* 11.5, 7.0 and 4.8, 7-H^{Maj and Minor}), 4.18 (1H, d, *J* 15.0, 2-benzyl H_A^{Min}), 3.79 (3H, s, OMe), 3.78 (3H, s, OMe), 3.78 (6H, s, OMe), 3.72–3.65 (4H, m, 1-methyl H₂^{Min} and 1-C^{Maj and Min}) 3.51 (2H, ddd, *J* 9.8, 5.7 and 2.7, 1-methy H₂^{Maj}), 3.26 (2H, dt, *J* 4.5 and 3.2, 4-H^{Maj and Min}), 3.13 (1H, dd, *J* 13.8 and 6.4, 4-benzyl H_A^{Maj}), 3.08 (1H, dd, *J* 13.8 and 6.5, 4-benzyl H_A^{Min}), 2.91 (1H, dd, *J* 13.8 and 6.4, 4-benzyl H_B^{Maj}), 2.90 (1H, dd, *J* 13.8 and 6.5, 4-benzyl H_B^{Min}), 2.27 (2H, dtd, *J* 14.2, 7.2, 6.6 and 1.7, 5-H_B^{Maj and Min}), 2.04 (2H, ddd, *J* 6.6, 4.8 and 1.7, 6H_B^{Maj and min}), 2.00–1.93 (2H, m, 5-H_A^{Maj and Min}), 1.93–1.82 (2H, m, 6-H_A^{Maj and Min}), 2× OH not observed; δ_C (125 MHz, CDCl₃); 164.3 (3-C (C=O)^{Maj}), 163.7 (3-C (C=O)^{Min}), 160.5 (DMB 4-C^{Min}), 160.4 (DMB 4-C^{Maj}), 158.3 (DMB 1-C^{Min}), 158.1 (DMB 1-C^{Min}), 135.9 (Ar^{Min}) 135.8 (Ar^{Maj}), 133.8 (Ar^{Maj}), 133.7 (Ar), 130.8 (DMB 2-C^{Min}), 130.7 (DMB 1-C^{Maj}), 130.3 (Ar^{Min}), 130.2 (Ar^{Maj}), 128.6 (Ar^{Min}), 126.9 (Ar^{Maj}), 126.8 (Ar^{Min}), 126.6 (Ar^{Maj}), 125.9 (Ar^{Min}), 125.8 (Ar^{Maj}), 117.8 (DMB 6-C^{Min}), 117.8 (DMB 6-C^{Maj}), 104.8 (DMB 5-C^{Maj}), 104.2 (DMB 5-C^{Min}), 98.5 (DMB 3-C^{Maj and Min}), 62.8 (1-methyl^{Maj}), 62.5 (1-methyl^{Min}), 60.3 (5-C^{Min}), 59.7 (5-C^{Maj}), 59.1 (1-

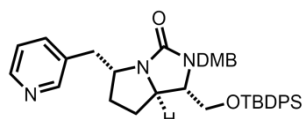
C^{Maj}), 59.0 (1-C^{Min}), 58.2 (7a-C^{Maj}), 58.1 (7a-C^{Maj}), 55.3 (OMe^{Maj}), 54.8 (OMe^{Min}), 54.7 (OMe^{Maj}), 54.6 (OMe^{Min}) 39.6 (2-benzyl^{Maj}), 39.2 (2-benzyl^{Min}), 38.7 (5-methyl^{Maj}), 38.6 (5-methyl^{Min}), 31.0 (6-C^{Min}), 30.9 (6-C^{Maj}), 28.2 (7-C^{Min}), 27.9 (7-C^{Maj}); HRMS Found: 431.1738 (C₂₃H₂₇ClN₂O₄ MH⁺ requires 431.1732).

Benzyl tert-butyl (1-((tert-butyldiphenylsilyl)oxy)hept-6-ene-2,3-diyl) dicarbamate (292)



By **General Method H**, using **285** (0.14 g, 0.26 mmol), 1-bromo-2-chlorobenzene (0.54 mmol), followed by flash chromatography, eluting with EtOAc–Hexane (90:10) gave **291** (94 mg, 57%). However analysis of 500 MHz ^1H NMR spectrum was non trivial; 1 M TBAF (0.12 mL) was added to **291** in THF (0.5M) and stirred for 2 h. H_2O (5 ml) was added and the aqueous layer was extracted with DCM (3×5 mL), dried (MgSO_4) and passed through a plug of silica eluting with DCM–EtOH– Et_3N (90:9:1) to give **292** (32 mg, d.r. 65:35, 54%); R_f : 0.15 (97:2:1 DCM–EtOH– NH_4OH); δ_{H} (500 MHz, CDCl_3); 8.49 (1H, dd, J 2.0 and 0.8, pyridinyl 2-H), 8.46 (1H, dd, J 4.8 and 2.0, pyridinyl 6-H), 7.68 (1H, dt, J 7.8 and 2.0, pyridinyl 4-H), 7.23 (1H, ddd, J 7.8, 4.8 and 0.8, pyridinyl 3-H), 7.04 (1H, d, J 8.3, DMB 6- H^{Min}), 6.98 (1H, d, J 8.3, DMB 6- H^{Maj}), 6.37 (1H, dd, J 8.3 and 2.4, DMB 4-H), 6.31 (1H, d, J 2.4, DMB 2-H), 4.54 (1H, d, J 15.2, 2' benzyl H_A), 4.17–4.07 (1H, m, 2' benzyl H_B), 3.94 (2H, d, J 13.7 and 9.6, 4- H^{Maj}), 3.91 (2H, d, J 15.2, 1 H^{Maj} and Min), 3.80 (3H, s, OMe^{Maj}), 3.77 (3H, s, $\text{OMe}^{\text{Minor}}$), 3.64–3.60 (2H, m, 3' benzyl), 3.59 (1H, d, J 5.0, 1-methy H_B^{Maj}), 3.56 (1H, d, J 8.6, 1-methy H_B^{Min}), 3.45 (3H, s, OMe), 2.96 (1H, dd, J 13.8 and 6.0, 6' benzyl H_B), 2.80 (1H, dd, J 13.8 and 7.3, 6' benzyl H_A), 1.80 (1H, dt, J 9.8, 5.0, 6 H_B), 1.61–1.44 (2H, m, 5- H_A and 6- H_A), 1.26 (1H, t, J 7.1, 5- H_B), 1.04 (9H, s, ^tBu), 0.98 (9H, s, ^tBu); δ_{C} (125 MHz, CDCl_3); 164.3 ($\text{C}=\text{O}^{\text{Maj}}$), 163.7 ($\text{C}=\text{O}^{\text{Min}}$), 160.5 (DMB 4- C^{Min}), 160.4 (DMB 4- C^{Maj}), 158.2 (DMB 1- C^{Min}), 158.1 (DMB 1- C^{Maj}), 150.8.0 (pyridinyl 2-C), 147.6 (pyridinyl 4-C), 136.8 (pyridinyl 6-C), 135.3 (pyridinyl 6-C), 133.1 (DMB 1-C), 125.7 (pyridinyl 5-C), 117.9 (DMB 1- C^{Min}), 117.8 (DMB 1- C^{Maj}), 104.8 (DMB 5- C^{Maj}), 104.2 (DMB 5- C^{Min}), 98.5 (DMB 3 Min), 98.5 (DMB 3 Maj), 62.8 (4-C) 62.5 (4- C^{Maj}), 61.0 (4- C^{Min}), 59.7 (1- C^{Min}), 58.9 (1- C^{Maj}), 58.3 (7- C^{Min}), 58.2(7- C^{Maj}), 55.4 (OMe^{Maj}), 54.1 (1-methyl Min and Maj), 55.5 (OMe^{Min}), 55.4(OMe^{Maj}), 55.4 (OMe^{Min}), 40.2 (2-benzyl), 39.7 (5-methyl), 31.6 (5-C), 26.8 (^tBu), 26.1 (6-C); $\nu_{\text{max}}/\text{cm}^{-1}$ (neat); ; m/z (ES) 398.2; HRMS Found: 398.2064, ($\text{C}_{22}\text{H}_{27}\text{N}_3\text{O}_4$ MH^+ requires 398.2074).

(1R,5R,7aR)-1-(((*tert*-Butyldiphenylsilyloxy)methyl)-2-(2,4-dimethoxybenzyl)-5-(pyridin-3-ylmethyl)tetrahydro-1H-pyrrolo[1,2-c]imidazol-3(2H)-one (295)

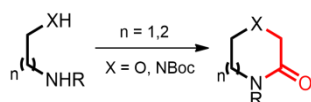


By **General Method H**, using **285b** (0.25 g, 0.45 mmol), 1-bromo-2-chlorobenzene (0.54 mmol), followed by flash chromatography, eluting with EtOAc–Hexane (90:10) gave the *title compound* (0.14 g, d.r. 93:7, 50%); R_f : 0.1 (97:2:1 DCM–EtOH–NH₄OH); δ_H (500 MHz, CDCl₃); 8.49 (1H, dd, J 2.0 and 0.8, pyridinyl 2-H^{Maj and Min}), 8.46 (1H, dd, J 4.8 and 2.0, pyridinyl 4-H^{Maj and Min}), 7.68 (1H, dt, J 7.8 and 2.0, pyridinyl 6-H^{Maj and Min}), 7.60–7.56 (2H, m, Ar^{Maj and Min}), 7.52–7.48 (2H, m, Ar^{Maj and Min}), 7.46–7.30 (6H, m, Ar^{Maj and Min}), 7.23 (1H, ddd, J 7.8, 4.8 and 0.8, pyridinyl 5-H^{Maj and Min}), 7.04 (1H, d, J 8.3, DMB 6-H^{Min}), 6.98 (1H, d, J 8.3, DMB 6-H^{Maj}), 6.37 (1H, dd, J 8.3 and 2.4, DMB 4-H^{Maj and Min}), 6.31 (1H, d, J 2.4, DMB 2-H^{Maj and Min}), 4.54 (1H, d, J 15.2, 2-methyl H_A^{Maj}), 4.53 (1H, d, J 14.7, 2-methyl H_a^{Min}), 4.12 (1H, ddd, J 10.2, 6.9 and 3.0, 7-H), 4.05 (1H, d, J 14.7, 2-methyl H_B^{Min}), 3.94 (1H, dt, J 13.6 and 9.6, 4-H^{Maj and Min}), 3.91 (1H, d, J 15.2, 2-methyl H_B^{Maj}), 3.80 (3H, s, OMe^{Maj and Min}), 3.65–3.54 (3H, m, 1-methyl H₂ and 1-H^{Maj and Min}), 3.45 (3H, s, OMe^{Maj and Min}), 2.96 (dd, J 13.8 and 6.0, 5-methyl H_B^{Maj and Min}), 2.80 (1H, dd, J 13.8 and 7.3, 5-methyl H_A^{Maj}), 2.73 (1H, dd, J 13.8 and 7.3, 5-methyl H_B^{Min}), 2.08–2.00 (1H, m, 5H_A^{Maj and Min}), 1.80 (1H, dt, J 10.2, 5.0, 6H_B^{Maj and Min}), 1.61–1.44 (2H, m, 5-H_A and 6-H_A^{Maj and Min}), 1.04 (9H, s, ^tBu^{Maj and Min}), 0.98 (9H, s, ^tBu^{Maj and Min}); δ_C (125 MHz, CDCl₃); 164.2 (C=O), 160.2 (DMB 4-C), 158.2 (DMB 1-C), 150.8 (pyridinyl 2-C), 147.6 (pyridinyl 4-C), 137.0 (pyridinyl 6-C), 135.5 (pyridinyl 1-C), 135.4 (Ar), 134.7 (Ar), 133.1 (DMB 2-C), 133.0 (Ar), 130.5 (Ar), 129.8 (Ar), 129.7 (Ar), 127.8 (Ar), 127.5 (Ar), 123.6 (pyridinyl 5-C), 117.8 (DMB 6-C), 104.8 (DMB 5-C), 98.5 (DMB 3-C), 62.8 (4-C), 59.7 (1-C), 58.6 (7-C), 55.4 (OMe), 55.0 (1-methyl), 54.9 (OMe), 40.2 (2-benzyl), 39.7 (5-methyl), 31.6 (5-C), 26.8 (^tBu), 26.1 (6-C) 19.1 (^tBu); ν_{max}/cm^{-1} (neat); ; m/z (ES) 636.3; HRMS Found: 636.3257, (C₃₈H₄₆N₃O₄Si MH^+ requires 636.3252).

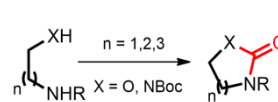
6 Appendices

6.1 Appendix 1: Cyclisation reactions

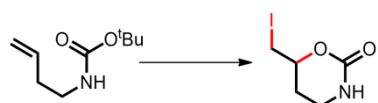
Ketopiperazine/Ketomorpholine^{187,188}



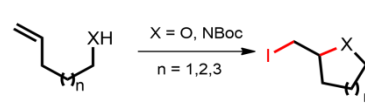
Carmamate/Urea formation⁹³



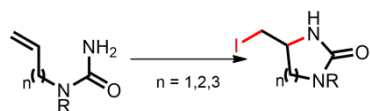
Carbamate cyclisation¹⁸⁹



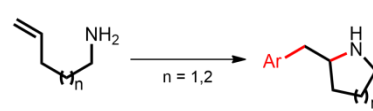
Iodine-mediated amination⁹²



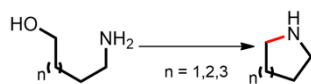
Iodine-mediated urea cyclisation⁸⁷



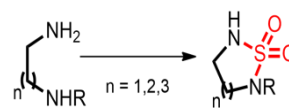
Pd-catalysed aminoarylation^{190,191}



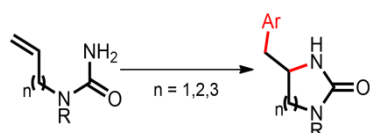
Mitsunobu/Appel^{192,193}



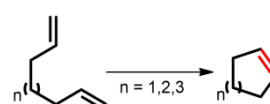
Sulfurea formation¹⁹⁴



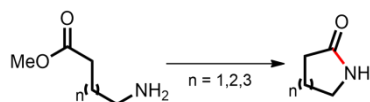
Pd-catalysed urea-arylation^{195,196}



Ring-closing metathesis⁹⁶⁻⁹⁸



Lactamisation¹⁹⁷



Heck¹⁹⁸

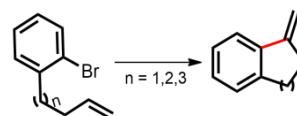


Figure 47: Choice of cyclisations used in the computational analysis.

6.2 Appendix 2: Diversification reactions

Following the enumeration; a series of functional group interconversions remove undesirable functional groups.

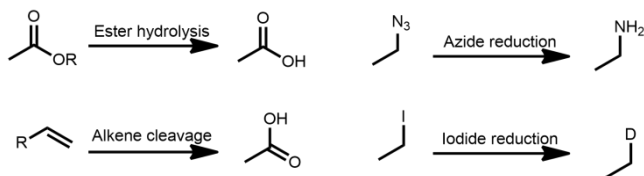


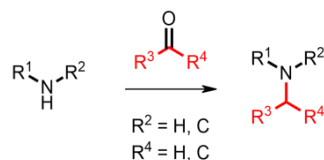
Figure 48: Functional group interconversions used in the protocol

Next, the scaffolds were decorated with capping groups (GSK provided a list of commonly used groups).

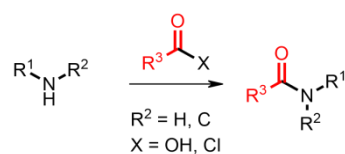
N-Alkylation



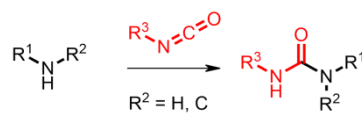
Reductive amination



Amide coupling



Urea formation



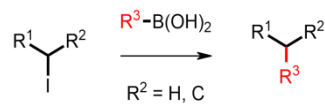
N-arylation



Sulfonamide coupling



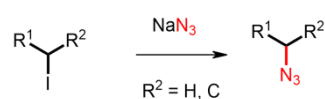
Suzuki coupling



S_n2 Etherification



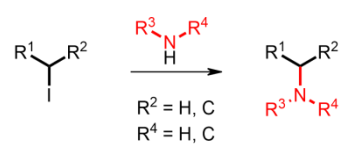
Azide displacement



S_N2 Sulfone



S_n2 Amination



O-Alkylation

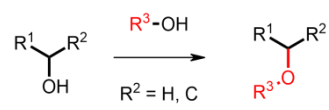
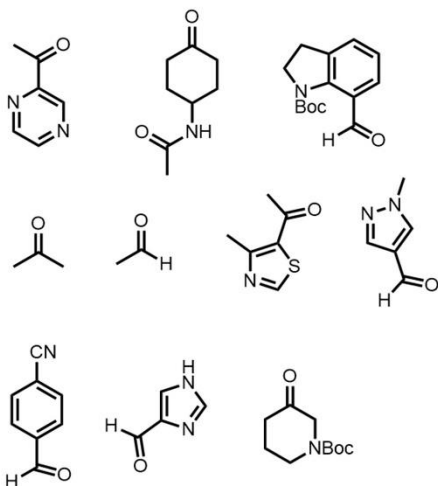


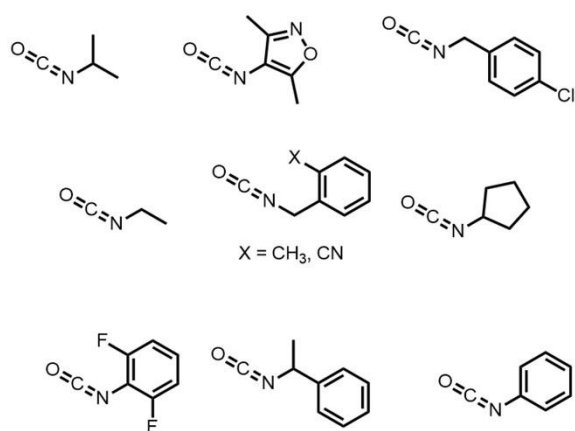
Figure 49: Summary of chemistries used in generating final compounds from scaffolds.

6.3 Appendix 3: Capping groups

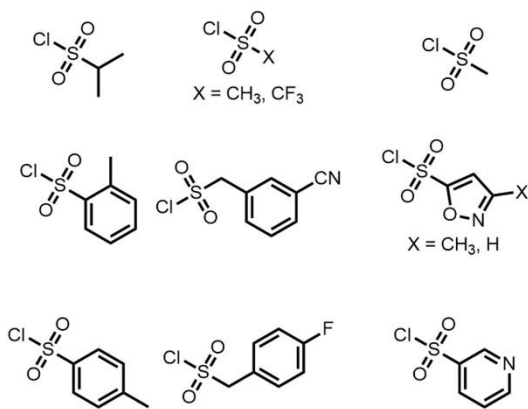
Aldehydes



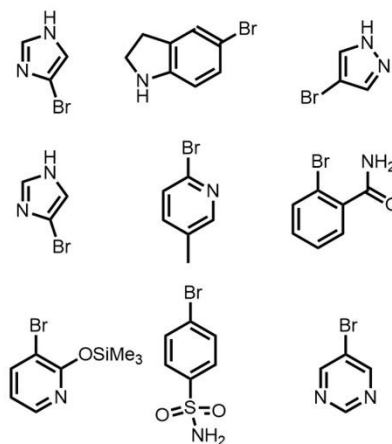
Isocyanates



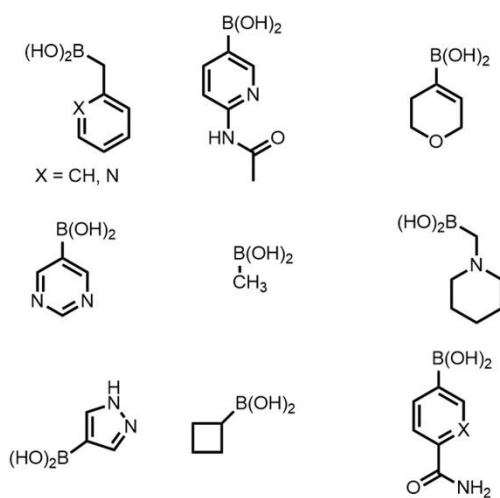
Sulfonylchloride



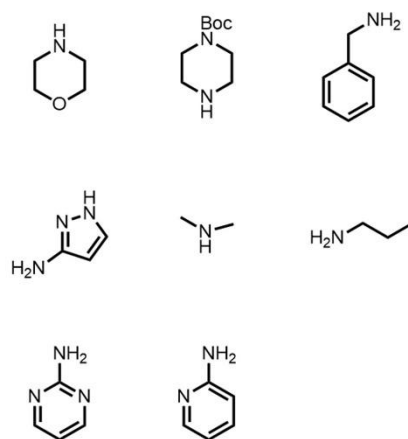
Aryl Bromides



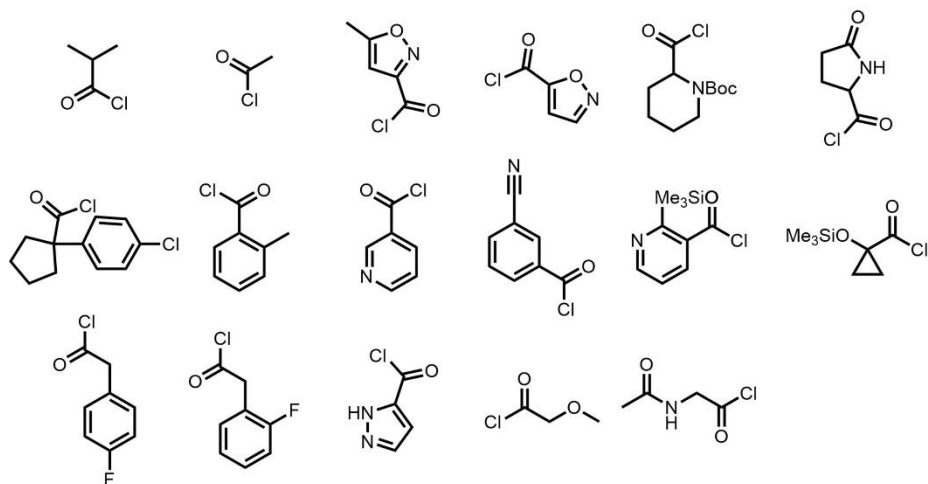
Boronic Acids



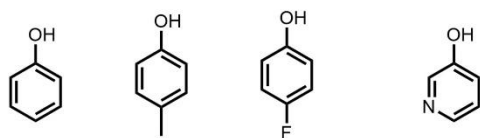
Amines



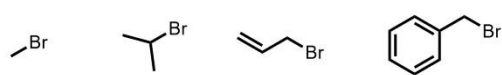
Acid chlorides



Phenols



Alkyl Bromides



Sulfones

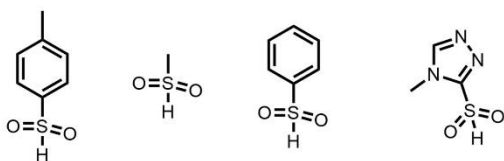


Figure 50: Capping groups used in the computational protocol

6.4 Appendix 4: Novelty Assessment

Novelty was assessed at the scaffold level by way of a substructure count against a reference database (Figure 51). Murcko fragments¹⁰⁷ without α -attachments are generated for each scaffold and these are compared with Murcko fragments without α -attachments generated from a random 2% of compounds (~150,000 compounds) from the ZINC database of commercially available compounds.¹⁰⁸ A penalty is incurred for the scaffold each time a match within the ZINC database is found. In addition, Murcko fragments with α -attachments are generated and these are also compared with the same randomly selected compounds from the ZINC database. With these two scores, it is possible to investigate both skeletal novelty (is the specific known without substituents) and appendage novelty (is the scaffold substitution pattern of the scaffold known).

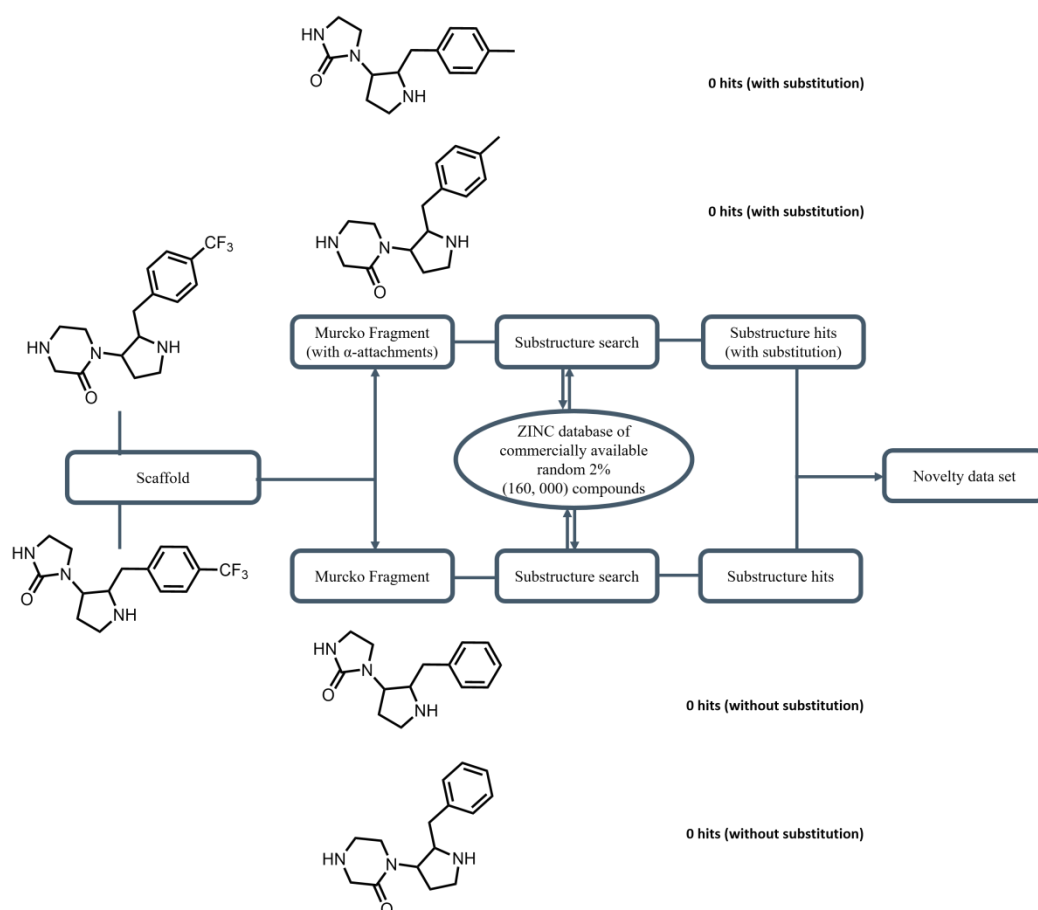
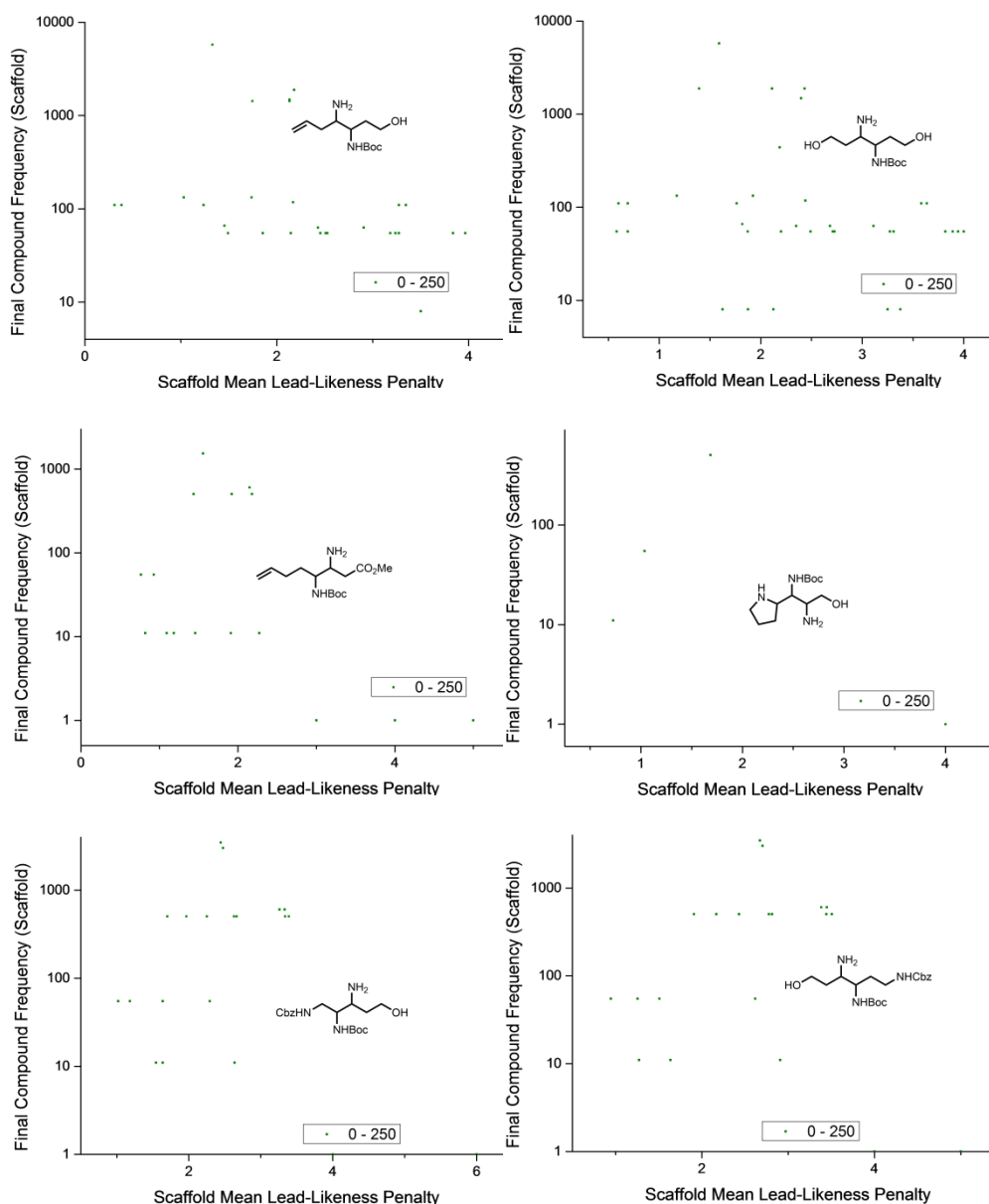
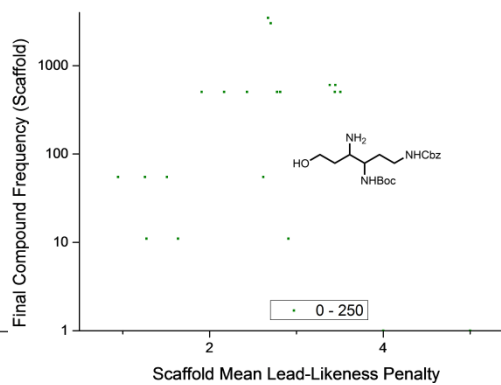
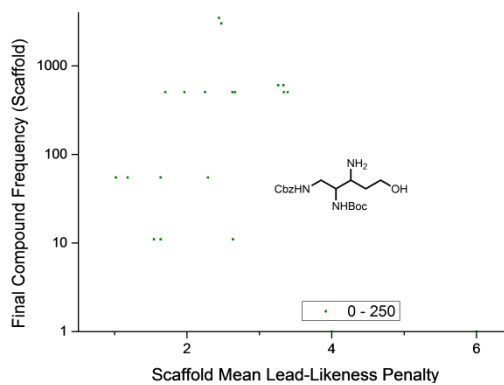
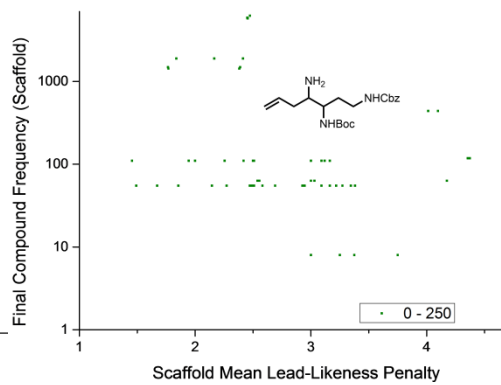
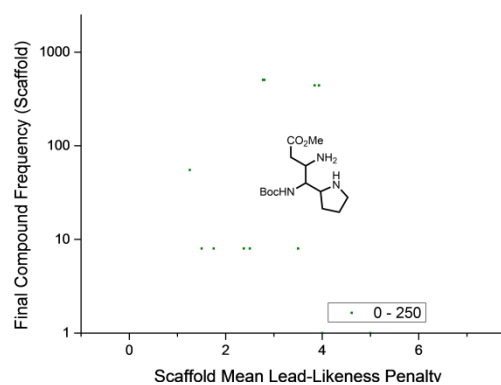
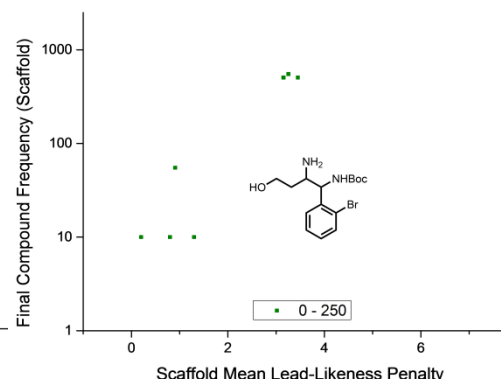
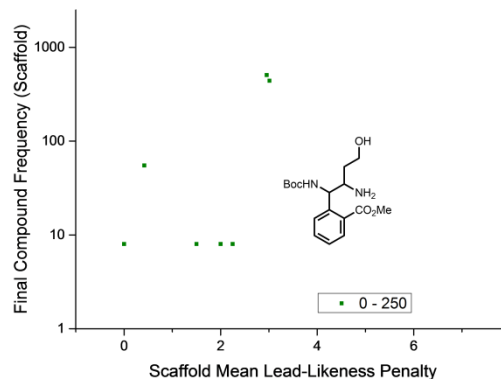
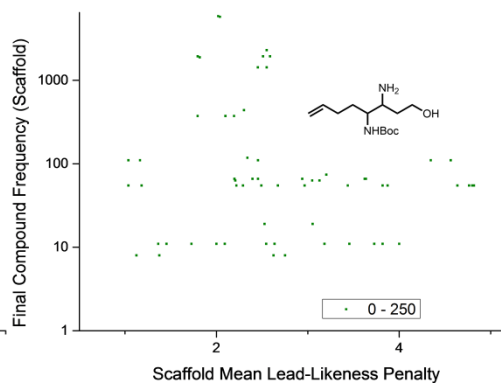
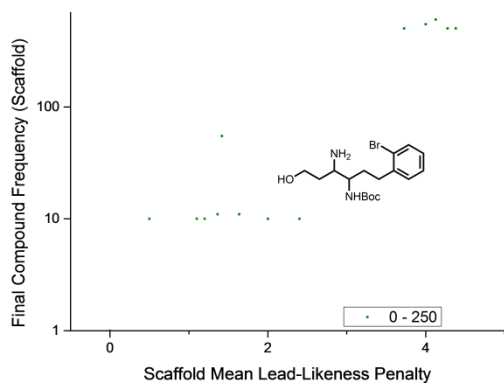


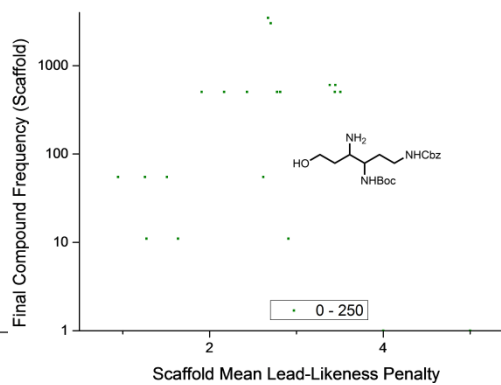
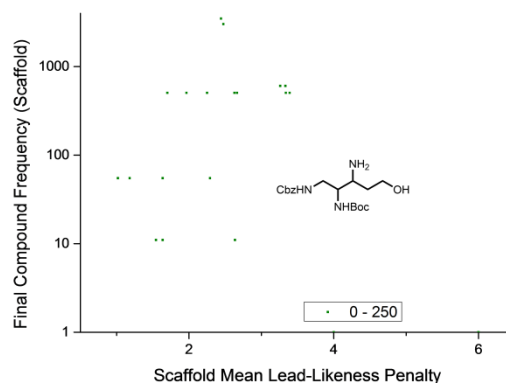
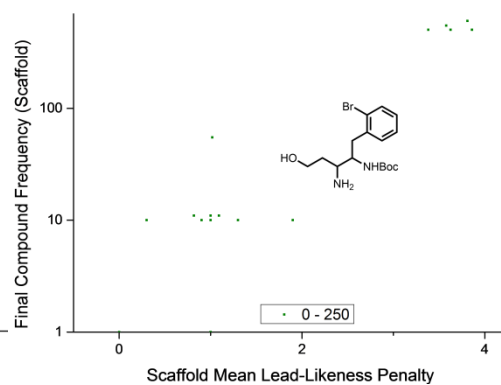
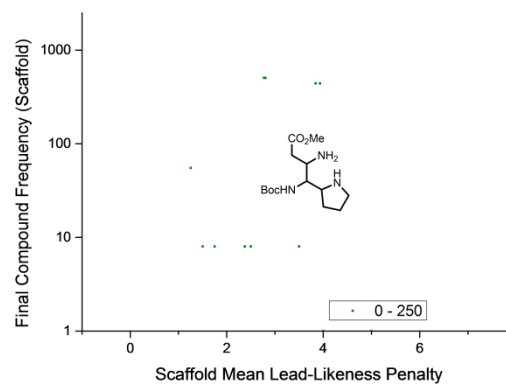
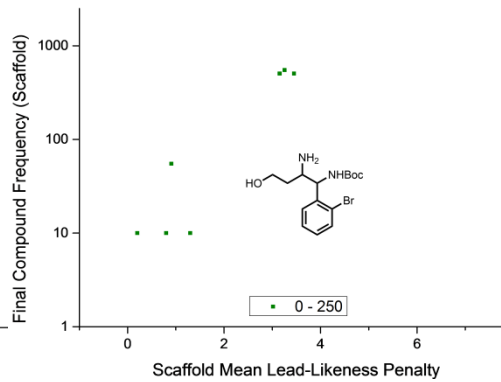
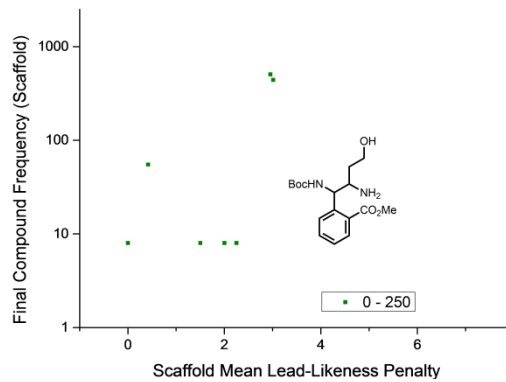
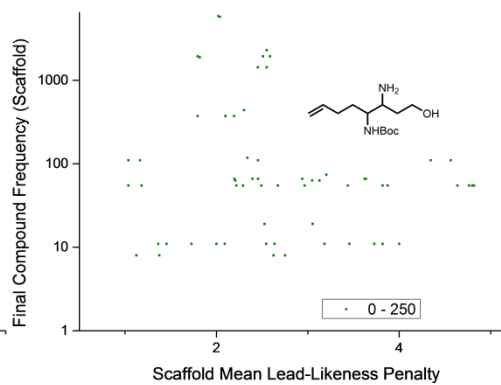
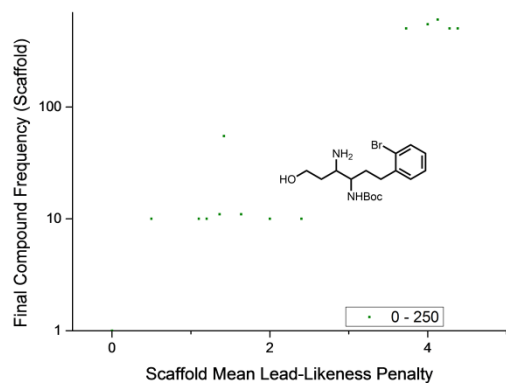
Figure 51: Novelty assessment. Two fragments are generated for each scaffold and compared with the ZINC database. Demonstrated with two exemplar scaffolds

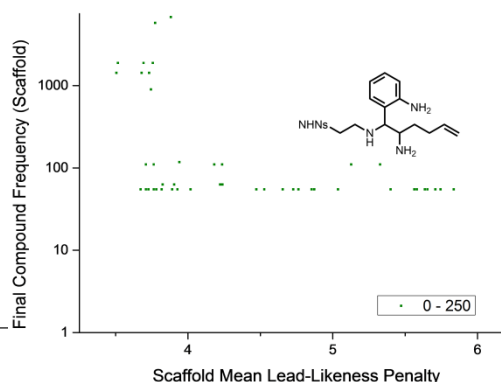
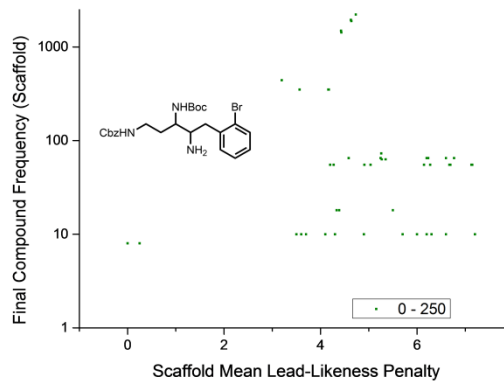
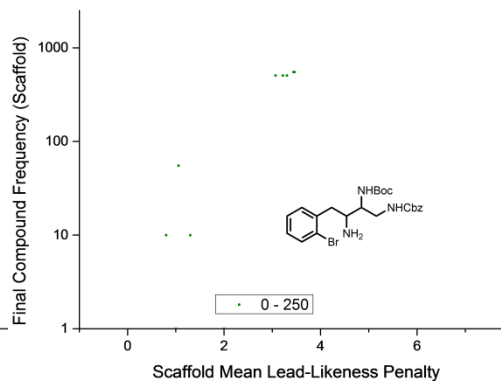
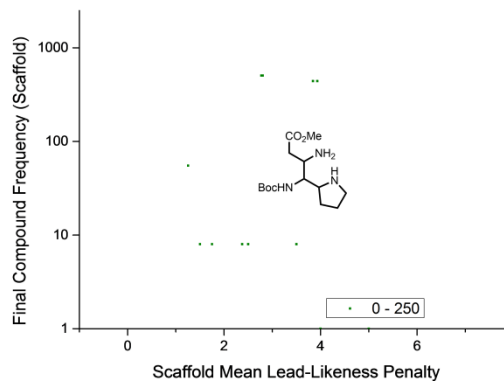
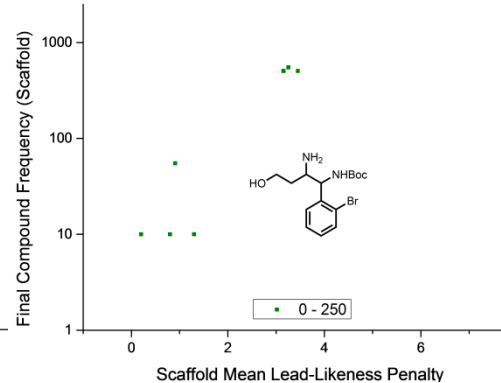
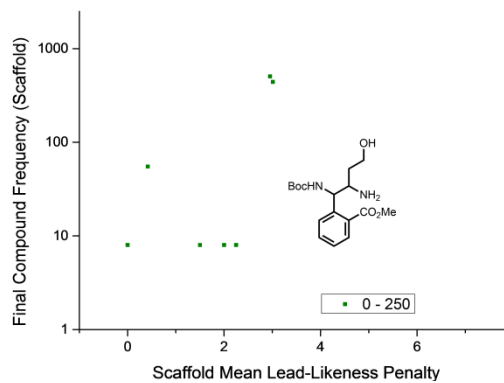
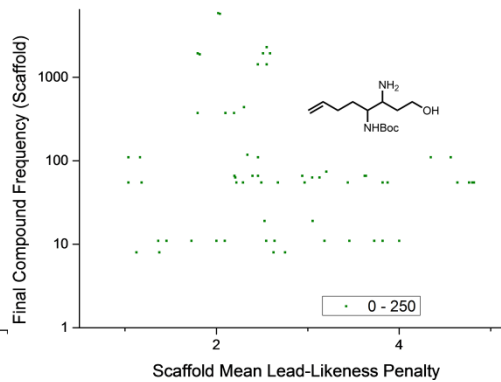
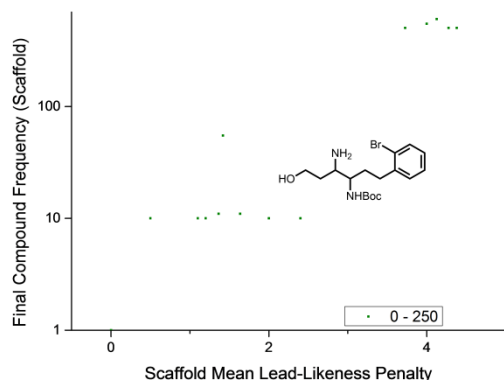
Appendix 5: Individual cyclisation data

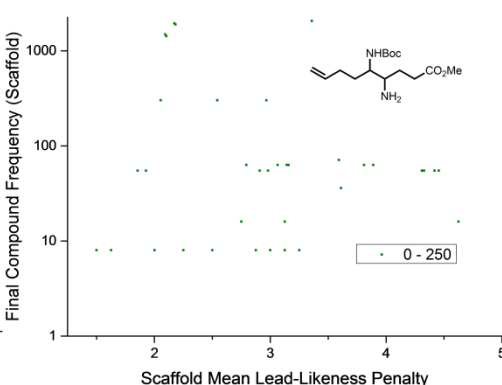
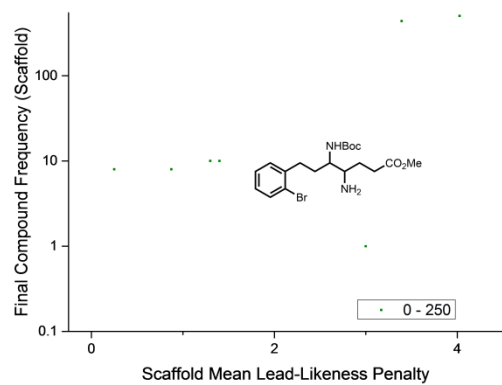
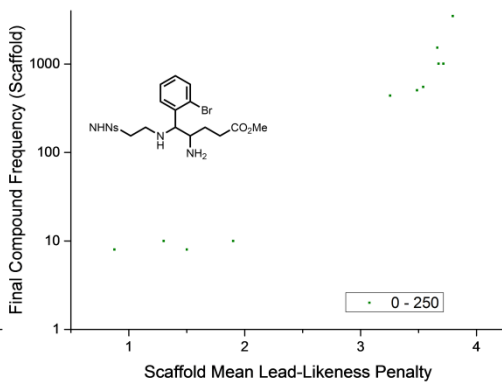
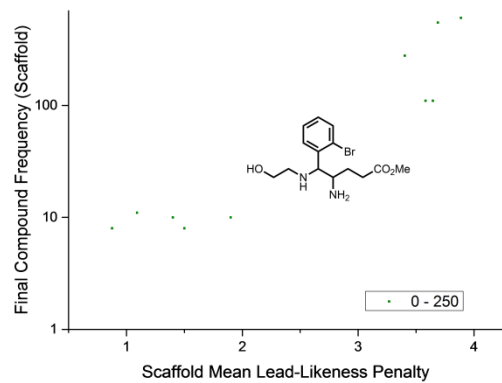
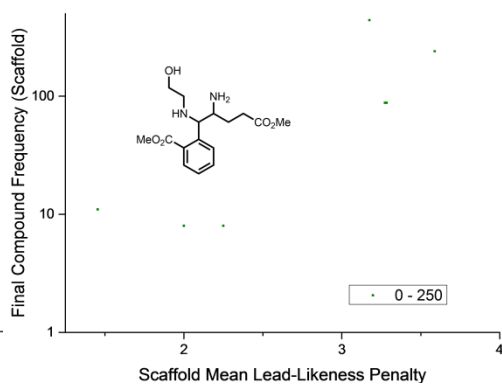
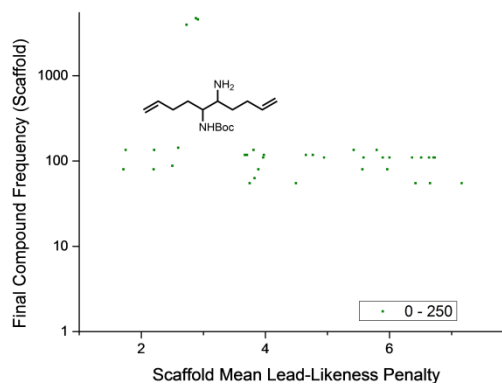
From the large nitro-Mannich reaction library, 42 cyclisation precursors were identified having significant potential for the synthesis of a library of scaffolds to be used in the generated of interrogating lead-like chemical space. It should be noted, that given the limitations of the protocol, that before synthetic effort was undertaken the precursor would be entered into pipeline pilot as a single entry. This ensures not potential scaffolds are lost due to identical scaffold from a different precursor











6.5 Appendix 6: Data for Molecular weight, F_{SP³} plots

A_{LogP} and number of heavy atoms were calculated using the tools within Pipeline Pilot. The fraction of sp³-hybridised carbon atoms (F_{SP³}) was calculated using Dotmatics Vortex (Vortex v2013.12.25046). The data were visualized and analysed using Vortex and Origin Pro v9.

The structural filtering was performed by interrogating two sets of SMARTS definitions with each of the final compounds using the substructure search tool within Pipeline Pilot. The first set contained 240 definitions as compiled by Shoichet, Simeonev *et al.* and used at the NIH Chemical Genomics Centre.²⁷ The second set contained 36 definitions and are examples from the ‘GSKB’ filter as described by Churcher *et al.*⁷ In addition, the structural element of the high throughput screening filter embedded in Pipeline Pilot was also used that comprised the filters for undesirable functionality outlined in Table 15.

Data from the lead-likeness assessment of both the ZINC database of compounds ‘available now’ and the virtual library (as summarised in Figure 42) are provided in Table 13-14. The distribution of the molecular properties of the virtual library based upon each scaffold is shown in Table 13.

For the purposes of the novelty assessment scaffolds were virtually deprotected but did not undergo manipulation. In each case, a substructure search was performed against the ZINC database (90 911).

Scaffold	Number of Final Compounds	Number of Lead-like Compounds	% Lead-like Compounds	Mean Fsp ³	Substructure Hits
ZINC (random 1%)	90911	20 932	23	0.335	n/a
Virtual Library	2414	1112	46	0.520	1733
1	33	6	19	0.539	0
2	40	7	18	0.509	0
3	16	12	86	0.458	0
4	9	6	67	0.470	0
5	66	34	57	0.549	1
6	633	312	50	0.471	142
7	1617	715	44	0.616	1592

Table 13: Number of final compounds derived from each scaffold, together with the number and percentage of compounds that are lead-like (i.e. pass all filters). Fsp³ data illustrated in Figure 43, Novelty assessment data as compared with random 2% of ZINC database.

Filter	Random 2% of ZINC Database (90911)	Virtual Library (19530)
	Successive Filtering	Successive Filtering
$14 \leq nHA \leq 26$	43971	1048
$-1 \leq ALogP \leq 3$	17828	200
Structural filter	8180	78
Pass All	20932 (23%)	1128 (46%)

Table 14: Lead-likeness assessment data. The data shown in Figure 42, Panels A and B was obtained by successive filtering by the number of heavy atoms, lipophilicity and structural filters.

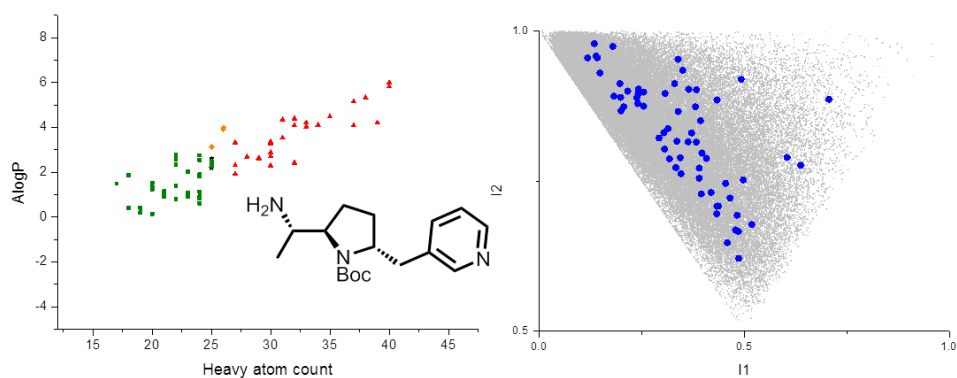
Filter		
Acyl halide	Disulfide	Dicarbonyl
Aldehyde	Hydrazine (terminal)	Quaternary ammonium
Alkyl halide	Isocyanate	Peroxide
Anhydride	Isothiocyanate	Diazo

Table 15: Undesirable functionality filters used in the 'HTS Filter' embedded in Pipeline Pilot.

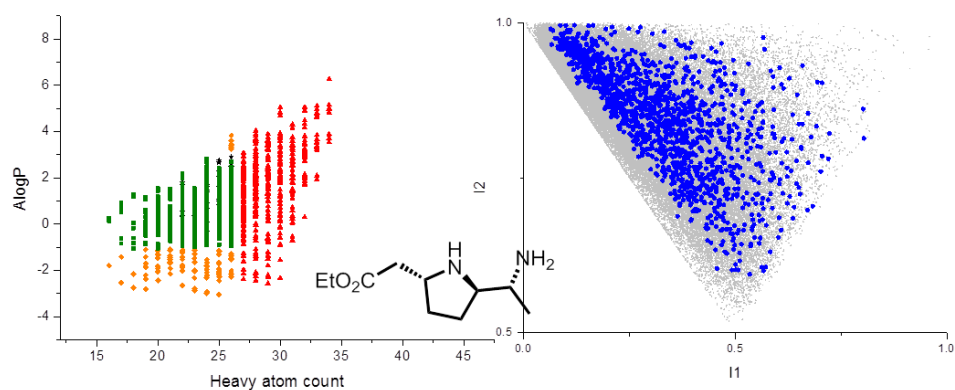
6.6 Appendix 7: Shape Analysis – Principal Moments of Inertia

3D structures were generated from the 2D Pipeline Pilot and the lowest energy conformer selected output using LLAMA.¹⁹⁹ The 3D structures were used to generate the three Principal Moments of Inertia (I_1 , I_2 and I_3) using LLAMA which then normalised the plots by dividing the two lower values by the largest (I_1/I_3 and I_2/I_3).¹⁹⁹ These Normalised PMI plots generate a triangular plot with the corners defined by a perfect sphere, a perfect disk and a perfect rod shape.²⁰⁰

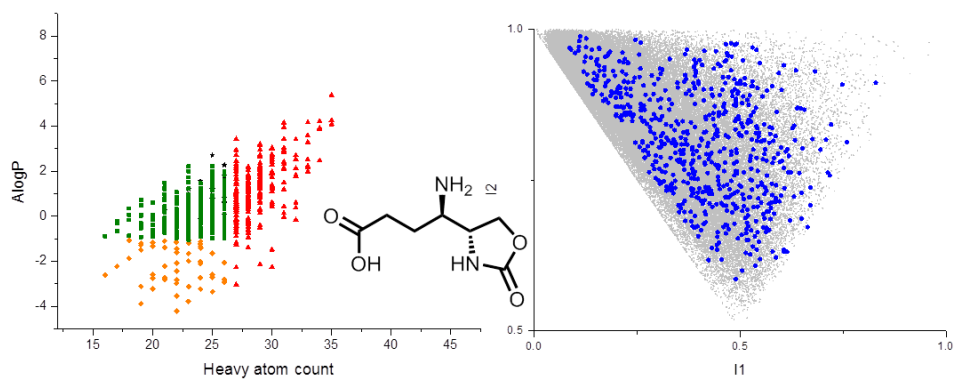
Scaffold 279



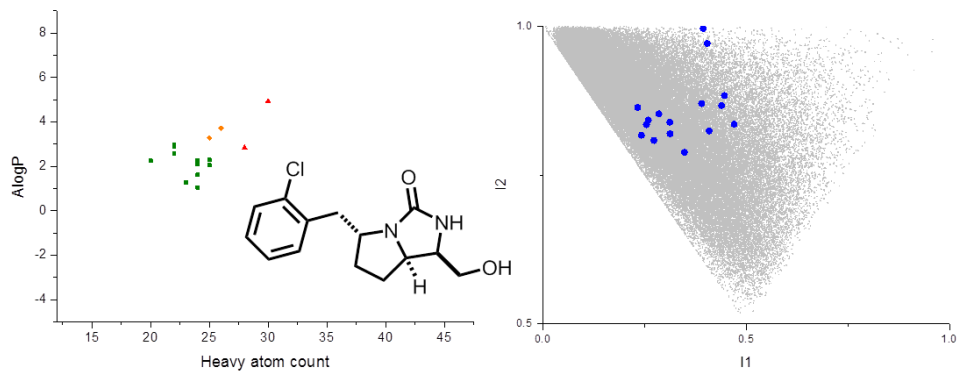
Scaffold 281



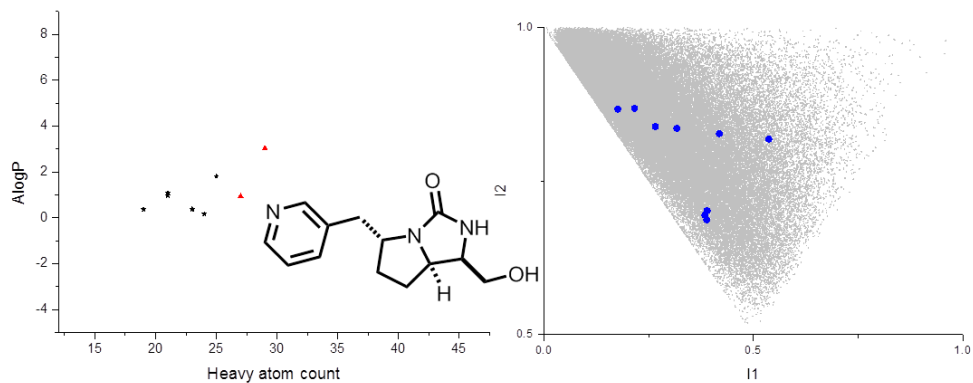
Scaffold 284



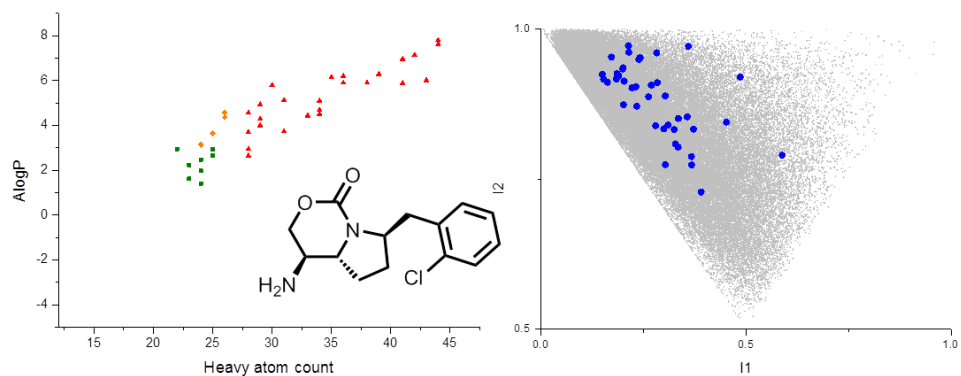
Scaffold 289



Scaffold 292



Scaffold 293



Scaffold 294

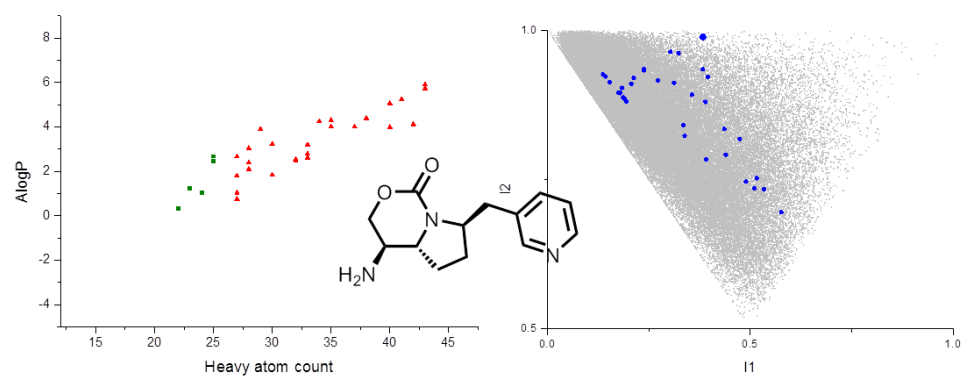


Figure 52: Distribution of the molecular properties of the virtual library on a scaffold basis. Compounds are successive filtering by molecular size ($14 \leq \text{number of heavy atoms} \leq 26$; failures shown in red) and lipophilicity ($-1 \leq \text{AlogP} \leq 3$; failures shown in orange) and various structural filters (failures shown in black) to give portion of lead-like compounds (green). A normalised principal moment of inertia plot to show the shapes of the 2413 virtual library on a scaffold basis in relation to three idealised shapes; a rod, disk and sphere.

6.7 Appendix 8: Crystallographic informations

The candidate crystallised **265** from EtOAc:Petrol. The crystals was subsequently assessed by Dr Chris Pask and a suitable crystal was selected and data obtained.

Measurements were carried out at 120K on an Agilent SuperNova diffractometer equipped with an Atlas CCD detector and connected to an Oxford Cryostream low temperature device using mirror monochromated Cu K α radiation ($\lambda = 1.54184 \text{ \AA}$ from a Microfocus Nova X-ray source. The structure was solved by direct methods using SHELXS²⁰¹ and refined by a full matrix least squares technique based on F² using SHELXL97.²⁰¹

The compound crystallised as colourless needles. The compound crystallised in a monoclinic cell and was solved in the *P*2₁/*c* space group, with one molecule in the asymmetric unit.

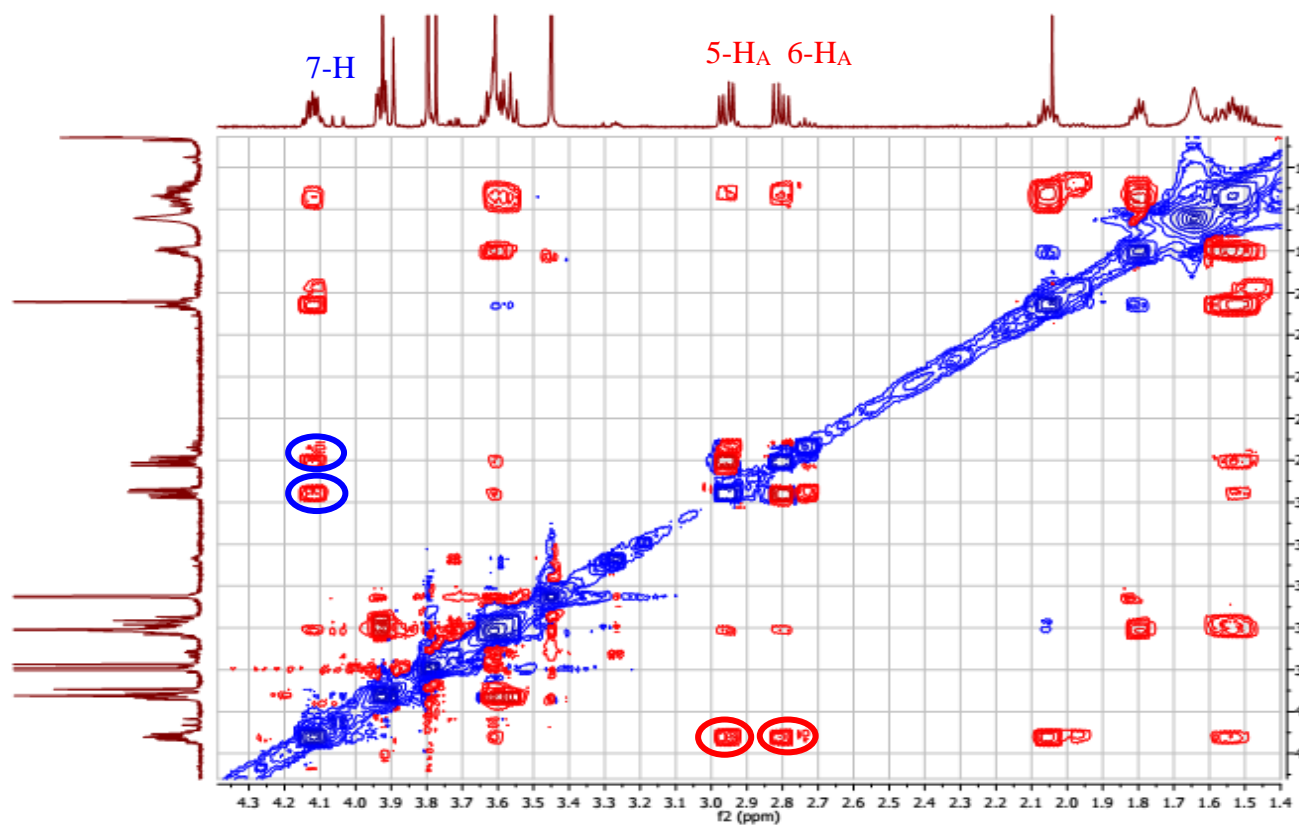
All non-hydrogen atoms were located in the Fourier Map and refined anisotropically. All hydrogen atoms were placed in calculated positions and refined isotropically using a “riding model”.

Pictures are presented with non-hydrogen atoms displayed as displacement ellipsoids, which are set at the 50% probability level.

Table 16: Crystal data and structure refinement for **265**

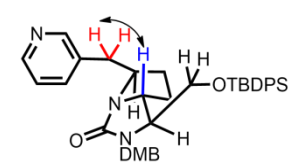
Empirical formula	C ₁₂ H ₂₂ N ₂ O ₄
Formula weight	258.32
Temperature/K	121(2)
Crystal system	monoclinic
Space group	P2 ₁ /c
a/Å	9.7870(10)
b/Å	16.958(2)
c/Å	9.1099(7)
α/°	90.00
β/°	94.166(9)
γ/°	90.00
Volume/Å ³	1507.9(3)
Z	4
ρ _{calc} /cm ³	1.138
μ/mm ⁻¹	0.704
F(000)	560.0
Crystal size/mm ³	0.11 × 0.03 × 0.03
Radiation	CuKα (λ = 1.54184)
2θ range for data collection/°	9.06 to 100.84
Index ranges	-8 ≤ h ≤ 9, -16 ≤ k ≤ 14, -9 ≤ l ≤ 8
Reflections collected	3306
Independent reflections	1554 [R _{int} = 0.0372, R _{sigma} = 0.0605]
Data/restraints/parameters	1554/0/167
Goodness-of-fit on F ²	1.127
Final R indexes [I ≥ 2σ (I)]	R ₁ = 0.0478, wR ₂ = 0.0998
Final R indexes [all data]	R ₁ = 0.0707, wR ₂ = 0.1151
Largest diff. peak/hole / e Å ⁻³	0.26/-0.17

6.8 Appendix 9: NOESY Spectra for 295



4-methyl H₂: 7-H

7-H: 4-methyl H₂



7 References

- 1 F. Pammolli, L. Magazzini and M. Riccaboni, *Nat. Rev. Drug Discov.*, 2011, **10**, 428–38.
- 2 D. Robbins, A. F. Newton, C. Gignoux, J.-C. Legeay, A. Sinclair, M. Rejzek, C. a. Laxon, S. K. Yalamanchili, W. Lewis, M. a. O’Connell, et al., *Chem. Sci.*, 2011, **2**, 2232–35.
- 3 J. P. Hughes, S. S. Rees, S. B. Kalindjian and K. L. Philpott, *Br. J. Pharmacol.*, 2011, **162**, 1239–1249.
- 4 G. L. Patrick, *An Introduction to Medicinal Chemistry*, Oxford University Press, 2005.
- 5 L. J. Gershell and J. H. Atkins, *Nat. Rev. Drug Discov.*, 2003, **2**, 321–7.
- 6 A. K. Ghose, V. N. Viswanadhan and J. J. Wendoloski, *J. Comb. Chem.*, 1998, **1**, 55–68.
- 7 A. Nadin, C. Hattotuwigama, I. Churcher, A. Nadin, C. Hattotuwigama and I. Churcher, *Angew. Chemie Int. Ed.*, 2012, **51**, 1114–22.
- 8 J. P. Garnier, *Harv. Bus. Rev.*, 2008, 68–76.
- 9 I. Kola and J. Landis, *Nat. Rev. Drug Discov.*, 2004, **3**, 711–5.
- 10 P. D. Leeson and J. R. Empfield, *Annu. Rep. Med. Chem.*, 2010, Volume 45, pp. 393–407.
- 11 C. a. Lipinski, F. Lombardo, B. W. Dominy and P. J. Feeney, *Adv. Drug Deliv. Rev.*, 1997, **23**, 3–25.
- 12 T. I. I. Oprea, A. M. M. Davis, S. J. J. Teague and P. D. D. Leeson, *J. Chem. Inf. Comput. Sci.*, 2001, **41**, 1308–15.
- 13 S. S. J. Teague, A. A. M. Davis, P. P. D. Leeson and T. Oprea, *Angew. Chemie - Int. Ed.*, 1999, **38**, 3743–3748.
- 14 J. F. Blake and B. James F, *Curr. Opin. Biotechnol.*, 2000, **11**, 104–107.
- 16 M. J. Waring, *Bioorg. Med. Chem. Lett.*, 2009, **19**, 2844–2851.
- 17 M. J. Waring, *Expert Opin. Drug Discov.*, 2010, **5**, 235–48.
- 18 M. J. Waring and C. Johnstone, *Bioorg. Med. Chem. Lett.*, 2007, **17**, 1759–1764.
- 19 P. D. Leeson and B. Springthorpe, *Nat Rev Drug Discov*, 2007, **6**, 881–890.
- 20 H. van de Waterbeemd, D. A. Smith, K. Beaumont and D. K. Walker, *J. Med. Chem.*, 2001, **44**, 1313–1333.
- 21 J. Gasteiger, *Handbook of Chemoinformatics: From Data to Knowledge*, Wiley-VCH, 2003.
- 22 R. Mannhold, H. Kubinyi and G. Folkers, *Molecular Drug Properties: Measurement and Prediction*, John Wiley & Sons, 2008.

- 23 C. A. Lipinski, *J. Pharmacol. Toxicol. Methods*, 2000, **44**, 235–249.
- 24 P. Ertl, B. Rohde and P. Selzer, *J. Med. Chem.*, 2000, **43**, 3714–3717.
- 25 A. Chuprina, O. Lukin, R. Demoiseaux, A. Buzko and A. Shivanyuk, *J. Chem. Inf. Model.*, 2010, **50**, 470–479.
- 26 G. M. Rishton and R. Gilbert M, *Drug Discov. Today*, 2003, **8**, 86–96.
- 27 A. Jadhav, R. S. Ferreira, C. Klumpp, B. T. Mott, C. P. Austin, J. Inglese, C. J. Thomas, D. J. Maloney, B. K. Shoichet and A. Simeonov, *J. Med. Chem.*, 2009, **53**, 37–51.
- 28 R. Gilbert M and G. M. Rishton, *Drug Discov. Today*, 1997, **2**, 382–384.
- 29 S. L. McGovern, E. Caselli, N. Grigorieff and B. K. Shoichet, *J. Med. Chem.*, 2002, **45**, 1712–1722.
- 30 E. Kerns and L. Di, *Drug-like Properties: Concepts, Structure Design and Methods: From ADME to Toxicity Optimization*, Elsevier Science, 2008.
- 31 P. D. Dobson and D. B. Kell, *Nat. Rev. Drug Discov.*, 2008, **7**, 205–20.
- 32 S. Oswald, M. Grube, W. Siegmund and H. K. Kroemer, *Xenobiotica*, 2007, **37**, 1171–1195.
- 33 U. Norinder and M. Haerberlein, *Adv. Drug Deliv. Rev.*, 2002, **54**, 291–313.
- 34 H. van de Waterbeemd, G. Camenisch, G. Folkers, J. R. Chretien and O. A. Raevsky, *J. Drug Target.*, 1998, **6**, 151–165.
- 35 S. G. Summerfield, A. J. Stevens, L. Cutler, M. del Carmen Osuna, B. Hammond, S.-P. Tang, A. Hersey, D. J. Spalding and P. Jeffrey, *J. Pharmacol. Exp. Ther.*, 2006, **316**, 1282–1290.
- 36 W.E. Glover, A.D.M. Greenfield and R.G. Shanks, *Br. J. Pharmacol. Chemother.*, 1962, **19**, 235–244.
- 37 J. W. Black, A. F. Crowther, R. G. Shanks, L. H. Smith and A. C. Dornhorst, *Lancet*, 1964, **283**, 1080–1081.
- 38 C. Hamlett, *Drug Discovery Using a Fragment-based Approach*, University of Leeds, 2011.
- 39 M. M. Hann and T. I. Oprea, *Curr. Opin. Chem. Biol.*, 2004, **8**, 255–263.
- 40 P. J. Hajduk, W. R. J. D. Galloway and D. R. Spring, *Nature*, 2011, **470**, 42–43.
- 41 R. A. E. Carr, M. Congreve, C. W. Murray and D. C. Rees, *Drug Discov. Today*, 2005, **10**, 987–992.
- 42 D. C. Rees, M. Congreve, C. W. Murray and R. Carr, *Nat Rev Drug Discov*, 2004, **3**, 660–672.
- 43 M. M. Hann, A. R. Leach and G. Harper, *J. Chem. Inf. Model.*, 2001, **41**, 856–864.
- 44 G. Bollag, P. Hirth, J. Tsai, J. Zhang, P. N. Ibrahim, H. Cho, W. Spevak, C. Zhang, Y. Zhang, G. Habets, et al., *Nature*, 2010, **467**, 596–599.
- 45 J. Tsai, J. T. Lee, W. Wang, J. Zhang, H. Cho, S. Mamo, R. Bremer, S. Gillette, J. Kong, N. K. Haass, et al., *Proc. Natl. Acad. Sci.*, 2008, **105**, 3041–

3046.

- 46 A. H. Lipkus, Q. Yuan, K. Lucas, S. Funk, W. F. Bartelt, R. J. Schenck and A. J. Trippe, *J. Org. Chem.*, 2008, **73**, 4443–51.
- 47 R. J. Spandl, M. Díaz-Gavilán, K. M. G. O’Connell, G. L. Thomas and D. R. Spring, *Chem. Rec.*, 2008, **8**, 129–142.
- 48 D. Morton, S. Leach, C. Cordier, S. Warriner and A. Nelson, *Angew. Chemie Int. Ed.*, 2009, **48**, 104–109.
- 49 M. Dow, M. Fisher, T. James, F. Marchetti and A. Nelson, *Org. Biomol. Chem.*, 2012, **10**, 17–28.
- 50 K. H. Bleicher, H.-J. Bohm, K. Muller and A. I. Alanine, *Nat Rev Drug Discov*, 2003, **2**, 369–378.
- 51 D. S. Tan, *Nat Chem Biol*, 2005, **1**, 74–84.
- 52 M. D. Burke and S. L. Schreiber, *Angew. Chem. Int. Ed. Engl.*, 2004, **43**, 46–58.
- 53 H. Oguri and S. L. Schreiber, *Org. Lett.*, 2004, **7**, 47–50.
- 54 R. J. Spandl, A. Bender and D. R. Spring, *Org. Biomol. Chem.*, 2008, **6**, 1149–1158.
- 55 T. E. E. Nielsen and S. L. L. Schreiber, *Angew. Chem. Int. Ed. Engl.*, 2008, **47**, 48–56.
- 56 S. L. Schreiber, *Science (80-.)*, 2000, **287**, 1964–1969.
- 57 D. R. Spring, *Org. Biomol. Chem.*, 2003, **1**, 3867–3870.
- 58 N. Kumagai, G. Muncipinto and S. L. Schreiber, *Angew. Chem. Int. Ed. Engl.*, 2006, **45**, 3635–8.
- 59 G. L. Thomas, R. J. Spandl, F. G. Glansdorp, M. Welch, A. Bender, J. Cockfield, J. A. Lindsay, C. Bryant, D. F. J. Brown, O. Loiseleur, et al., *Angew. Chemie Int. Ed.*, 2008, **47**, 2808–2812.
- 60 S. Sirois, G. Hatzakis, D. Wei, Q. Du and K.-C. Chou, *Comput. Biol. Chem.*, 2005, **29**, 55–67.
- 61 C.-V. T. Vo, G. Mikutis and J. W. Bode, *Angew. Chem. Int. Ed. Engl.*, 2013, **52**, 1705–8.
- 62 C.-V. T. Vo, M. U. Luescher and J. W. Bode, *Nat. Chem.*, 2014, **6**, 310–4.
- 63 M. He and J. W. Bode, *J. Am. Chem. Soc.*, 2008, **130**, 418–9.
- 64 S. M.-C. Pelletier, P. C. Ray and D. J. Dixon, *Org. Lett.*, 2009, **11**, 4512–5.
- 65 R. G. Doveston, P. Tosatti, M. Dow, D. J. Foley, H. Y. Li, A. J. Campbell, D. House, I. Churcher, S. P. Marsden and A. Nelson, *Org. Biomol. Chem.*, 2015, **13**, 859–865.
- 66 A. Dömling and I. Ugi, *Angew. Chem. Int. Ed. Engl.*, 2000, **39**, 3168–3210.
- 67 N. R. Candeias, F. Montalbano, P. M. S. D. Cal and P. M. P. Gois, *Chem. Rev.*, 2010, **110**, 6169–93.
- 68 J. Zhu and H. Bienaym, *Multicomponent Reactions*, John Wiley & Sons,

2006.

- 69 E. Ascic, S. T. Le Quement, M. Ishoey, M. Daugaard, T. E. Nielsen, S. T. Le Quement, M. Ishoey, M. Daugaard and T. E. Nielsen, *ACS Comb. Sci.*, 2012, **14**, 253–7.
- 70 N. R. Candeias, L. F. Veiros, C. a. M. Afonso and P. M. P. Gois, *European J. Org. Chem.*, 2009, 1859–1863.
- 71 E. Ascic, S.T. Le Quement, M. Ishoey, M. Daugaard and T. E. Nielsen, *ACS Comb. Sci.*, 2012, **17**, 19–23.
- 72 M. Ayaz, J. Dietrich and C. Hulme, *Tetrahedron Lett.*, 2011, **52**, 4821–4823.
- 73 F. Berre, *Tetrahedron Lett.*, 2001, **42**, 3591–3594.
- 74 T. J. Southwood, M. C. Curry and C. a. Hutton, *Tetrahedron*, 2006, **62**, 236–242.
- 75 N. A. Petasis and I. A. Zavialov, *J. Am. Chem. Soc.*, 1997, **7863**, 445–446.
- 76 N. A. Petasis, *Tetrahedron*, 1997, **53**, 16463–16470.
- 77 T. Koolmeister, M. Södergren and M. Scobie, *Tetrahedron Lett.*, 2002, **43**, 5969–5970.
- 78 G. Muncipinto, P. N. Moquist, S. L. Schreiber and S. E. Schaus, *Angew. Chem. Int. Ed. Engl.*, 2011, **50**, 8172–5.
- 79 P. Wu, M. Å. Petersen, A. E. Cohrt, R. Petersen, M. H. Clausen and T. E. Nielsen, *European J. Org. Chem.*, 2015, n/a–n/a.
- 80 T. Flagstad, M. R. Hansen, S. T. Le Quement, M. Givskov and T. E. Nielsen, *ACS Comb. Sci.*, 2015, **17**, 19–23.
- 81 S. T. Le Quement, T. Flagstad, R. J. T. Mikkelsen, M. R. Hansen, M. C. Givskov and T. E. Nielsen, *Org. Lett.*, 2012, **14**, 640–643.
- 82 G. Muncipinto, T. Kaya, J. A. Wilson, N. Kumagai, P. a. Clemons and S. L. Schreiber, *Org. Lett.*, 2010, **12**, 5230–3.
- 83 K. K. Nanda and B. Wesley Trotter, *Tetrahedron Lett.*, 2005, **46**, 2025–2028.
- 84 S. Wertz, S. Kodama and A. Studer, *Angew. Chemie - Int. Ed.*, 2011, **50**, 11511–11515.
- 85 S. Urig, J. Jacob, E. Amtmann, J. Moulinoux, S. Gromer, K. Becker and E. Davioud-charvet, *J. Med. Chem.*, 2005, **48**, 7024-7039.
- 86 W. M. Meylan and P. H. Howard, *J. Pharm. Sci.*, 1995, **84**, 83–92.
- 87 C. J. Moody, P. A. Hunt and C. Smith, *ARKIVOC*, 2000, **v**, 698–706.
- 88 M. D. Burke, E. M. Berger and S. L. Schreiber, *Science (80-.)*, 2003, **302**, 613–618.
- 89 Z. Hong, L. Liu, C.-C. Hsu and C.-H. Wong, *Angew. Chem. Int. Ed. Engl.*, 2006, **45**, 7417–21.
- 90 F. Dioury, E. Guéné, A. Di Scala-Rouilleau, C. Ferroud, A. Guy and M. Port, *Tetrahedron Lett.*, 2005, **46**, 611–613.
- 91 S. Ahmad and A. Sutherland, *Org. Biomol. Chem.*, 2012, **10**, 8251–9.

- 92 S. Bera and G. Panda, *ACS Comb. Sci.*, 2012, **14**, 1–4.
- 93 H. A. Staab, *Justus Liebigs Ann. Chem.*, 1957, **609**, 75–83.
- 94 D. Zhang, X. Xing and G. D. Cuny, *J. Org. Chem.*, 2006, **71**, 1750–3.
- 95 B. M. Bhanage, S. Fujita, Y. Ikushima and M. Arai, *Green Chem.*, 2004, **6**, 78.
- 96 L. a Marcaurelle, E. Comer, S. Dandapani, J. R. Duvall, B. Gerard, S. Kesavan, M. D. Lee, H. Liu, J. T. Lowe, J.-C. Marie, et al., *J. Am. Chem. Soc.*, 2010, **132**, 16962–76.
- 97 A. Fürstner and K. Langemann, *J. Am. Chem. Soc.*, 1997, **119**, 9130–9136.
- 98 R. H. Grubbs, S. J. Miller and G. C. Fu, *Acc. Chem. Res.*, 1995, **28**, 446–452.
- 99 G. O. Wilson, K. A. Porter, H. Weissman, S. R. White, N. R. Sottos and J. S. Moore, *Adv. Synth. Catal.*, 2009, **351**, 1817–1825.
- 100 C. C. and L. A. Oro, *Wiley: Iridium Complexes in Organic Synthesis - Luis A. Oro, Carmen Claver*, 2008.
- 101 J. F. Hartwig and L. M. Stanley, *Acc. Chem. Res.*, 2010, **43**, 1461–75.
- 102 G. Helmchen, A. Dahnz, P. Dübon, M. Schelwies and R. Weihofen, *Chem. Commun. (Camb.)*, 2007, 675–91.
- 103 R. Takeuchi and S. Kezuka, *Synthesis (Stuttg.)*, 2006, **2006**, 3349–3366.
- 104 R. Takeuchi, *Synlett*, 2002, **2002**, 1954–1965.
- 105 J. P. Janssen and G. Helmchen, *Tetrahedron Lett.*, 1997, **38**, 8025–8026.
- 106 R. Takeuchi and M. Kashio, *Angew. Chemie Int. Ed. English*, 1997, **36**, 263–265.
- 107 G. W. Bemis and M. A. Murcko, *J. Med. Chem.*, 1996, **39**, 2887–2893.
- 108 J. J. Irwin, T. Sterling, M. M. Mysinger, E. S. Bolstad and R. G. Coleman, *J. Chem. Inf. Model.*, 2012, **52**, 1757–68.
- 109 H. Fujieda, M. Kanai, T. Kambara and M. Dekker, *J. Am. Chem. Soc.* 1997, **119**, 2060-2061.
- 110 Z. Chen, L. Lin, M. Wang, X. Liu and X. Feng, *Chem. Eur. J.*, 2013, **19**, 7561–7567.
- 111 M. M. C. Lo and G. C. Fu, *J. Am. Chem. Soc.*, 2002, **124**, 4572–4573.
- 112 E. C. Lee, B. L. Hodous, E. Bergin, C. Shih and G. C. Fu, *J. Am. Chem. Soc.*, 2005, **127**, 11586–11587.
- 113 B. L. Hodous and G. C. Fu, *J. Am. Chem. Soc.*, 2002, **124**, 1578–1579.
- 114 S. Chen, E. C. Salo, K. a. Wheeler and N. J. Kerrigan, *Org. Lett.*, 2012, **14**, 1784–1787.
- 115 S. France, H. Wack, A. M. Hafez, A. E. Taggi, D. R. Witsil and T. Lectka, *Org. Lett.*, 2002, **4**, 1603–1605.
- 116 H. M. L. Davies and C. Venkataramani, *Org. Lett.*, 2001, **3**, 1773–1775.
- 117 H. M. L. Davies, R. E. J. Beckwith, E. G. Antoulinakis and Q. Jin, *J. Org. Chem.*, 2003, **68**, 6126–6132.

- 118 S. F. Zhu, B. Xu, G. P. Wang and Q. L. Zhou, *J. Am. Chem. Soc.*, 2012, **134**, 436–442.
- 119 H. M. L. Davies, T. Hansen and M. R. Churchill, *J. Am. Chem. Soc.*, 2000, **122**, 3063–3070.
- 120 B. Liu, S. Zhu, W. Zhang, C. Chen and Q. Zhou, *J. Am. Chem. Soc.*, 2007, 5834–5835.
- 121 H. M. L. Davies, C. Venkataramani, T. Hansen and D. W. Hopper, *J. Am. Chem. Soc.*, 2003, **125**, 6462–6468.
- 122 Z. Hou, J. Wang, P. He, J. Wang, B. Qin, X. Liu, L. Lin and X. Feng, *Angew. Chemie - Int. Ed.*, 2010, **49**, 4763–4766.
- 123 H. Finch, G. Nogami, M. Yokoyama, M. Barta and J.L. Havens, *ACS Comb. Sci.*, 2002, **30**, 2197–2199.
- 124 H. M. L. Davies, D. W. Hopper, T. Hansen, Q. Liu and S. R. Childers, *Bioorg. Med. Chem. Lett.*, 2004, **14**, 1799–1802.
- 125 N. T. Jui, J. a O. Garber, F. G. Finelli and D. W. C. MacMillan, *J. Am. Chem. Soc.*, 2012, **134**, 11400–11403.
- 126 H. Y. Jang, J. B. Hong and D. W. C. MacMillan, *J. Am. Chem. Soc.*, 2007, **129**, 7004–7005.
- 127 T. H. Graham, C. M. Jones, N. T. Jui and D. W. C. MacMillan, *J. Am. Chem. Soc.*, 2008, **130**, 16494–16495.
- 128 K. A. and D. W. C. M. T D. Beeson, A Mastracchio, J. B. Hong, *Science (80-.)*, 2007, **316**, 582–586.
- 129 H. Kim and D. W. C. Macmillan, *J. Am. Chem. Soc.*, 2008, **130**, 398–399.
- 130 J. F. Bower, P. Szeto and T. Gallagher, *Org. Lett.*, 2007, **9**, 4909–4912.
- 131 M. Eskici, A. Karanfil, M. S. Özer and C. Sarikürkcü, *Tetrahedron Lett.*, 2011, **52**, 6336–6341.
- 132 T. a. Moss, D. M. Barber, A. F. Kyle and D. J. Dixon, *Chem. - A Eur. J.*, 2013, **19**, 3071–3081.
- 133 J. F. Bower, P. Szeto and T. Gallagher, *Org. Biomol. Chem.*, 2007, **5**, 143–150.
- 134 A. J. Williams, S. Chakthong, D. Gray, R. M. Lawrence and T. Gallagher, *Org. Lett.*, 2003, **5**, 811–814.
- 135 J. F. Bower, J. Švenda, A. J. Williams, J. P. H. Charmant, R. M. Lawrence, P. Szeto and T. Gallagher, *Org. Lett.*, 2004, **6**, 4727–4730.
- 136 J. F. Bower, P. Szeto and T. Gallagher, *Tetrahedron*, 2007, 10–13.
- 137 A. Noble and J. C. Anderson, *Chem. Rev.*, 2013, **113**, 2887–2939.
- 138 H. G. Johnson, *J. Am. Chem. Soc.*, 1946, **68**, 12–14.
- 139 E. L. Hirst, J. K. N. Jones, S. Minahan, F. W. Ochynski, A. T. Thomas and T. Urbanski, *J. Chem. Soc.*, 1947, 924.
- 140 H. Adams, J. C. Anderson, S. Peace and A. M. K. Pennell, *J. Org. Chem.*, 1998, **63**, 9932–9934.

- 141 C.-J. Wang, X.-Q. Dong, Z.-H. Zhang, Z.-Y. Xue and H.-L. Teng, *J. Am. Chem. Soc.*, 2008, **130**, 8606–7.
- 142 D. M. Barber, H. J. Sanganee, D. J. Dixon and A. Park, *Org. Lett.*, 2012, 4064–4067.
- 143 K. M. Johnson, M. S. Rattley, F. Sladojevich, D. M. Barber, M. G. Nuñez, A. M. Goldys, D. J. Dixon, M. G. Nu, A. M. Goldys and D. J. Dixon, *Org. Lett.*, 2012, **14**, 2492–5.
- 144 J. M. B. Vu and J. L. Leighton, *Org. Lett.*, 2011, **13**, 4056–9.
- 145 J. C. Anderson, L. R. Horsfall, A. S. Kalogirou, M. R. Mills, G. J. Stepney and G. J. Tizzard, *J. Org. Chem.*, 2012, **77**, 6186–98.
- 146 T. Okino, S. Nakamura, T. Furukawa and Y. Takemoto, *Org. Lett.*, 2004, **6**, 625–7.
- 147 Z. Wang, *Comprehensive Organic Name Reactions and Reagents*, Wiley, 2009.
- 148 B. M. Nugent, R. a Yoder and J. N. Johnston, *J. Am. Chem. Soc.*, 2004, **126**, 3418–9.
- 149 N. Ono, in *The Nitro Group in Organic Synthesis*, John Wiley & Sons, Inc., 2002, pp. 159–181.
- 150 P. Ceccherelli, M. Curini, M. C. Marcotullio, F. Epifano and O. Rosati, *Synth. Commun.*, 2006, **28**, 3057–3064.
- 151 J. C. Anderson and H. a Chapman, *Org. Biomol. Chem.*, 2007, **5**, 2413–2422.
- 152 K. Yamada, G. Moll and M. Shibasaki, *Synlett*, 2001, **2001**, 980–982.
- 153 L. Bernardi, F. Fini, R. P. Herrera, A. Ricci and V. Sgarzani, *Tetrahedron*, 2006, **62**, 375–380.
- 154 E. Marqués-López, P. Merino, T. Tejero and R. P. Herrera, *European J. Org. Chem.*, 2009, **2009**, 2401–2420.
- 155 E. Gomez-Bengoa, A. Linden, R. López, I. Múgica-Mendiola, M. Oiarbide and C. Palomo, *J. Am. Chem. Soc.*, 2008, **130**, 7955–66.
- 156 C. Palomo, M. Oiarbide, R. Halder, A. Laso and R. López, *Angew. Chemie - Int. Ed.*, 2005, **45**, 117–120.
- 157 C. Palomo, M. Oiarbide, A. Laso and R. López, *J. Am. Chem. Soc.*, 2005, **127**, 17622–3.
- 158 J. S. Bandar and T. H. Lambert, *J. Am. Chem. Soc.*, 2013, **135**, 11799–802.
- 159 G. P. Marsh, P. J. Parsons, C. McCarthy and X. G. Corniquet, *Org. Lett.*, 2007, **9**, 2613–6.
- 160 W. He, Q. Wang, Q. Wang, B. Zhang, X. Sun and S. Zhang, *Synlett*, 2009, 1311–1314.
- 161 J. C. Anderson and P. J. Koovits, *Chem. Sci.*, 2013, **4**, 2897.
- 162 H. Y. Wang, Z. Chai and G. Zhao, *Tetrahedron*, 2013, **69**, 5104–5111.
- 163 T. a Davis, J. C. Wilt and J. N. Johnston, *J. Am. Chem. Soc.*, 2010, **132**, 2880–2.

- 164 C. A. Brown and V. K. Ahuja, *J. Org. Chem.*, 1973, **38**, 2226–2230.
- 165 *Encyclopedia of Reagents for Organic Synthesis*, John Wiley & Sons, Ltd, Chichester, UK, 2001.
- 166 P. G. M. Wuts and T. W. Greene, *Greene's Protective Groups in Organic Synthesis*, Wiley, 2006.
- 167 G. S. Lemen and J. P. Wolfe, *Org. Lett.*, 2010, **12**, 2322–5.
- 168 L. Bagnoli, S. Cacchi, G. Fabrizi, A. Goggiamani, C. Scarponi and M. Tiecco, *J. Org. Chem.*, 2010, **75**, 2134–7.
- 169 F. Lovering, J. Bikker and C. Humblet, *J. Med. Chem.*, 2009, **52**, 6752–6.
- 170 N. R. Candeias, P. M. S. D. Cal, V. André, M. T. Duarte, L. F. Veiros and P. M. P. Gois, *Tetrahedron*, 2010, **66**, 2736–2745.
- 171 H. Jourdan, G. Gouhier, L. Van Hijfte, P. Angibaud and S. R. Piettre, *Tetrahedron Lett.*, 2005, **46**, 8027–8031.
- 172 C. Gnamm, G. Franck, N. Miller, T. Stork, K. Brödner and G. Helmchen, *Synthesis (Stuttg.)*, 2008, **2008**, 3331–3350.
- 173 H.-O. Kim, D. Friedrich, E. Huber and N. P. Peet, *Synth. Commun.*, 1996, **26**, 3453–3469.
- 174 PCT, 9 167 193, 1999.
- 175 R. Gosain, A. M. Norrish and M. E. Wood, *Tetrahedron*, 2001, **57**, 1399–1410.
- 176 M. Nagarajan, X. Xiao, S. Antony, G. Kohlhagen, Y. Pommier and M. Cushman, *J. Med. Chem.*, 2003, **46**, 5712–24.
- 177 A. J. Murray, P. J. Parsons, E. S. Greenwood and E. M. E. Viseux, *Synlett*, 2004, 1589–1591.
- 178 A. S. Kende and J. S. Mendoza, *Tetrahedron Lett.*, 1991, **32**, 1699–1702.
- 179 C. G. Oliva, A. M. S. Silva, D. I. S. P. Resende, F. A. A. Paz and J. A. S. Cavaleiro, *European J. Org. Chem.*, 2010, **2010**, 3449–3458.
- 180 A. F. Kyle, P. Jakubec, D. M. Cockfield, E. Cleator, J. Skidmore and D. J. Dixon, *Chem. Commun. (Camb.)*, 2011, **47**, 10037–9.
- 181 L. Huang and W. D. Wulff, *J. Am. Chem. Soc.*, 2011, **133**, 8892–5.
- 182 Q. Wang, M. Leutzsch, M. van Gemmeren and B. List, *J. Am. Chem. Soc.*, 2013, **135**, 15334–7.
- 183 D. J. Miller, M. Bashir-Uddin Surfraz, M. Akhtar, D. Gani and R. K. Allemann, *Org. Biomol. Chem.*, 2004, **2**, 671–88.
- 184 L. Espelt, T. Parella, J. Bujons, C. Solans, J. Joglar, A. Delgado and P. Clapés, *Chemistry*, 2003, **9**, 4887–99.
- 185 N. Bischofberger, H. Waldmann, T. Saito, E. S. Simon, W. Lees, M. D. Bednarski and G. M. Whitesides, *J. Org. Chem.*, 1988, **53**, 3457–3465.
- 186 Y. Meyer, J.-A. Richard, M. Massonneau, P.-Y. Renard and A. Romieu, *Org. Lett.*, 2008, **10**, 1517–20.

- 187 A. Viso, R. Fernández de la Pradilla, A. Flores and A. García, *Tetrahedron*, 2007, **63**, 8017–8026.
- 188 S. Dugar, A. Sharma, B. Kuila, D. Mahajan, S. Dwivedi and V. Tripathi, *Synthesis*, 2014, **47**, 712–720.
- 189 S. G. Davies, J. R. Haggitt, O. Ichihara, R. J. Kelly, M. A. Leech, A. J. Price Mortimer, P. M. Roberts and A. D. Smith, *Org. Biomol. Chem.*, 2004, **2**, 2630.
- 190 M. L. Leathen, B. R. Rosen and J. P. Wolfe, *J. Org. Chem.*, 2009, 5107–5110.
- 191 J. S. Nakhla, D. M. Schultz and J. P. Wolfe, *Tetrahedron*, 2009, **65**, 6549–6570.
- 192 T. Ayad, Y. Génisson and M. Baltas, *Org. Biomol. Chem.*, 2005, **3**, 2626.
- 193 D. Savoia, S. Grilli and A. Gualandi, *Org. Lett.*, 2010, **12**, 4964–7.
- 194 M. C. Manfredi, Y. Bi, A. A. Nirschl, J. C. Sutton, R. Seethala, R. Golla, B. C. Beehler, P. G. Sleph, G. J. Grover, J. Ostrowski, et al., *Bioorg. Med. Chem. Lett.*, 2007, **17**, 4487–90.
- 195 D. Schultz, J. Wolfe, D. Schultz M. and J. Wolfe P., *Synthesis (Stuttg.)*, 2012, **44**, 351,361.
- 196 J. D. Neukom, A. S. Aquino and J. P. Wolfe, *Org. Lett.*, 2011, **13**, 2196–2199.
- 197 M. Kunishima, K. Hioki, T. Moriya, J. Morita, T. Ikuta and S. Tani, *Angew. Chemie, Int. Ed.*, 2006, **45**, 1252–1255.
- 198 T. W. Liwosz and S. R. Chemler, *J. Am. Chem. Soc.*, 2012, **134**, 2020–3.
- 199 A. Nelson, C. Empson, P. Craven, Z. Owen, I. Churcher, R. Doveston, S. Warriner, M. Dow and A. Horton, *Org. Biomol. Chem.*, 2015, **13**, 859-865.
- 200 W. H. B. Sauer and M. K. Schwarz, *J. Chem. Inf. Comput. Sci.*, 2003, **43**, 987.
- 201 G. M. Sheldrick, *Acta Crystallogr. A.*, 2008, **64**, 112–22.